

Advances in Experimental Medicine and Biology 1250

Heung Jae Chun
Rui L. Reis
Antonella Motta
Gilson Khang *Editors*

Biomimicked Biomaterials

Advances in Tissue Engineering and
Regenerative Medicine

 Springer

Advances in Experimental Medicine and Biology

Volume 1250

Editorial Board

WIM E. CRUSIO, *Institut de Neurosciences Cognitives et Intégratives d'Aquitaine, CNRS and University of Bordeaux UMR 5287, Pessac Cedex, France*

JOHN D. LAMBRIS, *University of Pennsylvania, Philadelphia, PA, USA*

HEINFRIED H. RADEKE, *Institute of Pharmacology & Toxicology, Clinic of the Goethe University Frankfurt Main, Frankfurt am Main, Germany*

NIMA REZAEI, *Research Center for Immunodeficiencies, Children's Medical Center, Tehran University of Medical Sciences, Tehran, Iran*

Advances in Experimental Medicine and Biology provides a platform for scientific contributions in the main disciplines of the biomedicine and the life sciences. This series publishes thematic volumes on contemporary research in the areas of microbiology, immunology, neurosciences, biochemistry, biomedical engineering, genetics, physiology, and cancer research. Covering emerging topics and techniques in basic and clinical science, it brings together clinicians and researchers from various fields.

Advances in Experimental Medicine and Biology has been publishing exceptional works in the field for over 40 years, and is indexed in SCOPUS, Medline (PubMed), Journal Citation Reports/Science Edition, Science Citation Index Expanded (SciSearch, Web of Science), EMBASE, BIOSIS, Reaxys, EMBiology, the Chemical Abstracts Service (CAS), and Pathway Studio.

2018 Impact Factor: 2.126.

More information about this series at <http://www.springer.com/series/5584>

Heung Jae Chun
Rui L. Reis • Antonella Motta
Gilson Khang
Editors

Biomimicked Biomaterials

Advances in Tissue Engineering
and Regenerative Medicine

 Springer

Editors

Heung Jae Chun
Institute of Cell & Tissue Engineering
and College of Medicine
Catholic University of Korea
Seoul, South Korea

Antonella Motta
Department of Industrial Engineering
and BIOTech Research Center
University of Trento
Trento, Italy

Rui L. Reis
3B's Research Group, I3Bs – Research
Institute on Biomaterials,
Biodegradables and Biomimetics,
Headquarters of the European Institute
of Excellence on Tissue Engineering
and Regenerative Medicine
University of Minho
Guimarães, Portugal

Gilson Khang
Department of BIN Convergence
Technology, Department of Polymer
Nano Science & Technology and
Polymer BIN Research Center
Jeonbuk National University
Jeonju, South Korea

ISSN 0065-2598 ISSN 2214-8019 (electronic)
Advances in Experimental Medicine and Biology
ISBN 978-981-15-3261-0 ISBN 978-981-15-3262-7 (eBook)
<https://doi.org/10.1007/978-981-15-3262-7>

© Springer Nature Singapore Pte Ltd. 2020

This work is subject to copyright. All rights are reserved by the Publisher, whether the whole or part of the material is concerned, specifically the rights of translation, reprinting, reuse of illustrations, recitation, broadcasting, reproduction on microfilms or in any other physical way, and transmission or information storage and retrieval, electronic adaptation, computer software, or by similar or dissimilar methodology now known or hereafter developed.

The use of general descriptive names, registered names, trademarks, service marks, etc. in this publication does not imply, even in the absence of a specific statement, that such names are exempt from the relevant protective laws and regulations and therefore free for general use.

The publisher, the authors, and the editors are safe to assume that the advice and information in this book are believed to be true and accurate at the date of publication. Neither the publisher nor the authors or the editors give a warranty, expressed or implied, with respect to the material contained herein or for any errors or omissions that may have been made. The publisher remains neutral with regard to jurisdictional claims in published maps and institutional affiliations.

This Springer imprint is published by the registered company Springer Nature Singapore Pte Ltd. The registered company address is: 152 Beach Road, #21-01/04 Gateway East, Singapore 189721, Singapore

Preface

Tissue engineering and regenerative medicine is an interdisciplinary field that involves the study and development of biomaterials, scaffolds, organs, and implants for the society. Tissue and organ shortage is a major public health challenge with only a percentage of deserving people receiving transplantation. Many of them are in waiting lists for the tissue and organ. The promising advancement in the field of tissue engineering and regenerative medicine results in the regeneration or replacement of a variety of organs and tissues including the heart, kidney, skin, and liver. In connection with this, we are very pleased to launch our next edition of the textbook *Biomimicked Biomaterials for Tissue Engineering and Regenerative Medicine* volume II smart materials, discussing on the recent advancement in this field using different materials and techniques. We have attempted to maintain the highest standard of excellence, truthfulness, and pedagogy developed by the publishers that address wide audience (including countless students of biological science, medicine, veterinary, dentistry, materials science, engineering, and physics worldwide; bachelor, master, PhD students; researchers, and company professionals) who intent to update and invent new biomaterials for the tissue engineering and regenerative medicine applications. At the same time, we are very focused on the evolving need of the students and researchers in updating their career in the developing field of bio-inspired materials. This book is a continuation of my previously published book *Novel Biomaterials for Regenerative Medicine* and comprehensive reviews on *Cutting-Edge Enabling Technology for Regenerative Medicine*.

The contents of this book are divided into 4 parts with 13 chapters addressing the recent findings and reports being investigated by a prominent researcher in this field from different parts of the world. **The first part of this book consists of two chapters discussing the novel biomimicked biomaterials for regenerative medicine.** Chapters 1 and 2 focused on the decellularized bone matrix and their application in the field of bone/tissue engineering and regenerative medicine. **The second part consists of four chapters discussing the novel biomimicked hydrogel for regenerative medicine.** Chapters 3, 4, and 5 deal with different types of hydrogels for protein, peptide delivery, and 3D cell encapsulation for tissue engineering and regenerative medicine, and Chap. 6 is about the application of *gellan gum* incorporated demineralized bone in enhancing osteochondral tissue regeneration. **The third part consists of four chapters discussing the control of stem cell fate by biomaterials for regenerative medicine.** Chapter 7 deals with the extracellular vesicle integrated biomaterial for bone regeneration, Chap. 8 gives an overview of the biocompatibility of biomaterial device, and Chaps. 9 and 10 discuss about the cell response to material and their patterns for biomedical engineering. **The fourth part consists of three chapters discussing the nano-intelligent biocomposites for**

regenerative medicine. Chapter 11 discusses about the polyphenols in the fibrillization of islet amyloid polypeptide while Chap. 12 about the recent advances on the biphasic calcium phosphate bioceramics for bone tissue regeneration. Finally, Chap. 13 gives an overview about the surface-modifying polymers for blood-contacting polymeric biomaterials.

Acknowledgment We would like to thank the International Research and Development Program (NRF-2017K1A3A7A03089427) that served as sponsor and inspiration for this book. We offer a special thanks to those who enthusiastically invested time, experience, and energy in submitting their impressive research results, being the backbone of this work, and also to the reviewers for their valuable suggestions in maintaining the quality of the book chapters. Finally, we appreciate the efforts of the publisher of *Advances in Experimental Medicine and Biology* (AEMB) by *Springer Nature* for his great effort in the timely publication of this book. We would also like to appreciate and thank Mr. Wonchan Lee, Ms. Jeong Eun Song, and Mr. Muthukumar Thangavelu from Gilson's Lab for e-mailing all authors, editing, formatting, pressing, and follow-ups in all technical aspects in publishing this book.

Special Dedication to Professor Claudio Migliaresi in Honor of His Retirement

This book is in honor of the retirement of Professor Claudio Migliaresi, University of Trento, Italy, for his extraordinary career and his great contribution in the development of new strategies and materials in the biomedical field, thanks to his advanced vision, challenging attitude, and curiosity. He is also one of the founders of the Department of Materials Engineering and Industrial Technologies, University of Trento, and leader in the biomedical field. He is professor of composite materials engineering and head of the BIOtech Research Center of the University of Trento. He built an international and multidisciplinary research group, thanks to the numerous projects that he coordinated, creating an inspiring and motivating work environment where people can exchange ideas and build new projects altogether. He is still spending energy for the group. He was also vice-rector for technological transfer and dean of Engineering School in Trento. He has published numerous papers on international journals and is editor of books in the field and international patents.



Heung Jae Chun, Institute of Cell & Tissue Engineering, College of Medicine, The Catholic University of Korea, 222 Banpo-daero, Seocho-gu, Seoul, South Korea.



Antonella Motta, Department of Industrial Engineering and BIOTech Research Center, University of Trento, Via Sommarive 9, 38123 Trento, Italy.



Rui L. Reis, 3B's Research Group – Biomaterials, Biodegradables and Biomimetics, University of Minho, Headquarters of the European Institute of Excellence on Tissue Engineering and Regenerative Medicine, AvePark – Parque de Ciência e Tecnologia, Zona Industrial de Gandra, 4805-017 Barco, Guimarães, Portugal; ICVS/3B's – PT Government Associated Laboratory, Braga/Guimarães, Portugal; The Discoveries Centre for Regenerative and Precision Medicine, Headquarters at University of Minho, Avepark, 4805-017 Barco, Guimarães, Portugal.



Gilson Khang, Department of BIN Convergence Technology, Department of Polymer Nano Science & Technology and Polymer BIN Research Center, Chonbuk National University, Deokjin-gu, Jeonju-si, Jeollabuk-do, 54896, South Korea.



Contents

Part I Novel Biomimicked Biomaterials for Regenerative Medicine

- 1 Bone Regeneration Using Duck's Feet-Derived Collagen Scaffold as an Alternative Collagen Source 3**
Jeong Eun Song, Muthukumar Thangavelu, Joohee Choi,
Hunhwi Cho, Byung Kwan Moon, Sun Jung Yoon,
Nuno M. Neves, and Gilson Khang
- 2 Decellularized Extracellular Matrices for Tissue Engineering and Regeneration. 15**
Fang Ge, Yuhe Lu, Qian Li, and Xing Zhang

Part II Novel Biomimicked Hydrogel for Regenerative Medicine

- 3 Injectable In Situ-Forming Hydrogels for Protein and Peptide Delivery 35**
Seung Hun Park, Yun Bae Ji, Joon Yeong Park,
Hyeon Jin Ju, Mijeong Lee, Surha Lee, Jae Ho Kim,
Byoung Hyun Min, and Moon Suk Kim
- 4 Alginate Hydrogels: A Tool for 3D Cell Encapsulation, Tissue Engineering, and Biofabrication 49**
Walter Bonani, Nicola Cagol, and Devid Maniglio
- 5 Design of Advanced Polymeric Hydrogels for Tissue Regenerative Medicine: Oxygen-Controllable Hydrogel Materials 63**
Jeon Il Kang, Sohee Lee, Jeong Ah An, and Kyung Min Park
- 6 Enhancing Osteochondral Tissue Regeneration of Gellan Gum by Incorporating *Gallus gallus* var *Domesticus*-Derived Demineralized Bone Particle 79**
Muthukumar Thangavelu, David Kim, Young Woon Jeong,
Wonchan Lee, Jun Jae Jung, Jeong Eun Song, Rui L. Reis,
and Gilson Khang

**Part III Control of Stem Cell Fate by Biomaterials
for Regenerative Medicine**

- 7 The Development of Extracellular Vesicle-Integrated Biomaterials for Bone Regeneration** 97
Yinghong Zhou and Yin Xiao
- 8 In Vivo Evaluation of the Biocompatibility of Biomaterial Device** 109
L. P. Frazão, J. Vieira de Castro, and Nuno M. Neves
- 9 Biocompatibility of Materials for Biomedical Engineering** 125
Yu-Chang Tyan, Ming-Hui Yang, Chin-Chuan Chang, and Tze-Wen Chung
- 10 Regulation of Stem Cell Functions by Micro-Patterned Structures** 141
Guoping Chen and Naoki Kawazoe

Part IV Nano-Intelligent Biocomposites for Regenerative Medicine

- 11 Natural Polyphenols as Modulators of the Fibrillization of Islet Amyloid Polypeptide** 159
Ana R. Araújo, Rui L. Reis, and Ricardo A. Pires
- 12 Recent Advances of Biphasic Calcium Phosphate Bioceramics for Bone Tissue Regeneration** 177
Sung Eun Kim and Kyeongsoon Park
- 13 Surface-Modifying Polymers for Blood-Contacting Polymeric Biomaterials** 189
Chung-Man Lim, Mei-Xian Li, and Yoon Ki Joung

Part I

**Novel Biomimicked Biomaterials
for Regenerative Medicine**



Bone Regeneration Using Duck's Feet-Derived Collagen Scaffold as an Alternative Collagen Source

Jeong Eun Song, Muthukumar Thangavelu, Joohee Choi, Hunhwi Cho, Byung Kwan Moon, Sun Jung Yoon, Nuno M. Neves, and Gilson Khang

Abstract

Collagen is an important component that makes 25–35% of our body proteins. Over the past decades, tissue engineers have been designing collagen-based biocompatible materials and studying their applications in different fields. Collagen obtained from cattle and pigs has been mainly used until now, but collagen derived from fish and other livestock has attracted more attention since the outbreak of mad cow disease, and they are also used as a raw material for cosmetics and foods. Due to the zoonotic infection using collagen derived from pigs and cattle, their application in developing biomaterials is limited; hence, the development of new animal-derived collagen

is required. In addition, there is a religion (Islam, Hinduism, and Judaism) limited to export raw materials and products derived from cattle and pig. Hence, high-value collagen that is universally accessible in the world market is required. Therefore, in this review, we have dealt with the use of duck's feet-derived collagen (DC) as an emerging alternative to solve this problem and also presenting few original investigated bone regeneration results performed using DC.

Keywords

Duck's feet · Collagen · Extraction · Biomaterial · Scaffold · Bone marrow stem cell · Differentiation · Bone · Regeneration · Tissue engineering

J. E. Song · M. Thangavelu · J. Choi · H. Cho
B. K. Moon · G. Khang (✉)
Department of BIN Convergence Technology,
Department of Polymer Nano Science & Technology
and Polymer BIN Research Center, Jeonbuk National
University, Jeonju, South Korea
e-mail: gskhang@jbnu.ac.kr

S. J. Yoon
Department of orthopedic surgery, Medical School,
Jeonbuk National University,
Jeonju, Republic of Korea

N. M. Neves
3B's Research Group—Biomaterials, Biodegradables
and Biomimetics, Headquarters of the European
Institute of Excellence on Tissue Engineering and
Regenerative Medicine, Guimarães, Portugal

1.1 Introduction

The body has homeostasis to maintain its normal physiological functions up to the certain limit for all external damages. When a disorder such as bone loss or bone defect occurs due to disease or trauma, signaling activation starts to recover to a normal state, and regeneration phenomenon occurs by removing damaged tissue cells [1]. Although the mild bone disorder can be cured through methods such as pharmacotherapy or

physiotherapy, and if recovery is not possible in such methods, the damaged tissue is recovered and transplanted (critical defects such as average diameters of 2 cm) [2, 3].

Autografts are known to be the most ideal method used till now because they contain important factors for bone formation in autogenous bone. However, autografts have limitations, since they are considered to leave bone defects in the withdrawal sites, with the risk of severe infection or pain in the defect area, and have limitations in the harvested bone volume [4–6]. Homografts are a typical substitution method, where the donors' availability is very limited, and after implantation immunosuppressants need to be administered to avoid immune rejection. However, there is a risk of infection with viral diseases [7], whereas, in the case of heterograft (xenograft), the bone is absorbed or it is immunologically problematic to the recipient.

Therefore, a bone substitute is prepared using a metal, ceramic, natural, or synthetic polymer to regenerate the physiological function of the removed tissue or replace the tissue itself with a material having a similar function [8, 9]. Among the biomaterials used for bone tissue engineering, bone fixation materials made of metal are considered and given first priority, followed by ceramics such as calcium phosphate, hydroxyapatite, and tricalcium phosphate (TCP) [10, 11]. However, in the case of conventional metals or ceramics, their structure plays a role of the extracellular matrix. Therefore, it cannot provide physiological activity functions necessary for cell survival. Thus, extracellular matrices are artificially extracted and cell culture tissues are to be reconstructed in the natural cellular biological environment to mimic them. In other words, research is underway to treat tissue engineering [8]. Bioabsorbable synthetic polymers such as polylactic acid (PLA), polyglycolic acid (PGA), poly lactic-co-glycolic acid (PLGA), etc., are biocompatible and biodegradable; hence they are widely used as biomaterials [12, 13]. However, they cannot actively induce bone formation. Therefore, as a study to produce natural bone, natural tissue was used to make scaffolds mim-

icking the morphology of the human tissue, and then the extracellular matrix was directly or indirectly provided for cell adhesion, proliferation, and differentiation. Biomaterials rich in type I collagen are widely used as bone regeneration materials in tissue engineering [14–16]. The bone is composed of a large amount of bone matrix existing between the cells. The majority of the bone matrix is composed of 35% of the organic component composed of the collagen fibers, 45% of the inorganic component composed of calcium, and 20% of the water [17, 18]. In particular, type I collagen is known to form bone and deposit minerals. It is also known that osteogenic proteins and osteoclast progenitor cells promote the action of these substances and serve as regulatory sites for cell attachment [19, 20]. In addition, collagen is biocompatible, non-cytotoxic, and biodegradable and has hemostatic properties and low inflammatory host response [21–24]. However, collagen alone is not as effective in bone formation. When combined with the ceramic material, it shows bone conductivity and when combined with bone marrow component and growth factors, it becomes bone-inducing substance.

Collagen extracted from pigs and cattle was widely used for bone tissue engineering biomaterial. However, these types of collagen may induce immune response or zoonotic infection (foot-and-mouth disease of the pig, mad cow disease of cattle, etc.) [25]. Also, these animals may cause religious issue (Islam, Hinduism, Judaism) which may limit the application. Alternatives have been suggested by extracting collagen from other resources. For example, collagen extracted from marine organisms have been reported to be safe in vivo and do not generate zoonotic infection when compared to collagen derived from cattle and pigs. However, despite its high biocompatibility, marine collagen is unstable for practical application due to its low denaturing temperature and rapid rate of biodegradation [26–29]. Thus, it is an important challenge to develop alternative collagen resources that do not produce toxic substance and have stable property.

Therefore, in this review, we will discuss the components of duck's feet-derived collagen (DC) that is biocompatible, stable, and free from zoonotic infection and their application in bone regeneration.

1.2 The Extraction Method and Components of DC

1.2.1 Components of DC

Collagen is a protein that accounts for 25–35% of the total protein in the human body. To date, about 29 types of collagen have been found [27, 30, 31]. Collagen has various types of α -chains depending on the type of protein in the connective tissue. And a large type of collagen is formed by a combination of these. Type I collagen is 30 nm in length and 1.5 nm in diameter. It is composed of about 1000 amino acids and has a triple helix structure (two α 1-chain and one α 2-chain) [32, 33]. In addition, type I collagen accounts for 90% of human collagen and is reported to be found in skin, bones, ligatures, vascular, connective tissue, etc. [34–36].

Kim and Ko et al. reported the molecular weight of DC by sodium dodecyl sulfate-

polyacrylamide gel electrophoresis (SDS-PAGE) and found two α -chains (α 1, α 2) with molecular weight ranging from 110 to 130 kDa and one β -chain molecular weight of 235 kDa (as shown in Fig. 1.1a) [37–39]. It was confirmed that the DC is same as the composition of type I collagen, and it has almost similar molecular weight as compared with commercially available porcine collagen (PC, Sewon Cellontech Co., Ltd.) and collagen from rat tail (Sigma-Aldrich, USA).

As a result of FTIR measurement, amide A peak was observed at 3300 cm^{-1} , together with amide B at 2876 cm^{-1} , amide I at 1634 cm^{-1} , amide II at 1544 cm^{-1} , and amide III at 1236 cm^{-1} , respectively. As a result, it was confirmed that similar peaks were also observed with PC (Fig. 1.1b). In addition, SIS and DBP analysis showed a similar peak as reported in Cha's study [40].

In addition, Sewon Cellontech Co., Ltd. conducted a test analysis based on ASTM F2212–11 (Standard guide for characterization of type I collagen as starting material for surgical implants and substrates for tissue-engineered medical products) for the characterization of a prototype of DC as shown in Table 1.1.

Based on these results, the collagen derived from flippers is expected to have a positive effect

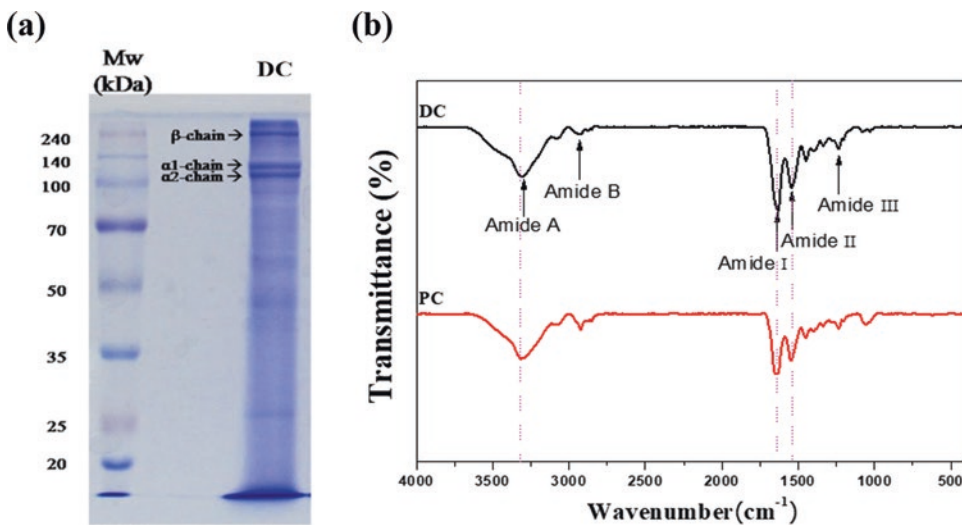
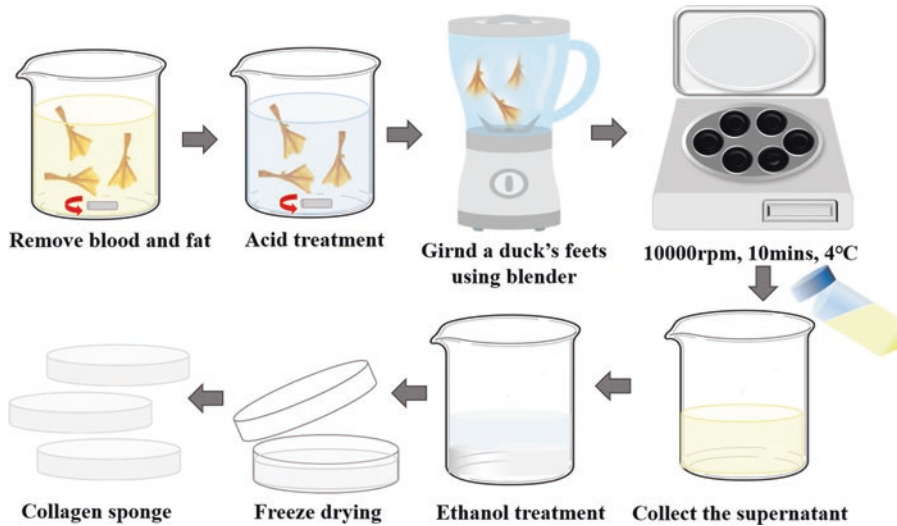


Fig. 1.1 (a) SDS-page of DC [37] and (b) FT-IR spectra of DC and PC (original data, not published)

Table 1.1 Component analysis of prototype DC of Sewon Cellontech

Type I collagen	Type III collagen	Lipid	Glycosaminoglycan	Elastin	Inorganic
Over 97.0%	2.0%	0.0%	0.0085%	0.0168%	0.00%

**Fig. 1.2** Schematic process of the extraction of the duck's feet collagen

on bone reconstruction and regeneration, as the major constituent is composed of type I collagen.

1.2.2 Extraction of DC

DC is extracted using the method followed by Song et al. [39, 40] (Fig. 1.2). Firstly, duck's feet were washed with distilled water. To remove blood from the flippers, they were cut using a blade and immersed in 70% alcohol for 3 h. Then, they are immersed into 0.5 M NaOH solution for 24 h to remove fat from tissue and followed by washing with methanol and chloroform solution in 3:1 ratio, acetone, alcohol, and distilled water, respectively. The duck's feet were stirred in 5% citric acid for 24 h. Then the mixture was crushed in a blender and mixed with 3 g pepsin for 48 h. After removal of a precipitate, the supernatant was collected and centrifuged at 12,000 rpm for 15 min. The precipitated collagen was treated with alcohol and centrifuged at 3500 rpm for 5 min. Subsequently, precipitated collagen was lyophilized.

1.3 Scaffolds Based on DC

1.3.1 Characteristics and Immunological Responses of Scaffolds Based on DC

First, physical properties and inflammatory response according to the type of DC scaffolds are evaluated. The scaffolds are prepared in different forms such as gel and fiber with the different manufacturing method including freeze-drying to lyophilize the solution, solvent casting, particulate leaching, phase separation, gas foaming, electrospinning, etc., [41–44]. Table 1.2 summarizes the different scaffold prepared and studied using DC till date. DC-related studies were mainly applied to skin and bone regeneration.

The research data from the articles in Table 1.2 shows the result of DC physical properties analysis; DC sponge showed compressive strength of 0.04~2 MPa, the pore size of 283~295 μm , and porosity between 52 and 87%. In addition, the

Table 1.2 Various forms of DC scaffold fabrication and their application

Form	polymers	Fabrication techniques	Cross-linking agent	Cell	Target tissue	Refs.
Sponge	DC	Freeze-drying	0.25% glutaraldehyde for 4 h, 0.1 M glycine for 24 h	RAW 264.7, NIH/3 T3	Skin	[40]
Sponge	DC/silk	Freeze-drying	0.3 w/v% Genipin for 24 h	NIH3T3	Skin	[37]
Hydrogel	DC/PVA	Freeze-thawing	–	NIH3T3	Skin	[45]
Sponge	DC/silymarin, hydroxyapatite (HAp)	Freeze-drying	0.25% glutaraldehyde for 4 h, 0.1 M glycine for 24 h	rBMSC	Bone	[46]
Sponge	DC/epigallocatechin gallate (EGCG)/HAp	Freeze-drying	0.25% glutaraldehyde for 4 h, 0.1 M glycine for 24 h	rBMSC	Bone	[47]
Sponge	DC/demineralized bone particles (DBP)	Freeze-drying	0.25% glutaraldehyde for 4 h, 0.1 M glycine for 24 h	rBMSC	Bone	[48]
Scaffold	DC/PLGA	Particulate leaching	–	RAW 264.7, NIH3T3, rBMSC	Bone	[39, 49, 50]

compressive strength of DC/HAp sponge, which is widely used for bone regeneration, was observed to be 0.14–3.5 MPa higher than that of DC sponge, whereas the pore size and porosity were decreased. This change was due to more attachment of HAp to the porous wall as the HAp penetrates between the pores in the collagen sponge when soaking them in the simulated body fluid (SBF) solution.

Kim et al., studied the production of reactive oxygen species (ROS) through flow cytometry analysis (FACS) to analyze the inflammatory response of DC/PLGA scaffolds prepared in different combination (0, 10, 20, 40, and 80 DC/PLGA) [50]. As a result, the 80 DC/PLGA group containing the maximum amount of DC was the closest to the negative control TCP, and with the weakest fluorescence intensity measurement (Fig. 1.3a). In addition, RT-PCR confirmed the expression of tumor necrosis factor- α (TNF- α), an inflammatory cytokine that was markedly decreased TNF- α expression in the 80 DC/PLGA scaffold with a high DC content (Fig. 1.3b). The inflammatory response of gellan gum (GG) and DC/GG sponge was confirmed by Song et al.; as a result, the expression of TNF- α , COX-2, and IL-1 β was observed to be lower in the DC/GG

sponge, and the number of ED-1-positive cells in DC/GG sponge was significantly decreased even in the immunochemical ED-1 staining [51]. These results are consistent with the conclusion that collagen and DC help in reducing inflammation [52–54].

1.3.2 Application of Scaffolds Based on Duck's Feet-Derived Collagen for Bone Regeneration

We prepared 2% DC and 2% PC sponge using DC prototypes (Sewon Cellontech Co., Ltd), and commercially available porcine collagen (PC, Sewon Cellontech Co., Ltd). Physiochemical characteristics, cell proliferation, ALP analysis, and animal experiments were compared. As a result of observing cell proliferation on the seventh day after seeding rabbit bone marrow stem cells (rBMSC) into a sponge, cell viability was high in DC and PC, similar with time (Fig. 1.4a) In order to confirm the degree of bone differentiation, ALP activity analysis showed that the PC sponge activity was more than DC sponge. Figure 1.4b shows that the difference is insignifi-

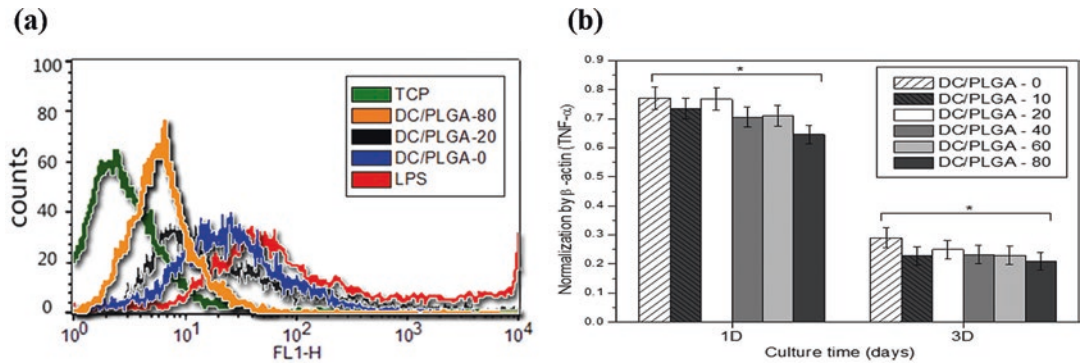


Fig. 1.3 Antioxidant and anti-inflammatory activity of DC/PLGA. (a) The flow cytometry analysis and (b) gene expression of TNF- α [50]

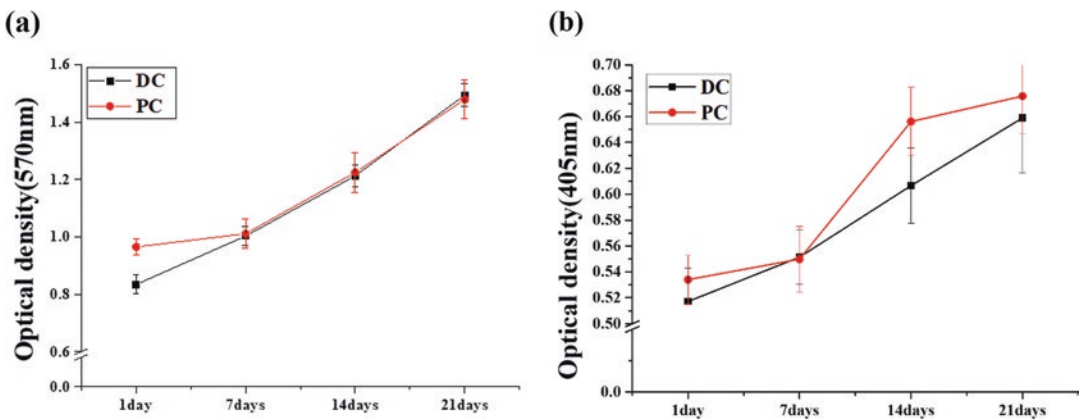


Fig. 1.4 Evaluation of rBMSCs proliferation through MTT assay (a) and ALP activity (b) on DC and PC sponges after 1, 7, 14, 21, and 28 days

cant. This demonstrates the feasibility of commercialization of DC as a prototype for the bone regeneration ability compared with PC, which is already a commercial product.

However, many studies have reported that the addition of polymers and biomolecules to DC can more effectively increase the mechanical properties and bone regeneration ability of these DC-based scaffolds. Therefore, in order to reinforce the mechanical properties of the fabricated DC sponge, studies using a HAp coating or a polymer blend along with bioactive molecules for enhancing bone conduction and induction were examined.

Kuk et al. evaluated the osteogenic effect of DC/PLGA scaffolds by adding DC (0, 10, 20, 40,

60, 80% of PLGA weight) to the PLGA solution [39]. The compressive strength of the PLGA scaffolds was about 4.4 Mpa, while the compressive strength was observed to be decreased as the content of DC increased. However, when the BMSC was seeded on the scaffolds, the higher the content of DC, the compressive strength increased with biocompatibility. It was reported that, as BMSC proliferated, the compressive strength increased due to the formation of ECM and mineral deposition. The MTT measurement showed that the proliferation of BMSCs was increased with time in the 80% DC/PLGA scaffold, and the ALP activity was also increasing with time in the 80% DC/PLGA scaffold. In addition, after subcutaneous implantation of the

scaffold in the nude mouse for 1 and 4 weeks, cytoplasm formation and osteogenesis were evaluated by H&E and von Kossa staining. As time increased in the 80% DC/PLGA group, mineral deposits were observed to be more active than the other groups.

Song et al., supported the *in vivo* study of bone regeneration effects of 80% DC/PLGA [49]. As a result, bone regeneration was observed in the order of blank, PLGA, PLGA + BMSC, 80 DC/PLGA, and 80 DC/PLGA + BMSC. In particular, it was confirmed that the DC/PLGA scaffold was superior to the PLGA scaffold. This is because type 1 collagen, a component of DC, promotes osteoblast differentiation and accelerates bone formation. Also, epigallocatechin gallate (EGCG), quercetin (Qtn), and silymarin (Smn) belonging to the group of flavonoid have been reported to help bone growth with their antioxidant and anti-inflammatory effects [55].

Kook et al. reported that EGCG, which is abundant in green tea, binds to tricalcium phosphate (TCP) particles and stimulates bone regeneration by increasing human osteoblast growth and mineralization in bone nodules [56]. After seeding the BMSCs in the sponge, cell proliferation and ALP activity were examined. As a result, the DC/HAp sponge had a higher cell proliferation rate and ALP activity at all the time points. However, the 1, 5 μM EGCG/DC/HAp sponge group containing EGCG showed better cell proliferation and ALP activity than the DC/HAp group. In addition, scaffolds were transplanted into nude mouse subcutaneously, H&E and von Kossa staining were performed. As a result, it was confirmed that calcium deposition was increased in 5 μM EGCG/DC/HAp sponge group with an increase in bone mineralization.

Qtn reduces the activity of osteoclasts and inhibits bone resorption. It is reported that Qtn affects the growth and development of osteoblasts, increases osteoblastic differentiation, effectively promotes bone differentiation in stem cells, and enhances the function of differentiated osteoblasts [57, 58].

Song et al. reported that among all the prepared sponges in different concentration (0, 25, 50, and 100 μM Qtn/DC/HAp), the cell prolifera-

tion rate, ALP activity, and Col I, OCN, and RUNX2 gene expression were observed to be higher in the 25 μM Qtn/DC/HAp sponge. This is because the Qtn acts as an inhibitor to inhibit cell proliferation. Therefore, it is described that when the concentration exceeds a certain level, the cell proliferation rate is lowered, and a 25 μM Qtn/DC/HAp sponge seeded with BMSC cells is added to the skull defect model; after transplantation, micro-CT and histologic examinations were performed and confirmed that bone mineralization increased significantly at 8 weeks. (Fig. 1.5).

Smn is known to be effective in bone fracture and osteoporosis treatment by controlling bone formation, as well as liver function improvement and antioxidant and anti-inflammatory effects [60]. Song et al. reported that 0, 25, 50, and 100 μM Smn/DC/HAp sponges were fabricated and cell proliferation and ALP activity of BMSCs seeded on sponges were observed to be increased as the concentration of smn increased [46]. In addition, since the expression of Col I and OCN were higher in the 100 μM Smn/DC/HAp sponge that may be due to Smn. Micro-CT and histological staining also showed higher bone mineralization in the 100 μM Smn/DC/HAp group than in the blank and DC/HAp groups, thus supporting this result (Fig. 1.6).

1.4 Conclusions

In this review, we have summarized the extraction method, the constituents of DC, and bone regeneration studies of DC-based scaffolds by mixing DC with bioactive molecules and polymers. The results of *in vitro* and *in vivo* evaluations showed that DC sponge alone exerts excellent effects on bone differentiation and regeneration. However, it was confirmed that the mixing of HAp, bioactive molecules, and polymers improves mechanical properties and promotes bone formation. This is because when HAp binds to DC sponge rich in type 1 collagen, which accounts for most of the extracellular matrix of bone, it is reconstituted with the bone matrix as minerals are deposited. In addition, bioactive molecules promote cell attachment,

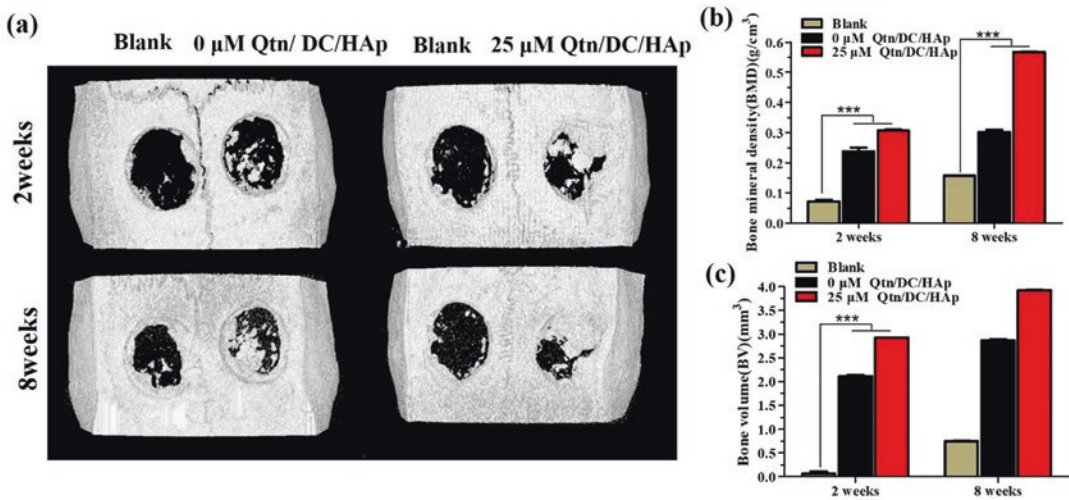


Fig. 1.5 SD-Rat cranial bone regeneration after implantation at 2 and 8 weeks: (a) Micro-CT images and (b) Bone mineral density (BMD) and (c) Bone volume (BV) [59]

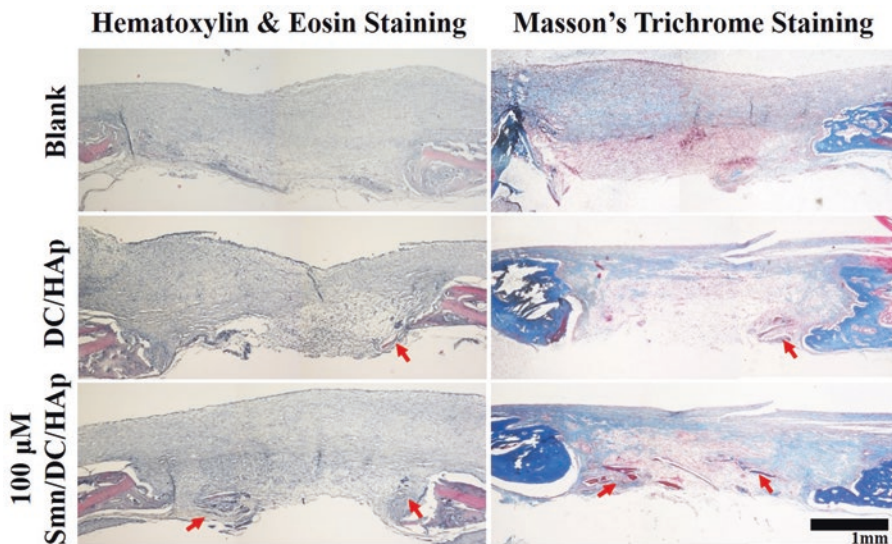


Fig. 1.6 Histological analysis of rat calvarial defects implanted with DC/HAp and Smn/DC/HA sponges after 8 weeks of implantation. H&E and MTS staining of the explant cross-section (Magnification = ×40, scale bar = 1 mm) [42]

proliferation, and bone differentiation. Thus, DC-based scaffolds are suitable as bone graft material because they provide an excellent environment for the bone grafting. In addition, it can be produced in the form of a hydrogel such as bio-ink, and it can be applied not only to bone graft materials but also to other organ regeneration.

Acknowledgments This research was supported by a grant of the Korea Health Technology R&D Project through the Korea Health Industry Development Institute (KHIDI), funded by the Ministry of Health & Welfare, Republic of Korea (HI15C2996) and the International Research & Development Program of the National Research Foundation of Korea (NRF) funded by the Ministry of Science, ICT & Future Planning (NRF-2017K1A3A7A03089427).

References

1. Tang D, Tare RS, Yang LY et al (2016) Biofabrication of bone tissue: approaches, challenges and translation for bone regeneration. *Biomaterials* 83:363–382
2. El-Rashidy AA, Roether JA, Harhaus L et al (2017) Regenerating bone with bioactive glass scaffolds: a review of in vivo studies in bone defect models. *Acta Biomater* 62:1–28
3. Oryan A, Kamali A, Moshiri A et al (2018) Chemical crosslinking of biopolymeric scaffolds: current knowledge and future directions of crosslinked engineered bone scaffolds. *Int J Biol Macromol* 107(Pt A):678–688
4. Lopes D, Martins-Cruz C, Oliveira MB et al (2018) Bone physiology as inspiration for tissue regenerative therapies. *Biomaterials* 185:240–275
5. Almubarak S, Nethercott H, Freeberg M et al (2016) Tissue engineering strategies for promoting vascularized bone regeneration. *Bone* 83:197–209
6. Tiffany AS, Gray DL, Woods TJ et al (2019) The inclusion of zinc into mineralized collagen scaffolds for craniofacial bone repair applications. *Acta Biomater* 93:86–96
7. Ho-Shui-Ling A, Bolander J, Rustom LE et al (2018) Bone regeneration strategies: engineered scaffolds, bioactive molecules and stem cells current stage and future perspectives. *Biomaterials* 180:143–162
8. He B, Zhao JQ, Ou YS et al (2018) Biofunctionalized peptide nanofiber-based composite scaffolds for bone regeneration. *Mater Sci Eng C Mater Biol Appl* 90:728–738
9. Yoon SJ, Yoo Y, Nam SE et al (2018) The cocktail effect of BMP-2 and TGF-1 loaded in visible light-cured glycol chitosan hydrogels for the enhancement of bone formation in a rat tibial defect model. *Mar Drugs* 16(10)
10. Anita LJ, Sundareswari M, Ravichandran K et al (2019) Fabrication and characterization of porous scaffolds for bone replacements using gum tragacanth. *Mater Sci Eng C Mater Biol Appl* 96:487–495
11. Yang DH, Lee DW, Kwon YD et al (2015) Surface modification of titanium with hydroxyapatite-heparin-BMP-2 enhances the efficacy of bone formation and osseointegration in vitro and in vivo. *J Tissue Eng Regen Med* 9(9):1067–1077
12. Yang D, Xiao J, Wang B et al (2019) The immune reaction and degradation fate of scaffold in cartilage/bone tissue engineering. *Mater Sci Eng C Mater Biol Appl* 104:109927
13. Shin YM, Shin HJ, Yang DH et al (2017) Advanced capability of radially aligned fibrous scaffolds coated with polydopamine for guiding directional migration of human mesenchymal stem cells. *J Mater Chem B* 5(44):8725–8737
14. Rubaiya Y, Kumar T, Doble M (2015) Design of biocomposite materials for bone tissue regeneration. *Mater Sci Eng C Mater Biol Appl* 57:452–463
15. He XC, Fan XL, Feng WP et al (2018) Incorporation of microfibrillated cellulose into collagen-hydroxyapatite scaffold for bone tissue engineering. *Int J Biol Macromole* 115:385–392
16. Park HK, Joo W, Gu BK et al (2018) Collagen/poly(D,L-lactic-co-glycolic acid) composite fibrous scaffold prepared by independent nozzle control multi-electrospinning apparatus for dura repair. *J Ind Eng Chem* 66:430–437
17. Zhu CL, Pongkitwitton S, Qiu JC et al (2018) Design and fabrication of a hierarchically structured scaffold for tendon-to-bone repair. *Adv Mater* 30(16):e1707306
18. Khan AF, Saleem M, Afzal A et al (2014) Bioactive behavior of silicon substituted calcium phosphate based bioceramics for bone regeneration. *Mater Sci Eng C Mater Biol Appl* 35:245–252
19. Li H, Nie B, Zhang S et al (2019) Immobilization of type I collagen/hyaluronic acid multilayer coating on enoxacin loaded titania nanotubes for improved osteogenesis and osseointegration in ovariectomized rats. *Colloids Surf B Biointerfaces* 175:409–420
20. Maghdouri-White Y, Bowlin GL et al (2014) Mammary epithelial cell adhesion, viability, and infiltration on blended or coated silk fibroin-collagen type I electrospun scaffolds. *Mater Sci Eng C Mater Biol Appl* 43:37–44
21. Magri AMP, Fernandes KR, Assis L et al (2019) Incorporation of collagen and PLGA in bioactive glass: in vivo biological evaluation. *Int J Biol Macromol* 134:869–881
22. Babrnakova J, Pavlinakova V, Brtnikova J et al (2019) Synergistic effect of bovine platelet lysate and various polysaccharides on the biological properties of collagen-based scaffolds for tissue engineering: scaffold preparation, chemo-physical characterization, in vitro and ex ovo evaluation. *Mater Sci Eng C Mater Biol Appl* 100:236–246
23. Koo Y, Choi EJ, Lee JY et al (2018) 3D printed cell-laden collagen and hybrid scaffolds for in vivo articular cartilage tissue regeneration. *J Ind Eng Chem* 66:343–355
24. Liu X, Zheng C, Luo X et al (2019) Recent advances of collagen-based biomaterials: multi-hierarchical structure, modification and biomedical applications. *Mater Sci Eng C Mater Biol Appl* 99:1509–1522
25. Bhuimbar MV, Bhagwat PK, Dandge PB (2019) Extraction and characterization of acid soluble collagen from fish waste: development of collagen-chitosan blend as food packaging film. *J Environ Chem Eng* 7(2):102983
26. Breaud S, Nuroy P, Malbouyres M et al (2019) Fishing for collagen function: about development, regeneration and disease. *Semin Cell Dev Biol* 89:100–110
27. Sun L, Li B, Yao D et al (2018) Effects of cross-linking on mechanical, biological properties and biodegradation behavior of Nile tilapia skin collagen sponge as a biomedical material. *J Mech Behav Biomed Mater* 80:51–58

28. Sun L, Hou H, Li B et al (2017) Characterization of acid- and pepsin-soluble collagen extracted from the skin of Nile tilapia (*Oreochromis niloticus*). *Int J Biol Macromol* 99:8–14
29. Mosquera M, Gimenez B, da Silva IM et al (2014) Nanoencapsulation of an active peptidic fraction from sea bream scales collagen. *Food Chem* 156:144–150
30. Bazrafshan Z, Stylios GK (2019) Spinnability of collagen as a biomimetic material: a review. *Int J Biol Macromol* 129:693–705
31. Zhang D, Wu X, Chen J et al (2018) The development of collagen based composite scaffolds for bone regeneration. *Bioact Mater* 3(1):129–138
32. Ferreira AM, Gentile P, Chiono V et al (2012) Collagen for bone tissue regeneration. *Acta Biomater* 8(9):3191–3200
33. Yang S, Shi XX, Li XM et al (2019) Oriented collagen fiber membranes formed through counter-rotating extrusion and their application in tendon regeneration. *Biomaterials* 207:61–75
34. Kim YA, Tarahovsky YS, Gaidin SG et al (2017) Flavonoids determine the rate of fibrillogenesis and structure of collagen type I fibrils in vitro. *Int J Biol Macromol* 104(Pt A):631–637
35. McCoy MG, Seo BR, Choi S et al (2016) Collagen I hydrogel microstructure and composition conjointly regulate vascular network formation. *Acta Biomater* 44:200–208
36. Oliveira PN, Montebault A, Sudre G et al (2019) Self-crosslinked fibrous collagen/chitosan blends: processing, properties evaluation and monitoring of degradation by bi-fluorescence imaging. *Int J Biol Macromol* 131:353–367
37. Kim SH, Park HS, Lee OJ et al (2016) Fabrication of duck's feet collagen-silk hybrid biomaterial for tissue engineering. *Int J Biol Macromol* 85:442–445
38. Ko H, Kim H, Ha H (2012) Extraction of collagen from livestock waste of duck's foot and its application of scaffold materials for tissue engineering. *Int J Tissue Regen* 3:103–110
39. Kuk H, Kim HM, Kim SM et al (2015) Osteogenic effect of hybrid scaffolds composed of duck feet collagen and PLGA. *Polymer Korea* 39(6):846–851
40. Cha SR, Jeong HK, Kim SY et al (2015) Effect of duck's feet derived collagen sponge on skin regeneration: in vitro study. *Polymer Korea* 39(3):493–449
41. Dave K, Gomes VG (2019) Interactions at scaffold interfaces: effect of surface chemistry, structural attributes and bioaffinity. *Mater Sci Eng C Mater Biol Appl* 105:110078
42. Bhattacharjee P, Kundu B, Naskar D et al (2017) Silk scaffolds in bone tissue engineering: an overview. *Acta Biomater* 63:1–17
43. Soundarya SP, Menon AH, Chandran SV et al (2018) Bone tissue engineering: scaffold preparation using chitosan and other biomaterials with different design and fabrication techniques. *Int J Biol Macromol* 119:1228–1239
44. Moreno MAP, Vrech SM, Sanchez MA et al (2019) Advances in additive manufacturing for bone tissue engineering scaffolds. *Mater Sci Eng C Mater Biol Appl* 100:631–644
45. Song JE, Tripathy N, Shin JH et al (2016) Skin regeneration using duck's feet derived collagen and poly (vinyl alcohol) scaffold. *Macromol Res* 24(4):359–336
46. Song JE, Jeon YS, Tian J et al (2019) Evaluation of silymarin/duck's feet-derived collagen/hydroxyapatite sponges for bone tissue regeneration. *Mater Sci Eng C Mater Biol Appl* 97:347–355
47. Kook YJ, Tian J, Jeon YS et al (2018) Nature-derived epigallocatechin gallate/duck's feet collagen/hydroxyapatite composite sponges for enhanced bone tissue regeneration. *J Biomater Sci Polym E* 29(7–9):984–996
48. Cha JG, Cha SR, Lee DH et al (2016) Evaluation of osteogenesis on duck's feet derived collagen and demineralized bone particles sponges. *Polymer Korea* 40(6):858–864
49. Song JE, Tripathy N, Shin JH et al (2017) In vivo bone regeneration evaluation of duck's feet collagen/PLGA scaffolds in rat calvarial defect. *Macromol Res* 25(10):994–999
50. Kim SM, Kim HM, Kuk H et al (2015) Characterization and effect of inflammatory reaction of duck-feet derived collagen/poly(lactic-co-glycolide)(PLGA) hybrid scaffold. *Polym Korea* 39(6):837–845
51. Song JE, Lee SE, Cha SR et al (2016) Inflammatory response study of gellan gum impregnated duck's feet derived collagen sponges. *J Biomater Sci Polym Ed* 27(15):1495–1506
52. Zhao YL, Liu WW, Liu W et al (2018) Phorbol ester (PMA)-treated U937 cells cultured on type I collagen-coated dish express a lower production of pro-inflammatory cytokines through lowered ROS levels in parallel with cell aggregate formation. *Int Immunopharmacol* 55:158–164
53. Offengenden M, Chakrabarti S, Wu J (2018) Chicken collagen hydrolysates differentially mediate anti-inflammatory activity and type I collagen synthesis on human dermal fibroblasts. *Food Sci Hum Wellness* 7(2):138–147
54. Court M, Malier M, Millet A (2019) 3D type I collagen environment leads up to a reassessment of the classification of human macrophage polarizations. *Biomaterials* 208:98–109
55. Preethi SS, Sanjay V, Haritha MA et al (2018) Effects of flavonoids incorporated biological macromolecules based scaffolds in bone tissue engineering. *Int J Biol Macromol* 110:74–87
56. Chu C, Wang Y, Wang Y et al (2019) Evaluation of epigallocatechin-3-gallate (EGCG) modified collagen in guided bone regeneration (GBR) surgery and modulation of macrophage phenotype. *Mater Sci Eng C Mater Biol Appl* 99:73–82

57. Song JE, Tripathy N, Lee DH et al (2018) Quercetin inlaid silk fibroin/hydroxyapatite scaffold promotes enhanced osteogenesis. *ACS Appl Mater Interfaces* 10:32955–32964
58. Gupta SK, Kumar R, Mishra NC (2017) Influence of quercetin and nanohydroxyapatite modifications of decellularized goat-lung scaffold for bone regeneration. *Mater Sci Eng C Mater Biol Appl* 71:919–928
59. Song JE, Tian J, Kook YJ et al (2019) A BMSCs-laden quercetin/duck's feet collagen/hydroxyapatite sponge for enhanced bone regeneration. *J Biomed Mater Res A* 108:784–794
60. Ying XZ, Sun LJ, Chen XW et al (2013) Silibinin promotes osteoblast differentiation of human bone marrow stromal cells via bone morphogenetic protein signaling. *Eur J Pharmacol* 721(1–3):225–230



Decellularized Extracellular Matrices for Tissue Engineering and Regeneration

2

Fang Ge, Yuhe Lu, Qian Li, and Xing Zhang

Abstract

Decellularized extracellular matrices (dECMs) from mammalian tissues and organs are particularly interesting as scaffolds for tissue engineering and regeneration when considering their ability to retain chemical compositions and three-dimensional (3D) microstructures that are similar to native ECMs. This review discusses the advantages and disadvantages of different decellularization methods that use various agents, such as ionic and nonionic detergents and biological enzymes. The applications of dECMs as scaffolds or hydrogels for tissue engineering of specific tissues including heart valves, blood vessels, and skin, as well as their performance in vitro and in vivo, are also discussed. In addition, whole organ regeneration (i.e., the

heart, kidney, liver) using dECM scaffolds has been explored, which are able to recapitulate partial functions of native organs.

Keywords

Decellularization · Recellularization · Extracellular matrices · Microstructure · Tissue engineering · Organ regeneration

Authors Fang Ge and Yuhe Lu have equally contributed to this chapter.

F. Ge · Q. Li
Institute of Metal Research, Chinese Academy of Sciences, Shenyang, Liaoning, China

Department of Chemistry, Northeastern University, Shenyang, Liaoning, China

Y. Lu
Institute of Metal Research, Chinese Academy of Sciences, Shenyang, Liaoning, China

School of Materials Science and Engineering, Northeastern University, Shenyang, Liaoning, China

2.1 Introduction

The replacement of damaged organs and tissues with artificial grafts has been widely performed to cure end-stage organ failure [1–7]. Because of a severe shortage of donated organs and complications that are associated after organ replacement, such as thromboembolism [4, 6, 8] and calcification [9], new strategies are needed for tissue repair and regeneration, including tissue engineering [6, 9, 10] and cell therapy [11]. Various materials, including natural [7, 12–15] and synthetic [8, 16–18] materials, have been

X. Zhang (✉)
Institute of Metal Research, Chinese Academy of Sciences, Shenyang, Liaoning, China

School of Materials Science and Engineering, University of Science and Technology of China, Hefei, Anhui, China
e-mail: xingzhang@imr.ac.cn

explored as scaffolds for tissue engineering and cell delivery. Among these scaffolds, decellularized extracellular matrices (dECMs) from mammalian tissues and organs are particularly interesting when considering their ability to retain chemical compositions and three-dimensional (3D) microstructures that are similar to native ECMs.

Extracellular matrices are native scaffolds for cells in different tissues and organs, comprising a complex mixture of fibrous proteins, such as collagen, elastin, proteoglycans (PGs), and glycosaminoglycans (GAGs) [19]. Extracellular matrices also serve as a reservoir of essential growth factors and signaling molecules. Extracellular matrices that are derived from tissues and organs can preserve native microstructures and compositions, such as proteins, growth factors, and GAGs, which is difficult to achieve with synthetic materials. Additionally, dECMs can be used as hydrogels that allow the delivery of cells, growth factors, and drugs to many sites of interest [20], including irregularly shaped anatomical sites [21], using minimally invasive methods. Notably, ECM structures and components can be damaged by the method of decellularization that is adopted [1, 22]. Extracellular matrix decellularization should preserve the ultrastructure and composition while completely removing resident cells.

The present review discusses the advantages and disadvantages of different decellularization methods that use various agents, such as ionic and nonionic detergents and biological enzymes. The applications of dECMs as scaffolds or hydrogels and their performance *in vitro* and *in vivo* are also discussed from the perspective of specific organs and tissues.

2.2 Decellularization Methods

Cellular components of different tissues (e.g., heart valves, the dermis, the small intestine, etc.) and organs (e.g., the heart, liver, kidney, etc.) can be removed from their ECMs using various methods, including mechanical methods (i.e., freezing-thawing), chemical treatment (e.g.,

ionic or nonionic detergents and hyper- or hypotonic solutions), and enzymatic treatment (e.g., trypsin, DNase, and RNase). These methods are discussed in detail below.

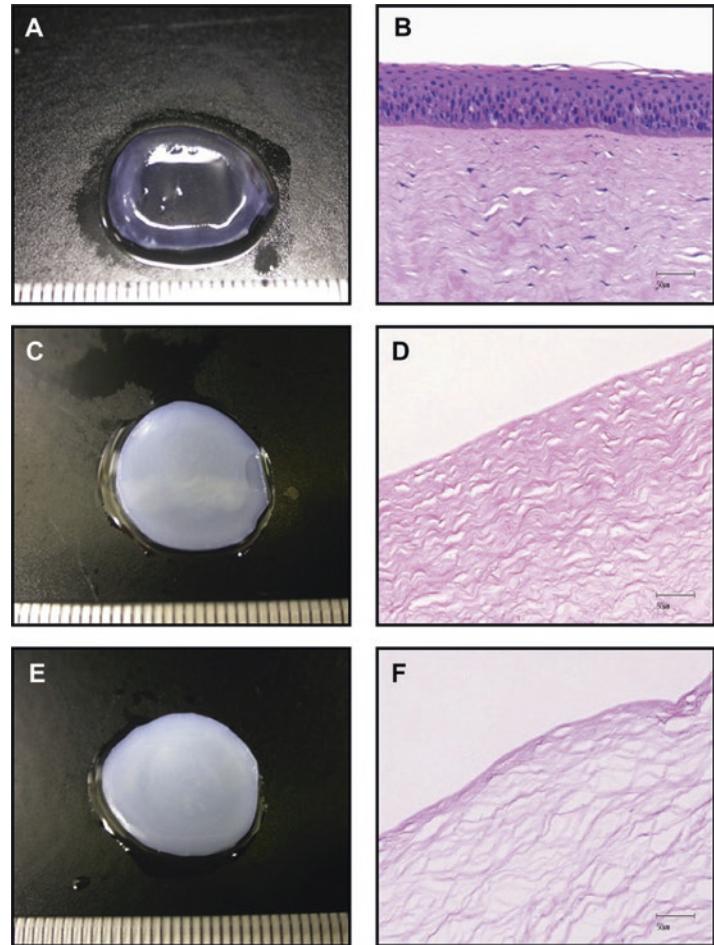
2.2.1 Physical Methods

Physical methods include non-thermal irreversible electroporation, hydrostatic pressurization, mechanical stirring, and snap freezing, which can be used to dissociate tissue components and facilitate tissue decellularization. For example, non-thermal irreversible electroporation (NTIRE) pulsed electrical fields can be used to cause nanoscale irreversible damage to the cell membrane for decellularization of living tissues [23]. Electrode clamps were applied close to rat carotid artery's bifurcation. An electric field of about 1750 V/cm, 100 μ s each, and a frequency of 1 Hz or 4 Hz were applied between the electrodes, which can efficiently ablate cells from the rat carotid artery. Compared with the control, NTIRE resulted in an artery that was largely decellularized 3 days posttreatment. After 5 days, histological analysis showed that the Vascular smooth muscle cells (VSMCs) were almost completely ablated when treated with NTIRE.

High-hydrostatic pressurization has been applied to prepare decellularized porcine cornea [24]. Porcine corneas were pressurized at 980 MPa at 10 °C or 30 °C for 10 min, which were further rinsed with an EGM-2 medium containing 3.5% w/v dextran for 72 h. Translucent corneas were obtained (Fig. 2.1c, e) after complete removal of the epithelial layer and stromal cells observed through HE staining (Fig. 2.1d, f). The superstructure of collagen fibrils can be retained in the sample treated with the pressurization at 980 MPa at 10 °C (Fig. 2.1d), while the collagen fibrils were slightly loosened in the sample with the pressurization at 980 MPa at 30 °C (Fig. 2.1f).

However, these physical methods are mainly used to disrupt cell membranes and inner structures. The complete removal of cells is difficult when using only these methods, unless they are combined with chemical or enzyme treatment.

Fig. 2.1 Representative images and HE staining of native cornea (a), (b) and corneas decellularized by high-hydrostatic pressurization. The corneas were pressurized for 10 minutes at 980 MPa, 10 °C (c), (d), 980 MPa, 30 °C (e), (f). Scale bars = 50 μ m. (Reprinted with permission from Elsevier [24])



2.2.2 Chemical Treatment

2.2.2.1 Detergents

Ionic and nonionic detergents have been commonly used for decellularization, which have presented different effects on ECM ultrastructures. Sodium dodecyl sulfate (SDS) and sodium deoxycholate (SDC) are the most widely used ionic detergents for decellularization. Porcine pulmonary leaflets can be decellularized by either 1% SDC or SDS in phosphate-buffered saline (PBS) at 37 °C for 24 h, resulting in the complete removal of cells. Sodium dodecyl sulfate treatment of valve leaflets almost completely retained collagen and elastin structures. In SDS-treated leaflets, elastic fibers become compact and micro-curved, whereas the appearance of collagen fibers is compact with an obvious loss of

structural details. Both of these decellularization protocols were shown to affect the human immunological response and increase thrombogenicity [25]. One disadvantage of SDS and SDC for decellularization, however, is residual detergents that remained in the ECM fibers after the process, which may cause toxicity to the host of these implants. Sodium dodecyl sulfate may cause greater disruption to native tissue structures because of the removal of GAGs and disruption of the collagen triple helix structure and elastin network. In one study, rat aortic conduit grafts were decellularized with four 12-h cycles with 0.5% SDS + 0.5% SDC, followed by thorough rinsing with distilled water and PBS. Decellularized aortic conduits were further surface-coated with fibronectin, which induced medial graft repopulation in the absence of an

inflammatory reaction or adverse gene expression when implanted into the systemic circulation in Wistar rats for up to 8 weeks [26].

Compared with ionic detergents, nonionic detergents, such as Triton X-100 and octyl-glucopyranoside (OGP), may cause the greater disruption of DNA-protein, lipid-lipid, and lipid-protein interactions and to a lesser degree protein-protein interactions, which may protect collagen from disruption. Porcine aortic valve leaflets were decellularized using 1% Triton X-100. The overall extensibility that is represented by areal strain at 60 N/m increased from 68.85% for native leaflets to 177.69% for decellularized leaflets. Effective flexural moduli decreased from 156.07 ± 24.6 kPa for native leaflets to 19.4 ± 8.9 kPa for decellularized leaflets. These results showed that decellularization with Triton X-100 resulted in substantial microscopic disruption, although the overall leaflet fiber architecture remained relatively unchanged. A novel nonionic detergent, OGP, was employed for the decellularization of porcine pericardium, which removed cells completely while preserving most ECM components and slightly decreasing GAG content [27]. Octyl-glucopyranoside presented advantages of high biodegradability, low irritation, and low toxicity. Porcine pericardium decellularization using environmentally friendly OGP resulted in similar mechanical properties to native specimens and lower toxicity compared with specimens that were decellularized by SDS treatment.

Ionic and nonionic detergents can also be combined for tissue decellularization. For example, porcine pulmonary valve conduits were decellularized using a mixture solution of 0.05% SDC and 0.05% Triton X-100 under continuous shaking for 48 h at 4 °C, which successfully preserved the structural integrity of ECMs [28]. Therefore, the types and amounts of detergents play significant roles in tissue decellularization. These factors can affect ECM compositions, ultrastructures, and mechanical properties.

2.2.2.2 Other Chemical Agents

Other chemical agents, including hypertonic and hypotonic solutions, acids, bases, alcohols, and

other solvents, have also been used for the decellularization of tissues and organs. For example, bovine vocal fold samples were decellularized by first treating them with highly hypertonic 3 M sodium chloride solution for 24 h followed by isotonic PBS solution for 24 h, resulting in the large osmotic influx of water, which broke down cell membranes. The cells were further subjected to a cycle of osmotic stress by incubation in 70% ethyl alcohol for 24 h followed by isotonic PBS solution for 48 h [10].

A supercritical carbon dioxide and ethanol co-solvent (scCO₂-EtOH) was developed to decellularize rat heart tissues for 6 h, which prevented ECM structure disruption and retained various angiogenic proteins in the dECMs compared with a detergent group that underwent a general decellularization method with 1% SDS for 14 h and 1% Triton X-100 for 30 min [29]. The dECMs powder was used to prepare hydrogels, which were subcutaneously injected in rats to estimate the effect of angiogenesis. Mature blood vessels were formed with more von Willebrand factor (vWF) and α -smooth muscle actin (α SMA)-positive regions in the scCO₂-EtOH group than in the detergent group, indicating the advantage of retaining angiogenic proteins in the dECMs using the novel supercritical co-solvent method.

2.2.3 Enzyme Treatment

Trypsin, collagenases, and nucleases (DNase and RNase) are enzymes that are typically used for decellularization. Trypsin is a highly specific enzyme that can cleave peptide bonds on the C-side of arginine (Arg) and lysine (Lys) and dissolve ECM constituents, such as collagen, laminin, fibronectin, elastin, and GAGs, thus disrupting ECM microstructures. Ethylenediaminetetraacetic acid (EDTA) and ethyleneglycoltetraacetic acid (EGTA) are chelating agents and protease inhibitors that are typically used in combination with trypsin to prevent the breakdown of collagen and elastin from the matrix structure when trypsin is used for cell dissociation. For example, rat hearts can be

perfused with 0.025% trypsin and 0.05% EDTA in PBS at 37 °C for 1 h, followed by 15 min with deionized water, 1 h with 3% Triton X-100 in deionized water, 15 min with deionized water only, 1 h with 4% deoxycholic acid in deionized water, 15 min with deionized water, and 1 h with 0.1% acetic acid in deionized water [30]. Moreover, DNase and RNase can be used to remove cell residues, especially DNA and RNA, thus reducing the risk of immune responses [28].

2.2.4 Combined Agents

Decellularization agents and their concentrations are crucially important to obtain cell-free, biocompatible ECM scaffolds while minimizing the disruption of ECM ultrastructures. As mentioned above, different agents have different effects on the microstructural and mechanical properties of ECMs [31]. Considering complex compositions and unique structures, the decellularization of tissues and organs is generally performed using multiple agents rather than any one agent alone [25, 30]. For example, cells were completely removed from porcine aortic valves using a detergent-enzyme digestion method. Treatment with a 0.05% trypsin solution with 0.02% EDTA, followed by a 1% SDC solution, resulted in the disruption of ECM fiber structures of aortic valves. Treatment with a 0.25% Triton X-100 solution, followed by a 0.25% SDC solution, preserved fibrous structures after decellularization.

Adult porcine tracheal matrices were processed in distilled water for 72 h at 4 °C, 4% SDC for 4 h, and 2000 kU DNase-I in 1 M NaCl for 3 h to eliminate cells. After 18 cycles of treatment, epithelial cells disappeared, but chondrocytes were still visible. Additional treatment cycles achieved completely decellularized tissue, but the structure of the trachea was disrupted [32]. Conconi et al. used this same method to harvest matrix from rat muscle material and then culture myoblasts as a promising tool for abdominal-wall repair [33].

A perfusion technique was recently employed for whole-organ decellularization. Theodoridis et al. decellularized porcine hearts by pulsatile

retrograde aortic perfusion to generate cardiac ECMs [34]. Various procedures using sequential treatment with different agents have been explored for the optimal decellularization of different organs [1] to ensure that biological scaffold material is safe for subsequent implantation [22].

Thus, the decellularization process can be used to preserve ECM components and 3D structures, decrease the risk of an immune response, and enhance anticalcification. Considering the different effects of various agents, optimal decellularization procedures need to be designed based on the composition and microstructure of individual tissues.

2.3 Characterization of Decellularized Extracellular Matrices

Histological staining was performed to detect cell removal and ECM structural integrity after decellularization. Hematoxylin-eosin staining was used to examine remaining cells after the decellularization of porcine pulmonary valves using trypsin-EDTA treatment. Observations of their morphology confirmed the complete removal of cellular components without disrupting ECMs [35]. Moreover, mechanical properties of samples before and after decellularization can be measured. For example, porcine pericardium samples that were decellularized by OGP presented an elastic modulus (58.49 ± 3.66 MPa) that was lower than native tissue samples (76.59 ± 10.34 MPa) but higher than samples that were decellularized by SDS (37.16 ± 5.49 MPa) and Triton X-100 (50.95 ± 5.49 MPa). Moreover, the ultimate tensile strength of dECM samples treated with OGP was 13.46 ± 0.55 MPa, close to that from native tissue (14.36 ± 0.82 MPa), significantly higher than that from the SDS group (8.41 ± 1.78 MPa) and Triton X-100 group (8.02 ± 1.78 MPa) [27].

The immunogenic response is a major concern for the application of dECMs. Both in vitro and in vivo immunogenicity assessments of dECM samples have been developed. For in vitro

tests, specific antibodies or antigens are used to characterize residual materials. For *in vivo* tests, dECM samples can be implanted into experimental animals for a specific period of time (usually 6–8 weeks). Interactions between cells and ECM scaffolds have been studied to evaluate the body's possible rejection or other acute responses to the ECM [36], generally by detecting immunoglobulin G (IgG) and IgM antibodies and T lymphocytes. The host's immune response to implanted ECM scaffolds has been partially characterized, but the true pathophysiological responses are still not fully understood [13].

Despite much effort, Simon et al. reported the death of three pediatric patients in clinical trials of decellularized porcine valve implants that induced inflammatory reactions, followed by the lymphocyte response and scaffold degeneration [37]. Another study evaluated immune responses in patients who received a bioprosthetic heart valve. Residual cells expressed α -Gal, which was considered the major reason for the rejection and failure of transported heart valves [9]. Therefore, the complete decellularization and removal of toxic agents are key to eliminating the immune response.

2.4 ECM Hydrogels

Decellularized ECMs (dECMs) that are derived from allogeneic or xenogeneic tissues possess ideal performance with regard to biocompatibility and bioactivity and have been used as scaffolds for tissue repair and tissue regeneration. Decellularized ECMs have been fabricated into different forms, such as sheets, powders, and hydrogels, for particular applications [20, 21]. Hydrogels with 3D networks that are fabricated using dECMs have been widely used in cell culture and tissue engineering [38].

Lyophilized dECM powder that retains essential native proteins and GAGs can be used to prepare bioactive hydrogels, which can be used to fill injured and irregular sites in organs or tissues by single or multiple injections. Extracellular matrix scaffolds were minced into powders after decellularization, which could be digested using

an acidic pepsin solution. Extracellular matrix components in the above solution were then dialyzed for purification and lyophilized to form a powder mixture, which could be further dissolved to form hydrogels by temperature-induced and/or pH-induced gelation [39]. A previous study showed that GAGs play an important role in hydrogel formation besides structural proteins. Glycosaminoglycans connected to ECM proteins, especially larger structural proteins (e.g., type I collagen), thus conferring a gel-like consistency to the ECMs [13]. In addition, ECM hydrogels contain various mixtures of GAGs that can bind growth factors and cytokines and promote water retention.

The pH-induced gelation from ECM components that were extracted from adipose and dermal tissues was found to be faster than temperature-induced gelation [40]. The pH-induced hydrogels from dermis-derived ECMs had fiber radii of $\sim 32 \pm 15$ nm and pore sizes of $\sim 160 \pm 64$ nm, whereas temperature-induced hydrogels had larger fiber radii ($\sim 55 \pm 14$ nm) and larger pore sizes ($\sim 359 \pm 143$ nm). The ECM hydrogels from decellularized porcine myocardial tissues showed the ability to gel *in vitro* at 37 °C and *in vivo* upon injection into rat myocardium [39]. The re-assembled nanofibers were approximately 40–100 nm in diameter. Moreover, Matrigel (Corning Life Sciences) is extracted from the Engelbreth-Holm-Swarm (EHS) mouse sarcoma, a tumor rich in such ECM proteins as laminin (a major component), collagen IV, heparan sulfate proteoglycans, entactin/nidogen, and a number of growth factors [41]. Matrigel has been widely used for 2D and 3D cell culture *in vitro*, which can improve the attachment and differentiation of different cells by mimicking *in vivo* environments.

The biocompatibility and biofunctionality of various ECM hydrogels have been assessed *in vitro* and *in vivo*. Rat cardiomyocytes were able to adhere and survive on the myocardial matrix gel fabricated using decellularized porcine myocardial matrix, comparable to collagen gels [39]. To assess chemoattraction of the myocardial matrix, human coronary artery endothelial cells (hCAECs) and rat aortic smooth muscle

cells (rASMCs) were cultured on top of myocardial matrix gel and collagen gel, respectively. The comparable activity of cardiomyocytes was found in these two groups. hCAECs and rASMCs migrated better in the myocardial matrix group than in the collagen gel group. These results showed that the myocardial matrix gels were nontoxic and chemoattractive to these cells. For in vivo test, 90 ml myocardial matrix solution was injected into the left ventricular wall of rats. Fibrous structures were observed after injection for 30 minutes, indicating that the injected matrix solution accomplished the gelation in situ. No immune response was found after implantation for 4 and 11 days. Endothelial cells and smooth muscle cells were found to migrate toward the myocardial matrix, with a significant increase in arteriole formation after implantation for 11 days. Therefore, the decellularized myocardial matrix and resultant hydrogel were biocompatible and suitable as scaffolds for tissue regeneration.

The ECM hydrogels prepared from decellularized porcine dermis and urinary bladder tissues were used to evaluate cell response in vitro and in vivo [20]. Dermal ECM hydrogels supported greater C2C12 myoblast fusion in vitro and less fibroblast infiltration and less fibroblast-mediated hydrogel contraction than urinary bladder ECM hydrogels (Fig. 2.2). Host cells, primarily macrophages, that were implanted in a rat abdominal wall defect infiltrated into both hydrogels (8 mg/ml) within 3 days of implantation. These ECM hydrogels almost completely degraded 35 days after implantation, and the UBM hydrogel degraded faster than the dermal ECM hydrogel. The UBM hydrogel promoted myogenesis more than the dermal ECM hydrogel, likely because of larger amounts of GAGs in the former, and both hydrogels accelerated the remodeling of muscle tissue [20]. These results indicate that the biofunctionality of an ECM hydrogel can be altered and at least partially controlled by specific ECM components and concentrations.

A precious study demonstrated the feasibility of using genetically engineered animals to create decellularized biologic scaffolds with favorable ECM properties. When a powdered form of acel-

lular dermis from thrombospondin-2 (TSP-2) knockout (KO) animals was implanted subcutaneously, it was able to promote enhanced vascularization over wide type (WT) [42]. Tunable hydrogels were further derived from genetically engineered acellular dermis. The hydrogels exhibited tunable cell invasion with a correlation between the content of TSP-2 KO hydrogel and the extent of cell invasion, when injected subcutaneously into healthy mice. Additionally, TSP-2 KO hydrogels significantly improved wound healing when applied to full-thickness wounds in diabetic mice for 10 and 21 days (Fig. 2.3) [43]. Thus, genetic engineering approaches impart tunability to ECM hydrogels, which result in novel materials capable of enhanced regeneration.

Thus, previous studies demonstrate that ECM hydrogels that are prepared from decellularized tissues are biocompatible and able to facilitate tissue remodeling and regeneration. Different functionality among various ECM hydrogels may be caused by variations of chemical components and different gelation methods. Some problems that can occur with these ECM hydrogels include damage to bioactive molecules, such as GAGs, proteins, and laminin, during the purification process [21]. The mechanical strength of these ECM hydrogels is also relatively low because of contraction of the gel when interacted with cells.

2.5 Decellularized Scaffolds for Tissue Repair and Regeneration

Decellularized ECMs have been widely employed as biologic scaffolds for tissue engineering, such as arterial and heart valve grafts, and skin and urinary tract reconstitution [13].

2.5.1 Blood Vessels

Cardiovascular disease (CVD) [44, 45] and coronary artery disease [46] are primary causes of death in the human population. Various surgical

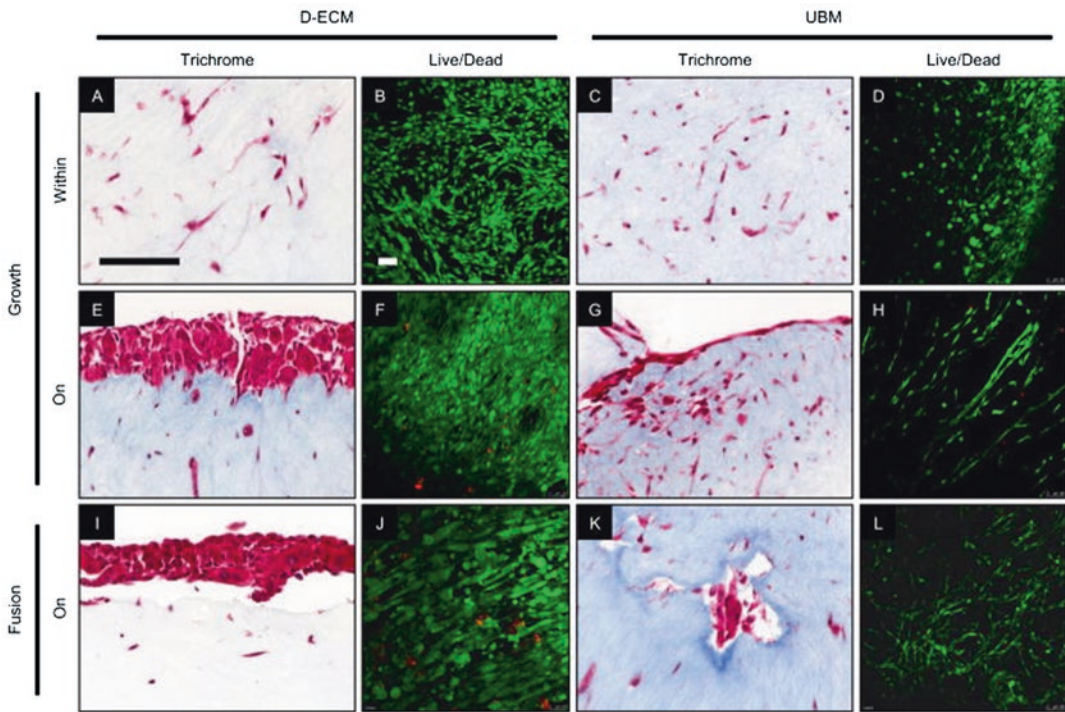


Fig. 2.2 Myogenic potential of ECM hydrogels in vitro. C2C12 myoblasts were cultured on the surface and within dermal ECM (D-ECM) and UBM hydrogels in growth and fusion conditions. Histologic analysis of Masson's Trichrome stained cross sections and Live/Dead staining

of the hydrogel surface for viable cells (green) and dead cell nuclei (red) were imaged with confocal microscopy. Scale bars = 100 μ m. (Reprinted with permission from Elsevier [20])

procedures and prostheses have been used to cure these diseases of blood vessels [5]. The replacement of damaged vessels has been performed since the 1950s. Many types of grafts have been implanted, including the transplantation of allogeneic, xenogeneic, and dECMs. Three-dimensional structures can be preserved, and such components as proteins and growth factors can be preserved by decellularization [44]. Both of these factors can reduce the incidence of an immune response when implanted in vivo [7].

Many decellularized approaches and ionic, nonionic, and enzymatic hydrolysis agents have been used to prepare dECMs as blood vessel grafts. Five different protocols utilizing the detergents sodium dodecyl sulfate (SDS), sodium deoxycholate (SDC), CHAPS, and Triton X-100 together with DNA-removing enzymes showed

similar efficacy for decellularization of porcine vena cava in a perfusion bioreactor setup [47]. However, Triton X-100 based protocols showed the greatest recellularization efficacy with Human Umbilical Vein Endothelial Cells (HUVECs) in vitro [47].

Intact human greater saphenous vein specimens were obtained by decellularization with 0.075% SDS. Luminal endothelial cells were completely removed, and 94% of cells were removed within the vessel wall. These results show that ECM basement membrane structures were well preserved, indicated by the immunohistochemical staining. Compared with fresh vein, decellularized vein showed similar in vitro burst pressure (2480 ± 470 vs 2380 ± 620 mmHg) and suture-holding strength (185 ± 30 vs 178 ± 66 gm) [44].

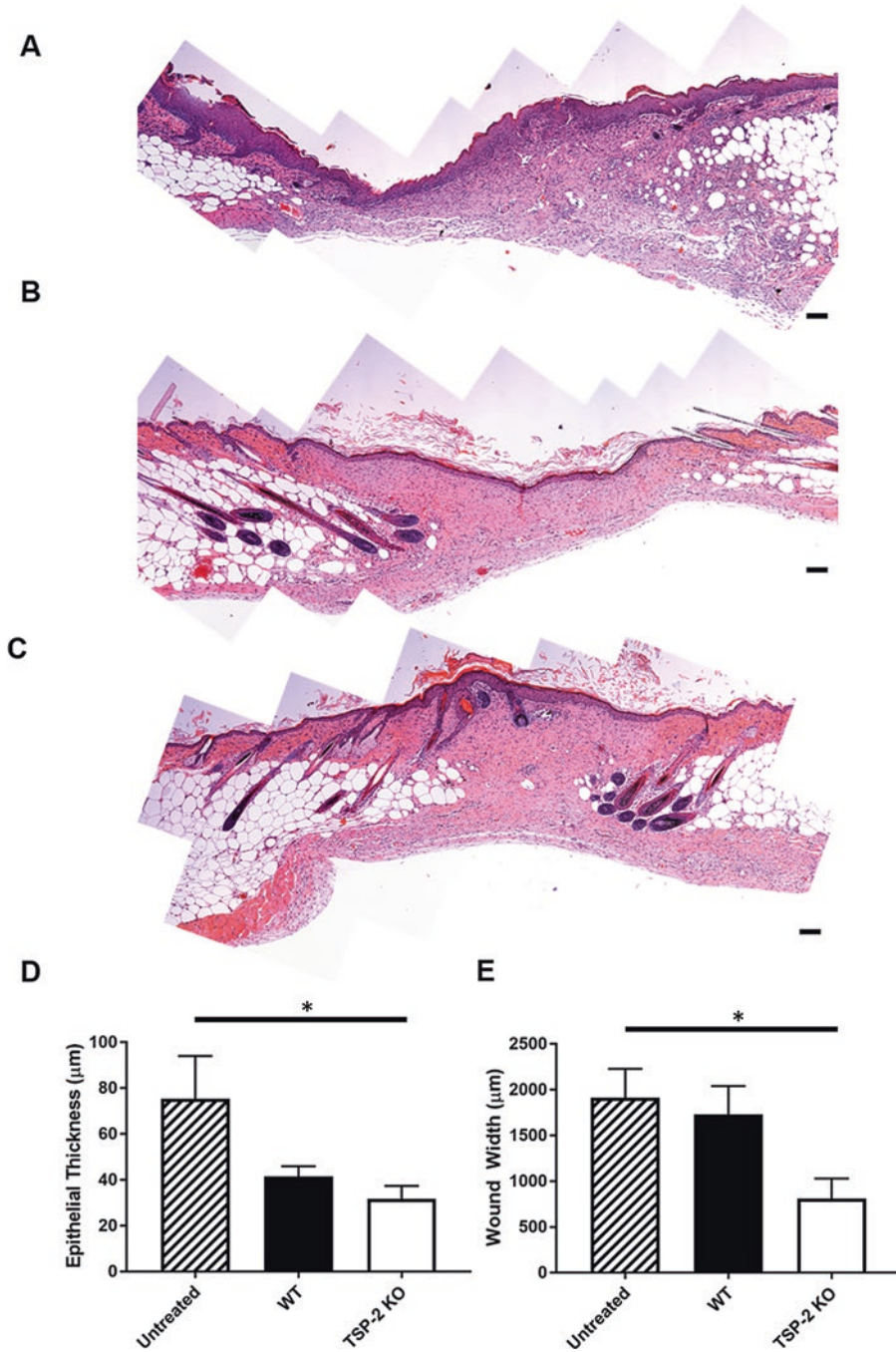


Fig. 2.3 TSP-2 KO hydrogels improved diabetic wound resolution compared to untreated wounds in mice. (a–c) Representative stitched images of entire wound beds from diabetic mice after 21 days of healing: (a) untreated, (b) WT gel-treated, or (c) TSP-2 KO gel-treated. (d) TSP-2

KO-treated wounds demonstrate decreased epithelial thickness by 21 days when compared to untreated control. (e) TSP-2 KO gel demonstrates decreased wound width at 21 days. Scale bars = 100 µm. * $p < 0.05$. (Reprinted with permission from ACS Publications [43])

The decellularization procedure for thicker tissue slabs (10–15 mm) of porcine cardiac extracellular matrix (pcECM) can be optimized to retain the inherent vasculature [31]. It was found that HUVECs repopulated and formed a monolayer that surrounded the inner lumen of the inherent acellular blood vessels, with no cell infiltration into the pcECM scaffold. These findings indicated that the decellularized blood vessels possessed recellularization proficiency.

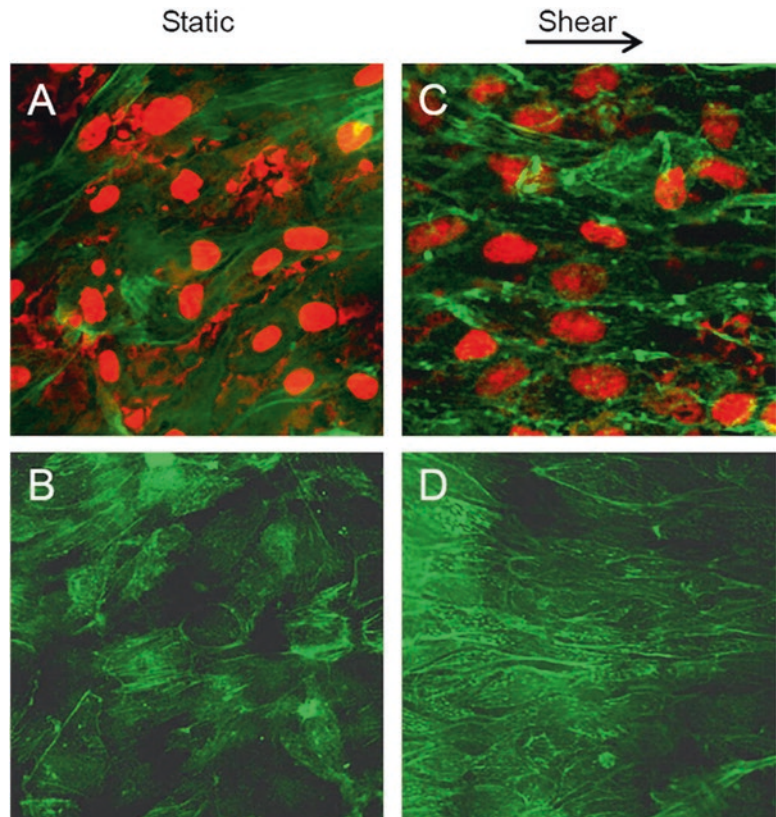
Amniotic membranes have been used to design tissue-engineered blood vessels (TEBVs) [48]. Amniotic membrane samples were decellularized by 0.25% trypsin for 10 min at room temperature and then crosslinked by treatment with 0.1% glutaraldehyde in 0.01 M acetic acid solution. Porcine vascular endothelial cells were cultured on decellularized amniotic membrane scaffolds under shear stress from 0.5 to 12 dyne cm^{-2} for 4 days and under static conditions. Cells in static culture were randomly oriented, while the actin filaments in cells exposed to shear stress

for 4 days were aligned in parallel to the direction of flow (Fig. 2.4). The junction proteins platelet endothelial cell adhesion molecule-1 and vascular endothelial cadherin were better developed by shear stress treatment. Additionally, the expression of $\beta 1$ integrin could be distracted from the cell surface by shear stress. These results suggest that denuded GA-crosslinked amniotic membrane tubes can be used as potential scaffolds for TEBVs. In clinical studies, TEBVs have been implanted in end-stage renal disease patients [49], with no indications of an immune response, rejection, or aneurysms in 28 patients.

2.5.2 Heart Valve

Mechanical and biological prostheses have been widely used clinically for heart valve replacement. Mechanical valves show advantage of long-term durability, but they require life-long anticoagulation. Biological valves retain charac-

Fig. 2.4 The tissue-engineered blood vessel (TEBV) was cultured under static conditions or subjected to a shear stress of 12 dyne cm^{-2} for 4 days. Cells in static culture were randomly oriented (a, b) as shown by the arrangement of actin (green fluorescence) and nucleus (red fluorescence). In cells exposed to shear stress for 4 days, the actin filaments were aligned in parallel to the direction of flow (c, d). \rightarrow : direction of flow. (Reprinted with permission from Elsevier [48])



teristics of good hemodynamic function and a low incidence of thromboembolism like native tissues, but calcification is a major limitation of their clinical application. Decellularized heart valve grafts presented a lower calcification risk and extended durability, suggesting their suitability for heart valve replacement.

Porcine aortic and pulmonary valves were decellularized using a low concentration SDS-based method [50]. Collagen and elastin fibers in the three layers of the organization were rearranged and looser than in the native samples, due to the removal of the cells. The tensile strength of decellularized leaflets was higher than that of native samples, while the elongation was comparable between native and decellularized samples. Immunofluorescent results showed colocalization of laminin and collagen IV in the organization of the ECM structures following decellularization, indicating that the basement membrane was not damaged.

Many studies have investigated the recellularization potential of dECMs of heart valve. Fibroblast cells (L929 cells) were shown to adhere to dECMs of porcine aortic valves that were decellularized by trypsin/EDTA treatment followed by SDS washing and detergent perfusion. These cells formed a surface monolayer but did not migrate inside the scaffold [51]. Pulmonary and aortic human allografts were harvested and decellularized using a SDS detergent-based cell extraction method. The luminal surface of the human matrix was successfully recellularized with HUVECs under dynamic flow conditions, leading to the formation of a confluent HUVEC monolayer [52]. Moreover, decellularized bovine pericardium that was transplanted into the pulmonary artery in sheep for 180 days presented good biocompatibility [53].

Despite the relatively good performance of dECMs of heart valve *in vivo*, possible immune responses of these xenogenic ECMs have been controversial in clinical applications. A previous study reported that 106 of 159 patients presented no immune response to bioprosthetic heart valves after decellularization (Matrix P plus®) or glu-

taraldehyde (GA) treatment, suggesting no toxicity and good biocompatibility of these ECMs in the human body [9]. However, existing antigens in decellularized heart valve grafts may elicit an immune response in recipients, such as acute rejection within days to weeks after transplantation because of the presence of low levels of circulating non-Gal xenoreactive natural antibodies. Therefore, advanced technical procedures for antigen removal should be further explored to produce high-quality bioprosthetic heart valves.

2.5.3 Skin

Abdominal wall reconstruction and dural defect recovery are still challenging clinical problems [54]. Many products, including human dermis (Alloderms®, Life Cell) and porcine SIS (Surgisis®, Cook Biotech; Restores®, DePuy Orthopaedics), are made from dECMs that can provide scaffolds for tissue incorporation and neovascularization [54]. Three products, AlloDerm, Surgisis, and Vicryl Woven Mesh, have been used for rat abdominal wall repair. Surgisis and AlloDerm had significantly greater ($p < 0.05$) amounts of collagen deposition and organization at 30 and 60 days compared to Vicryl Woven Mesh. The tensile strength of Surgisis® is 0.142 MPa, which is comparable to Alloderm® (0.091 MPa). Alloderm® and Surgisis® were shown to present no significant differences in tensile strength and collagen remodeling in a model of hernia in Sprague-Dawley rats (Fig. 2.5). However, neovascularization with Surgisis® mesh was better than Alloderm®.

An allogeneic acellular dermal matrix (ADM) was prepared by decellularization with 1.25 g/L trypsin solution and Triton X-100 in PBS at 4 °C for 24 h. A basic dermal architecture of collagen existed in both human and porcine ADMs. When transplanted in the area of a hypertrophic scar, the histological structures of the regenerative tissue were similar to native tissue, with no sign of rejection or hypertrophy [33].

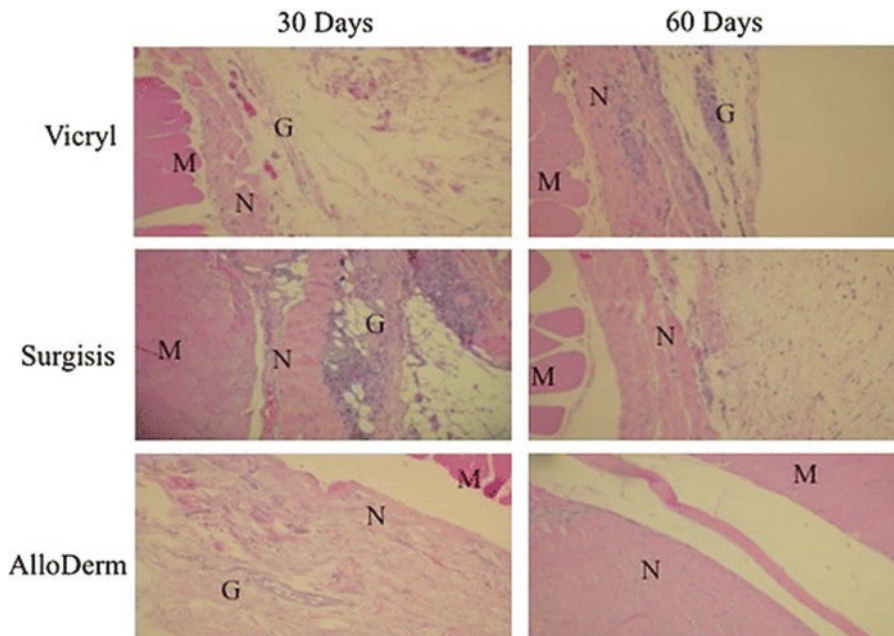


Fig. 2.5 Representative photomicrographs of graft-abdominal wall interface showing progressive increase in collagen deposition and organization. *M* abdominal wall

muscle, *G* graft, *N* new collagen. (Reprinted with permission from Springer [54])

2.6 Whole Organ Decellularization and Recellularization

Because of the notable shortage of functional organs that are ready for transplantation, a tremendous challenge is rescuing patients from end-stage organ failure. Various tissue engineering strategies have been applied to organ regeneration. One strategy for whole organ regeneration is to recellularize the acellular ECMs with original macro- and micro-structures including vasculature, which can create a new functional organ.

2.6.1 Heart

Approximately 22 million patients suffer from heart failure worldwide [55]. The ultimate treatment option for end-stage heart failure is heart transplantation. Considering the severe shortage of donor hearts, tissue engineering and regenerative medicine likely provide strategies for treatment of heart failure. Decellularized ECMs have

been used for scaffolds for heart regeneration. Ideal 3D structures, biochemical compositions, and biomechanical properties can be achieved when an intact decellularized heart is used as a scaffold. The most important aspect of organ engineering is cell proliferation and differentiation, which requires biological signaling between cells and the ECM scaffold.

Ott et al. [55] decellularized 140 rat hearts, after which the 3D structure was fully retained. Rat aortic endothelial cells were seeded on decellularized heart ECMs. Cell monolayers formed on the inner surfaces of coronary vessels after 7 days of cultivation. The cell density on the endocardial surface was 550.7 ± 99.0 cells/mm², whereas the cell density on the vessel branch was 264.8 ± 49.2 cells/mm². The recellularized scaffold presented contraction with loading and electrical stimulation of the work environment of the heart after 4 days, demonstrating pump function, although the extent of pump function was equivalent to a 16-week fetal human heart.

Ng et al. [56] seeded human embryonic stem cells (hESCs) and human mesendodermal cells

(hMECs) on decellularized rat hearts. These cells differentiated and expressed myosin light chain (My12, My17) and myosin heavy chain (Myh6) genes, which are crucially important characteristics of the myocardium. The reseeded heart was subcutaneously implanted into immune-compromised mice for 14 days. A better vascular network was observed in the hMECs-seeded scaffolds, while the hESCs-seeded scaffolds showed lesser blood vessels. Immunostaining of the explants revealed cardiac marker expressing cells within the scaffolds, but no beating function. These results demonstrated that the intact dECM of heart promoted the differentiation of stem/progenitor cells into the cardiac lineage.

Endothelial cells were present within vessels as evidenced by CD31 and von Willebrand factor (vWF) staining adjacent to lumen and appeared to be attached to the vessel wall, after short-term implantation (4–6 h) [57]. After long-term implantation (60 days), the dECM heart comprised complete vessels with both endothelial and smooth muscle cells. Adhesions with small blood vessels and presence of nascent muscles surrounding the heart scaffold were also found.

Thus, the ECM scaffold of the decellularized heart retained a vascular structure, which was used to transport cells into the scaffolds. Appropriate interactions between decellularized heart ECMs and seeded cells led to cell proliferation, migration, and differentiation toward a cardiac lineage, thus conferring the requisite functions of the heart.

2.6.2 Kidney

The number of patients who require kidney transplantation is increasing every year. In 2012, about 16,487 people received kidney transplants in the USA whereas 95,022 candidates were on the waiting list at the end of the year. Whole organ regeneration based on decellularization/recellularization techniques has provided the possibility to build functional kidney constructs as an alternative to donor organ transplantation [58]. Thus, decellularized ECMs of kidney that had appropriate compositions and microstructures were

used as 3D scaffolds for functional organ regeneration.

Rat kidneys were perfused with two detergents, SDS and SDC. The samples that were treated with SDS presented better decellularization compared with SDC treatment. After decellularization, the kidney scaffolds without cells were almost transparent, with preserved ECMs and vasculature [9]. Murine intra-arterial ESCs were seeded onto a decellularized kidney matrix [59], and these cells proliferated and distributed uniformly in the matrix after 6 days of culture. The cells migrated into microvessels and glomeruli within 7 days, which showed a reticular shape and almost fully filled the glomeruli and capillaries after 10 days. These results indicate that the co-culture of decellularized kidney ECMs and ESCs may direct the regeneration of a functional kidney.

Abolbashari et al. [60] decellularized porcine kidneys by perfusion with heparin and 0.5% SDS, following by enzymatic treatment with 0.0025 DNase and PBS rinse. The dECMs of kidneys were seeded with primary porcine renal cells. Fluorescent imaging showed that there was a significant amount of sodium uptake by the seeded renal cells, indicating these cells possessed electrolyte reabsorption capability (Fig. 2.6). Furthermore, the renal cells maintained hydrolases activity with the functional capability to transfer amino acids, as well as erythropoietin production. Moreover, Chani et al. evaluated the recellularization potential of decellularized scaffold of cryopreserved rat kidneys (3 months), which demonstrated that mesenchymal stem cells quickly repopulated the decellularized structures irrespective of the kidneys status, i.e., freshly isolated or the cryopreserved. Thus, cryopreserved kidneys can also be exploited as decellularized scaffolds for organ regeneration, which may provide alternatives to kidney transplantation.

2.6.3 Liver

End-stage liver failure is mainly caused by cirrhosis, chronic viral hepatitis, hepatocellular

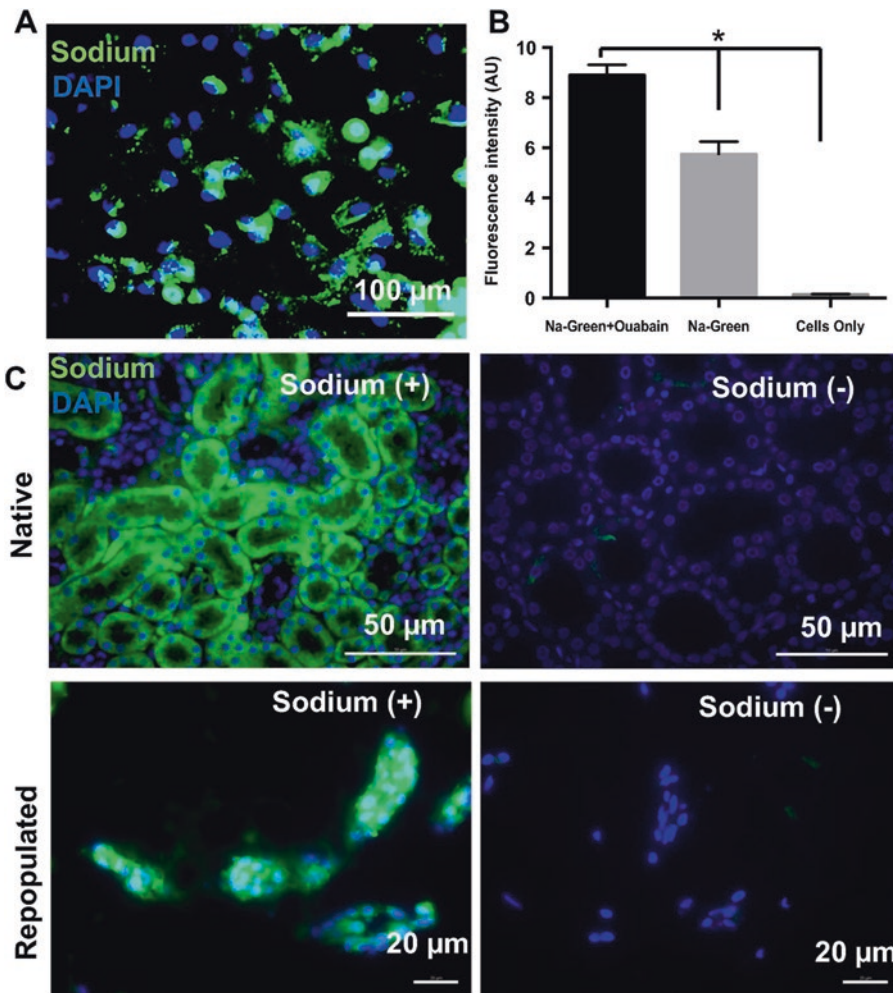


Fig. 2.6 Electrolyte reabsorption by the primary porcine renal cells on monolayer and the repopulated cells within the kidney construct. (a) In a fluorescent image, strong green fluorescence demonstrates sodium uptake by the primary porcine renal cells in monolayer culture with Ouabain treatment and (b) quantitative analysis confirms

specific uptake by the cells with significant difference ($*p < 0.0001$). (c) The tubular structures within the repopulated kidney scaffold also showed sodium uptake, as observed by the strong fluorescent signal. (Reprinted with permission from Elsevier [60])

carcinoma, etc. However, the number of liver donors is far to meet the transplantation needs. Biohybrid artificial liver (BAL) devices may provide temporary support for patients waiting for an allogeneic liver transplant, considering the regenerative capacity of liver. However, the inability of BAL to maintain the functionality of hepatocytes for long periods of time has limited clinical applications. The dECMs of liver support

the proliferation and differentiation of the hepatocytes, by providing appropriate cell-cell and cell-matrix interactions, which may provide solution for engineered functional liver constructs for temporary support or organ transplantation.

Zhou et al. [61] perfused rat livers sequentially with heparinized PBS, 1% SDS, and 1% Triton X-100 to obtain decellularized liver matrix (DLM). The removal of endogenous cellular

components and the preservation of the extracellular matrix proteins and vasculature were characterized. Subsequent reconstitution with human primary hepatocytes (hPHs) or human fetal hepatocytes immortalized by telomerase reconstitution (FH-hTERTs) in the DLM showed appropriate proliferation and improved expression of hepatic-specific genes compared with culture under standard conditions. DLMs were reconstituted with hPHs, which were implanted into the mice omenta. The results clearly demonstrated that DLM facilitated the survival of hPHs *in vivo* and maintained the liver-specific function of primary hepatocytes after implantation.

The dECM scaffolds of liver may remain thrombogenic even with anti-coagulation following transplantation. Bao et al. [62] showed that heparin can be immobilized on decellularized liver scaffolds, which prevented thrombosis in the dECM scaffolds of live with blood perfusion after implanted *in vivo*.

2.7 Conclusions and Future Perspectives

Tissue engineering and regenerative medicine can create functional tissues or whole organs, which may provide possible solutions to severe shortage of organ donors. Decellularized extracellular matrices (dECMs) are particularly interesting as scaffolds for tissue engineering and regeneration, due to their chemical compositions and hierarchical structures similar to native ECMs. A variety of decellularization methods have been developed in order to retain the microstructures (i.e., intact vasculature) and essential ECM components. The dECMs can be developed into hydrogels, which can be injected for tissue repair *in vivo*. Furthermore, decellularization and recellularization of the whole organ have been widely studied, which can recapitulate partial functions of native organs. In the future, tissue and organ regeneration may be achieved using dECMs with advanced techniques and proper cells.

References

1. Crapo PM, Gilbert TW, Badylak SF (2011) An overview of tissue and whole organ decellularization processes. *Biomaterials* 32(12):3233–3243
2. Gálvez-Montón C, Prat-Vidal C, Roura S et al (2013) Cardiac tissue engineering and the bioartificial heart. *Rev Esp Cardiol* 66(5):391–399
3. Kappetein AP, Feldman TE, Mack MJ et al (2011) Comparison of coronary bypass surgery with drug-eluting stenting for the treatment of left main and/or three-vessel disease: 3-year follow-up of the SYNTAX trial. *Eur Heart J* 32(17):2125–2134
4. L'Heureux N, Dusserre N, König G et al (2006) Human tissue-engineered blood vessels for adult arterial revascularization. *Nat Med* 12(3):361–365
5. Mangold S, Schrammel S, Huber G et al (2015) Evaluation of decellularized human umbilical vein (HUV) for vascular tissue engineering – comparison with endothelium-denuded HUV. *J Tissue Eng Regen Med* 9(1):13–23
6. Moroni F, Mirabella T (2014) Decellularized matrices for cardiovascular tissue engineering. *Am J Stem Cells* 3(1):1–20
7. Vorotnikova E, McIntosh D, Dewilde A et al (2010) Extracellular matrix-derived products modulate endothelial and progenitor cell migration and proliferation *in vitro* and stimulate regenerative healing *in vivo*. *Matrix Biol* 29(8):690–700
8. Lutolf MR, Weber FE, Schmoekel HG et al (2003) Repair of bone defects using synthetic mimetics of collagenous extracellular matrices. *Nat Biotechnol* 21(5):513–518
9. Bloch O, Golde P, Dohmen PM et al (2011) Immune response in patients receiving a bioprosthetic heart valve: lack of response with decellularized valves. *Tissue Eng Part A* 17(19–20):2399–2405
10. Xu CC, Chan RW, Tirunagari N (2007) A biodegradable, acellular xenogeneic scaffold for regeneration of the vocal fold lamina propria. *Tissue Eng* 13(3):551–566
11. Mann BK, Gobin AS, Tsai AT et al (2001) Smooth muscle cell growth in photopolymerized hydrogels with cell adhesive and proteolytically degradable domains: synthetic ECM analogs for tissue engineering. *Biomaterials* 22(22):3045–3051
12. Badylak SF (2002) The extracellular matrix as a scaffold for tissue reconstruction. *Semin Cell Dev Biol* 13(5):377–383
13. Badylak SF (2004) Xenogeneic extracellular matrix as a scaffold for tissue reconstruction. *Transpl Immunol* 12(3–4):367–377
14. Jarvelainen H, Sainio A, Koulou M et al (2009) Extracellular matrix molecules: potential targets in pharmacotherapy. *Pharmacol Rev* 61(2):198–223
15. Liang R, Fisher M, Yang G et al (2011) Alpha1,3-galactosyltransferase knockout does not alter the properties of porcine extracellular matrix bioscaffolds. *Acta Biomater* 7(4):1719–1727

16. Hong Y, Huber A, Takanari K et al (2011) Mechanical properties and in vivo behavior of a biodegradable synthetic polymer microfiber-extracellular matrix hydrogel biohybrid scaffold. *Biomaterials* 32(13):3387–3394
17. Lee KY, Bouhadir KH, Mooney DJ (2004) Controlled degradation of hydrogels using multi-functional cross-linking molecules. *Biomaterials* 25(13):2461–2466
18. Kloxin AM, Tibbitt MW, Anseth KS (2010) Synthesis of photodegradable hydrogels as dynamically tunable cell culture platforms. *Nat Protoc* 5(12):1867–1887
19. Bejleri D, Davis ME (2019) Decellularized extracellular matrix materials for cardiac repair and regeneration. *Adv Healthc Mater* 8(5):1801217
20. Wolf MT, Daly KA, Brennan-Pierce EP et al (2012) A hydrogel derived from decellularized dermal extracellular matrix. *Biomaterials* 33(29):7028–7038
21. Badylak SF, Freytes DO, Gilbert TW (2009) Extracellular matrix as a biological scaffold material: structure and function. *Acta Biomater* 5(1):1–13
22. Gilbert TW, Sellaro TL, Badylak SF (2006) Decellularization of tissues and organs. *Biomaterials* 27(19):3675–3683
23. Phillips M, Maor E, Rubinsky B (2010) Nonthermal irreversible electroporation for tissue decellularization. *J Biomech Eng* 132(9):091003
24. Hashimoto Y, Funamoto S, Sasaki S et al (2010) Preparation and characterization of decellularized cornea using high-hydrostatic pressurization for corneal tissue engineering. *Biomaterials* 31(14):3941–3948
25. Zhou J, Fritze O, Schleicher M et al (2010) Impact of heart valve decellularization on 3-D ultrastructure, immunogenicity and thrombogenicity. *Biomaterials* 31(9):2549–2554
26. Assmann A, Delfs C, Munakata H et al (2013) Acceleration of autologous in vivo recellularization of decellularized aortic conduits by fibronectin surface coating. *Biomaterials* 34(25):6015–6026
27. Dong J, Li Y, Mo X (2013) The study of a new detergent (octyl-glucopyranoside) for decellularizing porcine pericardium as tissue engineering scaffold. *J Surg Res* 183(1):56–67
28. Seebacher G, Grasl C, Stoiber M et al (2008) Biomechanical properties of decellularized porcine pulmonary valve conduits. *Artif Organs* 32(1):28–35
29. Seo Y, Jung Y, Kim SH (2018) Decellularized heart ECM hydrogel using supercritical carbon dioxide for improved angiogenesis. *Acta Biomater* 67:270–281
30. Akhyari P, Aubin H, Gwanmesia P et al (2011) The quest for an optimized protocol for whole-heart decellularization: a comparison of three popular and a novel decellularization technique and their diverse effects on crucial extracellular matrix qualities. *Tissue Eng Part C Methods* 17(9):915–926
31. Sarig U, Au-Yeung GC, Wang Y et al (2012) Thick acellular heart extracellular matrix with inherent vasculature: a potential platform for myocardial tissue regeneration. *Tissue Eng Part A* 18(19–20):2125–2137
32. Conconi MT, Coppi PD, Liddo RD et al (2005) Tracheal matrices, obtained by a detergent-enzymatic method, support in vitro the adhesion of chondrocytes and tracheal epithelial cells. *Transpl Int* 18(6):727–734
33. Conconi MT, Coppi PD, Bellini S et al (2005) Homologous muscle acellular matrix seeded with autologous myoblasts as a tissue-engineering approach to abdominal wall-defect repair. *Biomaterials* 26(15):2567–2574
34. Theodoridis K, Tudorache I, Calistru A et al (2015) Successful matrix guided tissue regeneration of decellularized pulmonary heart valve allografts in elderly sheep. *Biomaterials* 52:221–228
35. Schenke-Layland K, Vasilevski O, Opitz F et al (2003) Impact of decellularization of xenogeneic tissue on extracellular matrix integrity for tissue engineering of heart valves. *J Struct Biol* 143(3):201–208
36. Lim HG, Kim SH, Choi SY et al (2012) Anticalcification effects of decellularization, solvent, and detoxification treatment for genipin and glutaraldehyde fixation of bovine pericardium. *Eur J Cardiothorac Surg* 41(2):383–390
37. Simona P, Kasimira MT, Seebachera G et al (2003) Early failure of the tissue engineered porcine heart valve SYNERGRAFT (TM) in pediatric patients. *Eur J Cardiothorac Surg* 23(6):1002–1006
38. Li Z, Guan J (2011) Hydrogels for cardiac tissue engineering. *Polymers* 3(4):740–761
39. Singelyn JM, DeQuach JA, Seif-Naraghi SB et al (2009) Naturally derived myocardial matrix as an injectable scaffold for cardiac tissue engineering. *Biomaterials* 30(29):5409–5416
40. Uriel S, Labay E, Francis-Sedlak M et al (2009) Extraction and assembly of tissue-derived gels for cell culture and tissue engineering. *Tissue Eng Part C Methods* 15(3):309–321
41. Kleinman HK, Martin GR (2005) Matrigel: basement membrane matrix with biological activity. *Semin Cancer Biol* 15(5):378–386
42. Morris AH, Stamer DK, Kunkemoeller B et al (2018) Decellularized materials derived from TSP2-KO mice promote enhanced neovascularization and integration in diabetic wounds. *Biomaterials* 169:61–71
43. Morris AH, Lee H, Xing H et al (2018) Tunable hydrogels derived from genetically engineered extracellular matrix accelerate diabetic wound healing. *ACS Appl Mater Interfaces* 10(49):41892–41901
44. Schaner PJ, Martin ND, Tulenko TN et al (2004) Decellularized vein as a potential scaffold for vascular tissue engineering. *J Vasc Surg* 40(1):146–153
45. Song JJ, Ott HC (2011) Organ engineering based on decellularized matrix scaffolds. *Trends Mol Med* 17(8):424–432
46. Taylor PM, Cass AEG, Yacoub MH (2006) Extracellular matrix scaffolds for tissue engineering heart valves. *Prog Pediatr Cardiol* 21(2):219–225

47. Simsa R, Padma AM, Heher P et al (2018) Systematic in vitro comparison of decellularization protocols for blood vessels. *PLoS One* 13(12):e0209269
48. Lee PH, Tsai SH, Kuo L et al (2012) A prototype tissue engineered blood vessel using amniotic membrane as scaffold. *Acta Biomater* 8(9):3342–3348
49. Woods T, Gratzner PF (2005) Effectiveness of three extraction techniques in the development of a decellularized bone-anterior cruciate ligament-bone graft. *Biomaterials* 26(35):7339–7349
50. Roderjan JG, de Noronha L, Stimamiglio MA et al (2019) Structural assessments in decellularized extracellular matrix of porcine semilunar heart valves: evaluation of cell niches. *Xenotransplantation* 26(3):e12503
51. Wilczek P (2010) Heart valve bioprosthesis: effect of different acellularizations methods on the biomechanical and morphological properties of porcine aortic and pulmonary valve. *B Pol Acad Sci-Tech* 58(2):337–342
52. Weymann A, Schmack B, Okada T et al (2013) Reendothelialization of human heart valve neoscaffolds using umbilical cord-derived endothelial cells. *Circ J* 77(1):207–216
53. Collatusso C, Roderjan JG, Vieira ED et al (2011) Decellularization as an anticalcification method in stentless bovine pericardium valve prosthesis: a study in sheep. *Rev Bras Cir Cardiovasc* 26(3):419–426
54. Rice RD, Ayubi FS, Shaub ZJ et al (2010) Comparison of Surgisis, AlloDerm, and Vicryl Woven Mesh grafts for abdominal wall defect repair in an animal model. *Aesthet Plast Surg* 34(3):290–296
55. Ott HC, Matthiesen TS, Goh SK et al (2008) Perfusion-decellularized matrix: using nature's platform to engineer a bioartificial heart. *Nat Med* 14(2):213–221
56. Ng SL, Narayanan K, Gao S et al (2011) Lineage restricted progenitors for the repopulation of decellularized heart. *Biomaterials* 32(30):7571–7580
57. Taylor DA, Frazier OH, Elgalad A et al (2018) Building a total bioartificial heart: harnessing nature to overcome the current hurdles. *Artif Organs* 42(10):970–982
58. Orlando G, Booth C, Wang Z et al (2013) Discarded human kidneys as a source of ECM scaffold for kidney regeneration technologies. *Biomaterials* 34(24):5915–5925
59. Ross EA, Williams MJ, Hamazaki T et al (2009) Embryonic stem cells proliferate and differentiate when seeded into kidney scaffolds. *J Am Soc Nephrol* 20(11):2338–2347
60. Abolbashari M, Agcaoili SM, Lee MK et al (2016) Repopulation of porcine kidney scaffold using porcine primary renal cells. *Acta Biomater* 29:52–61
61. Zhou P, Lessa N, Estrada DC et al (2011) Decellularized liver matrix as a carrier for the transplantation of human fetal and primary hepatocytes in mice. *Liver Transpl* 17(4):418–427
62. Bao J, Wu Q, Sun J et al (2015) Hemocompatibility improvement of perfusion-decellularized clinical-scale liver scaffold through heparin immobilization. *Sci Rep* 5:10756

Part II

**Novel Biomimicked Hydrogel
for Regenerative Medicine**



Injectable In Situ-Forming Hydrogels for Protein and Peptide Delivery

Seung Hun Park, Yun Bae Ji, Joon Yeong Park, Hyeon Jin Ju, Mijeong Lee, Surha Lee, Jae Ho Kim, Byoung Hyun Min, and Moon Suk Kim

Abstract

Injectable in situ-forming hydrogels have been used clinically in diverse biomedical applications. These hydrogels have distinct advantages such as easy management and minimal invasiveness. The hydrogels are aqueous formulations, and a simple injection at the target site replaces a traditional surgical procedure. Here, we review injectable in situ-forming hydrogels that are formulated by physical and chemical methods to deliver proteins and peptides. Prospects for using in situ-forming hydrogels for several specific applications are also discussed.

Keywords

Injectable in situ forming hydrogels · Protein and peptide · Drug depot · Crosslinking · Physical interaction · Electrostatic interaction · Biomedical application of hydrogel ·

Authors Seung Hun Park and Yun Bae Ji have equally contributed to this chapter.

S. H. Park · Y. B. Ji · J. Y. Park · H. J. Ju · M. Lee
S. Lee · J. H. Kim · B. H. Min · M. S. Kim (✉)
Department of Molecular Science and Technology,
Ajou University, Suwon, South Korea
e-mail: hpt88@ajou.ac.kr; jyb26267@ajou.ac.kr;
pjy16@ajou.ac.kr; tssos@ajou.ac.kr; mjlee5567@ajou.ac.kr;
lsh5969@ajou.ac.kr; jhkim@ajou.ac.kr;
bhmin@ajou.ac.kr; moonskim@ajou.ac.kr

Drug delivery system · Click reaction · Covalent and non-covalent bonding · Protein and peptide loading

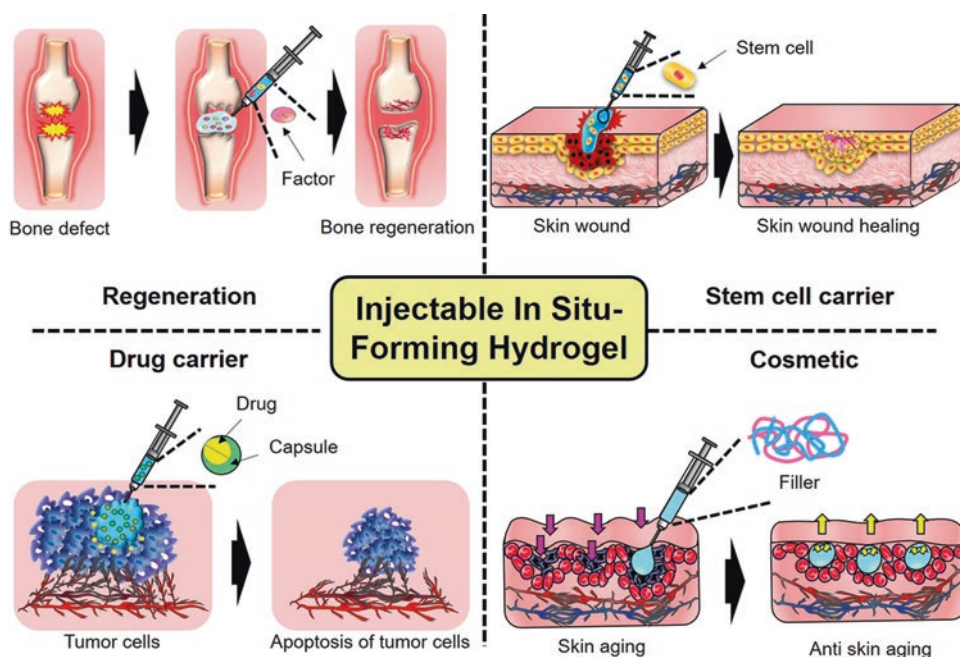
3.1 Introduction

Hydrogels are widely utilized in a variety of biomedical fields (Fig. 3.1) [1–4]. Hydrogels possess a three-dimensional network structure that swells from the absorption of large amounts of water. Since hydrogels can suitably adjust water content, they provide an environment similar to that of a biological tissue in vivo [5]. Hydrogels have been prepared by using natural, synthetic, and composite biomaterials with high biocompatibility [6].

Since conventional hydrogels are made in a hydrogel (solid) phase outside the body, they require a surgical delivery procedure. It can be difficult to fit hydrogels to the corresponding implantation sites because of variability between individuals [7]. To solve these problems, in situ-forming hydrogels, which can be injected into a desired target site in a minimally invasive manner, are being widely studied.

Injectable in situ-forming hydrogel formulations are prepared as solutions that become hydrogels in vivo after injection. Since injectable in situ-forming hydrogel formulations

Table of Content



(TOC was drawn by S.H.P. and Y.B.J. using Adobe Photoshop7.0)

are liquids prior to injection, various growth factors, cells, and chemical agents can be easily introduced by simple mixing [8].

Methods for formulating injectable in situ-forming hydrogels can be categorized into physical and chemical methods. Physical methods use non-covalent bonds such as hydrophobic bonds, electrostatic attraction bonds, and hydrogen bonds [9–11]; chemical methods form covalent bonds such as click chemistry or enzyme-mediated crosslinking [12, 13].

Protein- and peptide-based drugs have been developed for in vivo applications. Many studies are ongoing to develop carriers for these drugs. When protein/peptide drugs are administered orally, they can be degraded by enzymes or high acidity in the gastrointestinal tract or can have difficulty moving through the walls of the gastrointestinal tract [14].

Several approaches have been proposed to solve these problems [15, 16]. Parenteral administration methods have been investigated, and there has been growing interest in nasal, pulmonary, and transdermal delivery routes, but the low permeability of these substances presents challenges to the effective delivery of protein/peptide drugs [17].

Injectable in situ-forming hydrogels offer advantages for delivery of protein/peptide drugs into certain target sites without loss of efficacy as well as providing options for sustained release via the design of hydrogel characteristics.

Some attempts to control drug release involve the formation of a non-covalent or covalent interaction between the protein/peptide drugs and the in situ-forming hydrogel that controls the rate and efficiency of sustained release [18, 19, 20].

Here, we discuss injectable in situ-forming hydrogels formed by physical and chemical

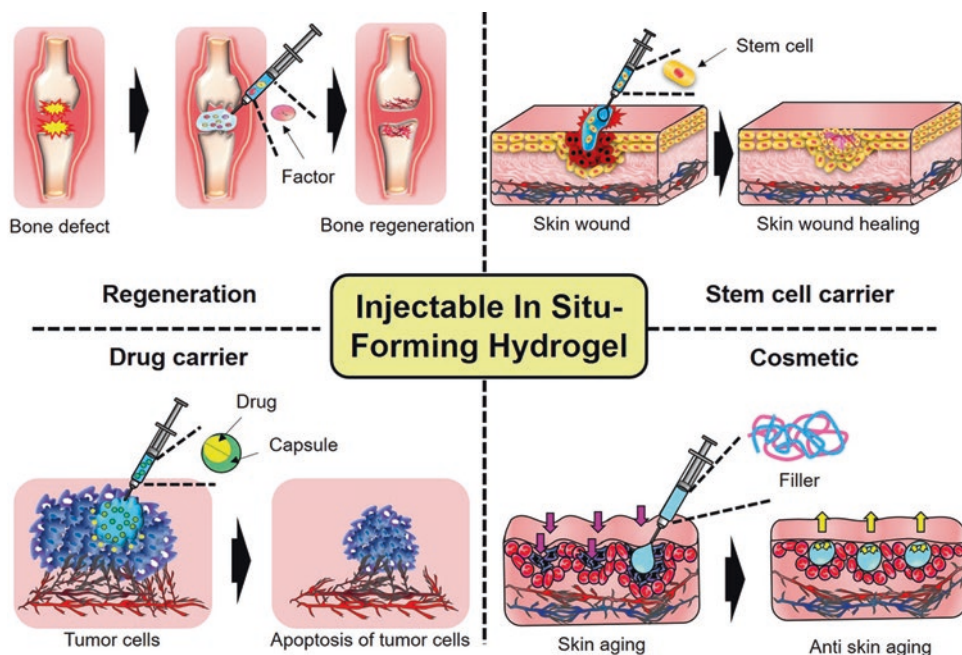


Fig. 3.1 Scheme image of injectable in situ-forming hydrogel for biomedical application. (The image was drawn by S.H.P. and Y.B.J. using Adobe Photoshop7.0)

methods, and then we discuss how these methods contribute to the controlled release of protein/peptide drugs. Finally, prospects for using in situ-forming hydrogels in several applications are discussed.

3.2 Injectable Hydrogel Formation via Physical Interaction

Injectable hydrogels that are formed in situ by physical crosslinking use hydrophobic bonding, electrostatic bonding, hydrogen bonding, etc. that leverage the change in environment that occurs when hydrogels transition from an in vitro state to an in vivo state postinjection (Fig. 3.2) [21]. For example, some hydrogels undergo reversible changes between a liquid phase to a hydrogel phase in response to external or internal factors such as temperature, pH, and shear stress. Examples of these injectable in situ-forming hydrogels are described below.

3.2.1 Injectable Hydrogel Formation via Hydrophobic Bonding Interaction

Hydrophobic molecules tend to aggregate by strong interactions when they are dispersed in highly polar water. Amphiphilic polymers are composed of hydrophilic and hydrophobic moieties [22]. An amphiphilic polymer suspension can be prepared in a liquid phase because the interaction between the hydrophilic moieties and water dominates under certain conditions. However, environmental changes such as temperature and pH can cause the hydrophobic moieties of the amphiphilic polymers to aggregate in water. Thus, injectable in situ-forming hydrogel formulations can be prepared by utilizing the tendency of hydrophobic moieties to aggregate in aqueous environments [22].

Polyethylene glycol (PEG) has a simple water-soluble structure and thus is one of the most widely studied hydrophilic moieties.

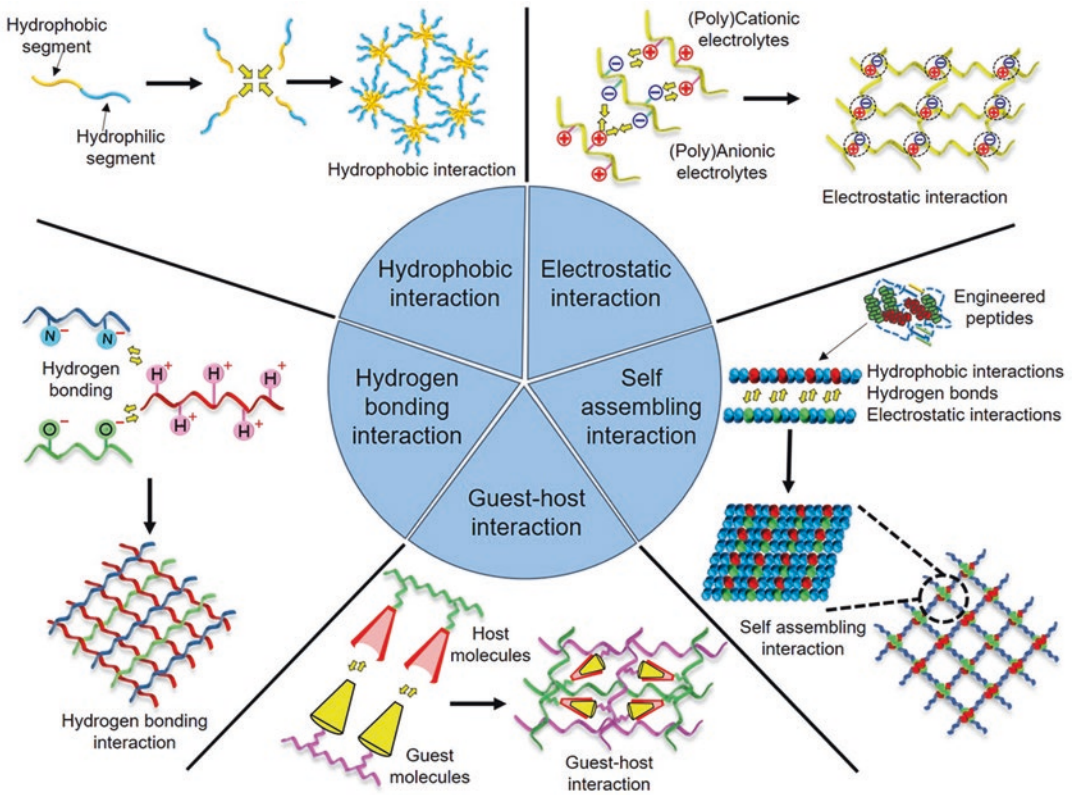


Fig. 3.2 Scheme image of injectable in situ-forming hydrogel via hydrophobic bonding, electrostatic bonding, hydrogen bonding, self-assembling, and host-guest inter-

action. (The image was drawn by S.H.P. and Y.B.J. using Adobe Photoshop7.0)

Polyesters, polyphosphazenes, polyamides, poly(*N*-isopropylacrylamide), poly(propylene oxide), poly(methacrylic acid), poly(trimethylene carbonate), polysebacic acids, etc. are among the most widely studied hydrophobic moieties [23–28]. Amphiphilic polymers are being manufactured as combinations of these hydrophilic and hydrophobic moieties.

Typically, injectable in situ-forming hydrogel formulations are prepared in vitro as a solution by dispersing amphiphilic polymers into solution under external conditions that favor the hydrophilic moiety-aqueous interaction (room temperature, etc.) [29]. After injection, these formulations become hydrogels in situ because the in vivo conditions (body temperature, etc.) favor hydrophobic bonding.

3.2.2 Injectable Hydrogel Formation via Electrostatic Interaction

Electrostatic interactions are among the most common intermolecular interactions that occur in nature [30]. When cationic and anionic electrolytes are mixed, they form an electrostatic bond. Typical natural polymeric anionic electrolytes are alginate, chondroitin sulfate, hyaluronate, heparin, sodium carboxymethylcellulose, pectin, dextran sulfate, and xanthan. Synthetic polymeric electrolytes include polyacrylic acids, poly-*L*-glutamates, and poly(methyl vinyl ether-co-maleic anhydride). Polymeric cationic electrolytes include chitosan, polyvinylamine hydrochloride, poly(allylamine hydrochloride), poly(diallyldimethylammonium chloride),

spermine, spermidine, polyethylenimine, polylysine, poly(2-dimethylaminoethyl methacrylamide), and poly[2-(trimethylammonio)ethyl methacrylate chloride] [31–47].

When a polymeric cationic and an anionic electrolyte or a monomeric cationic and an anionic electrolyte are mixed, they form a network structure through electrostatic interaction [46]. The properties of electrostatic interactions are primarily determined by the strength of the interaction between opposite charges, solubility, conductivity, turbidity, and pH [41].

Injectable hydrogels that form in situ via electrostatic interaction have very little or no electrostatic interaction between their constituent cationic and anionic electrolytes at room temperature, resulting in homogeneous solutions. Body temperature induces the electrostatic interaction between electrolytes to form viscous and macroscopic hydrogels. At higher temperatures, the electrostatic interaction can become too strong, and precipitation can occur. Consequently, injectable hydrogels that form in situ via electrostatic interaction can be controlled by the relationship between the strength of the electrostatic interaction between polymer components and temperature.

3.2.3 Injectable Hydrogel Formation via Hydrogen Bonding

A hydrogen bond is formed between a molecule having a hydrogen atom and a molecule containing electronegative atoms having unpaired electrons such as nitrogen, oxygen, and fluorine. Although hydrogen bonds are very weak bonds, molecular interactions via multiple hydrogen bonds play a very important role in nature [48].

Several materials including peptides, poly(acrylic acid), poly(acrylamide), poly(methacrylic acid), poly(methyl methacrylate), poly(L-glutamic acid), poly(L-lysine), phenylboronic acid, and 2-vinyl-4,6-diamino-1,3,5-triazine are used for forming hydrogen bonding [49–53].

If the hydrogen bonding between water and a polymer with unpaired electrons is strong, then the polymer remains in solution. However, when intra- or intermolecular hydrogen bonds among polymer molecules become strong, or the hydrogen bonds between water and polymer molecules become weak, a hydrogel will form as a polymeric network structure [54].

It is important that the polymer molecules easily form intra- and intermolecular hydrogen bonds to achieve a hydrogel. Therefore, proper regulation of the conditions under which intra- and intermolecular hydrogen bond formation occurs in the polymer molecules is very important in the development of injectable in situ-forming hydrogels.

3.2.4 Injectable Hydrogel Formation Using Other Interactions

Non-covalent bonding interactions that are used to design injectable in situ-forming hydrogels include self-assembly and host-guest interaction.

Generally, self-assembly occurs through non-covalent bonds such as hydrophobic interactions, hydrogen bonds, and electrostatic interactions, resulting in the formation of a network structure. Engineered peptides or proteins can induce self-assembly via these non-covalent bonding mechanisms either as inter- or intra-chain interactions with polymer molecules [55, 56]. Many of these interactions form very strong bonds and consequently resulting in the formation of injectable in situ-forming hydrogels.

Some materials can be made by in situ association between host molecules and guest molecules. When this host molecule and guest molecule structure are mixed, a host-guest interaction is formed between the host molecule and the guest molecule [36, 37]. There are several host molecules such as α -cyclodextrin, β -cyclodextrin, γ -cyclodextrin, dibenzo[24]crown [8], and cucurbit[8]uril. Guest molecules are PEG, poly(ethylene oxide), adamantane, ferrocene, bisammonium salts, phenylalanine, etc. [57–61]. Binding of host to guest molecules can

form injectable in situ-forming hydrogels. The type and number of host and guest molecules can control the properties of injectable in situ-forming hydrogels.

3.3 Injectable Hydrogel Formation via Chemical Crosslinking

Hydrogels formed by chemical reaction have stronger physical properties than hydrogels formed by non-covalent bonding. Although a hydrogel with good physical properties can be produced by a chemical reaction that occurs in situ after injection, the inconvenience of the manufacturing process, the residual materials introduced by manufacturing, and factors such as bioavailability and biocompatibility must be carefully considered in introducing such a hydrogel into a living body. Hydrogel preparation through various covalent bonds is possible, but in this review, hydrogel preparation by click reaction and enzyme reaction are discussed.

3.3.1 Injectable Hydrogel Formation via Click Crosslinking

In chemistry, click crosslinking has been widely studied as a useful reaction [6]. Click crosslinking is fast and highly specific, and its yield is high, but it is an irreversible reaction.

Studies have investigated ways to apply click crosslinking in biomedicine [62]. In this case, biocompatible materials must be used as the basic structure, and then a click reagent is introduced on the materials to induce the click crosslinking.

Some click reactions proceed in biological conditions to form stable click crosslinks. Therefore, many studies have focused on the design of injectable in situ-forming hydrogels using click reactions (Table 3.1) [63–87].

In vivo application of injectable hydrogels that form in situ via click reaction should include the following considerations: (1) no clogging inside the syringe during injection, (2) a rapid in

situ-formation of the hydrogel at the injection site, (3) biocompatibility, (4) persistence for a suitable period of time, and (5) properties that are adjustable for the target body tissue.

3.3.2 Injectable Hydrogel Formation via Enzyme-Mediated Crosslinking

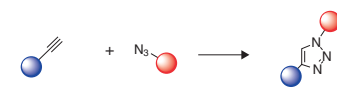
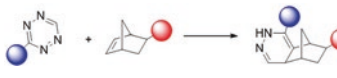
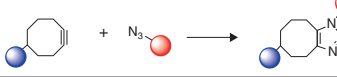
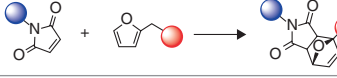
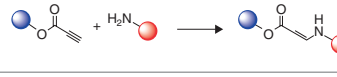

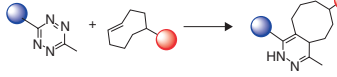

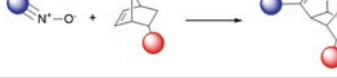
Enzymes catalyze various in vivo reactions. To prepare injectable hydrogels for in situ formation via enzyme-mediated crosslinking, an enzyme is immobilized onto some component that will form the hydrogel to prevent it from diffusing into the host tissue. The enzyme's substrate is either in an inactive conformation that is converted to an active conformation postinjection or the crosslinking requires a cofactor that is released from the polymer after injection to initiate the enzyme-mediated crosslinking, resulting in the formation in situ-forming hydrogel.

Table 3.2 summarizes examples of injectable hydrogels that are formed by the reaction of several substrates with specific enzyme-modified materials [13, 32, 88–98]. Since the enzymatic reactions need to occur postinjection, enzyme-mediated crosslinking must occur in the in vivo environment actively and safely. However, side effects such as the enzyme reacting with other tissues in the body or toxicity of the enzyme or any of its reaction products should be taken into consideration.

3.4 Injectable Hydrogels Formed as Therapeutic Protein/Peptide Drug Delivery Depots

Proteins and peptides play important roles in vivo, and in some cases, they have excellent therapeutic effects as drugs. However, protein/peptide drugs need be repeatedly used due to a short half-life under in vivo conditions. The short half-life of protein/peptide drugs can be solved by using hydrogels, because injectable in situ-forming hydrogels can act as a depot of protein/

Table 3.1 Injectable hydrogel formation via click crosslinking

Reaction type	Reaction mechanism	Material	Refs.
Copper (I)-catalyzed azide-alkyne cycloadditions (CuAAC)		HA, xylan	[63, 64]
Tetrazine-norbornene Diels-Alder reactions		Gelatin, alginate	[65, 66]
Strain-promoted azide-alkyne cycloadditions		PEG, HA, dextran, chitosan, gelatin	[67–72]
Diels-Alder cycloaddition		Chondroitin sulfate, Pluronic, PEG, HA, chitin, gelatin	[73–78]
Michael-type amino-ene(Yne) reaction		Chitosan, PEG, PAMAM	[79, 80]
Michael-type thiol-ene(Yne) reaction		HA, PEG, cysteine-TMV protein	[81, 82]
Tetrazine-trans-cyclooctene reaction		HA, SIS	[83, 84]
Oxime click chemistry		PEG, HA	[85, 86]
Nitrile oxide-norbornene click chemistry		PEG, gelatin	[87]

HA hyaluronic acid, PEG polyethylene glycol, PAMAM polyamidoamine, TMV tobacco mosaic virus, SIS small intestinal submucosa

Table 3.2 Injectable hydrogel formation via enzyme-mediated crosslinking

Materials	Enzyme	Substrate	Refs.
Collagen	Transglutaminase	Glutamine, lysine	[13]
Chondroitin sulfate	Tyrosinase	Tyramine	[88]
Chitosan	Tyrosinase	Tyrosine	[89]
Chitosan/HA	Glucose oxidase	Glucose	[32]
Dextran	Peroxidases	Tyramine/H ₂ O ₂	[90]
Gelatin	Transglutaminase	Glutamine, lysine	[91]
	Peroxidases	Tyramine/H ₂ O ₂	[92]
HA	Transglutaminase	Glutamine, lysine	[93]
	Peroxidases	Tyramine/H ₂ O ₂	[94]
Oligopeptide	Phosphatases	Phosphate	[95]
PEG	Glucose oxidase	Glucose	[96]
	Phosphopantetheinyl transferase	CoA	[97]
Poly(L-glutamic acid)/PEG	Peroxidases	Tyramine/H ₂ O ₂	[98]

peptide drugs as described in the previous section.

Several studies are investigating the application of injectable in situ-forming hydrogels as delivery systems for protein/peptide drug depots [99]. Injectable in situ-forming hydrogels can be easily prepared by simple mixing with proteins/peptides with little to no loss of the proteins/peptides. The protein/peptide-loaded hydrogel depot can be easily formed in vivo once injected into the body. The protein/peptide drugs become loaded into the hydrogel via physical loading during formation. The physically loaded protein/peptide drugs can be slowly released from hydrogel depots even when there is little to no interaction between the hydrogel depot and the protein/peptide drugs.

If protein/peptide drugs do interact with the hydrogel depot, the release of the drug can be controlled for a prolonged period compared with drugs that have little to no interaction with the hydrogel depot (Fig. 3.3). Several approaches have been explored to extend retention time of protein/peptide drugs inside hydrogel depots (Table 3.3) [35, 84, 100–108]. Here, we will describe two approaches: electrostatic interaction between the protein/peptide drugs and the hydrogel depot and covalent loading of protein/peptide drugs onto the hydrogel depot.

3.4.1 Electrostatic Loaded Proteins/Peptides Inside Hydrogel Depot

Proteins/peptides can have either a positive or a negative net charge in the biological environment. If the hydrogel has a net charge, then it can form an electrostatic interaction with proteins/peptides that have an opposite net charge.

Bone morphogenetic protein-2 (BMP2) is highly effective in inducing bone formation and bone differentiation [101]. However, when BMP2 is physically mixed with hydrogel, BMP2 is released rapidly in vivo. Because of this short release phenomenon, when BMP2 is used to induce osteogenesis, it is administered at a very high concentration or by repeated administrations, both of which can induce side effects.

BMP2 typically has a net negative charge in the biological environment [109]. Therefore, BMP2 can interact with cationic electrolytes. Kim et al. prepared an injectable cationic hydrogel to electrostatically interact with BMP2 and reported an enhancement of the in vivo osteogenic differentiation of human turbinate mesenchymal stem cells [100].

In the case of cancer treatment, administering anticancer drugs at the local site is often very effective. Moreover, direct intratumoral injection

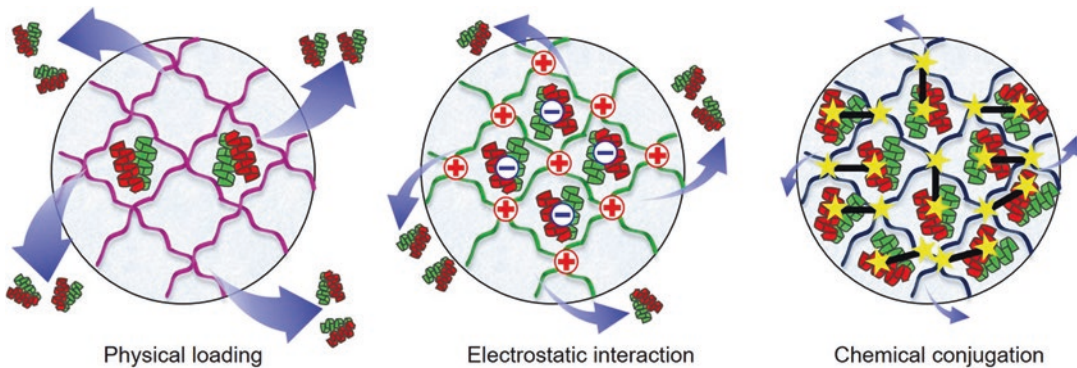


Fig. 3.3 Scheme image of injectable in situ-forming hydrogel for peptide and protein delivery application. (The image was drawn by S.H.P. and Y.B.J. using Adobe Photoshop7.0)

Table 3.3 Application of injectable hydrogels formed as therapeutic protein/peptide drug delivery depots

Application	Materials	Protein/peptide	Method for sustained release	Refs.
Bone regeneration	PCLA	BMP2	Electrostatic interaction	[100]
	PCL	BMP2	Covalent bond	[101]
Antitumor	PMNT-PEG-PMNT PCMS-PEG-PCMS	IL-12	Electrostatic interaction	[102]
Vascularization	Laponite/heparin	FGF-2	Electrostatic interaction	[103]
	Oligopeptide/PEG	TGF- β /VEGF	Covalent bond	[104]
Cartilage regeneration	HA	Cytomodulin	Covalent bond	[84]
		RGD	Covalent bond	[35]
Neural regeneration	Chitosan	IKVAV	Covalent bond	[105]
	HA/CMC	GRGDS	Covalent bond	[106]
Myocardial infarction	Chitosan/collagen	QHREDGS	Covalent bond	[107]
	Chitosan	RoY	Covalent bond	[108]

of anticancer drugs can suppress tumors very effectively and minimize toxicity against other organs [34, 110, 111].

Injectable in situ-forming hydrogels can easily be designed to contain anticancer drugs and deliver them directly by intratumoral injection. Several studies have reported on the anticancer effect using injectable in situ-forming hydrogel formulations. In one study, an injectable polyanionic hydrogel prepared was mixed with cationic protein (IL-12) to form an injectable hydrogel by electrostatic interaction to deliver IL-12 [102]. Cancer growth was inhibited with the injectable hydrogel to a greater extent than that seen when IL-12 was injected alone.

Ding et al. prepared an injectable in situ hydrogel using synthetic silicate laponite mixed with heparin and fibroblast growth factor-2 (FGF-2) [103]. The anionic hydrogel was injected subcutaneously into mice to slow the release of FGF-2 through electrostatic interaction between heparin and FGF-2. They reported that angiogenesis was enhanced when FGF-2 was administered with the injectable anionic hydrogel compared to when FGF-2 alone was injected.

3.4.2 Covalently Loaded Proteins/Peptides Inside Hydrogel

When proteins/peptides are introduced into a hydrogel through a chemical reaction, the release of proteins/peptides is slower than the release of

proteins/peptides that are physically loaded into hydrogels. However, the proteins/peptides may lose potency due to effects such as denaturation that occur during the chemical reaction. These problems can be solved either by milder reaction conditions or by using simple reactions rather than complex reactions at certain steps. As described in the previous section, the click reaction is useful for simply introducing proteins/peptides into a hydrogel. In addition, the reagents used in the reaction should be non-toxic and the by-products should be thoroughly removed if toxic.

Generally, the release of covalently loaded proteins/peptides is inhibited from hydrogel. If the hydrogel degrades slowly, the release of covalently loaded proteins/peptides occurs very slowly through breakdown of covalent bond between the proteins/peptides and the hydrogel.

Injectable covalent-loaded protein/peptide hydrogel can easily mix with stem cell. If proteins/peptides are differentiation factors, etc., the stem cells can differentiate to various tissues or organs through the inducing effect of proteins/peptides for a prolonged period.

Sun et al. have reported the enhancement of neural differentiation of neural stem cells in the hydrogel formed by chemically introducing the IKVAV peptide derived from laminin, one of the major components in neuron extracellular matrix [105].

Angiopoietin-1 can promote adhesion and growth of myocardial cells. Angiopoietin-1-

derived peptide (QHREDGS) has similar effect to angiotensin-1. An injectable in situ-forming chitosan hydrogel with chemically modified QHREDGS prepared and improved myocardial infarction by injecting into the myocardial infarction rats [107].

SVVYGLR peptide, which can induce angiogenesis, is chemically modified in the injectable gelatin hydrogel [112]. An injectable in situ-forming gelatin hydrogel with chemically modified SVVYGLR effectively formed new blood vessels by subcutaneous injecting into rats.

3.5 Summary and Outlook of Injectable In Situ-Forming Hydrogels

Recently, there have been a lot of studies to apply injectable in situ-forming hydrogels to biomedical field. Various methods are being developed to create clinically applicable injectable in situ-forming hydrogels. The successful results have been obtained in the clinical utilization of injectable in situ-forming hydrogels. However, many studies remain in the animal research stage, and thus much effort is needed to use them in clinical applications. The challenges are that clinical applications should minimize the immune response and avoid side effects and toxicity of injectable in situ-forming hydrogels. Additionally, the ultimate clinician should be easy to handle, and the patient should be minimally invasive and uncomfortable. Our knowledge of clinically relevant technologies for injectable in situ-forming hydrogel is now growing exponentially and will require collaborative research among biomaterial, biological, and clinical scientists.

Acknowledgment This study was supported by a grant from Creative Materials Discovery Program through the National Research Foundation (2019M3D1A1078938) and Priority Research Centers Program (2019R1A6A1A11051471) funded by the National Research Foundation of Korea (NRF).

References

1. Abedi-Koupai J, Sohrab F, Swarbrick G (2008) Evaluation of hydrogel application on soil water retention characteristics. *J Plant Nutr* 31(2):317–331
2. Narjary B, Aggarwal P, Singh A et al (2012) Water availability in different soils in relation to hydrogel application. *Geoderma* 187–188:94–101
3. Seo JY, Lee B, Kang TW et al (2018) Electrostatically interactive injectable hydrogels for drug delivery. *Tissue Eng Regen Med* 15(5):513–520
4. Park JH, Park SH, Lee HY et al (2018) An injectable, electrostatically interacting drug depot for the treatment of rheumatoid arthritis. *Biomaterials* 154:86–98
5. Chan BQY, Low ZW, Heng SJ et al (2016) Recent advances in shape memory soft materials for biomedical applications. *ACS Appl Mater Interfaces* 8:10070–10087
6. Cho KH, Uthaman S, Park IK et al (2018) Injectable biomaterials in plastic and reconstructive surgery: a review of the current status. *Tissue Eng Regen Med* 15(5):559–574
7. Bencherif SA, Sands RW, Bhatta D et al (2012) Injectable preformed scaffolds with shape-memory properties. *PNAS* 109(48):19590–19595
8. Kim DY, Kwon DY, Kwon JS et al (2015) Injectable in situ-forming hydrogels for regenerative medicines. *Polym Rev* 55:407–445
9. Jang JY, Park SH, Park JH et al (2016) In vivo osteogenic differentiation of human dental pulp stem cells embedded in an injectable in vivo-forming hydrogel. *Macromol Biosci* 16(8):1158–1169
10. Cui H, Zhuang X, He C et al (2015) High performance and reversible ionic polypeptide hydrogel based on charge-driven assembly for biomedical applications. *Acta Biomater* 11:183–190
11. Cui J, del Campo A (2012) Multivalent H-bonds for self-healing hydrogels. *Chem Commun (Camb)* 48(74):9302–9304
12. Gopinathan J, Noh I (2018) Click chemistry-based injectable hydrogels and bioprinting inks for tissue engineering applications. *Tissue Eng Regen Med* 15(5):531–546
13. Zhao L, Li X, Zhao J et al (2016) A novel smart injectable hydrogel prepared by microbial transglutaminase and human-like collagen: its characterization and biocompatibility. *Mater Sci Eng C Mater Biol Appl* 68:317–326
14. Gupta S, Jain A, Chakraborty M et al (2013) Oral delivery of therapeutic proteins and peptides: a review on recent developments. *Drug Deliv* 20(6):237–246
15. Almeida AJ, Souto E (2007) Solid lipid nanoparticles as a drug delivery system for peptides and proteins. *Adv Drug Deliv Rev* 59(6):478–490

16. Sontyana AG, Mathew AP, Cho KH et al (2018) Biopolymeric in-situ hydrogels for tissue engineering and bio-imaging applications. *Tissue Eng Regen Med* 15(5):575–590
17. Sood A, Panchagnula R (2001) Peroral route: an opportunity for protein and peptide drug delivery. *Chem Rev* 101(11):3275–3303
18. Koshy ST, Zhang DKY, Grolman JM et al (2018) Injectable nanocomposite cryogels for versatile protein drug delivery. *Acta Biomater* 65:36–43
19. Park MR, Seo BB, Song SC (2013) Dual ionic interaction system based on polyelectrolyte complex and ionic, injectable, and thermosensitive hydrogel for sustained release of human growth hormone. *Biomaterials* 34(4):1327–1336
20. Payyappilly S, Dhara S, Chattopadhyay S (2014) Thermoresponsive biodegradable PEG-PCL-PEG based injectable hydrogel for pulsatile insulin delivery. *J Biomed Mater Res A* 102(5):1500–1509
21. Huynh DP, Nguyen MK, Lee DS (2010) Controlling the degradation of pH/temperature-sensitive injectable hydrogels based on poly(β -amino ester). *Macromol Res* 18(2):192–199
22. Park JH, Lee BK, Park SH et al (2017) Preparation of biodegradable and elastic poly(ϵ -caprolactone-co-lactide) copolymers and evaluation as a localized and sustained drug delivery carrier. *Int J Mol Sci* 18(3):671
23. Hyun H, Park SH, Kwon DY et al (2014) Thermo-responsive injectable MPEG-polyester diblock copolymers for sustained drug release. *Polymers* 6(10):2670–2683
24. Lee BK, Park JH, Park SH et al (2017) Preparation of pendant group-functionalized diblock copolymers with adjustable thermogelling behavior. *Polymers* 9(6):239
25. Caykara T, Kiper S, Demirel G (2006) Thermosensitive poly(N-isopropylacrylamide-co-acrylamide) hydrogels: synthesis, swelling and interaction with ionic surfactants. *Eur Polym J* 42(2):348–355
26. Ni X, Cheng A, Li J (2009) Supramolecular hydrogels based on self-assembly between PEO-PPO-PEO triblock copolymers and alpha-cyclodextrin. *J Biomed Mater Res A* 88(4):1031–1036
27. Zhang J, Peppas N (2000) Synthesis and characterization of pH- and temperature-sensitive poly(methacrylic acid)/poly(n-isopropylacrylamide) interpenetrating polymeric networks. *Macromolecules* 33:102–107
28. Kim JI, Kim DY, Kwon DY et al (2012) An injectable biodegradable temperature-responsive gel with an adjustable persistence window. *Biomaterials* 33(10):2823–2834
29. Lee HY, Park JH, Ji YB et al (2018) Preparation of pendant group-functionalized amphiphilic diblock copolymers in the presence of a monomer activator and evaluation as temperature-responsive hydrogels. *Polymer* 137:293–302
30. Bidarra SJ, Barrias CC, Granja PL (2014) Injectable alginate hydrogels for cell delivery in tissue engineering. *Acta Biomater* 10(4):1646–1662
31. Lu S, Gao C, Xu X et al (2015) Injectable and self-healing carbohydrate-based hydrogel for cell encapsulation. *ACS Appl Mater Interfaces* 7(23):13029–13037
32. Tan H, Rubin JP, Marra KG (2010) Injectable in situ forming biodegradable chitosan-hyaluronic acid based hydrogels for adipose tissue regeneration. *Organogenesis* 6(3):173–180
33. Zhang L, Ma Y, Pan X et al (2018) A composite hydrogel of chitosan/heparin/poly (gamma-glutamic acid) loaded with superoxide dismutase for wound healing. *Carbohydr Polym* 180:168–174
34. Park SH, Kim DY, Panta P et al (2017) An intratumoral injectable, electrostatic, cross-linkable curcumin depot and synergistic enhancement of anticancer activity. *NPG Asia Mater* 9:e397
35. Chen F, Ni Y, Liu B et al (2017) Self-crosslinking and injectable hyaluronic acid/RGD-functionalized pectin hydrogel for cartilage tissue engineering. *Carbohydr Polym* 166:31–44
36. Yucel Falco C, Falkman P, Risbo J et al (2017) Chitosan-dextran sulfate hydrogels as a potential carrier for probiotics. *Carbohydr Polym* 172:175–183
37. Liu Z, Yao P (2015) Injectable thermo-responsive hydrogel composed of xanthan gum and methylcellulose double networks with shear-thinning property. *Carbohydr Polym* 132:490–498
38. Gulyuz U, Okay O (2014) Self-healing poly(acrylic acid) hydrogels with shape memory behavior of high mechanical strength. *Macromolecules* 47:6889–6899
39. Moreno E, Schwartz J, Larraneta E et al (2014) Thermosensitive hydrogels of poly(methyl vinyl ether-co-maleic anhydride) - Pluronic((R)) F127 copolymers for controlled protein release. *Int J Pharm* 459(1–2):1–9
40. Li Y, Liu C, Tan Y et al (2014) In situ hydrogel constructed by starch-based nanoparticles via a Schiff base reaction. *Carbohydr Polym* 110:87–94
41. Lawrence PG, Lapitsky Y (2015) Ionically cross-linked poly(allylamine) as a stimulus-responsive underwater adhesive: ionic strength and pH effects. *Langmuir* 31(4):1564–1574
42. Alatorre-Meda M, Taboada P, Krajewska B et al (2010) DNA-poly(diallyldimethylammonium chloride) complexation and transfection efficiency. *J Phys Chem B* 114(29):9356–9366
43. Soto AM, Koivisto JT, Parraga JE et al (2016) Optical projection tomography technique for image texture and mass transport studies in hydrogels based on gellan gum. *Langmuir* 32(20):5173–5182
44. Lopez-Cebral R, Paolicelli P, Romero-Caamano V et al (2013) Spermidine-cross-linked hydrogels as novel potential platforms for pharmaceutical applications. *J Pharm Sci* 102(8):2632–2643

45. Han SC, He WD, Li J et al (2009) Reducible polyethylenimine hydrogels with disulfide crosslinkers prepared by michael addition chemistry as drug delivery carriers: synthesis, properties, and in vitro release. *J Polym Sci A Polym Chem* 47(16):4074–4082
46. Lee HY, Park SH, Kim JH et al (2017) Temperature-responsive hydrogels via electrostatic interaction of amphiphilic diblock copolymers with pendant-ion groups. *Polym Chem* 8(43):6606–6616
47. Oupický D, Konák C, Ulbrich K (1999) DNA complexes with block and graft copolymers of N-(2-hydroxypropyl)methacrylamide and 2-(trimethylammonio)ethyl methacrylate. *J Biomater Sci Polym Ed* 10(5):573–590
48. Brovarets OO, Yurenko YP, Hovorun DM (2015) The significant role of the intermolecular CH...O/N hydrogen bonds in governing the biologically important pairs of the DNA and RNA modified bases: a comprehensive theoretical investigation. *J Biomol Struct Dyn* 33(8):1624–1652
49. Xiao XC, Chu LY, Chen WM et al (2005) Monodispersed thermoresponsive hydrogel microspheres with a volume phase transition driven by hydrogen bonding. *Polymer* 46(9):3199–3209
50. Kimura M, Fukumoto K, Watanabe J et al (2012) Hydrogen-bonding-driven spontaneous gelation of water-soluble phospholipid polymers in aqueous medium. *J Biomater Sci Polym Ed* 15(5):631–644
51. Zhang S, Fu W, Li Z (2014) Supramolecular hydrogels assembled from nonionic poly(ethylene glycol)-b-polypeptide diblocks containing OEGylated poly-l-glutamate. *Polym Chem* 5:3346–3351
52. Zhang YX, Chen YF, Shen XY et al (2016) Reduction- and pH-sensitive lipopeptide acid-modified poly(L-lysine) and polypeptide/silica hybrid hydrogels/nanogels. *Polymer* 86:32–41
53. Gao H, Wang N, Hu X et al (2013) Double hydrogen-bonding pH-sensitive hydrogels retaining high-strengths over a wide pH range. *Macromol Rapid Commun* 34(1):63–68
54. Chirila TV, Lee HH, Odon M et al (2014) Hydrogen-bonded supramolecular polymers as self-healing hydrogels: effect of a bulky adamantyl substituent in the ureido-pyrimidinone monomer. *J Appl Polym Sci* 131:39932
55. Yucel T, Cebe P, Kaplan DL (2009) Vortex-induced injectable silk fibroin hydrogels. *Biophys J* 97(7):2044–2050
56. Ozbas B, Kretsinger J, Rajagopal K et al (2004) Salt-triggered peptide folding and consequent self-assembly into hydrogels with tunable modulus. *Macromolecules* 37(19):7331–7337
57. Chen Y, Pang XH, Dong CM (2010) Dual stimuli-responsive supramolecular polypeptide-based hydrogel and reverse micellar hydrogel mediated by host-guest chemistry. *Adv Funct Mater* 20(4):579–586
58. Miyamae K, Nakahata M, Takashima Y et al (2015) Self-healing, expansion-contraction, and shape-memory properties of a preorganized supramolecular hydrogel through host-guest interactions. *Angew Chem Int Ed Engl* 54(31):8984–8987
59. Zhang M, Xu D, Yan X et al (2012) Self-healing supramolecular gels formed by crown ether based host-guest interactions. *Angew Chem Int Ed Engl* 51(28):7011–7015
60. Wu Y, Guo B, Ma PX (2014) Injectable electroactive hydrogels formed via host-guest interactions. *ACS Macro Lett* 3(11):1145–1150
61. Li C, Rowland MJ, Shao Y et al (2015) Responsive double network hydrogels of interpenetrating dna and CB[8] host-guest supramolecular systems. *Adv Mater* 27(21):3298–3304
62. Seo JY, Park SH, Kim MJ et al (2019) Injectable click-crosslinked hyaluronic acid depot to prolong therapeutic activity in articular joints affected by rheumatoid arthritis. *ACS Appl Mater Interface* 11(28):24984–24998
63. Piluso S, Hiebel B, Gorb SN et al (2018) Hyaluronic acid-based hydrogels crosslinked by copper-catalyzed azide-alkyne cycloaddition with tailorable mechanical properties. *Int J Artif Organs* 34(2):192–197
64. Pahimanolis N, Sorvari A, Luong ND et al (2014) Thermoresponsive xylan hydrogels via copper-catalyzed azide-alkyne cycloaddition. *Carbohydr Polym* 102:637–644
65. Koshy ST, Desai RM, Joly P et al (2016) Click-crosslinked injectable gelatin hydrogels. *Adv Health Mater* 5(5):541–547
66. Desai RM, Koshy ST, Hilderbrand SA et al (2015) Versatile click alginate hydrogels crosslinked via tetrazine-norbornene chemistry. *Biomaterials* 50:30–37
67. Hermann CD, Wilson DS, Lawrence KA et al (2014) Rapidly polymerizing injectable click hydrogel therapy to delay bone growth in a murine re-synostosis model. *Biomaterials* 35(36):9698–9708
68. Takahashi A, Suzuki Y, Sahara T et al (2013) In situ cross-linkable hydrogel of hyaluronan produced via copper-free click chemistry. *Biomacromolecules* 14(10):3581–3588
69. Jiang H, Qin S, Dong H et al (2015) An injectable and fast-degradable poly(ethylene glycol) hydrogel fabricated via bioorthogonal strain-promoted azide-alkyne cycloaddition click chemistry. *Soft Matter* 11(30):6029–6036
70. Wang X, Li Z, Shi T et al (2017) Injectable dextran hydrogels fabricated by metal-free click chemistry for cartilage tissue engineering. *Mater Sci Eng C Mater Biol Appl* 73:21–30
71. Fan M, Ma Y, Mao J et al (2015) Cytocompatible in situ forming chitosan/hyaluronan hydrogels via a metal-free click chemistry for soft tissue engineering. *Acta Biomater* 20:60–68
72. Truong VX, Tsang KM, Simon GP et al (2015) Photodegradable gelatin-based hydrogels prepared by bioorthogonal click chemistry for cell

- encapsulation and release. *Biomacromolecules* 16(7):2246–2253
73. Bai X, Lu S, Cao Z et al (2017) Dual crosslinked chondroitin sulfate injectable hydrogel formed via continuous Diels-Alder (DA) click chemistry for bone repair. *Carbohydr Polym* 166:123–130
 74. Fuhrmann T, Obermeyer J, Tator CH et al (2015) Click-crosslinked injectable hyaluronic acid hydrogel is safe and biocompatible in the intrathecal space for ultimate use in regenerative strategies of the injured spinal cord. *Methods* 84:60–69
 75. Bi B, Ma M, Lv S et al (2019) In-situ forming thermosensitive hydroxypropyl chitin-based hydrogel crosslinked by Diels-Alder reaction for three dimensional cell culture. *Carbohydr Polym* 212:368–377
 76. Abandansari HS, Ghania MH, Varzideh F et al (2018) In situ formation of interpenetrating polymer network using sequential thermal and click cross-linking for enhanced retention of transplanted cells. *Biomaterials* 170:12–25
 77. Fan M, Ma Y, Zhang Z et al (2015) Biodegradable hyaluronic acid hydrogels to control release of dexamethasone through aqueous Diels-Alder chemistry for adipose tissue engineering. *Mater Sci Eng C Mater Biol Appl* 56:311–317
 78. Wang G, Cao X, Dong H et al (2018) A hyaluronic acid based injectable hydrogel formed via photocrosslinking reaction and thermal-induced Diels-alder reaction for cartilage tissue engineering. *Polymers* 10(9):949
 79. Huang J, Jiang X (2018) Injectable and degradable pH-responsive hydrogels via spontaneous aminopyne click reaction. *ACS Appl Mater Interfaces* 10(1):361–370
 80. Wang J, He H, Cooper RC et al (2017) In situ-forming polyamidoamine dendrimer hydrogels with tunable properties prepared via Aza-Michael addition reaction. *ACS Appl Mater Interfaces* 9(12):10494–10503
 81. Dong Y, Saeed AO, Hassan W et al (2012) “One-step” preparation of thiol-ene clickable PEG-based thermoresponsive hyperbranched copolymer for in situ crosslinking hybrid hydrogel. *Macromol Rapid Commun* 33(2):120–126
 82. Maturavongsadit P, Luckanagul JA, Metavarayuth K et al (2016) Promotion of in vitro chondrogenesis of mesenchymal stem cells using in situ hyaluronic hydrogel functionalized with rod-like viral nanoparticles. *Biomacromolecules* 17(6):1930–1938
 83. Kim K, Park JH, Park SH et al (2016) An injectable, click-cross-linked small intestinal submucosa drug depot for the treatment of rheumatoid arthritis. *Adv Healthc Mater* 5(24):3105–3117
 84. Park SH, Seo JY, Park JY et al (2019) An injectable, click-crosslinked, cytomodulin-modified hyaluronic acid hydrogel for cartilage tissue engineering. *NPG Asia Mater* 11:30
 85. Hardy JG, Lin P, Schmidt CE (2015) Biodegradable hydrogels composed of oxime crosslinked poly(ethylene glycol), hyaluronic acid and collagen: a tunable platform for soft tissue engineering. *J Biomater Sci Polym Ed* 26(3):143–161
 86. Yang X, Shi L, Guo X et al (2016) Convergent in situ assembly of injectable lipogel for enzymatically controlled and targeted delivery of hydrophilic molecules. *Carbohydr Polym* 154:62–69
 87. Truong VX, Hun ML, Li F et al (2016) In situ-forming click-crosslinked gelatin based hydrogels for 3D culture of thymic epithelial cells. *Biomater Sci* 4(7):1123–1131
 88. Jin R, Lin C, Cao A (2014) Enzyme-mediated fast injectable hydrogels based on chitosan–glycolic acid/tyrosine: preparation, characterization, and chondrocyte culture. *Polym Chem* 5(2):391–398
 89. Park KM, Park KD (2018) In situ cross-linkable hydrogels as a dynamic matrix for tissue regenerative medicine. *Tissue Eng Regen Med* 15(5):547–557
 90. Jin R, Moreira Teixeira LS, Dijkstra PJ et al (2010) Enzymatically crosslinked dextran-tyramine hydrogels as injectable scaffolds for cartilage tissue engineering. *Tissue Eng Part A* 16(8):2429–2440
 91. Bode F, da Silva MA, Drake AF et al (2011) Enzymatically cross-linked tilapia gelatin hydrogels: physical, chemical, and hybrid networks. *Biomacromolecules* 12(10):3741–3752
 92. Park KM, Ko KS, Joung YK et al (2011) In situ cross-linkable gelatin–poly(ethylene glycol)–tyramine hydrogel via enzyme-mediated reaction for tissue regenerative medicine. *J Mater Chem* 21(35):13180
 93. Ranga A, Lutolf MP, Hilborn J et al (2016) Hyaluronic acid hydrogels formed in situ by transglutaminase-catalyzed reaction. *Biomacromolecules* 17(5):1553–1560
 94. Lee F, Chung JE, Kurisawa M (2008) An injectable enzymatically crosslinked hyaluronic acid–tyramine hydrogel system with independent tuning of mechanical strength and gelation rate. *Soft Matter* 4:880–887
 95. Yang Z, Xu B (2007) Supramolecular hydrogels based on biofunctional nanofibers of self-assembled small molecules. *J Mater Chem* 17(23):2385–2393
 96. Srinivasan G, Chen J, Parisi J et al (2015) An injectable PEG-BSA-coumarin-GOx hydrogel for fluorescence turn-on glucose detection. *Appl Biochem Biotechnol* 177(5):1115–1126
 97. Mosiewicz KA, Johnsson K, Lutolf M (2010) Phosphopantetheinyl transferase-catalyzed formation of bioactive hydrogels for tissue engineering. *J Am Chem Soc* 132(17):5972–5974
 98. Ren K, He C, Cheng Y et al (2014) Injectable enzymatically crosslinked hydrogels based on a poly(l-glutamic acid) graft copolymer. *Polym Chem* 5(17):5069–5076
 99. Vermonden T, Censi R, Hennink WE (2012) Hydrogels for protein delivery. *Chem Rev* 112(5):2853–2888
 100. Kim MG, Kang TW, Park JY et al (2019) An injectable cationic hydrogel electrostatically interacted with BMP2 to enhance in vivo osteogenic

- differentiation of human turbinate mesenchymal stem cells. *Mater Sci Eng C* 103:109853
101. Park SH, Kwon JS, Lee BS et al (2017) BMP2-modified injectable hydrogel for osteogenic differentiation of human periodontal ligament stem cells. *Sci Rep* 7(1):6603
 102. Ishii S, Kaneko J, Nagasaki Y (2016) Development of a long-acting, protein-loaded, redox-active, injectable gel formed by a polyion complex for local protein therapeutics. *Biomaterials* 84:210–218
 103. Ding X, Gao J, Wang Z et al (2016) A shear-thinning hydrogel that extends in vivo bioactivity of FGF2. *Biomaterials* 111:80–89
 104. Seliktar D, Zisch AH, Lutolf MP et al (2004) MMP-2 sensitive, VEGF-bearing bioactive hydrogels for promotion of vascular healing. *J Biomed Mater Res A* 68(4):704–716
 105. Yu LM, Kazazian K, Shoichet MS (2007) Peptide surface modification of methacrylamide chitosan for neural tissue engineering applications. *J Biomed Mater Res A* 8(1):243–255
 106. Tam RY, Cooke MJ, Shoichet MS (2012) A covalently modified hydrogel blend of hyaluronan–methyl cellulose with peptides and growth factors influences neural stem/progenitor cell fate. *J Mater Chem* 22(37):19402–19411
 107. Reis LA, Chiu LL, Wu J et al (2015) Hydrogels with integrin-binding angiopoietin-1-derived peptide, QHREDGS, for treatment of acute myocardial infarction. *Circ Heart Fail* 8(2):333–341
 108. Shu Y, Hao T, Yao F et al (2015) RoY peptide-modified chitosan-based hydrogel to improve angiogenesis and cardiac repair under hypoxia. *ACS Appl Mater Interfaces* 7(12):6505–6517
 109. Chung EJ, Chien KB, Aguado BA et al (2012) Osteogenic potential of BMP-2-releasing self-assembled membranes. *Tissue Eng Part A* 19(23–24):2664–2673
 110. Seo HW, Kim DY, Kwon DY et al (2013) Injectable intratumoral hydrogel as 5-fluorouracil drug depot. *Biomaterials* 34(11):2748–2757
 111. Kim DY, Kwon DY, Kwon JS et al (2016) Synergistic anti-tumor activity through combinational intratumoral injection of an in-situ injectable drug depot. *Biomaterials* 85:232–245
 112. Park KM, Lee Y, Son JY et al (2012) In situ SVVYGLR peptide conjugation into injectable gelatin-poly(ethylene glycol)-tyramine hydrogel via enzyme-mediated reaction for enhancement of endothelial cell activity and neo-vascularization. *Bioconjug Chem* 23(10):2042–2050



Alginate Hydrogels: A Tool for 3D Cell Encapsulation, Tissue Engineering, and Biofabrication

Walter Bonani, Nicola Cagol, and Devid Maniglio

Abstract

A wide variety of hydrogels have been proposed for tissue engineering applications, cell encapsulation, and bioinks for bioprinting applications. Cell-laden hydrogel constructs rely on natural hydrogels such as alginate, agarose, chitosan, collagen, gelatin, fibroin, and hyaluronic acid (HA), as well as on synthetic hydrogels such as poloxamers (Pluronic[®]) and polyethylene glycol (PEG). Alginate has become more and more important in the last years, thanks to the possibility to prepare alginate hydrogels suitable for cell encapsulation mainly because of the mild and reversible cross-linking conditions. In this paper alginate will be described in detail with respect to its chemistry, cross-linking behavior, biocompatibility, manufacturing capacity, and possible modifications.

Keywords

Sodium alginate · Hydrogels · Cell encapsulation · Bioprinting

4.1 Introduction

Hydrogels represent one of the most common scaffolding materials in tissue engineering and are used to provide bulk and mechanical constitution to a tissue construct, whether cells and bioactive compounds are adhered to or suspended within the 3D gel framework [1, 2].

Hydrogels possess many properties which are attractive as stand-alone tissue scaffolds or vehicles to deliver drugs, growth factors, or cell therapies: cytocompatibility, tissue mimetic water content, support of cell migration and tissue integration, sustained release of growth factors, and controllable physical properties [3, 4].

Hydrogels used in tissue engineering applications are predominantly based on natural derived polymers, including alginate, gelatin, collagen, chitosan, silk fibroin, fibrin, and hyaluronic acid, because of their inherent excellent cytocompatibility, low toxicity, and susceptibility to enzymatic degradation [5]. Natural hydrogels, derived from polysaccharide or proteins, offer inherent bioactivity except for agarose and alginate and display a chemical and structural resemblance to ECM [6]. Synthetic hydrogels which lack bio-

W. Bonani
Directorate for Nuclear Safety and Security,
European Commission, Joint Research Centre,
Karlsruhe, Germany

Department of Industrial Engineering and BIOTech
Research Center, University of Trento, Trento, Italy

N. Cagol · D. Maniglio (✉)
Department of Industrial Engineering and BIOTech
Research Center, University of Trento, Trento, Italy
e-mail: devid.maniglio@unitn.it

logic stimuli often require modification to introduce chemical and physical signals for instructive cell and tissue responses [4, 7].

Natural and synthetic hydrogels are particularly attractive for biofabrication as artificial ECM to generate physiologically relevant 3D scaffolds for cell and tissue growth. In fact, hydrogels are good candidates for encapsulating cells during their fabrication process: cell-laden hydrogel can serve as building blocks for the assembly of organ-like or tissue-like structures [7, 8] or can be used in conjunction with a set of additive manufacturing techniques that go under the name of bioprinting [9, 10]. The principle of bioprinting can be defined as the use of automated 3D robotic technologies in order to place cell-laden materials into spatially defined structures. The raw materials of bioprinting process, soft biomaterials loaded with living cells, are called “bioinks” [9, 11]. Various key properties including concentration, molecular weight, viscosity, gelation kinetics, and stiffness can be selected according to the specific bioink requirements [9, 11, 12].

Moreover, hydrogels are also suitable to keep cells and fluid separate while allowing diffusion of soluble factors within their structure. This property can be used to encapsulate cells in micron- to millimeter-size capsules that can serve as delivery vehicles for cell-based therapies [2, 13]. These microcapsules can also be engineered to allow for the diffusion of nutrients and removal of metabolites while prohibiting interaction of encapsulated cells with the immune system, therefore avoiding the rejection of the implant by the host [13, 14]. Therefore, encapsulation of cell offers several potential applications as the encapsulated cells can be transplanted within a host organism, permitting immune system insulation but allowing secretion and delivery of specific disease-treating molecules (e.g., against diabetes [15], anemia [16], or hemophilia [17]), as better described in 1.2.

A wide variety of hydrogels have been experimented within biofabrication, both for encapsulating cell into building blocks or as bioink for bioprinting applications [1–8]. Cell-laden hydrogel formulations utilize natural hydrogels such as

alginate, agarose, chitosan, collagen, gelatin, fibroin, and hyaluronic acid (HA), as well as synthetic hydrogels such as Pluronic (poloxamer) and polyethylene glycol (PEG), or blends. Several review papers have been published about hydrogels used for tissue engineering, and for detailed information about a wide variety of materials, the reader is referred to the works of Gasperini et al. [2], Ahmed [9], Peppas et al. [10], and Kuen Yong Lee and David J Mooney [11]. Natural hydrogels, derived from polysaccharide or proteins, offer inherent bioactivity, except for agarose and alginate, and display a chemical and structural resemblance to ECM [12–16].

Sodium alginate, or alginate, is a naturally occurring polysaccharide derived from brown seaweeds. Microbeads obtained by gelation of a sodium alginate solution were used for the first time in the 1980s to encapsulate pancreatic islets and are currently used for encapsulating different cell types and therapeutic agents [17, 18]. Alginate is the material of choice for many cell encapsulation applications because of its proven cytocompatibility, rapid ionic gelation property with divalent cation, hydrophilic nature, and tunable properties [19]. It has been used as a biomaterial in clinic for different applications, such as wound healing, bone graft substitute for spine fusion, and cell therapy [18, 20]. For the peculiar characteristics (particularly gelling capacity, low toxicity, high availability, and low cost), alginate hydrogels are widely adopted as base materials for scaffold realization, particularly for bone tissue engineering, or for bioink formulation [21]. In fact, alginate hydrogels can constitute an optimal substrate for cell loading and, as a consequence of the fast ionic cross-linking, they can be easily injected, making them outperforming with respect to other materials used for solid scaffold fabrication.

4.1.1 Alginate Structure and Chemistry

Alginic acid, or algin, is a natural anionic polysaccharide occurring mainly in the intracellular matrix of brown algae like many seaweeds from

the class Phaeophyceae. The term “alginate” is commonly used to define the metal salts of the alginic acid. Commercially available alginates are extracted from algae, but synthesis by microbial fermentation is possible and well documented [27]. Within the algae cell walls, alginate is in the form of an insoluble hydrated gel containing metal counterions like sodium, calcium, magnesium, strontium, and barium, which also contribute to stabilize the gel. First, algae are harvested, and water-insoluble alginic acid is extracted from dried algal tissue by acid conversion of insoluble alginate salts. Then, insoluble alginic acid is converted into water-soluble sodium alginate by alkali neutralization with sodium hydroxide or sodium carbonate. After a series of flocculation/floatation and filtration/centrifugation steps to remove seaweed residues, the water-soluble sodium salt of alginic acid is recovered by acid or alcohol precipitation [22, 28].

Alginates are linear polymers consisting of (1'4')-linked residues of β -D-mannuronic acid (M) and α -L-guluronic acid (G). Depending on the derivative algae species, the polymer backbone structure can consist of pure (G) blocks, pure (M) blocks, (GM-alternating) blocks and (GM-random) blocks with different length and organization [22]. The arrangement and relative amount of the different blocks depend also from the harvesting time and the extraction procedures itself [30]. The ratio between (G) and (M) blocks influences the mechanical properties of the alginate hydrogel as the (G) blocks are involved in the cross-linking mechanism of alginate hydrogels [2]. In fact, alginate molecules undergo ionotropic gelation in water solution in the presence of divalent cations, typically Ca^{2+} , Mg^{2+} , or Ba^{2+} , that interact with (G) blocks to form ionic interchain bridges [31].

The water solubility of sodium alginate and the viscosity of the resulting solution are pH-related. At physiological condition, alginate molecules are fully solubilized and present an extended random coil conformation; when reducing pH, alginate chains develop intermolecular hydrogen bonds, resulting in an increase of solution viscosity and, eventually, in the for-

mation of gelatinous precipitates at extremely low pH [22].

4.1.1.1 Alginate Hydrogels

The gelation of sodium alginate solutions can occur via two different processes: ionic or covalent cross-linking. The ionic gelation occurs in the presence of divalent cations such as Ca^{2+} , Sr^{2+} , and Ba^{2+} . When they are added to a water-based sodium alginate solution, they bind two adjacent residues allowing the formation of ionic interchain bridges that cause a fast sol-gel transition. The amount and the type of the gel-forming ions and the gelling conditions, such as temperature, also affect the network structure and permeability. In fact, the alginate gel is characterized by a wide pore size distribution, and its porosity is strongly influenced by the nature and concentration of gelling ions [12, 22].

Once the gel is formed, it can be dissolved by the exchange of ions with a buffer (e.g., phosphate buffer saline without calcium) or by treatment with a chelating agent for divalent cations such as ethylenediaminetetraacetic acid (EDTA) or sodium citrate. This can be useful to gently release cells entrapped in alginate hydrogels for further downstream processing [22]. On the other side, because these gels can be dissolved due to release of divalent cations into the surrounding media, a critical drawback of ionically cross-linked alginate gels is the limited long-term stability in physiological condition. The formation of an intermolecular gel network is compatible with the survival of cells that will be evenly distributed throughout the hydrogel if suspended in the alginate solution prior to gelation [22, 23]. In alternative to ionic cross-linking, covalently cross-linked hydrogels can be obtained with chemically modified sodium alginate. Different diamines and dihydrazides have been used to covalently cross-link alginate, and photo-cross-linkable hydrogels can be obtained in the presence of a photoinitiator and UV light after conjugating methacrylate groups onto the alginate backbone. Covalent cross-linked hydrogels allow better control over the physical properties and provide better chemical stability. However, covalent cross-linking reagents may be toxic, and the process is not as easily reversible as in the case of ionic gelation

[22, 23]. Moreover, the possibility of delayed gelation was exploited to develop in situ injectable hydrogels for cell delivery [33].

4.1.2 Therapeutic Applications of Cell-Laden Alginate Hydrogels

Pancreatic islets were the first cells immobilized in calcium alginate matrices by Lim and Sun at the end of the 1970s in order to treat diabetes [17]. From that time, several approaches and adaptations of mammalian cell culture have utilized alginate gels as a model system in biomedical studies and for manufacturing cell therapy constructs [20, 24]. Alginate gels can be adapted to serve as either 2D or 3D culture systems, being the latter more relevant from a physiological standpoint. Alginate gels may serve as an ideal blank slate, due to the low protein adsorption and lack of mammalian cell receptors for alginate. The limited inherent cell adhesion and cellular interaction can be an advantage for cell encapsulation applications, but can limit the use of cell-laden constructs for tissue engineering applications [25, 26]. Different biochemical modifications can be used to adapt alginate matrix to guide adhesion and function of specific cells and will be discussed later. The use of alginate hydrogels for the realization of scaffolds and cellular constructs as an alternative to cell culture in 2D includes the formation of beads, fibers, membranes, meshes, foams, and other hydrogel structures that can serve as building blocks according to the biofabrication paradigm [22, 27]. The role of alginate in pharmaceuticals and biomedical engineering includes also different applications. Alginate is a commonly used polymer for sustained and localized drug delivery applications, and different binding and gelation mechanisms allow to tune the sequence and rate of release [28]. In the form of sponges, hydrogels, and electrospun materials, alginate-based wound dressings have been used as substrates for the treatment of acute and chronic wounds, as they offer many advantages including hemostatic

capability and gel-forming ability upon adsorption [19].

Encapsulation in alginate hydrogels has shown to be an easy, non-toxic, and versatile method for immobilization of cells, and many studies describe the use of this technique for treating different diseases comprehending liver failure [29], Parkinson's disease [30], anemia [31], brain tumors [30], cartilage [32], and bone injuries [33]. In this process, living cells are suspended in alginate solution that is then dripped or extruded into a bath containing calcium chloride or other divalent ions. Since the ionic cross-linking reaction is instantaneous, the cells remain entrapped inside the hydrogel matrix. Oxygen and nutrients can diffuse into the gel, and cell products can diffuse outside the matrix. However, the hydrogel represents a barrier to antibodies and immune cells, and implantation studies into animals and diabetic patients have demonstrated long-term functionality of alginate hydrogel constructs containing cells [18]. Therefore, cell-laden alginate hydrogel constructs can be implanted into animals or humans and serve as "biofactory" for the continuous production of proteins or therapeutic agents as, for example, insulin [18, 20]. Alginate hydrogels have been also broadly used for the sustained and localized delivery of encapsulated drugs or growth factor by controlled release from the cross-linked matrix. Growth factor can promote or impede cell migration, differentiation, and proliferation, and they can be combined and delivered from the hydrogel by exploiting different mechanisms, which allows tuning the sequence and rate of release [26]. As an example, Li and colleagues investigated the release of vascular endothelial growth factor (VEGF), a potent angiogenic molecule, from poly-L-lysine-coated VEGF/alginate microspheres for promoting the vascularization of tissue-engineered bone graft [34].

4.1.3 Alginate-Based Cell Encapsulation Systems

A major disadvantage of alginate constructs and bioinks is the formation of relatively soft gels at

lower concentrations, even after cross-linking. On the other hand, high-concentration gels possess high stiffness and low diffusion properties, thus hampering cell proliferation and functionality. Therefore, it is challenging to print multilayered structures which can recapitulate the complexity of tissue-like structures [35]. In this framework, modular approaches would confer the ability to scale up by assembling layer by layer building blocks to create macroscopic tissue constructs.

The size of the hydrogel constructs is another critical parameter for biomedical application of encapsulated cells. The bead, fiber, or printed bioinks must be large enough to contain the biological material, and larger constructs are also easier to handle during washing or further assembling processes. However, the absence of convection movement within a capsule induces an oxygen and nutrient gradient from the surface to the construct resulting in necrosis of the inner cells [36]. In fact, although the nanoscale porosity of alginate gel permits the diffusion of solutes through its network, this process is limited when the size of the construct increases. A study published by Gasperini et al. identified a critical diffusion distance of about 400 μm for the long-term survival of B50 rat neuronal cells in the case of 2%_{wt} alginate hydrogels loaded with a cell density of five million cells per mL [37]. Specific types of geometry should be designed in order to counterbalance issues regarding the size of an alginate-based cell culture system.

4.1.3.1 Alginate Microbeads

One of the most studied supports for alginate cell encapsulation are microbeads that can be produced through electro-hydrodynamic process. In this process, an electrostatic potential is applied to a needle and used to deposit alginate droplets in the coagulation bath where gelation occurs [37]. Cells encapsulated with this technique remain viable inside the beads and are able to proliferate once released from the matrix, as demonstrated in the work of Liaudanskaya et al. [38].

Other techniques that can be used to encapsulate cells in alginate beads include coaxial air

or liquid flow [39], the use of micromolding platform [40], microfluidic-based emulsification [41], and the use of superhydrophobic substrates [42]. Alginate has been used for encapsulating pancreatic islets since it provides some advantages over other system. It does not interfere with cellular functions, encapsulation can be done at physiological conditions, and it can facilitate the functional survival of the islets when enveloped in microcapsules before long-term tissue culture [43].

4.1.3.2 Alginate Microfibers

Cell-laden microfibers are recognized as another appropriate form of building blocks for assembling cell-laden constructs in vitro because many important human tissue and organs are composed of fiber-based or network-like structures [44, 45]. Meter-long cell-laden fibers can be formed starting from a solution of alginate containing cells using techniques like electrospinning, wet spinning, microfluidic spinning, interfacial complexation, and melt spinning [44, 45]. In addition to cell-encapsulating structures, microfibers can also function as support for cell seeding and thus represent a versatile framework [46, 47]. The use of cell-laden fibers allows the use of textile technologies for making fabrics and cell-laden structures with precise control over the distribution of different cell types and anisotropic mechanical properties within the constructs. In fact, these fibers can be further assembled by weaving, knitting, and reeling into macroscopic cellular structures with various spatial patterns and used as templates for the reconstruction of fiber-shaped functional tissues that mimic muscle fibers, blood vessels, or nerve networks in vivo [45, 46]. Alginate is the most frequently used material for manufacturing cell-laden microfibers, thanks to its easy handling properties and its prepolymer solution, gelation agent, and coagulation bath being all compatible with living cells. Alginate-based microfibers can be easily formed with wet-spinning method, extruding the pre-gel solution containing cells into a gelator solution where it continuously polymerizes by using a syringe needle or micronozzle array. As an example, Lee and colleagues reported the successful encapsulation

of cells within alginate and alginate-chitosan fibers using a wet-spinning microfluidic chip [48]. Nevertheless, since cells cannot adhere on the surface of the alginate hydrogel due to its biological inertia, alginate-based microfibers are typically employed as cell-encapsulating building blocks. In addition, alginate-based microfibers with cell-adhesive materials have been fabricated in order to improve cell adhesion. For example, Onoe et al. developed a double-coaxial laminar flow microfluidic device to create meter-long functional microfibers with a mixture of extracellular matrix proteins and cells as the core and alginate hydrogel as the shell [49]. Akbari and colleagues reported the use of alginate hydrogels containing cells as coatings for synthetic polymer cores in order to create composite living fibers, subsequently assembled using regular textile processes [50]. Alginate microfibers found also application for treating various diseases. In the work of Jue et al., primary pancreatic islets and hepatocytes in the form of hybrid spheroids were encapsulated in collagen-alginate composite microfibers using a microfluidic chip. The xenogenic transplantation of these constructs in vivo showed great promises for treating end-stage liver diseases [51].

4.1.3.3 Alginate Hydrogels as Bioinks for Bioprinting

Alginate hydrogels are also widely used as a bioink for bioprinting applications, due to their compatibility with cells, fast gelation rate, and the ability to control biodegradation. In fact, alginate is reasonably easy to print, as it is easy to process and extrude while protecting the encapsulated cells [22, 27]. Moreover, using alginate it is possible to create long-term persistent cell-laden structures, whereas the slow degradation kinetics of the hydrogel can be tuned by oxidation or by modifying the molecular weight distribution of the polymer itself [52–54].

Alginate hydrogels possess shear thinning properties, and, therefore, their viscosity is dependent on the strain rate. The viscosity of alginate is concentration-dependent, and, generally, lower concentrations of alginate are recommended for high cell viability [27, 35].

However, low-concentration alginate exhibits poor mechanical properties and cannot be used for achieving good resolution in printing applications. Many attempts to optimize the resolution of alginate bioinks have been reported, including optimization of alginate concentration, incorporation of high molecular weight polymers, and different hydrogel fabrication methods [35, 55].

Different bioprinting approaches can be used for integrating living cells into three-dimensional alginate hydrogels, and these methods can be classified into three main categories: extrusion-based bioprinting (EBB) performed with the use of a piston or a screw or other pneumatic method; inkjet-based bioprinting (IBB), performed by a piezoelectric actuator or a heater that creates bubbles; and laser-assisted bioprinting (LAB), performed by a laser pulse that discharges bioink droplets from a donor slide onto an energy-adsorbing layer [56, 57]. In the case of laser-assisted methods, the processes involve high-temperature and high-energy radiations which make them unsuitable for bioprinting of cell-laden constructs [35]. Therefore, extrusion and inkjet printing are the two major technologies which can be used for printing cell-laden constructs under physiological conditions. Inkjet-based methods have been used for printing 3D cell-laden constructs due to the ability to provide good cell viability (around 90%). On the other side, the employed bioinks must be less viscous in comparison to extrusion printing, and cell density also must be lower. For these reasons, the most employed printing solution for alginate-based bioinks relies on the extrusion process, since it provides a platform to print cell-laden constructs efficiently and in a controllable manner compatible with cell survival [35].

In EBB methods, cells are blended with a hydrogel and loaded into sterilized syringes. The cell-laden hydrogel or cell spheroids are then dispensed by air pressure or a motorized plunger through a micronozzle onto the substrate, according to a customized design. Different EBB systems have been experimented for printing living cells onto target-specific positions while encapsulating them in alginate hydrogel. In a recently published review, Ozbolat and coauthors reported

a summary of these mechanisms which are (i) bioplotting, (ii) bioprinting hydrogel with a secondary nozzle using cross-linker deposition or a spraying system, (iii) bioprinting using a coaxial nozzle-assisted system, (iv) bioprinting pre-cross-linked alginate and further cross-linking it thereafter, and (v) bioprinting alginate with an aerosol cross-linking process [55]. There are many reports detailing various extrusion-based 3D tissue-printing systems and the parameters requested for an efficient printing, like printing speed, dispensing pressure, and movement distance. As an example, Gasperini et al. presented a bioprinting technique that exploits the electrohydrodynamic process to create a jet of liquid alginate beads containing cells [58]. The beads were placed at predefined positions and cross-linked on a calcium-donor substrate, to build block-by-block a cell-laden hydrogel scaffold. Tabriz and colleagues developed a new extrusion-based bioprinting technique to produce complex alginate hydrogel structures by dividing alginate hydrogel cross-linking process into three steps [65], each step corresponding to an increase in cross-linking level. With this technique they were able to successfully print complex 3D constructs in the shape of branched vascular structures [59].

4.1.4 Modification of Alginate Hydrogels

Although alginate is extremely cytocompatible, due to its highly hydrophilic nature, proteins are minimally adsorbed, thus hampering cell attachment on this material. Moreover, despite the intrinsic properties of alginate that make it a favorable material for tissue engineering applications, chemical modifications are often required to promote desirable cellular functions, provide a greater range of mechanical properties, and facilitate controlled release of encapsulated factors. In order to overcome its limitations, alginate can be modified by covalently grafting extracellular matrix peptides to provide molecule binding sites for cell adhesion, like the RGD (arginine-glycine-aspartate) motif found in collagen or the REDV (arginine-glutamate-aspartate-valine) peptides

found in fibronectin [60–62]. Another strategy consists in mixing alginate with protein-based cell-adhesive components such as collagen [63], gelatin [61], keratin [64], or silk fibroin [65] in order to obtain hybrid hydrogels with improved biocompatibility and enhanced degradation rate. These proteins contain cellular binding motifs, which support cellular attachment in a manner similar to the extracellular matrix (ECM). Different approaches have been proposed in this regard:

- In their well-known paper from 1999, Rowley and colleagues covalently modified alginate polysaccharides with RGD-containing cell adhesion ligands utilizing aqueous carbodiimide chemistry [60]. Mouse skeletal myoblasts were cultured on the obtained alginate hydrogel surface, where they proliferated and differentiated toward skeletal muscle lineage. The suitability of alginate as an ideal material with which to confer specific cellular interactive properties was thus demonstrated.
- Singh et al. compared the growth of vascular cells on different hydrogel substrates containing alginate (2%, wt/vol) blended in solutions with different proteins (silk fibroin, gelatin, keratin, or elastin at 1%, wt/vol) [66]. The analysis of cell proliferation, metabolic activity, and colonization was carried out in 2D, and the most promising results were obtained with silk fibroin- and keratin-containing hydrogels, which supported the growth of all types of vascular cells.
- Boccaccini et al. published several papers regarding alginate modification for enhancing its biocompatibility by resembling the mechanical, structural, and chemical properties of the native extracellular matrix. In their works, they developed modified alginate hydrogels in which cell-adhesive functionality was conferred by blending with gelatin [25], silk fibroin [67], and keratin [64]. They used this hybrid material to fabricate hydrogel films and hydrogel microcapsules. Cells were either seeded onto prefabricated hydrogel substrates (2D) or encapsulated during hydrogel microcapsule formation obtained with pressure-

driven extrusion technique (3D). Their results indicated that such novel hybrid hydrogels supported cell attachment, spreading, and proliferation and thus represent promising materials for biomedical applications in tissue engineering and regeneration. As an example, the presence of silk fibroin in the blend makes the gel stiffer compared with pure alginate and improves the physical-chemical properties in both the geometries of the blend [67]. As far as cell interaction is concerned, they showed that silk fibroin provides anchorage and a growth-supporting environment for both cells seeded on the films and for cells encapsulated in the microcapsule compared with structure of pure alginate [67]. However, they did not compare the behavior of cells processed with the different hydrogel systems.

- Cell sheet culture substrates were developed by Yan and coworkers using the ability of calcium alginate hydrogels to be dissolved under mild conditions [62]. The alginate was modified by conjugating the integrin binding peptide sequence RGD to the alginate solution in order to confer cell attachment sites to the hydrogel. The modified alginate hydrogel supported the attachment and growth of fibroblast and human corneal epithelial cell (HCEC) sheets, subsequently detached from the substrate through chelating the calcium using citrate. The cell-cell connections were retained following this release, and the cell layers adhered to each other and grew after being stacked (Table 4.1).

4.1.5 Challenges and Future Directions

Novel hydrogels for tissue engineering applications should be designed and engineered to fulfill a number of physical, chemical, and biological requirements: for example, hydrogel systems should be able to sustain cell viability and promote cell adhesion, proliferation, aggregation, and differentiation toward multiple lineages; demonstrate mechanical integrity and structural stability after gel formation; and allow integra-

tion with the endogenous tissue without minimal inflammatory response.

Alginate-based hydrogels have been widely explored in cell encapsulation and bioprinting applications due to large availability, limited cost, mild cross-linking conditions with no need for aggressive cross-linking agents, and reversible gelation.

Due to the high water content and the lack of cell binding sites, alginate hydrogels have shown limited protein adsorption, cell adhesion ability, and long-term stability. The limited inherent cell adhesion and cellular interaction can be an advantage for cell encapsulation applications but can limit the use of cell-laden constructs for tissue engineering applications. Alginate molecules can be chemically modified by covalent cross-linking with extracellular matrix components to provide molecule binding sites for cell adhesion. Similarly, hydrogel long-term stability can be greatly improved using dialdehydes or methacrylated alginate to form covalent intermolecular cross-linking bonds. However, additional research is necessary to fully understand the effect of chemical cross-linkers on the encapsulated cells and on long-term mechanical properties, stability, and, eventually, degradation of the hydrogels.

Conversely, new alginate-based formulations should be engineered to obtain hydrogel systems with finely tunable biological, mechanical, and degradation behavior.

Alginate hydrogels were used for the realization of 3D scaffolds and cellularized constructs in an alternative to 2D cell culture systems in the form of beads, fibers, membranes, meshes, foams, and hydrogel building blocks for biofabrication. Similarly, alginate systems with delayed gelation were exploited to develop in situ cross-linkable injectable hydrogels for bioprinting applications. This extended knowledge in material preparation and cell encapsulation should now be used to design and develop multicomponent structures populated with multiple cell lines which can recapitulate the complexity of tissue-like structures. In this framework, modular approaches would confer the ability to scale up

Table 4.1 Selected examples of alginate-based solutions for cell encapsulation, cell-laden injectable gels, tissue engineering and bioinks, and drug delivery systems

Application	Material	Physical form	Relevant findings	References
<i>Cell encapsulation, immobilization, and storage</i>				
	Alginate	Coated microcapsules	Dextran-spermine coated microcapsules of alginate containing viable Langerhans islets. Co-encapsulation of anti-inflammatory drugs increased resistance against lymphocytes and prevented fibrosis	[68]
	Alginate	Microbeads	Cell-laden microbeads prepared by electro-jetting of alginate droplets in CaCl ₂ coagulation bath. Encapsulated cells remained viable and were able to proliferate once released from the matrix.	[37] [38]
	Alginate/gelatin	Microbeads	Osteoblasts-like MG-63 cells microencapsulated in alginate-based hydrogels covalently cross-linked with gelatin showed good cell adhesion, spreading, migration, and proliferation ability	[25]
	Alginate/chitosan	Microfibers	Encapsulation of human hepatocellular carcinoma (HepG2) cells within pure alginate microfibers and alginate-chitosan fibers by wet-spinning using a coaxial microfluidic chip	[48]
	Chemically modified alginate	Injectable, multiple presentations	Alginate hydrogels cross-linked via bi-orthogonal click chemistry to obtain cell encapsulation in bulk gels with high post-encapsulation viability, minimal inflammatory reaction, and long-term stability	[69]
<i>Building blocks for organs and tissues assembly in vitro</i>				
	Alginate	Core-shell microfibers	A laminar flow microfluidic device was designed to manipulate coaxial microfibers with alginate hydrogel shell and carrying a cell suspension in the core. With a double capillary system, microfibers could be weaved to create stable 3D networks with multiple architecture	[49]
	BMP-modified alginate	Self-assembling microbeads	Cell-laden alginate microgels modified with three separate combinations of binding pair molecules (BPM) demonstrated the ability to self-assemble forming structures with loosely packed configurations	[70]
<i>Cell sheet technology</i>				
	RGD-modified alginate	Film	Cell-adhesive culture substrates for growth of fibroblasts and human corneal epithelial cells; the confluent cell layer was later detached from the substrate using citrate buffer while maintaining functional cell-to-cell interaction	[61]
<i>Injectable alginate-based hydrogels</i>				
	Oxidized alginate/gelatin	Self-cross-linked injectable hydrogel	Fast-gelling injectable hydrogel by self-cross-linking of sodium periodate-oxidized alginate and gelatin in the presence of borax for cartilage tissue engineering. Encapsulated chondrocytes demonstrated good viability, normal phenotype, and proliferation and migration ability within the matrix	[71]

(continued)

Table 4.1 (continued)

Application	Material	Physical form	Relevant findings	References
	Oxidized alginate/hyaluronate	Injectable hydrogel	An injectable, biodegradable, partially oxidized alginate/hyaluronate hydrogel infused with primary chondrocytes into mice demonstrated effective cartilage regeneration after 6 weeks with convincing expression of chondrogenic markers	[72]
	Alginate/carboxymethyl chitosan	Injectable hydrogel	An injectable alginate/O-carboxymethyl chitosan hydrogel loaded with fibrin nanoparticles was used to encapsulate adipose-derived stem cells leading to favorable cell adhesion, proliferation, and differentiation into adipocytes	[73]
	Alginate	Injectable hydrogel	Chondrocytes were resuspended in an alginate solution with porous polymeric microspheres containing calcium gluconate as a calcium source for delayed gelation. The resulting hydrogel was shown to integrate well in the bone defects and deliver cartilage cells in situ.	[74]
<i>Alginate-based bioinks</i>				
	Collagen Type I/alginate	3D bioprinted construct	Alginate/collagen bioinks loaded with chondrocytes were used to build 3D-printed constructs that facilitated cell adhesion and cell proliferation and enhanced the expression of cartilage-specific marker genes. The addition of collagen improved both mechanical strength and bioactivity of the bioinks while preserving chondrocyte phenotype	[63]
	Alginate/gelatin methacryloyl/PEG-tetra-acrylate	3D bioprinted construct	A cell-loaded bioink able to promote the proliferation and early maturation of vascular cells was used to bioprint complex 3D vascular networks using a multicomponent coaxial nozzle designed for continuous generation of hollow constructs. The system demonstrated the formation of functional vessel-like structures	[75]
<i>Drug delivery</i>				
	Alginate/poly-l-lysine	Coated microspheres	The release of vascular endothelial growth factor from poly-l-lysine-coated alginate microspheres promoted neo-vascularization of tissue-engineered bone graft	[34]

by assembling layer by layer building blocks to create macroscopic tissue constructs.

Cellularized bioprinted and biofabricated tissues can provide an immeasurable benefit in the development of new drug formulations by allowing testing and high-throughput screening of new and promising chemicals on functional human tissue in vitro. Moreover, the engineering of functional tissue constructs can help in improving understanding of tissue physiology and functions, leading to the development of refined TE strategies. For example, in vitro tumor models could be used to investigate cancer microenviron-

ment, growth, and metastasis, thus supporting the early stages of clinical trials.

In addition, the limited nutrient perfusion and oxygen diffusion in alginate hydrogels – similar to other hydrogel systems – restrict the possibility to develop functional cellularized constructs with clinically relevant dimensions and limit the integration of the new tissue in vitro and in vivo. Despite the great progress in biofabrication approaches, building a perfusable hierarchical vascular network remains a major challenge. Therefore, it is pivotal to provide a viable solution for vascularization to facilitate the clinical

translation of tissue-engineered constructs. Newly engineered alginate-based hydrogels can play an important role in the implementation of innovative biofabrication and bioprinting strategies for the development of vascularized tissue-engineered constructs.

References

- Ozbola IT (2015) Bioprinting scale-up tissue and organ constructs for transplantation. *Trends Biotechnol* 33(7):395–400
- Gasperini L, Mano JF, Reis RL (2014) Natural polymers for the microencapsulation of cells. *J R Soc Interface* 11(100):20140817
- Zimmermann H, Ehrhart F, Zimmermann D et al (2007) Hydrogel-based encapsulation of biological, functional tissue: fundamentals, technologies and applications. *Phys A* 89(4):909–922
- Yao H, Wang J, Mi S (2017) Photo processing for biomedical hydrogels design and functionality: a review. *Polymers (Basel)* 10(1):11
- Hospodiuk M, Dey M, Sosnoski D et al (2017) The bioink: a comprehensive review on bioprintable materials. *Biotechnol Adv* 35(2):217–239
- Murphy SV, Skardal A, Atala A (2013) Evaluation of hydrogels for bio-printing applications. *J Biomed Mater Res A* 101(1):272–284
- Wang S, Lee JM, Yeong WY (2015) Smart hydrogels for 3D bioprinting. *Int J Bioprint* 1(1):3–14
- Jen AC, Wake MC, Mikos AG (2000) Review: hydrogels for cell immobilization. *Biotechnol Bioprocess Eng* 50(4):357–364
- Ahmed EM (2015) Hydrogel: preparation, characterization, and applications: a review. *J Adv Res* 6(2):105–121
- Peppas NA, Hilt JZ, Khademhosseini A et al (2006) Hydrogels in biology and medicine: from molecular principles to bionanotechnology. *Adv Mater* 18(11):1345–1360
- Lee KY, Mooney DJ (2001) Hydrogels for tissue engineering. *Chem Rev* 101(7):1869–1879
- Rinaudo M (2008) Main properties and current applications of some polysaccharides as biomaterials. *Polym Int* 57(3):397–430
- Ji S, Guvendiren M (2017) Recent advances in bioink design for 3D bioprinting of tissues and organs. *Front Bioeng Biotechnol* 5:1–8
- Catoira MC, Fusaro L, Di Francesco D et al (2019) Overview of natural hydrogels for regenerative medicine applications. *J Mater Sci Mater Med* 30:115
- Varghese SA, Rangappa SM, Siengchin S et al (2020) Natural polymers and the hydrogels prepared from them. In: Chen Y (ed) *Hydrogels based on natural polymers*. Elsevier, Chennai, pp p17–p47
- Geckil H, Xu F, Zhang X et al (2010) Engineering hydrogels as extracellular matrix mimics. *Nanomedicine* 5(3):469–484
- Lim F, Sun A (1980) Microencapsulated islets as bioartificial endocrine pancreas. *Science* 210(4472):908–910
- Zimmermann H, Shirley SG, Zimmermann U (2007) Alginate-based encapsulation of cells: past, present, and future. *Curr Diab Rep* 7(4):314–320
- Lee KY, Mooney DJ (2012) Alginate: properties and biomedical applications. *Prog Polym Sci* 37(1):106–126
- Nicodemus GD, Bryant SJ (2008) Cell encapsulation in biodegradable hydrogels for tissue engineering applications. *Tissue Eng Part B Rev* 14(2):149–165
- Hernández-González AC, Téllez-Jurado L, Rodríguez-Lorenzo M (2019) Alginate hydrogels for bone tissue engineering, from injectables to bioprinting: a review. *Carbohydr Polym* 229:115514
- Andersen T, Auk-Emblem P, Dornish M (2015) 3D cell culture in alginate hydrogels. *Microarrays* 4(2):133–161
- Pawar SN, Edgar KJ (2012) Alginate derivatization: a review of chemistry, properties and applications. *Biomaterials* 33(11):3279–3305
- Orive G, Santos E, Pedraz JL et al (2014) Application of cell encapsulation for controlled delivery of biological therapeutics. *Adv Drug Deliv Rev* 67–68:3–14
- Sarker B (2015) Alginate-based hydrogels with improved adhesive properties for cell encapsulation. *Int J Biol Macromol* 78:72–78
- Augst AD, Kong HJ, Mooney DJ (2006) Alginate hydrogels as biomaterials. *Macromol Biosci* 6(8):623–633
- Axpe E, Oyen M (2016) Applications of alginate-based bioinks in 3D bioprinting. *Int J Mol Sci* 17(12):1976
- Sun J, Tan H (2013) Alginate-based biomaterials for regenerative medicine applications. *Materials (Basel)* 6(4):1285–1309
- Jitraruch S (2014) Alginate microencapsulated hepatocytes optimised for transplantation in acute liver failure. *PLoS One* 9(12):1–23
- Bhujbal SV, de Vos P, Niclou SP (2014) Drug and cell encapsulation: alternative delivery options for the treatment of malignant brain tumors. *Adv Drug Deliv Rev* 67–68:142–153
- Murua A, Orive G, Hernández RM et al (2009) Xenogeneic transplantation of erythropoietin-secreting cells immobilized in microcapsules using transient immunosuppression. *J Control Release* 137(3):174–178
- Nguyen D (2017) Cartilage tissue engineering by the 3D bioprinting of iPS cells in a nanocellulose/alginate bioink. *Sci Rep* 7(1):658
- Venkatesan J, Nithya R, Sudha PN et al (2014) Role of alginate in bone tissue engineering. *Adv Food Nutr Res* 73:45–57
- Li Q, Hou T, Zhao J et al (2011) Vascular endothelial growth factor release from alginate microspheres

- under simulated physiological compressive loading and the effect on human vascular endothelial cells. *Tissue Eng Part A* 17(13–14):1777–1785
35. Panwar A, Tan L (2016) Current status of bioinks for micro-extrusion-based 3D bioprinting. *Molecules* 21(6):685
 36. Novosel EC, Kleinhans C, Kluger PJ (2011) Vascularization is the key challenge in tissue engineering. *Adv Drug Deliv Rev* 63(4–5):300–311
 37. Gasperini L, Maniglio D, Migliaresi C (2013) Microencapsulation of cells in alginate through an electrohydrodynamic process. *J Bioact Compat Polym* 28(5):413–425
 38. Liaudanskaya V, Gasperini L, Maniglio D et al (2015) Assessing the impact of electrohydrodynamic jetting on encapsulated cell viability, proliferation, and ability to self-assemble in three-dimensional structures. *Tissue Eng Part C Methods* 21(6):631–638
 39. Barron C, He JQ (2017) Alginate-based microcapsules generated with the coaxial electrospray method for clinical application. *J Biomater Sci Polym Ed* 28(13):1245–1255
 40. Lee BR (2012) In situ formation and collagen-alginate composite encapsulation of pancreatic islet spheroids. *Biomaterials* 33(3):837–845
 41. Liu L (2013) Preparation of monodisperse calcium alginate microcapsules via internal gelation in microfluidic-generated double emulsions. *J Colloid Interface Sci* 404:85–90
 42. Song W, Lima AC, Mano JF (2010) Bioinspired methodology to fabricate hydrogel spheres for multi-applications using superhydrophobic substrates. *Soft Matter* 6(23):5868–5871
 43. De Vos P, Faas MM, Strand B et al (2006) Alginate-based microcapsules for immunoisolation of pancreatic islets. *Biomaterials* 27(32):5603–5617
 44. Onoe H, Takeuchi S (2015) Cell-laden microfibers for bottom-up tissue engineering. *Drug Discov Today* 20(2):236–246
 45. Tamayol A, Akbari M, Annabi N et al (2013) Fiber-based tissue engineering: Progress, challenges, and opportunities. *Biotechnol Adv* 31(5):669–687
 46. Onoe H, Gojo R, Tsuda Y et al (2010) Core-shell gel wires for the construction of large area heterogeneous structures with biomaterials. In: 2010 IEEE 23rd international conference on micro electro mechanical systems (MEMS) 2010, pp 248–251
 47. Takeuchi S (2013) (2013) cell-laden hydrogel beads, fibers and plates for 3D tissue construction. 2013 transducers and Eurosensors XXVII: the 17th international conference on solid-state sensors, actuators and microsystems. *Transducers Eurosensors* 6:1515–1518
 48. Lee BR, Lee KH, Kang E et al (2011) Microfluidic wet spinning of chitosan-alginate microfibers and encapsulation of HepG2 cells in fibers. *Biomicrofluidics* 5(2):022208
 49. Onoen H (2013) Metre-long cell-laden microfibres exhibit tissue morphologies and functions. *Nat Mater* 12(6):584–590
 50. Akbari M (2014) Composite living fibers for creating tissue constructs using textile techniques. *Adv Funct Mater* 24(26):4060–4067
 51. Jun Y (2013) 3D co-culturing model of primary pancreatic islets and hepatocytes in hybrid spheroid to overcome pancreatic cell shortage. *Biomaterials* 34(15):3784–3794
 52. Li X, Xu A, Xie H et al (2010) Preparation of low molecular weight alginate by hydrogen peroxide depolymerization for tissue engineering. *Carbohydr Polym* 79(3):660–664
 53. Bouhadir KH, Lee KY, Alsberg E et al (2001) Degradation of partially oxidized alginate and its potential application for tissue engineering. *Biotechnol Prog* 17(5):945–950
 54. Mao S, Zhang T, Sun W et al (2012) The depolymerization of sodium alginate by oxidative degradation. *Pharm Dev Technol* 17(6):763–769
 55. Ozbolat IT, Hospodiuk M (2016) Current advances and future perspectives in extrusion-based bioprinting. *Biomaterials* 76:321–343
 56. Hölzl K, Lin S, Tytga L et al (2016) Bioink properties before, during and after 3D bioprinting. *Biofabrication* 8(3):032002
 57. Datta P, Ayan B, Ozbolat IT (2017) Bioprinting for vascular and vascularized tissue biofabrication. *Acta Biomater* 51:1–20
 58. Gasperini L, Maniglio D, Motta A et al (2015) An electrohydrodynamic bioprinter for alginate hydrogels containing living cells. *Tissue Eng Part C Methods* 21(2):123–132
 59. Tabriz AG, Hermida MA, Leslie NR et al (2015) Three-dimensional bioprinting of complex cell laden alginate hydrogel structures. *Biofabrication* 7(4):045012
 60. Rowley JA, Madlambayan G, Mooney DJ (1999) Alginate hydrogels as synthetic extracellular matrix materials. *Biomaterials* 20(1):45–53
 61. Grigore A, Sarker B, Fabry B et al (2014) Behavior of encapsulated MG-63 cells in RGD and gelatine-modified alginate hydrogels. *Tissue Eng Part A* 20(15–16):2140–2150
 62. Yan J, Chen F, Amsden BG (2016) Cell sheets prepared via gel-sol transition of calcium RGD-alginate. *Acta Biomater* 30:277–284
 63. Yang X, Lu Z, Wu H et al (2018) Collagen-alginate as bioink for three-dimensional (3D) cell printing based cartilage tissue engineering. *Mater Sci Eng C* 83:195–201
 64. Silva R (2014) Hybrid hydrogels based on keratin and alginate for tissue engineering. *J Mater Chem B* 2(33):5441–5451
 65. Wang Y (2016) A biomimetic silk fibroin/sodium alginate composite scaffold for soft tissue engineering. *Sci Rep* 6(1):39477
 66. Singh R (2016) Evaluation of hydrogel matrices for vessel bioplotting: vascular cell growth and viability. *J Biomed Mater Res Part A* 104(3):577–585

67. Silva R (2016) Soft-matrices based on silk fibroin and alginate for tissue engineering. *Int J Biol Macromol* 93(Pt B):1420–1431
68. Azadi SA, Vasheghani-Farahani E, Hashemi-Najafabadi S et al (2016) Co-encapsulation of pancreatic islets and pentoxifylline in alginate-based microcapsules with enhanced immunosuppressive effects. *Prog Biomater* 5(2):101–109
69. Desai RM, Koshy ST, Hilderbrand SA et al (2015) Versatile click alginate hydrogels crosslinked via tetrazine–norbornene chemistry. *Biomaterials* 50:30–37
70. Hu Y, Mao AS, Desai RM et al (2017) Controlled self-assembly of alginate microgels by rapidly binding molecule pairs. *Lab Chip* 17(14):2481–2490
71. Balakrishnan B, Joshi N, Jayakrishnan A et al (2014) Self-crosslinked oxidized alginate/gelatin hydrogel as injectable, adhesive biomimetic scaffolds for cartilage regeneration. *Acta Biomater* 10(8):3650–3663
72. Park H, Lee KY (2014) Cartilage regeneration using biodegradable oxidized alginate/hyaluronate hydrogels. *J Biomed Mater Res A* 102(12):4519–4525
73. Jaikumar D (2015) Injectable alginate-O-carboxymethyl chitosan/nano fibrin composite hydrogels for adipose tissue engineering. *Int J Biol Macromol* 74:318–326
74. Liao J, Wang B, Huang Y et al (2017) Injectable alginate hydrogel cross-linked by calcium gluconate-loaded porous microspheres for cartilage tissue engineering. *ACS Omega* 2(2):443–454
75. Jia W (2016) Direct 3D bioprinting of perfusable vascular constructs using a blend bioink. *Biomaterials* 106:58–68



Design of Advanced Polymeric Hydrogels for Tissue Regenerative Medicine: Oxygen-Controllable Hydrogel Materials

Jeon Il Kang, Sohee Lee, Jeong Ah An,
and Kyung Min Park

Abstract

Engineered polymeric hydrogels have been extensively utilized in tissue engineering and regenerative medicine because of their biocompatibility, tunable properties, and structural similarity in their native extracellular microenvironment. The native extracellular matrix (ECM) has been implicated as a crucial factor in the regulation of cellular behaviors and their fate. The emerging trend in the design of hydrogels involves the development of advanced materials to precisely recapitulate the native ECM or to stimulate the surrounding tissues via physical, chemical, or biological stimuli. The ECM presents various parameters such as ECM components, soluble factors, cell-to-cell and cell-to-matrix interactions, physical forces, and physicochemical environments. Among these environmental factors, oxygen is considered as an essential signaling molecule. In particular, abnormal oxygen tension such as a lack of oxygen (defined as hypoxia) and an excess supply of oxygen (defined as hyperoxia) plays a pivotal

role during early vascular development, tissue regeneration and repair, and tumor progression and metastasis. In this chapter, we discuss how engineered polymeric hydrogels serve as either an artificial extracellular microenvironment to create engineered tissues or as an acellular matrix to stimulate the native tissues for a wide range of biomedical applications including tissue engineering and regenerative medicine, wound healing, and engineered disease models. Specifically, we focus on emerging technologies to create advanced polymeric hydrogel materials that accurately mimic or stimulate the native ECM.

Keywords

Polymeric hydrogels · Oxygen · Artificial extracellular matrix · Tissue engineering · Regenerative medicine

J. I. Kang · S. Lee · J. A. An · K. M. Park (✉)
Department of Bioengineering and Nano-
Bioengineering, Incheon National University,
Incheon, Republic of Korea
e-mail: kji0805@inu.ac.kr; dlthgml0327@inu.ac.kr;
jeongah95@inu.ac.kr; kmpark@inu.ac.kr

5.1 Introduction

The native extracellular matrix (ECM) is a complex three-dimensional (3D) framework composed of fibrous proteins, proteoglycans, and various soluble molecules immersed in body fluids [1]. The native ECM provides a structural frame to maintain structural integrity, support cell adhesion, and regulate cells behaviors. The

microenvironments have been implicated as critical factors in regulating cellular behaviors such as migration, proliferation, and differentiation, as well as the sequestering of growth factors (GFs) in various biological processes [2]. In the fields of tissue engineering and regenerative medicine, the recapitulation of the native cellular microenvironment using various bioinspired materials is an emerging trend.

Polymeric hydrogels are 3D hydrophilic networks that absorb excess water without dissolving. They have attracted much attention as a promising artificial ECM due to their similarity to native ECM, including moisture environment, hydrophilic networks, biocompatibility, and ease of incorporating biochemical agents such as genes, growth factors, and enzymes [3–6]. To develop advanced hydrogels that mimic native ECM, many researchers have attempted to recapitulate various parameters of native ECM (e.g., mechanical properties, physical forces, topographies, porosities, cell-to-cell and cell-to-matrix interactions, and the incorporation of biochemical molecules including growth factors, nutrients, and oxygen) by considering the type of polymers, cross-linking density, hydrophilicity, and encapsulation of the growth factors and other physiological molecules [2, 3, 7, 8].

Oxygen is an essential element as a metabolic substrate and as a signaling molecule in various biological processes including embryo development, homeostasis, and tissue regeneration. Oxygen condition can be classified in three levels: hypoxia (lack of oxygen below 21% pO_2), normoxia (normal oxygen tension; 21% pO_2), and hyperoxia (excessive supply of oxygen above 21% pO_2) [9, 10]. In particular, recent approaches have focused on the recapitulation of a lack or excessive oxygen condition for mimicking biological conditions and facilitating different biological processes. Hypoxia occurs during embryonic development, tissue regeneration, and tumor development, resulting in vascular development and tumor progression [11, 12]. Hyperoxia is induced by an artificial oxygen supply and facilitates cell proliferation, collagen maturation, neovascularization, reepithelialization, and the recruitment of stem/progenitor cells

[13, 14]. The available evidence in the literature is considered to be critical in the design of advanced polymeric hydrogels that are better mimic the native ECM and stimulating the surrounding host.

In this chapter, we discuss the design of oxygen-controllable hydrogels as artificial cellular microenvironments or dynamic acellular matrices for tissue regeneration. In particular, we focus on the recently reported approaches for the design of advanced hydrogel materials for various therapeutic applications.

5.2 Advanced Polymeric Hydrogel as Artificial ECMs and Dynamic Matrices

The various types of polymers have been utilized to create hydrogel matrices. Within the engineered microenvironments, polymers play the role of the backbone of artificial ECM, similar to a fibrous protein and proteoglycan in a native ECM. This results in the determination of physical forces, cell-to-cell and cell-to-matrix interaction, and the encapsulation of biochemical molecules [3, 7]. The polymeric biomaterials are classified as natural, synthetic, and semisynthetic polymers. Natural polymers (e.g., collagen, gelatin (Gtn), hyaluronic acid (HA), fibrin, chitosan, and alginate) have suitable properties such as hydrophilicity, biocompatibility, cell adhesive, and degradable sites; however, their use is limited due to their weak mechanical properties and batch-to-batch variation [8, 15]. Synthetic polymers, including poly(ethylene glycol) (PEG), poly(vinyl alcohol) (PVA), and poly(ethylene oxide)-poly(propylene oxide)-poly(ethylene oxide) (PEO-PPO-PEO) are utilized because of their stable matrix formation, precise tunability, and minimal variation of components. However, they lack bioactive moieties such as cell adhesive and degradable sites. To develop desirable polymers, semisynthetic polymers (e.g., gelatin-folic acid (Gtn-FA), thiolated gelatin (GtnSH), and Gtn-methacryloyl (GelMA)) have been developed in recent studies. These are chemically modified natural polymers that offer the advan-

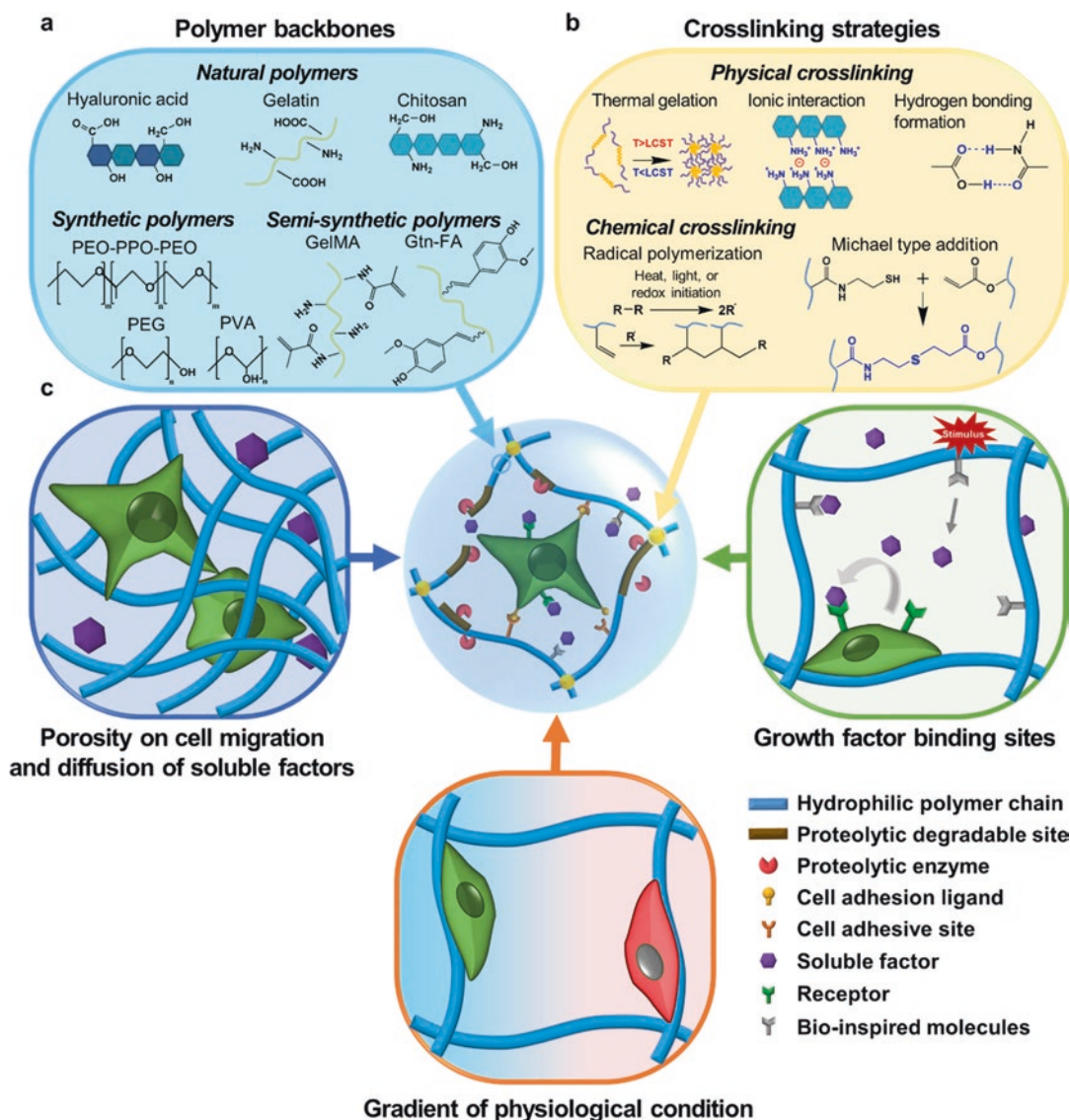


Fig. 5.1 Design of the artificial ECM hydrogels. (a) Various polymers and (b) cross-linking strategies used to develop the artificial ECM hydrogels. (c) Diverse parameters for the artificial ECM hydrogels

tages of both polymers (Fig. 5.1a) [12, 16, 17]. With these various polymers, diverse cross-linking reactions have been considered as an important factor in the development of polymeric hydrogels. Physical cross-linking reactions (e.g., hydrophobic interaction, ionotropic interaction, hydrogen-bonding formation) occur via non-covalent bond formation under mild condition. Although these reactions have some benefits, such as reversibility without chemical reagents,

they result in low-stability hydrogels with weak mechanical properties compared to hydrogels formed via chemical cross-linking reactions. Chemical cross-linking reactions (e.g., radical polymerization, Michael-type addition, disulfide bond formation, Schiff base reaction, and enzyme-mediated reaction) are formed by covalent bonds. While these reactions can form a stable hydrogel network with controllable mechanical properties, the chemical reagent used

and their reactions are associated with potential problems, including toxicity to cells and organs or even at the systemic level (Fig. 5.1b) [8, 18]. Considering diverse polymers and cross-linking strategies, many researchers are attempting to precisely reconstruct the native ECM conditions into hydrogels with various parameters, including the physicochemical and biological cues.

In the design of artificial ECM hydrogels, the structural framework and its properties are important factors. The structural framework in the hydrogels provides an environment for cell survival, attachment, migration, and proliferation via cell-to-cell and cell-to-matrix interaction during biological processes [2]. To provide the optimal conditions for cellular response, polymers should be hydrophilic and possess charge [3]. The diffusion of bioactive molecules such as GFs, cytokines, and gaseous exchange (e.g., oxygen and carbon dioxide) is important because they create a proper environment for the maintenance of cell survival. Indeed, cell adhesive sites (e.g., RGD, VPVG, and REDV) and proteolytic degradable sites decomposed by biological enzymes (e.g., metalloproteinases (MMPs), elastases, and serine proteases) should be incorporated into the polymers to assist in their 3D cell growth and to regulate their fate. Cell adhesive sites assist in the anchorage of cells and proteolytic degradable sites facilitate the establishment of a tunnel for cell migration [1, 2, 19]. Another factor that is considered for cell growth is the cross-linking density. The cross-linking density determines the physicochemical properties of hydrogels, such as their stiffness, porosity, and swelling ratio. In particular, the porosity provides a cage for cell migration and diffusion of bioactive molecules [1]. Although proper pore size facilitates cell migration, diffusion of bioactive molecules, and gaseous exchange, unsuitable pore size limited cell migration and the penetration of molecules or the burst-diffusion rate. Various GFs and cytokines are secreted from the cells and stimulate the cell migration, proliferation, and differentiation via autocrine and paracrine binding [8, 20]. The diffusion of these molecules are coordinated

not only by charges of the polymer chain, pore size, and biodegradability but also by the external stimuli (e.g., magnetic field, ultrasound, and electrical impulse or light) and bioinspired molecules (e.g., heparin, integrin, and ligands and adhesive protein) [3, 21]. The incorporation of these physicochemical and biological stimuli can release the signaling molecules that are spatially and temporally similar to the native ECM [1, 3]. Finally, hydrogels should provide an optimal environment for cell growth and differentiation by controlling the pH, oxygen level, and nutrient response to changes of the external condition [8, 22]. Commonly, cells exhibit a decrease in the pH via the increase of lactic acid as a metabolite and a deficiency of oxygen and nutrients [22, 23]. This poor environment limits cell viability, proliferation, and differentiation, resulting in apoptosis (Fig. 5.1c). Nevertheless, several biological processes including inflammation, angiogenesis, and granulation tissue formation associated with wound healing occur in this poor environment [22]. Although various parameters have been extensively investigated to develop artificial ECM-like matrix, the reconstruction of the oxygen environment in the native ECM is necessary to generate the artificial ECM completely.

In tissue engineering and regenerative medicine, the use of engineered implants consisting of hydrogels, cells, and tissues as therapeutic approaches has been plagued by the critical hurdle, such as oxygen deficiency. To overcome this limitation, various strategies have been investigated that involve the inducement of neovascularization or the infiltration of the surrounding vessel, utilization of the cells and GFs, and the control of physicochemical properties such as stiffness and topography, gradient of nutrients, pH, and oxygen level. In particular, strategies that involve the tuning of oxygen tension have been developed by reconstructing the angiogenic environment or the exploitation of extreme environments that temporally stimulate the cells or tissues. We hereby discuss how to create oxygen-controllable hydrogel matrices and their uses in a broad range of biomedical applications.

5.3 Engineered Hypoxic Microenvironment

Hypoxia is a condition in which the partial pressure of oxygen (pO_2) falls below 5% in the body or local region of the body. This has a crucial effect on metabolism, survival, cell-to-cell interactions, proliferation, and migration [24, 25]. In addition, oxygen levels have been shown to regulate the differentiation of mesenchymal stem cells (MSCs) and to control their paracrine functions [26, 27]. Cellular responses to oxygen deprivation are primarily regulated by hypoxia-inducible factors (HIFs) that accumulate under low-oxygen conditions. HIFs are transcriptional activators composed of β and α subunits [28, 29]. In normoxic conditions, the α subunits are hydroxylated by HIF prolyl hydroxylase (HIF-PH), and ubiquitin ligase recognizes and labels them for rapid degradation by proteasome. However, when cells experience hypoxia, degradation of the α subunits is inhibited, and they accumulate, are translocated into the nucleus, and activate downstream signaling pathways [30]. HIFs activate the expression of various angiogenic factors that could promote angiogenesis and vasculogenesis such as vascular endothelial growth factor (VEGF), VEGF receptor 2 (VEGFR2), angiopoietin (ANG1), and MMPs [31–34]. Hypoxia occurs in a wide variety of situations such as embryonic development, wound healing, tissue ischemia, and tissue regeneration. Recently, many researchers have investigated the effect of hypoxia on cell fate. In this regard, there have been several attempts to mimic the hypoxic condition.

Park et al. developed hypoxia-inducible (HI) hydrogels as the artificial hypoxic microenvironments to facilitate vascular differentiation and morphogenesis of endothelial progenitor cells (EPCs) [12]. They conjugated ferulic acid (FA) to the Gtn backbone via a carbodiimide-mediated reaction. The HI hydrogel was fabricated via laccase-mediated dimerization of the FA molecules during oxygen consumption (Fig. 5.2a). They monitored the dissolved oxygen (DO) levels at the bottom of hydrogels and determined that increasing laccase concentrations from 3.1 to

25.0 U/mL decreased both the DO levels and the time to reach the minimum DO level. In addition, they compared the experimental DO values and numerical DO values, demonstrating that the oxygen consumption kinetics during hydrogel formation follows the Michaelis-Menten equation. These results demonstrated that the oxygen levels and gradients within the HI hydrogels were predictable and controllable (Fig. 5.2b). To investigate the cellular responses to the hypoxic environment, endothelial colony-forming cells (ECFCs) were encapsulated within the HI hydrogel matrices and cultured. Interestingly, the DO levels of the hydrogels decreased distinctly for the first 30 min and retained prolonged low-oxygen levels for up to 50 h due to oxygen consumption of the cells. After 3 days of incubation, the ECFCs within the hypoxic hydrogels underwent tubulogenesis, forming complex network structures (Fig. 5.2c). It was determined that ECFCs cultured in hypoxic gels exhibited significantly higher expression of genes related to angiogenesis such as HIF-1 α , HIF-2 α , MMP, VEGF, VEGFR2, and ANG1 compared to nonhypoxic gels. The HI hydrogels were injected subcutaneously in mice to examine in vivo blood vessel formation. The results indicated a higher density and larger size of microvasculature in hypoxic hydrogel matrices (Fig. 5.2d, e). This demonstrated that HI hydrogels could induce acute hypoxia in the surrounding tissues and stimulate blood vessel recruitment and infiltration.

Although HI hydrogel has potential as an engineered scaffold for hypoxia-related applications, the oxygen levels of the hydrogel over an extended period of time depends on the oxygen consumption by the encapsulated cells and the oxygen levels in the surrounding tissues. This is because of the limited conjugation efficiency of FA molecules that can consume oxygen during cross-linking reactions. To overcome this limitation and to control and maintain continuous hypoxic condition, Park et al. developed dextran-based HI (Dex-HI) hydrogels. Dextran has been used for various biomedical applications because of its hydrophilic, biocompatibility, and biodegradability properties [35]. They synthesized Dex-HI hydrogels by conjugating tyramine (TA)

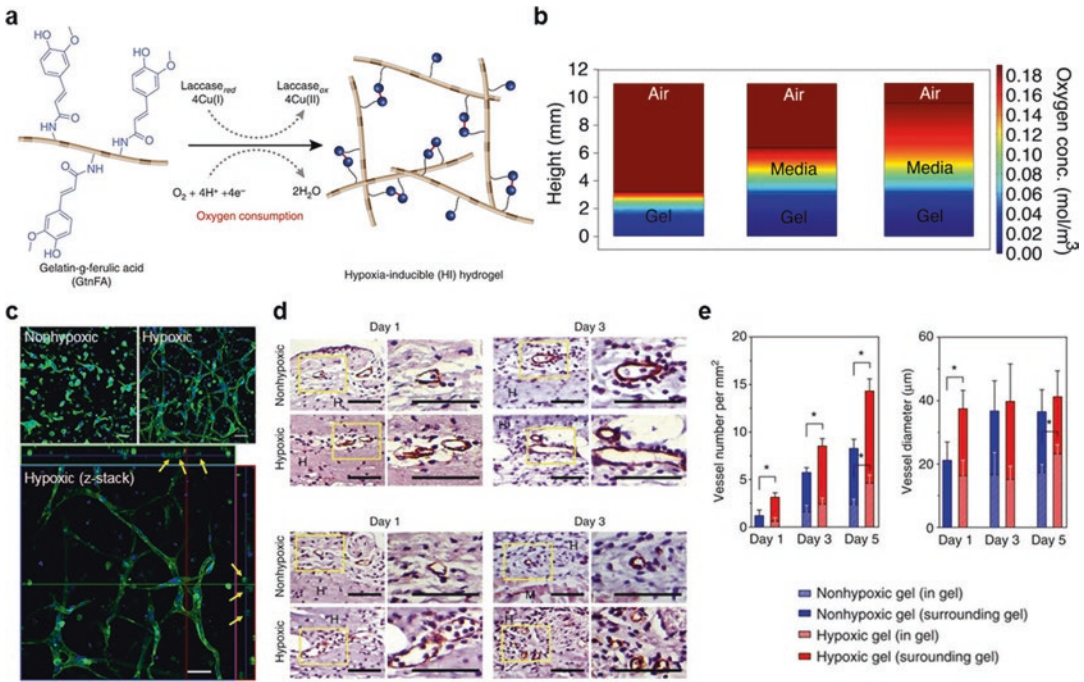


Fig. 5.2 Hypoxia-inducible hydrogels as an artificial hypoxic microenvironment. **(a)** Schematic representation of HI hydrogel formation. Oxygen-consuming cross-linking reaction by laccase resulting in the oxidation of FA molecules to form diferulic acid (DiFA). **(b)** Model predictions of oxygen levels and gradients after 30 min of hydrogel formation in the three-layer model (air–media–gel). **(c)** Confocal microscopy images of ECFCs encapsulated within the nonhypoxic gel and hypoxic gel; yellow

arrows indicate lumen formation within the vascular networks (green, phalloidin, and blue, nuclei). Scale bars presents 50 μm. **(d)** Histological sections 1 and 3 days after the hydrogel injection stained with α-SMA (upper panel) and CD31 (lower panel) and **(e)** quantification of blood vessel number and diameter surrounding and penetrating into the hydrogels. Results in **(d)** are shown as the average value ± SD, **P* < 0.05. (Reprinted with permission from [12] Copyright (2014) Springer Nature)

molecules to Dex using PEG as a linker. The DO levels within Dex-HI hydrogels decreased dramatically during the initial 30 min and maintained low-oxygen tension (<0.5%) up to 8 h depending on the polymer concentration. As the polymer concentration was increased from 3 w/v% to 10 w/v%, the hydrogels exhibited a faster oxygen consumption rate and longer hypoxic conditions up to 12 h. These results indicated that Dex-HI hydrogels could generate extended hypoxic conditions (up to 12 h) compared to Gtn-HI hydrogels (up to 1 h).

Hypoxia is an important regulator of stem cell function including proliferation, maintenance of the cell condition and function, and differentiation [36]. Sathy et al. developed dimethylloxalylglycine (DMOG)-releasing hydrogels to control the differentiation of transplanted MSCs [37].

DMOG is an HIF-PH inhibitor and can mimic the effect of low-oxygen conditions by stabilizing HIF-1α and inducing HIF-1-dependent downstream pathways. DMOG delivered hydrogels were prepared by mixing DMOG and RGD-alginate solution. Firstly, RGD (GGGGRGDSP) peptides were covalently linked to alginate via carbodiimide chemistry and cross-linked with agarose (3%) containing 50 mM calcium chloride via an ionic cross-linking reaction. DMOG was added to the RGD-alginate hydrogel solution with different concentrations (2.1, 4.2, 6.3 mg/mL). The hydrogel burst and released DMOG over the first 3 h with a sustained release for 72 h. MSCs encapsulated in DMOG-releasing hydrogels expressed a higher ratio of nuclear to cytoplasmic HIF-1α, indicating that DMOG could stabilize HIF-1α. To determine whether DMOG

delivery and HIF-1 α levels could regulate the differentiation of adult stem cells, the MSCs encapsulated within the hydrogels were cultured in the presence of TGF- β 3. The expression of key chondrogenic genes such as type-II collagen and aggrecan increased. In addition, there was also an increase in the level of Smad 2/3, which is known to play a key role in chondrogenesis and osteogenesis in MSCs. It was also determined that co-delivery of TGF- β 3 and BMP-2 by DMOG hydrogels increased the expression of Sox-9, type-II collagen, and type-X collagen, resulting in enhanced chondrogenesis compared to the delivery of DMOG or growth factors only.

Cobalt ion (Co²⁺) also has the potential to imitate hypoxia by artificially stabilizing HIF-1 α [38, 39]. HIF-1 α then translocates into the nucleus to stimulate the upregulation of pro-vascularogenic genes such as VEGF [40]. Quinlan et al. designed novel hypoxia-mimicking cobalt bioactive glasses with collagen-glycosaminoglycan (CG) scaffolds to enhance angiogenesis and bone repair [41]. They developed a highly porous collagen-CG scaffold that has an optimized composition using a controlled freeze-drying process to facilitate osteogenesis and to enhance bone repair. They incorporated cobalt bioactive glass into CG scaffolds to improve the mechanical and structural properties, in addition to angiogenesis. To fabricate this scaffold, 2.8 mg and 7 mg of cobalt bioactive glasses were added to preformed CG slurry and freeze-dried at a cooling rate of 1 °C/min for 24 h at a final freezing temperature of -40 °C. The compressive strength of the scaffolds was significantly increased by the addition of cobalt bioactive glasses, and a high degree of porosity of 98% was maintained. To investigate cellular responses to the cobalt-CG scaffold, human umbilical vein endothelial cells (HUVECs) and MC3T3-E1 were seeded onto the scaffolds. VEGF gene expression and protein production of HUVECs were upregulated for the scaffolds with cobalt bioactive glass. Enhanced vascular tubule formation was observed compared to the bioactive glass-free CG control. The osteogenic activities of MC3T3-E1 cells were measured by monitoring alkaline phosphatase (ALP) activity and alizarin red staining. The

results indicated an upregulation of ALP activity (2.2–2.6 fold) and enhanced calcium deposition within the cobalt bioactive glass-CG scaffolds. This demonstrates that the cobalt bioactive glass-CG scaffolds enhance angiogenic activity and influence osteogenesis.

Yegappan et al. also used DMOG as an inhibitor of HIF-PH and whitlockite (WH), which is an unusual form of calcium phosphate and the second most abundant bone mineral in human, to evaluate osteogenic and angiogenic properties [42]. They developed injectable carrageenan (crg) nanocomposite hydrogels by mixing 2% crg solution with WH nanoparticles and DMOG and allowed them to cool at room temperature. Additionally, cross-linking was performed by immersing the nanocomposite gel in CaCl₂ solution. To investigate the effect of hydrogels on cell migration, HUVECs were seeded onto transwell inserts and hydrogels were injected into the bottom chamber. As a result, cell migration toward crg + DMOG and nanocomposite hydrogel (DMOG+WH) was significantly higher than that of the other groups, demonstrating that DMOG in hydrogels could mimic a hypoxia microenvironment. It has been shown that the presence of DMOG mimics the hypoxic condition that leads to overexpression of WNT11, which can stimulate cell migration. Additionally, it was determined that nanocomposite hydrogel and crg + DMOG gel exhibited increased tube formation compared to the other groups. Rat adipose-derived mesenchymal stem cells (rADSCs) that were cultured in nanocomposite hydrogel exhibited an increase in ALP concentration and enhanced expression of RUNX2 and collagen (COL) and osteopontin (OPN).

Hypoxia is also a key feature of various diseases. Many pathological conditions exhibit hypoxic or a low-oxygen tension compared to normal conditions such as chronic inflammatory disease, rheumatoid arthritis, ischemia/reperfusion injury, diabetes, and cancer [43–45]. In particular, many researchers have developed engineered hydrogels that can mimic various cues of tumor microenvironments and ECM-cell interactions to investigate tumor growth and drug responses of cancer cells. During tumor growth,

cells inevitably undergo depletion of nutrients, including oxygen, due to extensive growth [46, 47]. Shen et al. developed a 3D culture system to study the effects of matrix stiffness and oxygen tension on cancer cell behavior [48]. They presented a modular culture system using an acrylated hyaluronic acid (AHA) hydrogel to produce a functional human microvascular network and to stimulate endothelial cell (EC) proliferation and angiogenesis [49, 50]. HA is an abundant element in the ECM and can be applied to the study of cancers and angiogenesis because it can facilitate cancer progression, invasion, and migration [51]. Acrylated HA was cross-linked with MMP-1 and MMP-2 containing two cysteines and conjugated RGD peptide that contained one cysteine. The thiol groups of cysteines reacted with acrylates; by controlling the concentration of MMP, they could alter the cross-linking density of hydrogels to form three hydrogels with different viscoelasticity (soft, 78 ± 16 Pa; medium, 309 ± 57 Pa; and stiff, 596 ± 73 Pa). HT 1080, which is highly angiogenic and metastatic, was encapsulated in the hydrogels. After 24 hours, the cells in the medium and stiff hydrogels began to spread, but those in the soft hydrogels started to form aggregates. Interestingly, after the cell encapsulation, the stiffness of the hydrogels was slightly decreased because of the cell clusters. In addition, it was determined that the DO levels of the hydrogels depend on both the diffusion of oxygen from the air to the culture media and the consumption of oxygen by the cells. Oxygen tension was measured under three different conditions (1, 5, and 21%) with different cell concentrations (1, 5, and 10×10^6 cells/mL) based on mathematical modeling. Using 1×10^6 cells/mL at 5% oxygen, HT1080 cells underwent a constant distribution of 5% oxygen tension throughout the hydrogels. It was demonstrated that encapsulated HT1080 cells were restored more quickly from the apoptosis under hypoxia than under atmospheric conditions. With the addition of stromal cell-derived factor-1 (SDF-1 α) and sphingosine-1-phosphate (S1P), hypoxia enhanced EC proliferation and invasion and upregulated angiogenic-related genes (VEGF and ANG-1) by HT1080 in the hydrogels.

Lewis et al. used oxygen-controllable hydrogels (Gtn-based HI hydrogel) to create in vitro physiopathological oxygen levels to analyze the effect of hypoxia on soft tissue sarcoma invasion and migration [52]. They determined the DO levels during the growth of primary mouse sarcoma tumors (*Kras*^{G12D/+}; *Ink4a/Arf*^{fl/fl} (KIA) tumors). The results indicated that 50% of the large tumors (>300 mm³) are hypoxic ($\leq 0.1\%$ pO_2), and the smaller tumors exhibited hypoxic gradients throughout the tumor mass (0.1–6% pO_2) (Fig. 5.3a). Tumor biopsies from smaller tumors were grafted into the hypoxic and nonhypoxic gels (Fig. 5.3b), demonstrating that tumors in a hypoxic matrix invaded further into the hydrogels and away from the primary graft (after 1 week, 610 ± 210 μm) compared to the tumor in nonhypoxic gels (Fig. 5.3c). The grafted tumor exhibited a higher migration speed, larger migrating distances, and significantly longer distance in the z -direction in the hypoxic matrices (Fig. 5.3d). Individual sarcoma cells were encapsulated in the HI hydrogels to more accurately investigate the effect of the DO gradients. The cells in the HI hydrogels exhibited higher proteolytic degradation (Fig. 5.3e) and upregulation of collagen1 A1 (COL1A1), lysyl oxidase (LOX), and 2-oxoglutarate 5-dioxygenase (PLOD2) after 7 days of culture compared to the nonhypoxic gels. This is suggestive of remodeling the matrix in the hypoxic gel (Fig. 5.3f). In addition, individual cells in 3D hydrogels present greater and faster cell movement in the hypoxic matrix. Importantly, cells migrate in the direction of increased oxygen tension.

In sum, many researchers have endeavored to replicate the microenvironment of various human tissues or pathological conditions using in vitro models. In particular, the results of the recent studies have demonstrated that oxygen tension, specifically hypoxia, is a critical factor in molecular signaling during embryonic development, tissue regeneration, and tumor progression. For this reason, various artificial ECMs that can mimic the hypoxic condition of tissues have been developed using oxygen-consuming molecules or HIF-1 α stabilizing molecules. These engineered artificial ECMs are important in the study

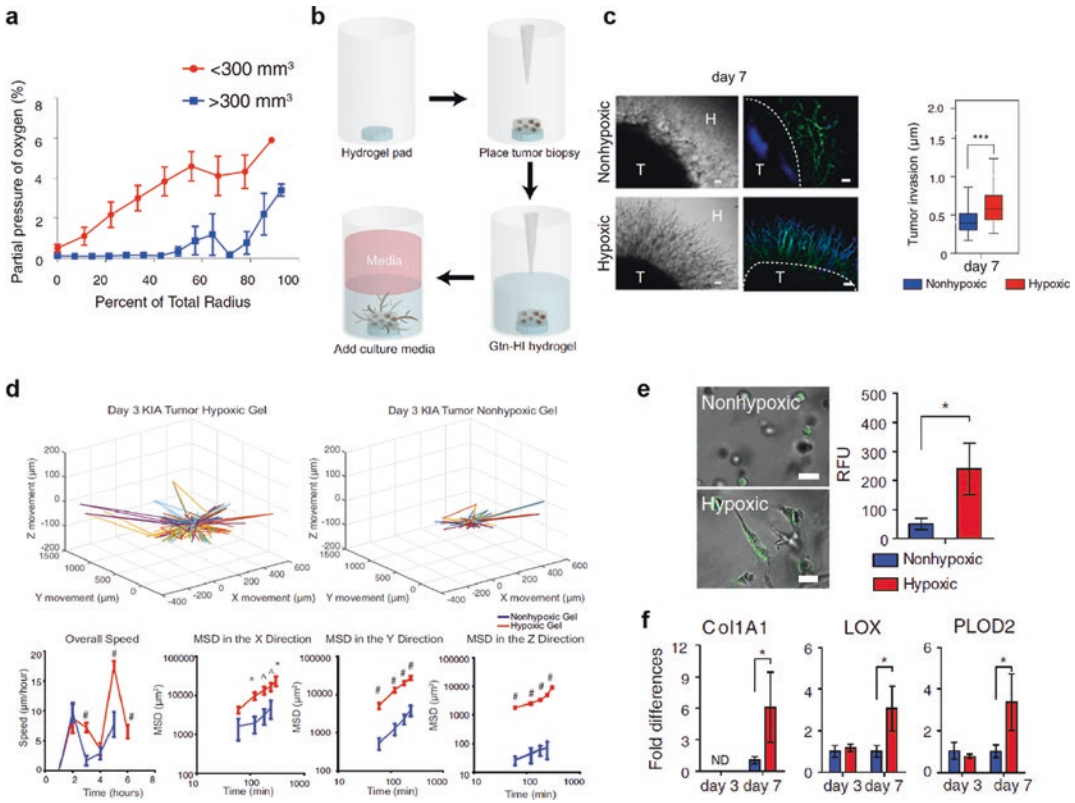


Fig. 5.3 Oxygen-controllable hydrogels as engineered tumor microenvironments. **(a)** In situ DO measurements in KIA tumors. **(b)** Schematic illustration of tumor encapsulation within HI hydrogel. **(c)** Light-microscopy and fluorescence microscopy images of sarcoma tumors encapsulated within the nonhypoxic and hypoxic gels (green, phalloidin, and blue, nuclei). H, hydrogels; T, tumors. Scale bars presents 100 μm . Quantitative analysis of the sarcoma tumor invasion into the hydrogel matrix (***) $P < 0.001$. **(d)** Dynamic cell movements were tracked

in the x-, y-, and z-directions. The overall speed and mean square displacement (MSD) in each direction ($^*P < 0.05$, $^{\#}P < 0.01$, $^{\#}P < 0.001$). **(e)** The fluorescence microscopy images of sarcoma cells encapsulated within HI hydrogels incorporated with DQ Gtn for 3 days. Scale bars presents 25 μm . The quantitative analysis of relative fluorescence intensity ($^*P < 0.05$). **(f)** Real-time RT-PCR analysis of collagen modification genes ($^*P < 0.05$). (Reprinted with permission from [52] Copyrights (2016) National Academy of Sciences)

of cellular behavior and the investigation of the tissue regeneration mechanism, metastatic processes, and the evaluation of therapeutic agents for the treatment of cancer.

5.4 Artificial Hyperoxia

In recent years, oxygen has been demonstrated as an essential molecule, such as the signaling of molecules to control cellular activities, such as cell survival, proliferation, migration, and differentiation of organisms [24]. In particular, it is widely known that a higher oxygen tension rela-

tive to the atmosphere (defined as hyperoxia) facilitates wound healing processes, including inflammation, proliferation, collagen synthesis, and angiogenesis [53, 54]. Hyperbaric oxygen can promote wound healing process via transient oxidative stress, resulting in upregulation of intracellular reactive oxygen species (ROS) and nitric oxide (NO) levels. These reactive molecules promote secretion of various GFs and cytokines, such as VEGF, platelet-derived growth factor (PDGF), transforming growth factor beta 1 (TGF- β 1), keratinocyte growth factor (KGF), and epidermal growth factor (EGF). In particular, ROS regulates cell proliferation, cell death (either

apoptosis or necrosis), and the activation of several signaling pathways [13, 55, 56]. Due to these characteristics, oxygen treatment using hyperbaric oxygen tanks, perfluorocarbons (PFCs), and oxygen-generating materials (calcium peroxide (CaO_2), magnesium peroxide (MgO_2), sodium carbonate (Na_2CO_3), hydrogen peroxide (H_2O_2), etc.) has been widely utilized as an advanced therapeutic tools. However, there are still several noteworthy limitations, such as limited oxygen diffusion, pulmonary damage, and uncontrollable burst releasing oxygen. For this reason, advanced oxygen-generating biomaterials are still under investigation. The ultimate goal of oxygen-generating biomaterials is to promote wound healing and tissue regeneration.

To achieve sustained and prolonged oxygen delivery, many researchers have investigated the development of advanced oxygen-generating biomaterials. Alemdar et al. reported on oxygen-generating photo-cross-linkable hydrogels for cardiac progenitor cell survival by the reduction of necrosis due to hypoxia [57]. Gelatin methacryloyl (GelMA) with cardiac side population cells (cSPCs) and CaO_2 were cross-linked via photo-cross-linking. Gelatin methacryloyl (GelMA) hydrogels with CaO_2 provided sustained release of oxygen for at least 5 days, and the use of CaO_2 could increase the oxygen tension in a dose-dependent manner. In vitro studies have been conducted in which CSPs were cultured depending on different concentrations of CaO_2 under hypoxic conditions to determine the effect of the oxygen-generating hydrogels on cell survival. The results showed that CaO_2 -GelMA also significantly improved cell survival. Moreover, CaO_2 reduced hypoxia-induced necrosis of CSPs by increasing oxygen availability under conditions that mimic an infarcted heart. Therefore, the oxygen-generating hydrogels are expected to improve tissue-engineered strategies by strengthened cell and tissue survival and by the amelioration of hypoxic stress and the reduction of necrosis-induced cell and tissue damage. Using a different cross-linking reaction method, Park et al. fabricated hyperbaric oxygen-generating hydrogels using GtnSH with CaO_2 (Fig. 5.4a). In this research, GtnSH polymer was synthesized

by conjugating Traut's reagent (TR) to a Gtn backbone. The GtnSH could then form hydrogel networks via oxidative stress mediated by CaO_2 [16]. Furthermore, controllable oxygen tension of the hydrogel could be controlled by regulating CaO_2 concentrations such that the induced CaO_2 content increased with the DO_{max} level (G5C0.25, 139.0% $p\text{O}_2$; G5C0.5, 160.0% $p\text{O}_2$; G5C0.75, 163.9% $p\text{O}_2$) (Fig. 5.4b). Variation of the feed of the TR, polymer, and CaO_2 content could regulate the mechanical properties of the hydrogels. All the groups with catalase exhibited enhanced cell viability, a predominantly viable cell population, in addition to cell spreading and elongation on the plate. To confirm the in vivo angiogenic effect of the hyperbaric oxygen-generating hydrogels, a subcutaneous mouse model was used for up to 7 days. Higher densities of vascular endothelial cells (CD31+) with capillary-like structures were observed within the hyperbaric matrices compared to the normoxic matrices. This suggested that the hyperbaric oxygen-generating hydrogels facilitated tissue infiltration and vascular recruitment from the host tissues via acute hyperbaric stimulation (Fig. 5.4c, d). Based on these results, it is suggested that the CaO_2 -mediated oxygen-generating hydrogels have great potential as advanced oxygen-generating biomaterials for a wide range of applications, including treatment of wound and vascular disorders, as well as in tissue regenerative medicine.

There are some kinds of hydrogels that can form a 3D network structure without chemical modification. Kang et al. demonstrated that oxygen-generating alginate-based hydrogels accelerated wound healing in full-thickness wounds [58]. The oxygen-generating alginate hydrogel (OGA) was fabricated by mixing alginate and CaO_2 solutions. It was determined that the mechanical properties of OGA hydrogels increased by increasing of the concentration of the polymer and CaO_2 : G' of hydrogels (with 0.3 wt% of CaO_2), depending on the alginate content 0.5–3 wt%, 2–1590 Pa and G' of hydrogels (with 2.0 wt% of alginate), depending on the CaO_2 concentration 0–0.9 wt%. The oxygen tension was measured using an invasive oxygen sensor. The oxygen tension of OGA

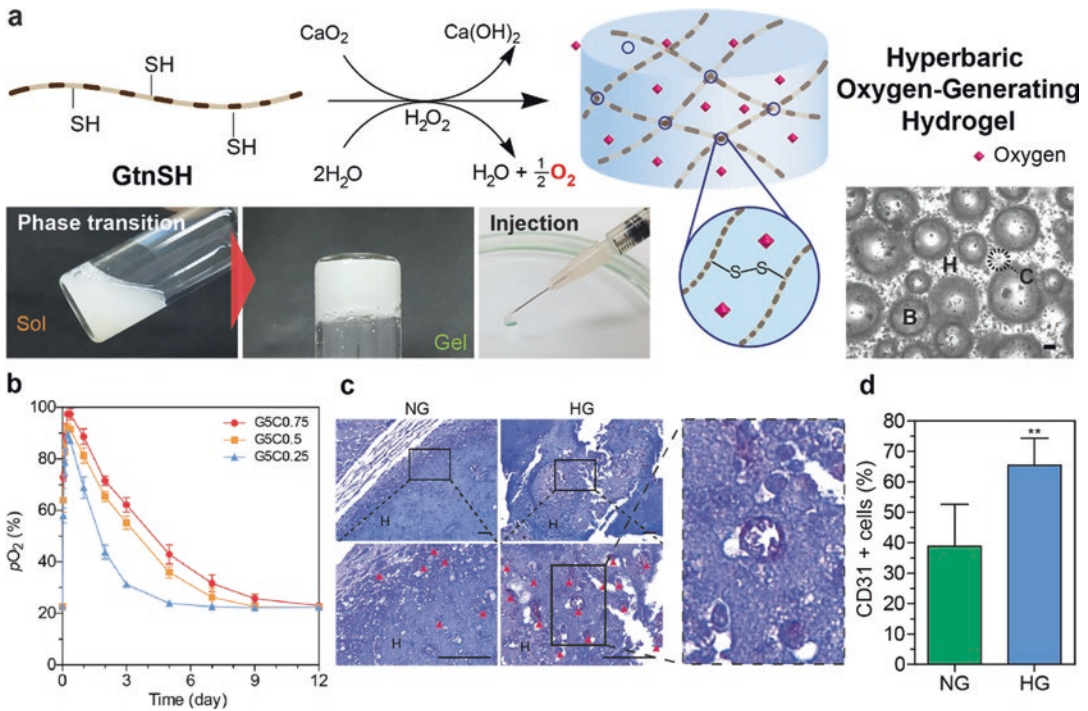


Fig. 5.4 Gelatin-based hyperbaric oxygen-generating hydrogels for wound healing and tissue regeneration. (a) Schematic representation of gel formation and digital images of the sol-gel phase transition, hydrogel injection, and oxygen bubbles in the hydrogel matrix. (b) DO was measured for oxygen-generating kinetics. (c) Histological sections stained with CD31. (d) Quantification of CD31-

positive cells within the hydrogels. H, hydrogels; \blacktriangle , CD31-positive cells. Scale bars represent 50 μm . The results in (d) are shown as the average values \pm SD ($n = 4-6$). (*) indicates a statistically significant difference between the groups (** $P < 0.01$). (Reprinted with permission from [16] Copyrights (2018) Elsevier)

hydrogels increased to 81.0% with the increasing CaO_2 content with catalase in the generation of additional oxygen within hydrogel matrices via the decomposition of H_2O_2 . None of the groups of OGA hydrogel with catalase exhibited significant cytotoxicity. In addition, the results of in vivo studies demonstrated that the hyperbaric hydrogel accelerates wound closing and wound remodeling compared to the normoxic gel (oxygen-free) via acute hyperoxic oxidative stress at the hydrogel-tissue interface.

Ben-Newland et al. reported that gellan gum-based oxygen-generating hydrogels enhanced chemotherapeutic efficiency in the core of tumors with low-oxygen-concentration environments [59]. A gellan gum hydrogel structure was fabricated using divalent calcium cation derived from CaO_2 . The generation of oxygen from gellan gum

was analyzed using a noninvasive oxygen sensor. The Gellan gum-based oxygen-generating hydrogels elevated oxygen levels (0.5% oxyGG, 220% O_2 and 1% oxyGG, 485% O_2) for up to 48 h under normoxic conditions. In addition, under hypoxic conditions (0.5% oxyGG and 1% oxyGG), the use of the hydrogels resulted that oxygen levels elevated above the phosphate-buffered saline (PBS) control for between 24 h and 64 h, and both periods were longer than that of the PBS-controlled baseline. It was demonstrated that for the rat glioblastoma cell line, C6 cells used to study the amount of oxygen released from oxyGG hydrogels could improve the action of doxorubicin. Although oxyGG hydrogels with doxorubicin did not enhance toxicity in a 2D in vitro culture of C6 glioma, it has the capacity to affect the efficacy of oxygen-dependent anti-

cancer therapy strategies such as radiotherapy and photodynamic therapy.

Shiekh et al. investigated oxygen-releasing antioxidant cryogel scaffolds for tissue engineering applications. In this study, to fabricate oxygen-generating 3D scaffolds with a sustained oxygen release, CaO₂ was included as an oxygen-generating material in an antioxidant polyurethane polymeric material (PUAO) [60]. H9C2 cells were seeded on PUAO–CaO₂ cryogels during *in vitro* studies, and the metabolic activity was studied over a period of 10 days under hypoxic conditions. Although 3% of the PUAO–CaO₂ cryogels exhibited significant cell toxicity with decreased metabolic activity, 1% and 2% of the PUAO–CaO₂ exhibited increased metabolic activity. Furthermore, this CaO₂–PUAO showed increased cell viability compared with PU cryogels. An *in vivo* study using a skin flap model was conducted by implanting oxygen-releasing scaffolds on the backs of mice. Although there was no statistically significant difference in the tissue survival rates between the PUAO and PUAO–CaO₂ groups at day 3, the PUAO–CaO₂ group showed decreased necrosis of up to $6.7 \pm 0.2\%$ compared to $41.6 \pm 12.4\%$ in the PU group. Thus, the oxygen-generating scaffold exhibited antioxidant behavior with the sustained release of oxygen, and it was also particularly useful for the regeneration of tissue under ischemic conditions such as myocardial infarction and chronic wound healing.

To produce oxygen-releasing biomaterials, an oxygen delivery system was also utilized. Kim et al. reported on oxygen-releasing microparticle for cell survival and differentiation ability for effective bone regeneration. Perfluorocarbons (PFCs), which have a high solubility for oxygen and carbon dioxide, facilitated the appropriate and controlled release of oxygen to cells without hypoxia and hyperoxia [61]. In this investigation, human periosteal-derived cells (HPDCs) were seeded on PFO–HPs and PBS–HPs, and only the PFO–HPs were incubated under the hypoxic conditions over a period of 10 days (Fig. 5.5a). Hollow microparticles with the emulsion of the oxygen carrier perfluorooctane (PFO–HPs) could supply oxygen to surrounding cells in low-oxy-

gen environments without releasing a burst of oxygen (hyperoxia). The number of viable *h*PDCCs on the PFO–HPs increased up to ~ 2.5 -folds after 5 days (Fig. 5.5b), demonstrating that PFO–HPs provided a suitable oxygen environment for cell survival and proliferation for 5 days of hypoxia. After 5 days, the viable cell number decreased over time because of the limited oxygen in the PFO emulsion. Moreover, hypoxia-related biomarker (HIF-1 α) expression was reduced and delayed in PFO–HPs compared with that in PBS–HPs (Fig. 5.5c). In the Hyp–Nor/PFO–HP and Nor/PBS–HP groups, ALP activity increased gradually, plateaued at 2 weeks, and then declined (Fig. 5.5d). In addition, calcium deposition (mineralization) by the cells increased continuously over time as they differentiated into osteoblasts (Fig. 5.5e). In *in vivo* studies based on the mandibular bone defects model, miniature pigs were used to investigate the capacity of PFO–HPs to supply sufficient oxygen for the survival of *h*PDCCs and the maintenance of osteogenic differentiation potency to facilitate new bone formation. New bone formation was observed via plain radiographs of CT scans for up to 10 weeks. The *h*PDCCs/PBS–HP group exhibited greater bone regeneration than the PFO–HP group without *h*PDCCs, but the difference was not statistically significant. The *h*PDCCs/PFO–HP group formed new bone at a faster rate and with a higher bone density at each time point compared to the *h*PDCCs/PBS–HP and PFO–HP groups (Fig. 5.5f–h). The bony defects in all the groups were almost completely filled with new bone; however, the *h*PDCCs/PFO–HP group exhibited more effective bone reconstruction based on the extent of the haversian system (osteon) which houses blood vessels and is the basic unit of the bone (Fig. 5.5i). Thus, PFO–HPs is a promising delivery system for various functional cells, including stem cells and progenitor cells, to produce clinically applicable tissues and organs.

Another oxygen-generating material was reported by Harrison et al. [62]. Poly (D, L-lactide-co-glycolide) (PLGA) films that incorporated sodium percarbonate (SPO) were fabricated using a solvent casting process. The release

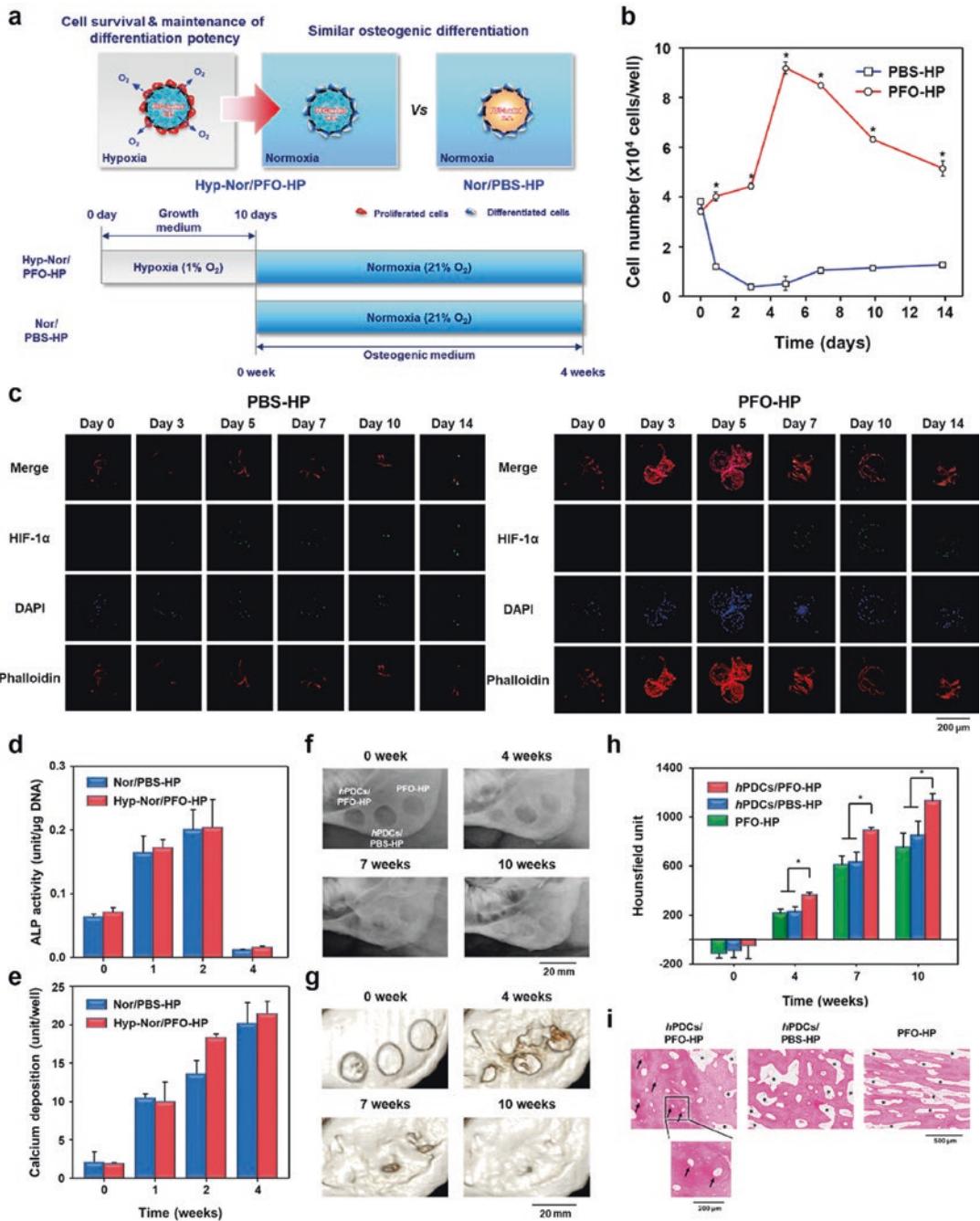


Fig. 5.5 Representation of oxygen-releasing microparticles for effective bone regeneration. (a) Schematic showing the expected events in the PFO-HP groups during in vitro cell culture, which includes hypoxia followed by normoxia and in vivo bone regeneration. (b) Cell survival in PBS-HP and PFO-HP. (c) Immunocytochemical analysis of HPDCs cultured on PBS-HPs and PFO-HPs under hypoxia (blue, cell nucleus; red, phalloidin; green, HIF-1 α), (d) quantitative ALP activity, and (e) calcium deposition. Representative bone regeneration data from implantation of HPDCs/PFO-HP, HPDCs/PBS-HP, and PFO-HP into mandibular defects in miniature pigs. (g) Radiographs of CT scan and (h) HU measurements; $n = 3$; $*P < 0.05$, and (i) histological section; arrow; Haversian system; asterisks, PCL HPs of the reconstructed bone at 10 weeks after implantation. (Reprinted with permission from [61] Copyrights (2019) American Chemical Society)

of oxygen revealed steadily over 24 h. A skin flap model was used for *in vivo* studies. After the creation of rectangular dorsal skin flaps, an oxygen-generating film was placed in the subcutaneous layer, and the surgical wound was closed. The size of tissue necrosis was measured up to 7 days. A reduction in necrosis was observed in the polymeric oxygen-generating (POG) group for the early time points (up to 3 days). In addition, the histological analysis of the tissue sections revealed better protection of general tissue architecture, epidermis height, hair follicles, and sebaceous glands in the POG group. As a result, the oxygen-producing biomaterials can release oxygen into hypoxic tissues, resulting in a delayed onset of necrosis.

Abdi et al. reported on an oxygen-producing micro-system for regenerative therapy [63]. They demonstrated the efficacy of the polymer matrix of poly (D, L-lactide-co-glycolide) (PLGA) with the direct encapsulation of H_2O_2 via the double emulsion solvent evaporation method. Microspheres were embedded in a secondary alginate matrix with the catalase pre-immobilized to the chain. It is well-known that the decomposition of H_2O_2 is very slow under the presence of a catalyst, and this slow decomposition could be problematic for practical applications. As a result, catalase was added to decompose the H_2O_2 within the secondary layer, which minimizes the possibility of the release of the free H_2O_2 from the microsystem. Eventually, oxygen is released into the environment without H_2O_2 . *In vitro* investigations demonstrated that the direct contact of H_2O_2 with cells resulted in toxic effects that severely impacted cell viability; however, the controlled release of H_2O_2 and the introduction of barrier layers between the cell and H_2O_2 resulted in improved cell viability. As a result, an oxygen-producing micro-system can provide a suitable environment for cells under a hypoxic environment, resulting in an improvement in cell survival.

5.5 Conclusion

Recently, numerous bioengineered hydrogels have been designed to mimic the native ECMs by controlling physicochemical properties such as matrix stiffness, porosity, cell-to-cell interaction, and nutrients. Although many studies have been conducted with the goal of replicating the different physicochemical and biological parameters in native ECM, it is still challenging to precisely recapitulate the spatiotemporal complex of the native tissues. Recently, oxygen has attracted much attention as not only essential molecules for recapitulating the native ECM conditions. Although tissue engineering approaches typically focused on promoting the viability of cells or tissues by oxygen supplying, the recent strategies have advanced the use of oxygen as a signaling molecule for improved neovascularization and wound healing process. Many researchers have developed various types of oxygen-controllable matrices as engineered cellular microenvironment or as dynamic acellular matrices for tissue engineering and regenerative medicine. These innovative approaches allow to develop advanced therapeutic tools for improved wound healing and tissue regeneration. Thus, the oxygen-controllable hydrogels hold great potential either as therapeutic implants or as therapeutic vehicles for the tissue regenerative applications as well as other biomedical applications.

Acknowledgement This work was supported by the Incheon National University International Cooperative Research Grants in 2017.

References

1. Hussey GS, Dziki JL, Badylak SF (2018) Extracellular matrix-based materials for regenerative medicine. *Nat Rev Mater* 3(7):159–173
2. Geckil H, Xu F, Zhang X et al (2010) Engineering hydrogels as extracellular matrix mimics. *Nanomedicine* 5(3):469–484
3. Dimatteo R, Darling NJ, Segura T (2018) In situ forming injectable hydrogels for drug delivery and wound repair. *Adv Drug Deliv Rev* 127:167–184

4. Nguyen MK, Jeon O, Dang PN et al (2018) RNA interfering molecule delivery from in situ forming biodegradable hydrogels for enhancement of bone formation in rat calvarial bone defects. *Acta Biomater* 75:105–114
5. Wang Y-W, Chen L-Y, An F-P et al (2018) A novel polysaccharide gel bead enabled oral enzyme delivery with sustained release in small intestine. *Food Hydrocoll* 84:68–74
6. Brovold M, Almeida JI, Pla-Palacín I et al (2018) Naturally-derived biomaterials for tissue engineering applications. In: Chun HJ, Park K, Kim CH, Khang G (eds) *Novel biomaterials for regenerative medicine, Advances in experimental medicine and biology*, vol 1077. Springer, Singapore, pp 421–449
7. Madl CM, Heilshorn SC (2018) Engineering hydrogel microenvironments to recapitulate the stem cell niche. *Annu Rev Biomed Eng* 20:21–47
8. Park S, Park K (2016) Engineered polymeric hydrogels for 3D tissue models. *Polymers* 8(1):23
9. Koh MY, Powis G (2012) Passing the baton: the HIF switch. *Trends Biochem Sci* 37(9):364–372
10. Kilgannon JH, Jones AE, Shapiro NI et al (2010) Association between arterial hyperoxia following resuscitation from cardiac arrest and in-hospital mortality. *JAMA* 303(21):2165–2171
11. Simon MC, Keith B (2008) The role of oxygen availability in embryonic development and stem cell function. *Nat Rev Mol Cell Biol* 9(4):285–296
12. Park KM, Gerecht S (2014) Hypoxia-inducible hydrogels. *Nat Commun* 5:4075
13. André-Lévine D, Modarressi A, Pepper M et al (2017) Reactive oxygen species and NOX enzymes are emerging as key players in cutaneous wound repair. *Int J Mol Sci* 18(10):1–28
14. Fosen KM, Thom SR (2014) Hyperbaric oxygen, vasculogenic stem cells, and wound healing. *Antioxid Redox Signal* 21(11):1634–1647
15. Chowdhury SR, Mh Busra MF, Lokanathan Y et al (2018) Collagen type I: A versatile biomaterial. In: Chun HJ, Park K, Kim CH, Khang G (eds) *Novel biomaterials for regenerative medicine, Advances in experimental medicine and biology*, vol 1077. Springer, Singapore, pp 389–414
16. Park S, Park KM (2018) Hyperbaric oxygen-generating hydrogels. *Biomaterials* 182:234–244
17. Hong Y, Zhou F, Hua Y et al (2019) A strongly adhesive hemostatic hydrogel for the repair of arterial and heart bleeds. *Nat Commun* 10(1):2060
18. Yang J-A, Yeom J, Hwang BW et al (2014) In situ-forming injectable hydrogels for regenerative medicine. *Prog Polym Sci* 39(12):1973–1986
19. Kim MS, Lee MH, Kwon BJ et al (2018) Influence of biomimetic materials on cell migration. In: Noh I (ed) *Biomimetic medical materials, Advances in experimental medicine and biology*, vol 1064. Springer, Singapore, pp 93–107
20. Kuttappan S, Mathew D, Jo JI et al (2018) Dual release of growth factor from nanocomposite fibrous scaffold promotes vascularisation and bone regeneration in rat critical sized calvarial defect. *Acta Biomater* 78:36–47
21. Wang Z, Wang Z, Lu WW et al (2017) Novel biomaterial strategies for controlled growth factor delivery for biomedical applications. *NPG Asia Mater* 9(10):e435
22. Castano O, Perez-Amodio S, Navarro-Requena C et al (2018) Instructive microenvironments in skin wound healing: biomaterials as signal releasing platforms. *Adv Drug Deliv Rev* 129:95–117
23. Gholipourmalekabadi M, Zhao S, Harrison BS et al (2016) Oxygen-generating biomaterials: a new, viable paradigm for tissue engineering? *Trends Biotechnol* 34(12):1010–1021
24. Semenza GL (2007) Life with oxygen. *Science* 318(5847):62–64
25. Pugh CW, Ratcliffe PJ (2003) Regulation of angiogenesis by hypoxia: role of the HIF system. *Nat Med* 9(6):677–684
26. Sheehy EJ, Buckley CT, Kelly DJ (2012) Oxygen tension regulates the osteogenic, chondrogenic and endochondral phenotype of bone marrow derived mesenchymal stem cells. *Biochem Biophys Res Commun* 417(1):305–310
27. Paquet J, Deschepper M, Moya A et al (2015) Oxygen tension regulates human mesenchymal stem cell paracrine functions. *Stem Cells Transl Med* 4(7):809–821
28. Wang GL, Jiang BH, Rue EA et al (1995) Hypoxia-inducible factor 1 is a basic-helix-loop-helix-PAS heterodimer regulated by cellular O₂ tension. *Proc Natl Acad Sci U S A* 92(12):5510–5514
29. Semenza GL, Prabhakar NR (2012) The role of hypoxia-inducible factors in oxygen sensing by the carotid body. In: Nurse C, Gonzalez C, Peers C, Prabhakar N (eds) *Arterial chemoreception, Advances in experimental medicine and biology*, vol 758. Springer, Dordrecht, pp 1–5
30. Huang LE, Arany Z, Livingston DM et al (1996) Activation of hypoxia-inducible transcription factor depends primarily upon redox-sensitive stabilization of its α subunit. *J Biol Chem* 271(50):32253–32259
31. Ben-Yosef Y, Lahat N, Shapiro S et al (2002) Regulation of endothelial matrix metalloproteinase-2 by hypoxia/reoxygenation. *Circ Res* 90(7):784–791
32. Augustin HG, Koh GY, Thurston G et al (2009) Control of vascular morphogenesis and homeostasis through the angiopoietin–tie system. *Nat Rev Mol Cell Biol* 10(3):165
33. Gassmann M, Fandrey J, Bichet S et al (1996) Oxygen supply and oxygen-dependent gene expression in differentiating embryonic stem cells. *Proc Natl Acad Sci U S A* 93(7):2867–2872
34. Kurihara T, Westenskow PD, Friedlander M (2014) Hypoxia-inducible factor (HIF)/vascular endothelial growth factor (VEGF) signaling in the retina. In: Ash J, Grimm C, Hollyfield J, Anderson R, La Vail

- M, Bowes Rickman C (eds) *Retinal degenerative diseases, Advances in experimental medicine and biology*, vol 801. Springer, New York, pp 275–281
35. Park KM, Blatchley MR, Gerecht S (2014) The design of dextran-based hypoxia-inducible hydrogels via in situ oxygen-consuming reaction. *Macromol Rapid Commun* 35(22):1968–1975
 36. Mohyeldin A, Garzón-Muvdi T, Quiñones-Hinojosa A (2010) Oxygen in stem cell biology: a critical component of the stem cell niche. *Cell Stem Cell* 7(2):150–161
 37. Sathy BN, Daly A, Gonzalez-Fernandez T et al (2019) Hypoxia mimicking hydrogels to regulate the fate of transplanted stem cells. *Acta Biomater* 88:314–324
 38. Wu C, Zhou Y, Fan W et al (2012) Hypoxia-mimicking mesoporous bioactive glass scaffolds with controllable cobalt ion release for bone tissue engineering. *Biomaterials* 33(7):2076–2085
 39. Fan W, Crawford R, Xiao Y (2010) Enhancing in vivo vascularized bone formation by cobalt chloride-treated bone marrow stromal cells in a tissue engineered periosteum model. *Biomaterials* 31(13):3580–3589
 40. Park KM, Gerecht S (2014) Harnessing developmental processes for vascular engineering and regeneration. *Development* 141(14):2760–2769
 41. Quinlan E, Partap S, Azevedo MM et al (2015) Hypoxia-mimicking bioactive glass/collagen glycosaminoglycan composite scaffolds to enhance angiogenesis and bone repair. *Biomaterials* 52:358–366
 42. Yegappan R, Selvaprithiviraj V, Amirhalingam S et al (2019) Injectable angiogenic and osteogenic carrageenan nanocomposite hydrogel for bone tissue engineering. *Int J Biol Macromol* 122:320–328
 43. Heddleston J, Li Z, Lathia J et al (2010) Hypoxia inducible factors in cancer stem cells. *Br J Cancer* 102(5):789–795
 44. Maltepe E, Simon MC (1998) Oxygen, genes, and development: an analysis of the role of hypoxic gene regulation during murine vascular development. *J Mol Med* 76(6):391–401
 45. Semenza GL (2001) Hypoxia-inducible factor 1: oxygen homeostasis and disease pathophysiology. *Trends Mol Med* 7(8):345–350
 46. Abramovic Z, Hou H, Julijana K et al (2011) Modulation of tumor hypoxia by topical formulations with vasodilators for enhancing therapy. In: LaManna J, Puchowicz M, Xu K, Harrison D, Bruley D (eds) *Oxygen transport to tissue XXXII, Advances in experimental medicine and biology*, vol 701. Springer, Boston, pp 75–82
 47. Vaupel P, Mayer A (2014) Hypoxia in tumors: pathogenesis-related classification, characterization of hypoxia subtypes, and associated biological and clinical implications. In: Swartz HM, Harrison DK, Bruley DF (eds) *Oxygen transport to tissue XXXVI, Advances in experimental medicine and biology*, vol 812. Springer, New York, pp 19–24
 48. Shen YI, Abaci HE, Krupski Y et al (2014) Hyaluronic acid hydrogel stiffness and oxygen tension affect cancer cell fate and endothelial sprouting. *Biomater Sci* 2(5):655–665
 49. Gerecht S, Hanjaya-Putra D, Bose V et al (2011) Controlled activation of morphogenesis to generate a functional human microvasculature in a synthetic matrix. *J Thromb Haemost* 9:953–954
 50. Hanjaya-Putra D, Wong KT, Hirotsu K et al (2012) Spatial control of cell-mediated degradation to regulate vasculogenesis and angiogenesis in hyaluronan hydrogels. *Biomaterials* 33(26):6123–6131
 51. Dickinson LE, Ho CC, Wang GM et al (2010) Functional surfaces for high-resolution analysis of cancer cell interactions on exogenous hyaluronic acid. *Biomaterials* 31(20):5472–5478
 52. Lewis DM, Park KM, Tang V et al (2016) Intratumoral oxygen gradients mediate sarcoma cell invasion. *Proc Natl Acad Sci U S A* 113(33):9292–9297
 53. Rodriguez PG, Felix FN, Woodley DT et al (2008) The role of oxygen in wound healing: a review of the literature. *Dermatol Surg* 34(9):1159–1169
 54. Winter GD (1978) Oxygen and epidermal wound healing. In: Silver IA, Ercińska M, Bicher HI (eds) *Oxygen transport to tissue — III, Advances in experimental medicine and biology*, vol 94. Springer, New York, pp 673–678
 55. Lee JB, Shin YM, Kim WS et al (2018) ROS-responsive biomaterial design for medical applications. In: Noh I (ed) *Biomimetic medical materials, Advances in experimental medicine and biology*, vol 1064. Springer, Singapore, pp 237–251
 56. Steiner T, Seiffart A, Schumann J et al (2018) Hyperbaric oxygen therapy in necrotizing soft tissue infections: a retrospective study. In: Thews O, LaManna J, Harrison D (eds) *Oxygen transport to tissue XL, Advances in experimental medicine and biology*, vol 1072. Springer, Cham, pp 263–267
 57. Alemdar N, Leijten J, Camci-Unal G et al (2016) Oxygen-generating photo-cross-linkable hydrogels support cardiac progenitor cell survival by reducing hypoxia-induced necrosis. *ACS Biomater Sci Eng* 3(9):1964–1971
 58. Kang JI, Park KM, Park KD (2019) Oxygen-generating alginate hydrogels as a bioactive acellular matrix for facilitating wound healing. *J Ind Eng Chem* 69:397–404
 59. Newland B, Baeger M, Eigel D et al (2017) Engineering, oxygen-producing gellan gum hydrogels for dual delivery of either oxygen or peroxide with doxorubicin. *ACS Biomater Sci Eng* 3(5):787–792
 60. Shiekh PA, Singh A, Kumar A (2018) Oxygen-releasing antioxidant cryogel scaffolds with sustained oxygen delivery for tissue engineering applications. *ACS Appl Mater Interfaces* 10(22):18458–18469
 61. Kim HY, Kim SY, Lee HY et al (2019) Oxygen-releasing microparticles for cell survival and differentiation ability under hypoxia for effective bone regeneration. *Biomacromolecules* 20(2):1087–1097
 62. Harrison BS, Eberli D, Lee SJ et al (2007) Oxygen producing biomaterials for tissue regeneration. *Biomaterials* 28(31):4628–4634
 63. Abdi SIH, Ng SM, Lim JO (2011) An enzyme-modulated oxygen-producing micro-system for regenerative therapeutics. *Int J Pharm* 409(1–2):203–205



Enhancing Osteochondral Tissue Regeneration of Gellan Gum by Incorporating *Gallus gallus var Domesticus*-Derived Demineralized Bone Particle

Muthukumar Thangavelu, David Kim, Young Woon Jeong, Wonchan Lee, Jun Jae Jung, Jeong Eun Song, Rui L. Reis, and Gilson Khang

Abstract

Treatment for the osteochondral defects (ODs) is more challenging nowadays that needs to be addressed by developing alternative bone tissue engineering materials. Gellan gum (GG) is a widely used natural polysaccharide in the field of tissue engineering (TE) and regenerative medicine due to its versatile properties. There are many reports about the successful application of GG in cartilage tissue engineering and guiding bone formation. Functional coatings and porous composite materials have been introduced in next-generation materials for treating OD, whereas osteoconductive materials, such as demineralized bone particle (DBP) or bone derivatives, are used. However, modifi-

cation of porosity, biocompatibility, cell proliferation, and mechanical properties is needed. DBP can activate human mesenchymal stem cells to differentiate into osteoblast cells. In this chapter, the potential application of GG with DBP in different combinations was reviewed, and the best suitable combinations were selected and further studied in small animal models for the soft and hard tissue engineering applications; also its application in the osteochondral integration fields were briefly discussed.

Keywords

Osteochondral defect · Gellan gum · Demineralized bone particle · Osteoarthritis · Biomaterial · Scaffold · Osteochondral defects · Tissue engineering · Hydrogel

M. Thangavelu · D. Kim · Y. W. Jeong · W. Lee
J. J. Jung · J. E. Song · G. Khang (✉)
Department of BIN Convergence Technology,
Department of Polymer Nano Science & Technology
and Polymer BIN Research Center, Jeonbuk National
University, Jeonju, South Korea
e-mail: gskhang@jbnu.ac.kr

R. L. Reis
3B's Research Group, I3Bs – Research Institute on
Biomaterials, Biodegradables and Biomimetics,
Headquarters of the European Institute of Excellence
on Tissue Engineering and Regenerative Medicine,
University of Minho, Guimarães, Portugal

6.1 Introduction

Osteochondral defect is a common disease caused by natural degradation due to severe traumas, athletic injuries, or physical diseases (osteoarthritis), which results in joint pain and deformity, as well as functional disability [1, 2]. With the aging population, the natural wear of the

cartilage tissue and injuries to the joint affected by traumas and sports are always developing into osteoarthritis (OA) which is a major cause for the osteochondral defect (OD) [3]. As of 2008, it was assessed that over 39 million people in the European Union and 31 million Americans suffered from OA; by 2012, among them, 9.2% had OD [4, 5]. As the number of patients affected by OA is growing, it is estimated that by 2030, approximately 67 million Americans will suffer from OA (prevalence of doctor-diagnosed arthritis and arthritis-attributable activity limitation – United States, 2007–2009 [6]). Cartilage lesions in OA at the early stages are characterized by pain and swelling of the articular joints. OD includes injury or degeneration in the bone, cartilage, and the bone cartilage interface. For treating or repairing the OD defects, it is very important to consider each of the components in an account. In the late 1970s, clinical treatment has been studied by which OD could be repaired [7]. Treating cartilage lesion is a great challenge in clinics. Many different types of treatments were attempted for focal, osteochondral lesions. Currently available surgical treatment includes different forms of abrasion chondroplasty, transplantation of osteochondral plugs, microfracture, and autologous cultured chondrocytes [8]. The focal treatments for ODs are presently associated with a variety of risks and limitations, including donor site morbidity, poor attachment of the graft to the surrounding tissue, inadequate availability, delamination of the graft, and inferior mechanical property at the treatment site [9–11]. Biochemically, cartilage is a complex tissue that comprises water, chondrocytes, and protein network (proteoglycan and type II collagen), whereas subchondral bone comprises water, hydroxyapatite (HA), and type I collagen [12]. Furthermore, cartilage and subchondral bone have different physiological properties and natural structures; hence, osteochondral regeneration remains an important task in clinics [13–15].

There are many research studies based on the depth of understanding osteochondral structure. In spite of the existing clinical strategies for treating cartilage OC defects, that include autologous chondrocyte implantation, microfracture, auto-

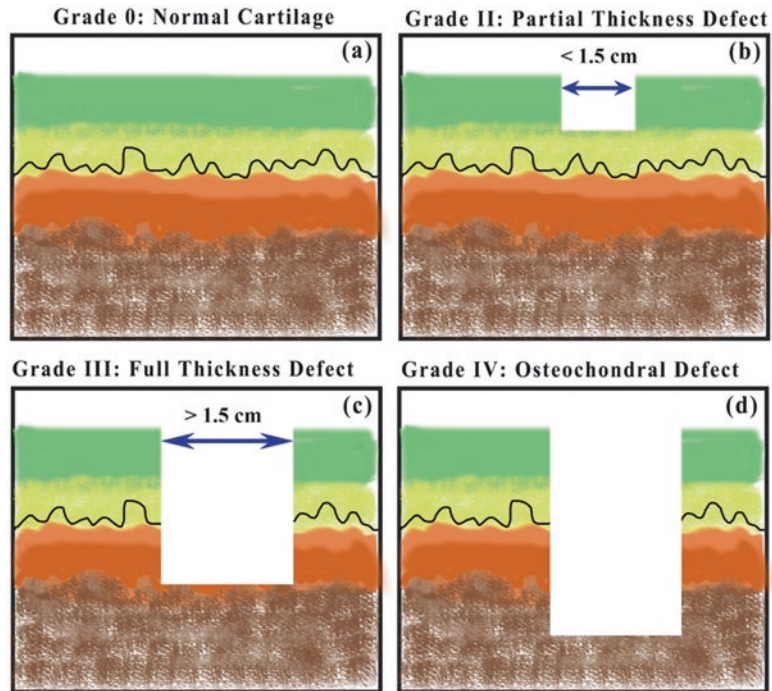
allograft, and joint replacement and mosaicplasty, the long-term bio-functionality of the repaired tissue that cannot be ensured are available for the treatment of OD [16–18]. Even though the available therapies can reduce pain and improve the quality of patients' lives, so far there is no surgical therapy available that could facilitate complete healing of OD, exclusively for complete cartilage regeneration [19–21]. Microfracture treatment can be considered as a low cost and minimally invasive procedure for cartilage repair [22, 23]. Recent studies have shown some positive results after marrow stimulation treatment; they are only palliative, not curative. On the other note, allograft use presents limitations in terms of immune rejection and disease transmission. Hence, there is an urge to develop alternative clinical treatments that will effectively address the pathology and to develop potential alternative therapies for treating OD.

In this chapter, we will be discussing the challenges in treating osteochondral defects, the existing strategies, and the application of GG with different combinations of DBP for its potential application in tissue engineering.

6.2 Challenges in Treating Osteochondral Defects and Existing Strategies

OD comprises the articular cartilage, subchondral bone, and osteochondral interface, and the bioactive properties of these three tissues are significantly different [24]. Based on the size and depth factors, OD can be classified differently based on the available methods. For medical and scientific purposes, OD are also classified using a number of different systems, the most popular one is the outerbridge classification system [25]. They are classified as grade 0 (normal cartilage), grade II (partial thickness defect), grade III (full-thickness defect), and grade IV OD, as shown in Fig. 6.1 [26, 27]. Along with the outerbridge classification, there are many other different methods available describing lesion types such as the Noyes and Stabler method [28] and the histological/histochemical grading system [29], as well as the osteoarthritis research society international

Fig. 6.1 Osteochondral defect classification. Graphical representation of the modified outerbridge classification scheme for cartilage injury: (a) grade 0, normal cartilage; (b) grade II, partial thickness defect; (c) grade III, full-thickness defect; and (d) grade IV, osteochondral defect



and the cartilage histopathology assessment system for classifying the and assessing osteoarthritis [30]. Histologically, articular cartilage has no vascular, nervous and lymphatic systems, while the subchondral bone is rich in blood supply, lymphatics, and nerve [27]. The subchondral bone exchanges nutrients over the blood and lymphatic vessels, and aerobic respiration are the primary means for the energy intake of the subchondral bone [31]. Along with this, there is an interdependent and interactive relationship among articular cartilage and subchondral bone. Subsequently, the most difficult challenge for osteochondral regeneration is to regenerate the articular cartilage, subchondral bone, and osteochondral interface simultaneously.

Articular damage can occur at any age, often seen in athletic young adults. Whereas the rate of injury differ, more than 60% of people who suffer from knee arthroscopies are from grade III or grade IV type [32]. Among the people between the age group of 25 and 75 from the USA, 12.1% have OA [33]. In the USA alone, there are 500 000 cartilage and OD repair treatments that were done roughly [34]. This number is increasing day

by day due to the increasing number of age and life expectancy of the population. The approximate treatment may cost around \$1.5 billion in the near future [34].

6.3 Gellan Gum (GG) as an Ideal Material for OD

More recently, hydrogels are attracting a great deal of attention for treating OD. One among them is GG; GG is a linear polysaccharide resulting from the fermentation process of *Sphingomonas elodea* bacteria. GG is a linear and anionic polysaccharide with repeating units consisting of α -L-rhamnose, β -D-glucose, and β -D-glucuronate [35, 36], being the major component of the extracellular polymeric substance (EPS), which can form ionic cross-linked hydrogels with thermosensitive behavior suitable as injectable formulations that jellify in situ at body temperature [37]. GG was discovered by Kelco (San Diego, USA) in 1987, during a large-scale screening program to identify polysaccharides with useful mechanical properties

[38]. Their low-cost production and great availability have turned GG an industrially relevant polymer widely applied in different areas like medical, pharmaceutical, and food industries. GG was approved by the FDA and EU as E418 for these reasons, and since then, several commercial products based on this polymer have been available in the market. Gelzan™, Gel-Gro, GELRITE, KELCOGEL®, and Phytigel™ are the trade names of the commercial products of GG with applications as a gelling agent for nonclinical and clinical applications. This can present a different degree of acetylation, acetylated form (high-acyl gellan gum (HAGG)) in its native state and the deacetylated form (low-acyl gellan gum (LAGG)). These are the types of GG commonly used in the commercial products ranging from a molecular weight around ~500 kDa [39, 40]. Over the past decade, GG has been effectively applied in the field of tissue engineering and regenerative medicine (TERM) approaches [41–49]. GG is isolated from natural origin material [50], biocompatible [51], not toxic, has highly hydrated polymeric network conjugated to their chemical nature altogether its ability to mimic the extracellular matrix (ECM), making GG as a promising biomaterial candidate for tissue engineering (TE) applications [52–54] [55]. In spite of its attractive properties, GG has some limitations that hurdle its use in a different application. Their disadvantages include high-processing and high-gelling temperature (90–100 °C; ~50 °C), weak mechanical properties, and lack of specific motifs for cell adhesion [37]. However, some of these limitations can be overcome, since the backbone of the polymer possesses functional reactive groups responsive to easy functionalization/modification. GG has been proposed for engineering cartilage substitute [53, 56–59] and has already received a great attention in in vivo experiments [58, 60–62]. It has been reported that blood vessel ingrowth and reinnervation from the subchondral bone into the articular cartilage is a major impediment to achieving tissue regeneration and form an aging pain [63]. Hence, it is beneficial to use non-angiogenic or antiangiogenic biomaterials that prevent blood

vessel ingrowths into the lesion site. Moreover, the injectability, cell encapsulation, and in situ gelling abilities of GG hydrogels turned this biomaterial an attractive nominee to be used as an advanced cell carrier in noninvasive approaches [64]. It was also observed that the different types of monovalent or divalent cations impact the viscoelastic behavior of GG solutions. Ca²⁺ was more remarkable than Mg²⁺ and K⁺ more than Na⁺ [64]. GG's beneficial use in the biomedical applications includes its lack of toxicity, ability to be used as an injectable system, processability under mild conditions, and structural similarity; in the cartilage, it has glycosaminoglycans with glucuronic acid residues in its repeating unit [65, 66].

The high affinity of GG to Ca²⁺ prompted its application in bone regeneration strategies [67, 68]. Mostly, Ca deficiencies result in hypertension, diabetes, neurodegenerative diseases, arteriosclerosis, degenerative joint diseases, and malignant tumors [69]. The national and international guidelines recommend that the daily dietary allowance of Ca is 1–1.2 g for osteoporosis patients [70]. Numerous postmenopausal women do not obtain the recommended amount of Ca from their diet, and they are dependent on Ca supplements [71]. Hence there is a need for us to search for an Ca supplements or naturally occurring ingredient, mainly from animal origins that may help us to prevent osteoporosis without affecting. Ca stimulates differentiation of osteoblast to osteocyte, as observed by increasing the expression of runt-related transcription factor 2 (RUNX2), bone morphogenetic protein-2 (BMP-2), thrombospondin-related anonymous protein (TRAP), receptor activator of nuclear factor kappa B (RANK), cathepsin K, and extracellular signal-regulated kinase (ERK).

6.4 Demineralized Bone Particle from *Gallus gallus var domesticus*

Gallus gallus var domesticus (GD), also known as Yeonsan Ogolgye, is a natural mutant black chicken in Korea. It has specific features such as

cockscorn of mulberry shape, muscle and internal organs with black-gray color, a beak with blue-white or black color, and flesh, leather, and bones with dark blue color. When the melanin ingredient is added into the above-mentioned parts of Yeosan Ogojye alkaline phosphate (ALP) activity increases and bones are strengthened, causing bone mineralization [72, 73]. It also retains unique morphological properties like black fluffy head feathers, pupils, earlobes, four toes, and feathers. GD was reported to efficiently promote red blood cell formation in the bone marrow, and also it shows medical effects, such as, treating anemia, hypertension, and bleeding; having antioxidant and anti-inflammatory properties; and being used as substitute to analgesics [72]. Oligopeptide particle formed from GD has beneficial antioxidant effects [74]; the water extract of GD enhances ALP activity, inhibits bone resorption, and promote mineralization of the bone. Their incorporation to the DBP was used in many tissue engineering applications [75–78]. The incorporation of DBP is similar to that of autogenous graft, where the growth factor triggers an endochondral ossification cascade and helps in the new bone formation at the site of the implantation [79].

6.5 Gellan Gum in Osteochondral Tissue Regeneration

GG, a new biomaterial in the recent times, is projected for tissue engineering applications mainly for the cartilage regeneration [80, 81]. According to the recent studies of Oliveira et al. 2010, GG were used as an encapsulating agent in the tissue engineering support for human articular chondrocytes [58]; their study reported that the GG gel exhibited low-viscosity, which is between 42 °C and 41 °C, enabling an efficient and homogeneous mixture of the cells, forming a stable gel that will entrap cells when reaching body temperature. The in vitro study showed that after 56 days of culturing, the human articular chondrocytes encapsulated in GG were observed to produce hyaline-like ECM along with the significant

increase in collagen II. GG was used and combined with many other biomaterials for cartilage regeneration applications by several researchers. In our previous studies, we used saponin (Sa)-loaded GG hydrogel scaffold for the cartilage regeneration; we observed that the scaffold possesses antiinflammatory, antioxidant, and anticancer properties. The chondrocyte cells seeded on the Sa-loaded GG hydrogels were evaluated for cell adhesion, viability, and proliferation ability. The results revealed that the surface morphology using scanning electron microscopy (SEM), live images using fluorescence images, and MTT assay showed that the cell adhesion and propagation were maintained at the highest level on the 0.025 wt% of the Sa-loaded GG hydrogel, and the cells were covered with ECM. mRNA expression was observed to be more, and thereafter, it tended to decrease with increasing Sa content. Figure 6.2 shows the field emission scanning electron microscopy (FESEM) images of the Sa-loaded GG hydrogels cultured with chondrocytes for 3 weeks, showing the adherence and proliferation of the cells on the hydrogel scaffold.

In another study, GG was blended with agar for the cartilage regeneration application, where the different concentrations of GG solutions (0.2, 0.4, 0.6, and 0.8 wt% of agar) were prepared; they were characterized in an in-vitro model. The results showed that the materials morphology has a suitable porous microstructure with a porosity ranging from 70 to 180 μm that allows water uptake and increased mechanical properties with optimal nutrients, oxygen diffusion, and cells ingrowth. Figure 6.3 shows the surface morphology of the pristine hydrogel and the GG with different ratios of agar and the SEM images showing the adhered cells on the scaffold cultured for a period of 14 days. From all the scaffold concentrations studied, the 0.8 wt% of GG–A was found to be more suitable for cartilage regeneration [56].

Pereira et al. 2018 have studied the GG with hydroxyapatite-based bilayered hydrogel composite for osteochondral tissue regeneration and reported that, based on the architectural observations through stereomicroscope and micro-

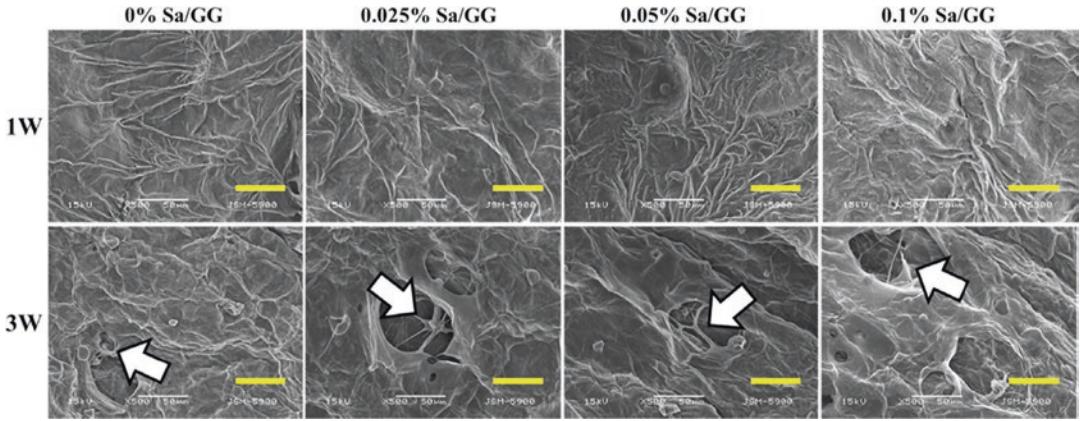


Fig. 6.2 FESEM images of 1 week and 3 weeks saponin–gellan gum (Sa-loaded GG) hydrogels (with a magnification of 500, scale bar represents 50 μm , and arrow denotes the 3-week formation of ECM from chondrocytes) [57]

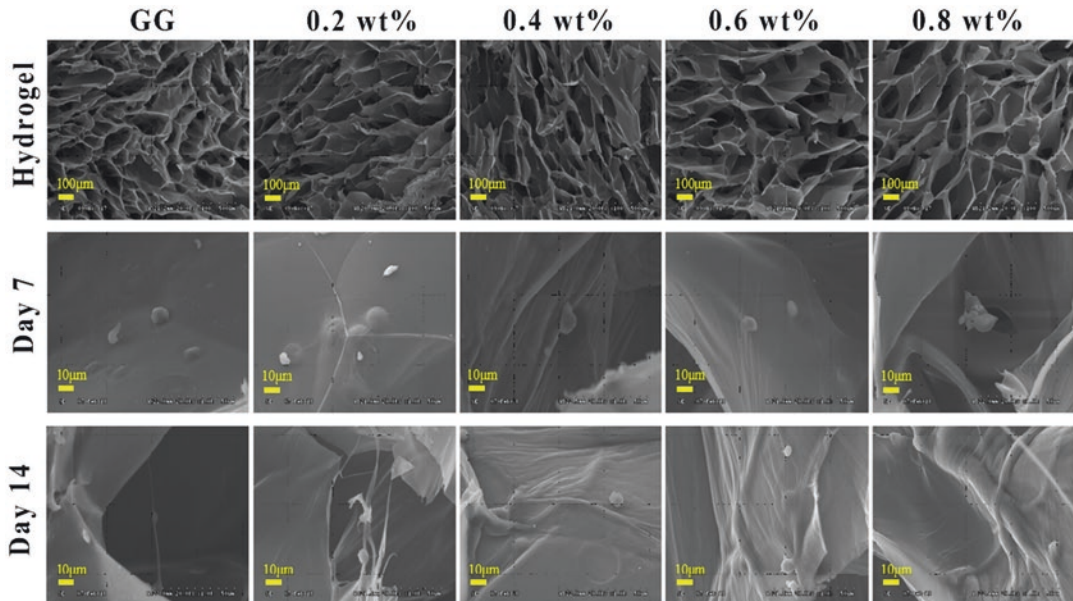


Fig. 6.3 SEM images showing the surface morphology of the pristine hydrogel and the chondrocytes cultured on the GG and GG–A hydrogel for 7 and 14 days [56]

computed tomography ($\mu\text{-CT}$), it demonstrated a connected stratified morphology with good ceramic dispersion within the bone-like layer. The swelling, degradation, as well as the mechanical analysis data revealed a stable viscoelastic construct under dynamic forces. The scaffold was biomimetic toward the bone formation

and was observed to be biocompatible and non-toxic. Their *in vivo* study 4 weeks after the implantation in the orthopedic knee model showed good integration with the surrounding tissue demonstrating that the bilayer scaffold with unique features can be used for OC regeneration [82].

6.6 Demineralized Bone Particle with GG for Bone Tissue Regeneration

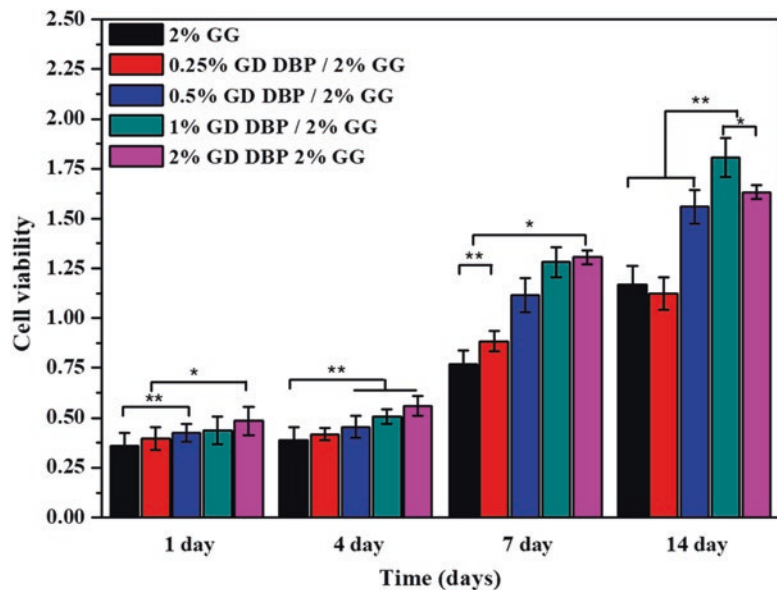
DBP, an effective bone regeneration material, has a trace quantity of ions and bone mineral element. Especially, GD (*Gallus gallus var domesticus*) derived DBP has a unique property, which has melanin, for strengthening bones, improving ALP activity and bone mineralization, compared to other available biomaterials. A recent study on the effect of different concentrations of the demineralized bone particles with GG porous scaffold for the application of bone tissue regeneration was reported [83]. The prepared scaffolds were characterized by their physicochemical properties, and further, they were studied for their biocompatibility and toxicity in vitro using BMSCs cells and in vivo in the rat as an animal model. The biocompatibility study showed that the rate of cell growth was higher by 2% in the GD with DBP–GG scaffold than 2% of the GG scaffold. Figure 6.4 shows the biocompatibility study results of the OD in different days. Initially, 2% samples showed higher BMSCs growth rate; later it was changed on day 14, where the 1% GD

DBP–GG samples showed significantly higher cell growth. The same pattern of cell growth was observed in days 4 and 7 and on the 1% and 2% of the GD with DBP–GG scaffolds. Reposts say the native bone tissue collagen plays a significant role in maintaining the structural integrity of the ECM [84]. The collagen and other ECM proteins using the adhesive transmembrane molecules will increase cell adhesion properties [85].

This was further confirmed by the LIVE/DEAD® viability assay results using confocal images, where live cells are stained green and the dead cells are stained red. Figure 6.5 shows the presence of live dead cells on the surface of the scaffold captured using confocal laser microscopy stained after 1, 7, and 14 days. Histological analysis was also presented for use in the in vitro analysis.

Hematoxylin and eosin and von Kossa staining shows the proliferation of BMSCs on the scaffold after 7 and 14 days of culture the images were shown in Fig. 6.6 The image clearly shows the proliferation and mineralization of BMSCs into scaffolds in all the groups. The BMSCs in the 1% sample were observed to be significantly proliferated after 14 days, and the rate of mineralization was also higher. The expression of ECM

Fig. 6.4 Cell viability of BMSCs on GD with DBP–GG scaffolds of different concentrations 1, 4, 7, and 14 days after cell culture analyzed by MTT ($p < 0.05$, $p^{***} < 0.01$, and $p^{****} < 0.001$) [83]



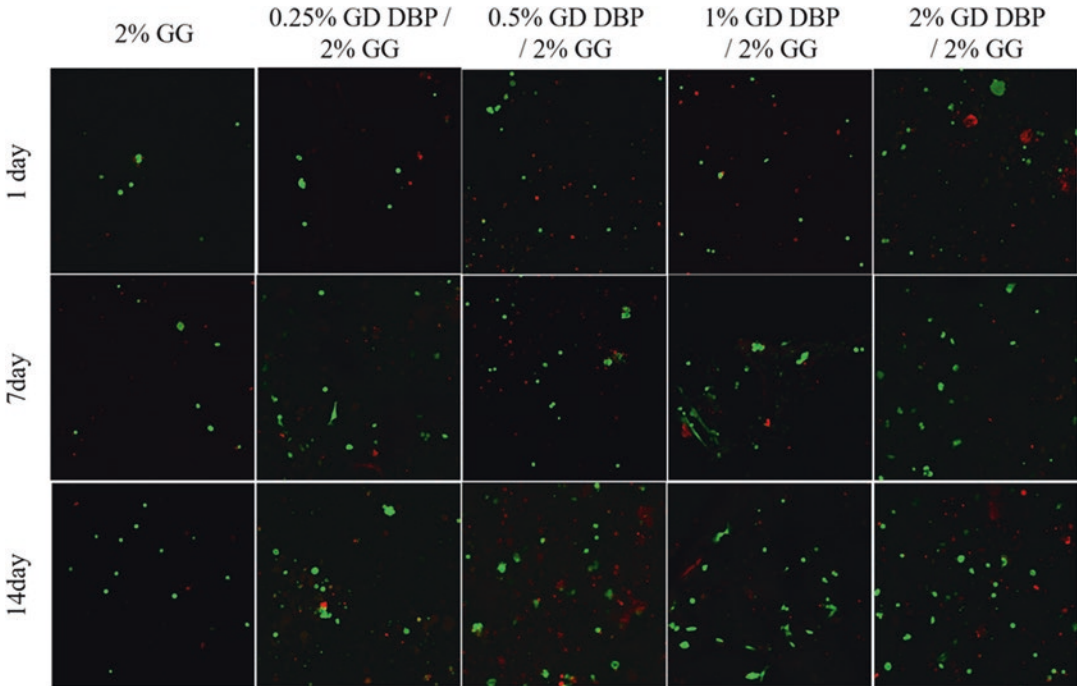


Fig. 6.5 Confocal microscopy images showing LIVE/DEAD® viability assay of BMSCs cultured for 1, 4, 7, and 14 days. Live cells are indicated by green, while dead

cells are indicated by red color (1×10^5 BMSCs into the scaffolds were seeded initially)

was stained using H&E, and it showed that the osteoblast was embedded in ECM. The von Kossa staining verified the phosphate group used in the study to recognize the mineralized bone matrix present inside the scaffolds.

The *in vivo* experimental results showed that the 1% samples were highly suitable for bone regeneration; they were supported by the animal studies using μ -CT and histology results. The regeneration properties of implanted graft were studied at the defeated site of the rat's skull using μ -CT analysis data of the 3D reconstruction of calvarial bone after *in vivo* experimental period on 2 and 4 weeks shown in Fig. 6.7 along with the (b) bone mineral density (BMD), (c) bone surface (BS), (d) bone volume (BV), (e) percent of bone volume (PBV), (f) trabecular number (Tb.N), and (g) trabecular separation.

The μ -CT analysis data clearly shows that the new bone formation in the control groups was less and was wide open, whereas in the treated groups on 4th week showed bone tissue filling

along with the mineralization. They are evident from the quantitative analysis data that play an important role in measuring the bone regeneration and strength of the bone. Increased bone mineralization density at 4th week was reported. One percent of the scaffold-treated groups showed significant increase in the bone volume over a period of 4 weeks. Study results clearly represent the density of the bone was significantly higher in treated groups. They were further supported by the histological analysis data using the H&E, von Kossa, Masson's trichrome, and ED-1 staining and is shown in Fig. 6.8. The H&E images showed one irregular regeneration on the 2nd and 4th week in the blank groups. The von Kossa staining showed that a large amount of phosphate group showed brownish-black color in 4 weeks of all the treated groups. Compared with 2nd week, where the cytoplasm and nuclei are dyed pink and red, the bone matrix in the scaffold was observed to be well mineralized [86]. MTS results are similar to that of the H&E results: at

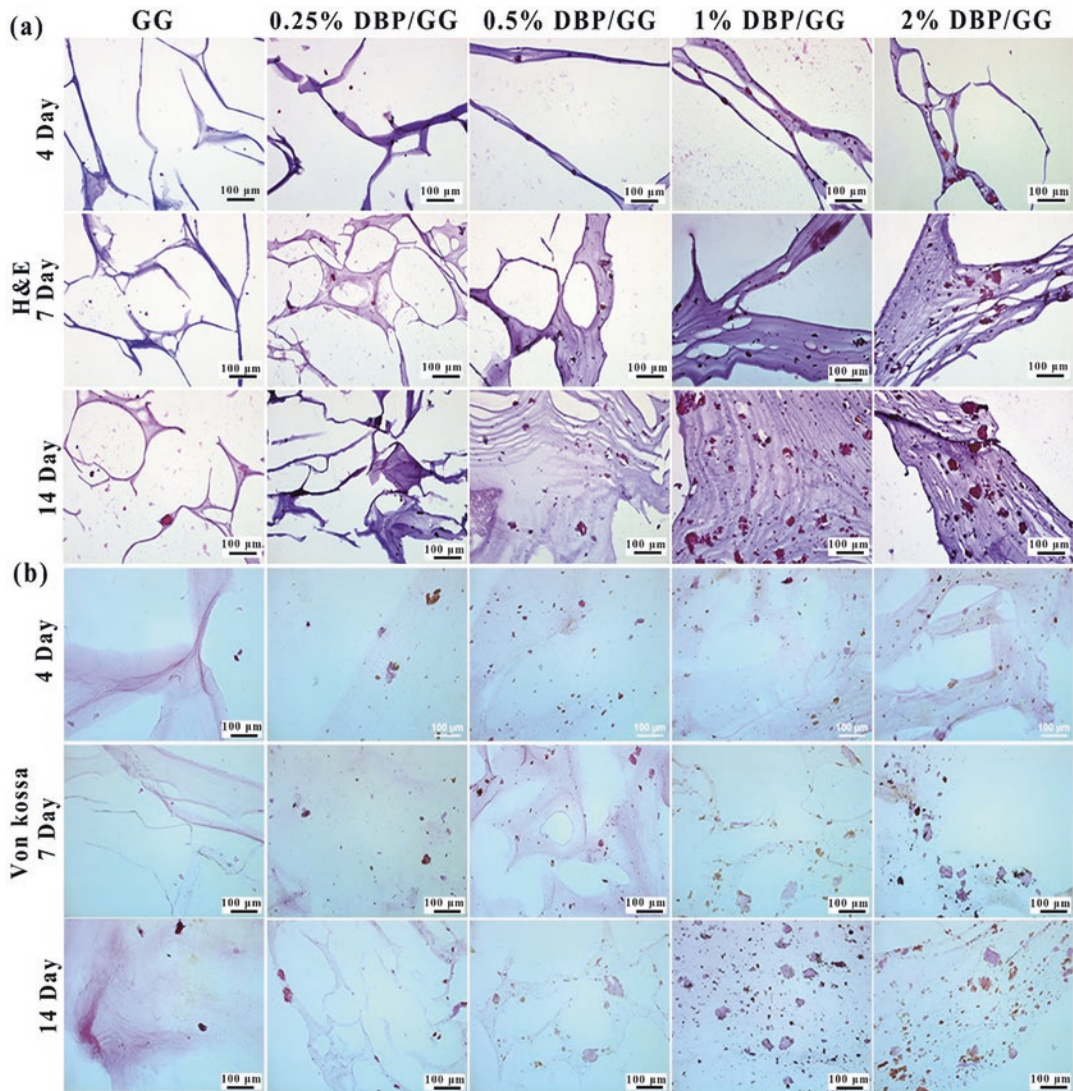


Fig. 6.6 Showing the histology staining of H&E (a), von Kossa (b), and the staining 4, 7, and 14 days after the cryosection of the 2% GG and 0.25% GD with DBP, 2%

GG and 0.5% GD with DBP, 2% GG and 1% GD with DBP, 2% GG and 2% GD with DBP and 2% GG respectively [83]

2 weeks the collagen content was less, whereas at 4 weeks the collagen content was observed to be increased in the 1% treated group compared with control and the other groups [87]. The microglia and invading macrophages were positively stained with ED1 (CD68) antibody, and the glycosylated antigen expressed activation of phagocytes [88]. Only a few macrophages were reported in the 1% treated groups that are expressed as dark brown color.

6.7 Conclusions

Different combinations of biomaterials are studied by the scientific community as a promising material for osteochondral tissue regeneration. Among the many materials successfully applied in the biomedical and clinical applications, the GG and DBP have received considerable attention separately due to their incredible flexibility. The nature of the GG and DBP, such as biological

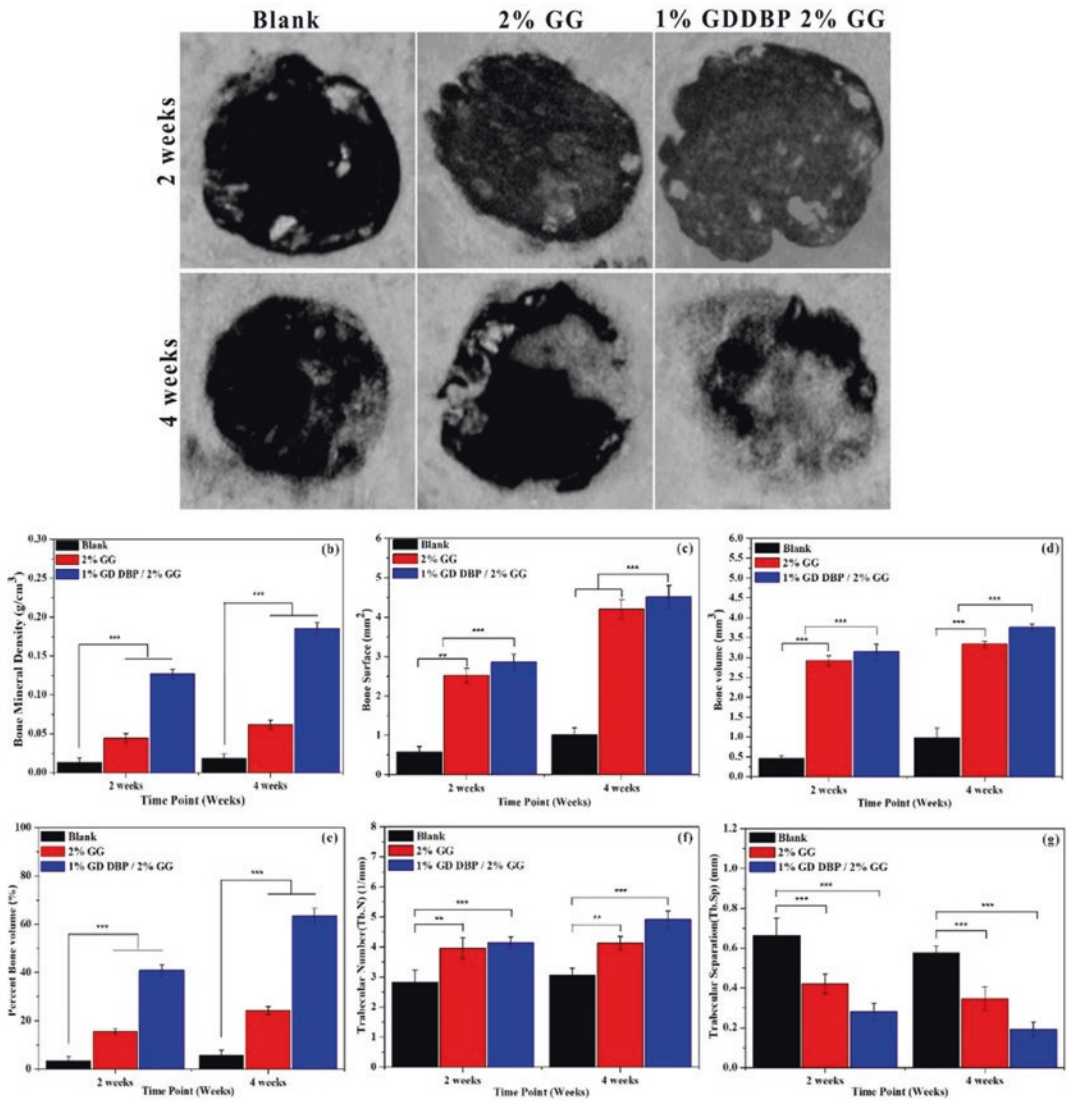


Fig. 6.7 (a) Micro-CT images after in vivo samples of the second- and fourth-week implantation of blank: 2% GG and 1% GD with DBP and 2% GG samples. (b) Bone mineral density (BMD), (c) bone surface (BS), (d) bone volume (BV), (e) percent of bone volume (PBV), (f) trabecular number (Tb.N), and (g) trabecular separation (Tb.Sp). (**p* < 0.05, ***p* < 0.01, ****p* < 0.001)

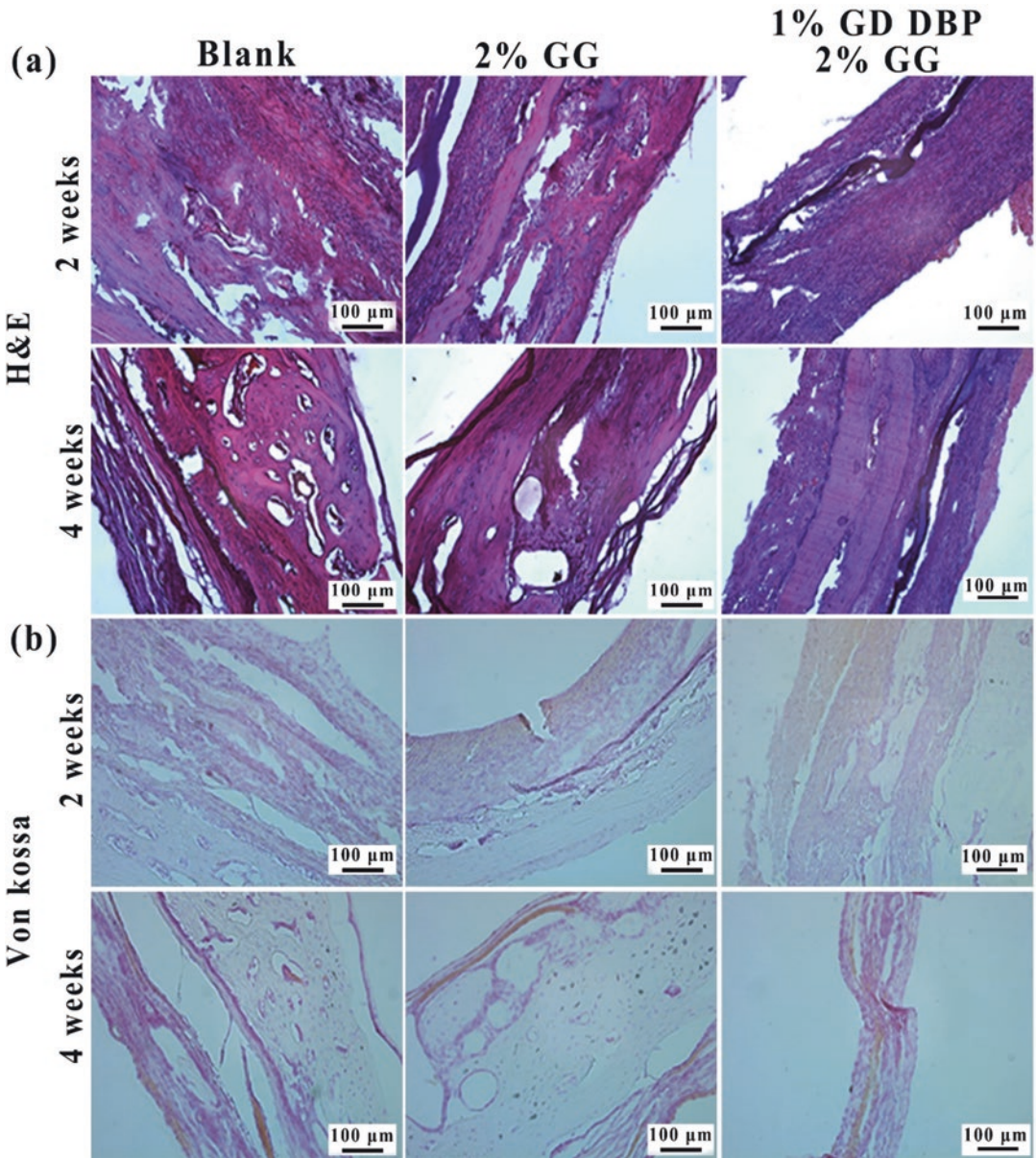


Fig. 6.8 The H&E (a), von Kossa (b), and Masson’s trichrome (c) staining (d) reported results in the 1% treated group after in vivo at 2 and 4 weeks

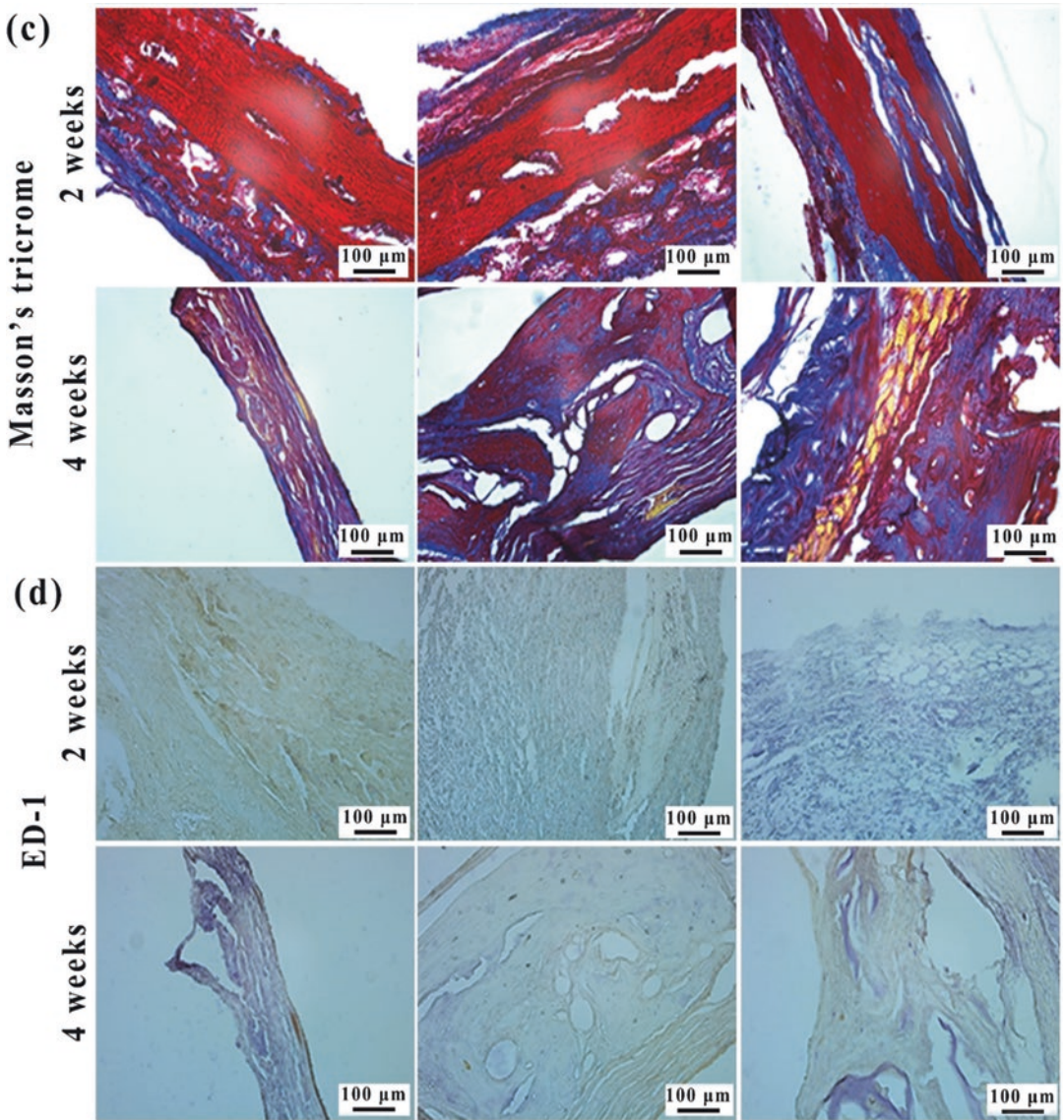


Fig. 6.8 (continued)

performance, and their application in osteochondral tissue regeneration field were discussed in this chapter. Different concentration of DBP with GG were used to prepare biomaterial scaffold that has biocompatible properties along with considerable preclinical studies have confirmed the potential of this scaffold as osteochondral tissue regeneration material. They can be constructed into scaffold and hydrogels that are injectable

and printable and encapsulated with other active components. However, GG applications as a bifunctional incorporated system for bone regeneration/repair still remain as a challenging field, so only a few studies have reported on the application of GG-based hydrogels for cartilage regeneration. The combination of GG with DBM is observed to be suitable material for the clinical implant for bone regeneration.

Acknowledgment This research was supported by a grant of the Korea Health Technology R&D Project through the Korea Health Industry Development Institute (KHIDI), funded by the Ministry of Health and Welfare, Republic of Korea (grant number: HI15C2996), and the International Research and Development Program of the National Research Foundation of Korea (NRF) funded by the Ministry of Science, ICT and Future Planning (NRF-2017K1A3A7A03089427).

References

- Hunter DJ (2009) Risk stratification for knee osteoarthritis progression: a narrative review. *Osteoarthr Cartil* 17(11):1402–1407
- Li X, Ding J, Wang J et al (2015) Biomimetic biphasic scaffolds for osteochondral defect repair. *Regen Biomater* 2(3):221–228
- Lee WY, Wang B (2017) Cartilage repair by mesenchymal stem cells: clinical trial update and perspectives. *J Orthop Translat* 9:76–88
- Csaki C, Schneider PR, Shakibaei M (2008) Mesenchymal stem cells as a potential pool for cartilage tissue engineering. *Ann Anat* 190(5):395–412
- Murphy L, Helmick CG (2012) The impact of osteoarthritis in the United States: a population-health perspective: a population-based review of the fourth most common cause of hospitalization in U.S. adults. *Orthop Nurs* 31(2):85–91
- Centers for Disease Control and Prevention (2010) Prevalence of doctor-diagnosed arthritis and arthritis-attributable activity limitation. United States, 2007–2009. <https://www.cdc.gov/mmwr/preview/mmwrhtml/mm5939a1.htm>
- Laskin RS (1978) Unicompartmental tibiofemoral resurfacing arthroplasty. *J Bone Joint Surg Am* 60(2):182–185
- Jakobsen RB, Engebretsen L, Slauterbeck JR (2005) An analysis of the quality of cartilage repair studies. *J Bone Joint Surg Am* 87(10):2232–2239
- Lynn AK, Brooks RA, Bonfield W et al (2004) Repair of defects in articular joints. Prospects for material-based solutions in tissue engineering. *J Bone Joint Surg (Br)* 86(8):1093–1099
- Redman SN, Oldfield SF, Archer CW (2005) Current strategies for articular cartilage repair. *Eur Cell Mater* 9:23–32. discussion 23–32
- Sgaglione NA (2004) The future of cartilage restoration. *J Knee Surg* 17(4):235–243
- Nooeaid P, Salih V, Beier JP et al (2012) Osteochondral tissue engineering: scaffolds, stem cells and applications. *J Cell Mol Med* 16(10):2247–2270
- Deng C et al (2019) Micro/nanometer-structured scaffolds for regeneration of both cartilage and subchondral bone. *Adv Funct Mater* 29(4):1806068
- Deng C et al (2018) Bioactive scaffolds for regeneration of cartilage and subchondral bone interface. *Theranostics* 8(7):1940–1955
- Magill P, Byrne DP, Baker JF et al (2011) Review article: Osteochondral reconstruction and grafting. *J Orthop Surg (Hong Kong)* 19(1):93–98
- Das RK, Gocheva V, Hammink R et al (2016) Stress-stiffening-mediated stem-cell commitment switch in soft responsive hydrogels. *Nat Mater* 15(3):318–325
- Liu X, Jin X, Ma PX (2011) Nanofibrous hollow microspheres self-assembled from star-shaped polymers as injectable cell carriers for knee repair. *Nat Mater* 10(5):398–406
- Seo SJ, Mahapatra C, Singh RK et al (2014) Strategies for osteochondral repair: focus on scaffolds. *J Tissue Eng* 5:2041731414541850
- Brittberg M, Lindahl A, Nilsson A et al (1994) Treatment of deep cartilage defects in the knee with autologous chondrocyte transplantation. *N Engl J Med* 331(14):889–895
- da Cunha Cavalcanti FM, Doca D, Cohen M et al (2015) Updating on diagnosis and treatment of chondral lesion of the knee. *Rev Bras Ortop* 47(1):12–20
- Shimomura K et al (2010) The influence of skeletal maturity on allogenic synovial mesenchymal stem cell-based repair of cartilage in a large animal model. *Biomaterials* 31(31):8004–8011
- Makris EA, Gomoll AH, Malizos KN et al (2015) Repair and tissue engineering techniques for articular cartilage. *Nat Rev Rheumatol* 11(1):21–34
- Mithoefer K et al (2006) Chondral resurfacing of articular cartilage defects in the knee with the microfracture technique. Surgical technique. *J Bone Joint Surg Am* 88(Suppl 1, Pt 2):294–304
- He A, Liu L, Luo X et al (2017) Repair of osteochondral defects with in vitro engineered cartilage based on autologous bone marrow stromal cells in a swine model. *Sci Rep* 7:40489
- Deng C, Chang J, Wu C (2018) Bioactive scaffolds for osteochondral regeneration. *J Orthop Translat* 17:15–25
- Hunziker EB, Quinn TM, Hauselmann HJ (2002) Quantitative structural organization of normal adult human articular cartilage. *Osteoarthr Cartil* 10(7):564–572
- Zhang Y, Wang F, Tan H et al (2012) Analysis of the mineral composition of the human calcified cartilage zone. *Int J Med Sci* 9(5):353–360
- Noyes FR, Stabler CL (1989) A system for grading articular cartilage lesions at arthroscopy. *Am J Sports Med* 17(4):505–513
- Acebes C, Roman-Blas JA, Delgado-Baeza E et al (2009) Correlation between arthroscopic and histopathological grading systems of articular cartilage lesions in knee osteoarthritis. *Osteoarthr Cartil* 17(2):205–212
- Custers RJH, Creemers LB, Verbout AJ et al (2007) Reliability, reproducibility and variability of the traditional histologic/histochemical grading system vs the new OARSIS osteoarthritis cartilage histopathology assessment system. *Osteoarthr Cartil* 15(11):1241–1248

31. Ulrich-Vinther M, Maloney MD, Schwarz EM et al (2003) Articular cartilage biology. *J Am Acad Orthop Surg* 11(6):421–430
32. Curl WW, Krome J, Gordon ES et al (1997) Cartilage injuries: a review of 31,516 knee arthroscopies arthroscopy. *Arthroscopy* 13(4):456–460
33. Upmeier H, Brügggenjürgen B, Weiler A et al (2007) Follow-up costs up to 5 years after conventional treatments in patients with cartilage lesions of the knee. *Knee Surg Sports Traumatol Arthrosc* 15(3):249–257
34. McNickle AG, Provencher MT, Cole BJ (2008) Overview of existing cartilage repair technology. *Sports Med Arthrosc Rev* 16(4):196–201
35. Gantar A, da Silva LP, Oliveira JM et al (2014) Nanoparticulate bioactive-glass-reinforced gellan-gum hydrogels for bone-tissue engineering. *Mater Sci Eng C* 43:27–36
36. Khang G et al (2015) Biological evaluation of intervertebral disc cells in different formulations of gellan gum-based hydrogels. *J Tissue Eng Regen Med* 9(3):265–275
37. Stevens LR, Gilmore KJ, Wallace GG et al (2016) Tissue engineering with gellan gum. *Biomater Sci* 4(9):1276–1290
38. Morris ER, Nishinari K, Rinaudo M (2012) Gelation of gellan – a review. *Food Hydrocoll* 28(2):373–411
39. Fialho AM, Moreira LM, Granja AT et al (2008) Occurrence, production, and applications of gellan: current state and perspectives. *Appl Microbiol Biotechnol* 79(6):889–900
40. Kim HS et al (2019) Engineering retinal pigment epithelial cells regeneration for transplantation in regenerative medicine using PEG/gellan gum hydrogels. *Int J Biol Macromol* 130:220–228
41. Anandan D, Madhumathi G, Nambiraj NA et al (2019) Gum based 3D composite scaffolds for bone tissue engineering applications. *Carbohydr Polym* 214:62–70
42. Bonifacio MA et al (2018) Antibacterial effectiveness meets improved mechanical properties: Manuka honey/gellan gum composite hydrogels for cartilage repair. *Carbohydr Polym* 198:462–472
43. Bonifacio MA et al (2018) Data on Manuka honey/gellan gum composite hydrogels for cartilage repair. *Data Brief* 20:831–839
44. Costa L, Silva-Correia J, Oliveira JM et al (2018) Gellan gum-based hydrogels for osteochondral repair. *Adv Exp Med Biol* 1058:281–304
45. Prajapati VD, Jani GK, Zala BS et al (2013) An insight into the emerging exopolysaccharide gellan gum as a novel polymer. *Carbohydr Polym* 93(2):670–678
46. Song JE, Lee SE, Cha SR et al (2016) Inflammatory response study of gellan gum impregnated duck's feet derived collagen sponges. *J Biomater Sci Polym Ed* 27(15):1495–1506
47. Vieira S, Da Silva MA, Garet E et al (2019) Self-mineralizing Ca-enriched methacrylated gellan gum beads for bone tissue engineering. *Acta Biomater* 93:74–85
48. Vuornos K et al (2019) Bioactive glass ions induce efficient osteogenic differentiation of human adipose stem cells encapsulated in gellan gum and collagen type I hydrogels. *Mater Sci Eng C Mater Biol Appl* 99:905–918
49. Xu Z, Li Z, Jiang S et al (2018) Chemically modified Gellan gum hydrogels with tunable properties for use as tissue engineering scaffolds. *ACS Omega* 3(6):6998–7007
50. EFSA Panel on Food Additives and Nutrient Sources added to Food (ANS), Younes M, Aggett P et al (2018) Re-evaluation of gellan gum (E 418) as food additive. *EFSA J* 16(6):e05296
51. Mano JF et al (2007) Natural origin biodegradable systems in tissue engineering and regenerative medicine: present status and some moving trends. *J R Soc Interface* 4(17):999–1030
52. Ciardelli G et al (2005) Blends of poly-(epsilon-caprolactone) and polysaccharides in tissue engineering applications. *Biomacromolecules* 6(4):1961–1976
53. Oliveira JT et al (2010) Gellan gum: a new biomaterial for cartilage tissue engineering applications. *J Biomed Mater Res A* 93(3):852–863
54. Vilela CA et al (2018) In vitro and in vivo performance of methacrylated gellan gum hydrogel formulations for cartilage repair. *J Biomed Mater Res A* 106(7):1987–1996
55. Pereira DR, Silva-Correia J, Oliveira JM et al (2018) Nanocellulose reinforced gellan-gum hydrogels as potential biological substitutes for annulus fibrosus tissue regeneration. *Nanomed Nanotechnol Biol Med* 14(3):897–908
56. Baek JS et al (2019) Evaluation of cartilage regeneration in gellan gum/agar blended hydrogel with improved injectability. *Macromol Res* 27(6):558–564
57. Jeon HY, Shin EY, Choi JH et al (2018) Evaluation of Saponin loaded gellan gum hydrogel scaffold for cartilage regeneration. *Macromol Res* 26(8):724–729
58. Oliveira JT et al (2010) Gellan gum injectable hydrogels for cartilage tissue engineering applications: in vitro studies and preliminary in vivo evaluation. *Tissue Eng Part A* 16(1):343–353
59. Shin EY, Park JH, Shin ME et al (2019) Evaluation of chondrogenic differentiation ability of bone marrow mesenchymal stem cells in silk fibroin/gellan gum hydrogels using miR-30. *Macromol Res* 27(4):369–376
60. Carvalho CR et al (2018) Gellan gum-based luminal fillers for peripheral nerve regeneration: an in vivo study in the rat sciatic nerve repair model. *Biomater Sci* 6(5):1059–1075
61. Silva-Correia J, Miranda-Gonçalves V, Salgado AJ et al (2012) Angiogenic potential of gellan-gum-based hydrogels for application in nucleus Pulposus regeneration: in vivo study. *Tissue Eng Part A* 18(11–12):1203–1212
62. Sun J, Zhou Z (2018) A novel ocular delivery of brinzolamide based on gellan gum: in vitro and in vivo evaluation. *Drug Des Devel Ther* 12:383–389

63. McWilliams DF, Walsh DA, Wilson D et al (2010) Angiogenesis and nerve growth factor at the osteochondral junction in rheumatoid arthritis and osteoarthritis. *Rheumatology (Oxford)* 49(10):1852–1861
64. Miyoshi E, Takaya T, Nishinari K (1996) Rheological and thermal studies of gel-sol transition in gellan gum aqueous solutions. *Carbohydr Polym* 30(2–3):109–119
65. Jen AC, Wake MC, Mikos AG (1996) Review: hydrogels for cell immobilization. *Biotechnol Bioeng* 50(4):357–364
66. Ruoslahti E (1989) Proteoglycans in cell regulation. *J Biol Chem* 264(23):13369–13372
67. Douglas TEL et al (2017) Composites of gellan gum hydrogel enzymatically mineralized with calcium–zinc phosphate for bone regeneration with antibacterial activity. *J Tissue Eng Regen Med* 11(5):1610–1618
68. Douglas TEL et al (2014) Injectable self-gelling composites for bone tissue engineering based on gellan gum hydrogel enriched with different bioglasses. *Biomed Mater* 9(4):045014
69. Kang SC, Kim HJ, Kim MH (2013) Effects of Astragalus membranaceus with supplemental calcium on bone mineral density and bone metabolism in calcium-deficient Ovariectomized rats. *Biol Trace Elem Res* 151(1):68–74
70. Rasch LA, De van der Schueren MAE, Van Tuyl LHD et al (2017) Content validity of a short calcium intake list to estimate daily dietary calcium intake of patients with osteoporosis. *Calcif Tissue Int* 100(3):271–277
71. Adluri RS, Zhan L, Bagchi M et al (2010) Comparative effects of a novel plant-based calcium supplement with two common calcium salts on proliferation and mineralization in human osteoblast cells. *Mol Cell Biochem* 340(1–2):73–80
72. Yoo HS, Chung KH, Lee KJ et al (2017) Melanin extract from *Gallus gallus domesticus* promotes proliferation and differentiation of osteoblastic MG-63 cells via bone morphogenetic protein-2 signaling. *Nutr Res Pract* 11(3):190–197
73. Yoo HS, Kim GJ, Song DH et al (2017) Calcium supplement derived from *Gallus gallus domesticus* promotes BMP-2/RUNX2/SMAD5 and suppresses TRAP/RANK expression through MAPK signaling activation. *Nutrients* 9(5):504
74. Liu W et al (2013) Isolation and identification of antioxidative peptides from pilot-scale black-bone silky fowl (*Gallus gallus domesticus* Brisson) muscle oligopeptides. *J Sci Food Agric* 93(11):2782–2788
75. Han KS, Song JE, Kang SJ et al (2015) Effect of demineralized bone particle/poly(lactic-co-glycolic acid) scaffolds on the attachment and proliferation of mesenchymal stem cells. *J Biomater Sci Polym Ed* 26(2):92–110
76. Jo H, Hong M, Shim JB et al (2015) The role of demineralized bone particle in a PLGA scaffold designed to create a media equivalent for a tissue engineered blood vessel. *Macromol Res* 23(11):986–993
77. Kim SH, Song JE, Lee D et al (2012) Demineralized bone particle impregnated poly(l-Lactide-co-Glycolide) scaffold for application in tissue-engineered intervertebral discs. *J Biomater Sci Polym Ed* 23(17):2153–2170
78. Song JE, Kim EY, Ahn WY et al (2015) The potential of DBP gels containing intervertebral disc cells for annulus fibrosus supplementation: in vivo. *J Tissue Eng Regen Med* 9(11):E98–E107
79. Khan SN, Cammisa FP Jr, Sandhu HS et al (2005) The biology of bone grafting. *J Am Acad Orthop Surg* 13(1):77–86
80. Gong Y, Wang C, Lai RC et al (2009) An improved injectable polysaccharide hydrogel: modified gellan gum for long-term cartilage regeneration in vitro. *J Mater Chem* 19(14):1968–1977
81. Smith AM, Shelton RM, Perrie Y et al (2007) An initial evaluation of gellan gum as a material for tissue engineering applications. *J Biomater Appl* 22(3):241–254
82. Pereira DR et al (2018) Injectable gellan-gum/hydroxyapatite-based bilayered hydrogel composites for osteochondral tissue regeneration. *Appl Mater Today* 12:309–321
83. Kim D, Thangavelu M, Song C et al (2019) Effect of different concentration of demineralized bone powder with gellan gum porous scaffold for the application of bone tissue regeneration. *Int J Biol Macromol* 134:749–758
84. Teti A (1992) Regulation of cellular functions by extracellular matrix. *J Am Soc Nephrol* 2(10 Suppl):S83
85. Masuda H, Ishihara S, Harada I et al (2014) Coating extracellular matrix proteins on a (3-aminopropyl) triethoxysilane-treated glass substrate for improved cell culture. *BioTechniques* 56(4):172–179
86. Relucenti M, Heyn R, Petruzzello L et al (2010) Detecting microcalcifications in atherosclerotic plaques by a simple trichromic staining method for epoxy embedded carotid endarterectomies. *Eur J Histochem* 54(3):e33–e33
87. Sieren JC et al (2010) An automated segmentation approach for highlighting the histological complexity of human lung cancer. *Ann Biomed Eng* 38(12):3581–3591
88. McMenamin PG, Djano J, Wealthall R et al (2002) Characterization of the macrophages associated with the tunica Vasculosa Lentis of the rat eye. *Invest Ophthalmol Vis Sci* 43(7):2076–2082

Part III

Control of Stem Cell Fate by Biomaterials for Regenerative Medicine



The Development of Extracellular Vesicle-Integrated Biomaterials for Bone Regeneration

7

Yinghong Zhou and Yin Xiao

Abstract

The clinical need for effective bone regeneration remains in huge demands. Although autologous and allogeneic bone grafts are generally considered “gold standard” treatments for bone defects, these approaches may result in various complications. Furthermore, safety considerations of gene- and cell-based therapies require further clarification and approval from regulatory authorities. Therefore, developing new therapeutic biomaterials that can empower endogenous regenerative properties to accelerate bone repair and regeneration is of great significance. Extracellular vesicles (EVs) comprise a heterogeneous population of naturally derived nanoparticles that play a critical role in mediating cell–cell communication. The vast amount of biological processes that EVs are involved in, such as

immune modulation, senescence, and angiogenesis, and the versatility of manner in which they can influence the behavior of recipient cells make EVs an interesting source for both diagnostic and therapeutic applications. Advancement of knowledge in the fields of immunology and cell biology has sparked the exploration of the potential of EVs in the field of regenerative medicine. EVs travel between cells and deliver functional cargoes, such as proteins and RNAs, thereby regulating the recruitment, proliferation, and differentiation of recipient cells. Numerous studies have demonstrated the pivotal role of EVs in tissue regeneration both in vitro and in vivo. In this chapter, we will outline current knowledge surrounding EVs, summarize their functional roles in bone regenerative medicine, and elaborate on potential application and challenges of EV-integrated biomaterials in bone tissue engineering.

Y. Zhou (✉) · Y. Xiao

Institute of Health and Biomedical Innovation,
Queensland University of Technology (QUT),
Brisbane, QLD, Australia

Key Laboratory of Oral Medicine, Guangzhou
Institute of Oral Disease, Stomatology Hospital of
Guangzhou Medical University, Guangzhou, China

The Australia-China Centre for Tissue Engineering
and Regenerative Medicine (ACCTERM),
Queensland University of Technology (QUT),
Brisbane, QLD, Australia
e-mail: yinghongzhou@qut.edu.au; yin.xiao@qut.edu.au

Keywords

Extracellular vesicles · Osteoblasts ·
Biomaterials · Bone regeneration ·
Osteogenesis

7.1 A Brief History of Extracellular Vesicles (EVs)

Extracellular vesicles (EVs) are a heterogeneous population of biological particles naturally released from most cell types, which play a critical role in intercellular communication [1]. The first observation of EVs was reported as platelet-derived particles in normal plasma in 1946 by Chargaff and West [2]. The presence of phospholipid-rich particulates within the platelets was then acknowledged and referred to as “platelet dust” by Wolf in 1960s [3]. It was noted that these particulates could be separated by ultracentrifugation and displayed procoagulant properties [3]. Early observations by Anderson [4] and Bonucci [5] in 1967 also included matrix vesicles identified during cartilage development and calcification. In 1980, Trams and colleagues uncovered the essential role that EVs played in the intercellular transport of trophic substances or nutrients [6], and such vesicles ranging from 40 to 1 000 nm were initially suggested to be referred to as exosomes, although the subcellular origin of these vesicles remained unclear. Around the same time, the first observations of tumor-originating membrane fragments were made [7], and they were also shown to be procoagulant [8]. Later in the 1980s, the secretory vesicles were reported to mediate reticulocyte maturation through recycling of transferrin and its receptor [9, 10]. Subsequent detailed ultrastructural studies showed that these nano-sized messengers were also released by multivesicular bodies (MVBs) fusing with the cell membrane during the differentiation of immature red blood cells [11, 12]. One decade later, pioneering studies by Raposo and colleagues discovered that EVs derived from the Epstein-Barr virus-transformed B lymphocytes incorporated and transported functional antigen-presenting complexes and were able to stimulate T cell responses [13]. From then on, many studies have further demonstrated that EVs are derived from professional antigen-presenting cells, such as dendritic cells (DCs), express class I and class II major histocompatibility complex (MHC), adhesion, and

co-stimulatory molecules that can directly activate CD4⁺ and CD8⁺ T cells [14, 15].

From the late 2000s onward, several key works have revealed the role of tumor EVs in promoting cancer growth and metastasis [16–18], and highlighted their potential utility as biomarkers [19]. In 2006–2007, further research discovered that EVs contain RNA, including microRNA, which fueled renewed interest in EVs as mediators of cell–cell communication [20, 21]. An important step in the recent advancement of the EV field has been the enthusiastic collaborative work since 2011 by the members of the International Society for Extracellular Vesicles (ISEV). Although a full consensus has yet to be achieved regarding specific markers of EV subtypes, such as endosome-origin exosomes and plasma membrane-derived ectosomes, it is suggested by the ISEV that referring to EV subtypes can be based on (a) physical characteristics, such as size, with ranges of diameter or density defined; (b) biochemical composition; or (c) descriptions of conditions or cell of origin [22]. Based on size, morphology, origin, and other biological features, EVs are commonly classified into exosomes, microvesicles (MVs), and apoptotic bodies (Table 7.1) [23, 24]. Exosomes are 40–100 nm cup-shaped vesicles produced by endosomal multivesicular bodies (MVBs), which are released into the extracellular microenvironment through fusion of the membrane of MVBs with the plasma membrane [23, 25]. MVs are generally 100–1000 nm in size and released from the cell by the outward budding of the plasma membrane [25, 26]. Apoptotic bodies can be formed during cell death and by blebbing of the plasma membrane [27, 28].

7.2 The Functional Role of EVs in Bone Regenerative Medicine

Regenerative medicine aims at the functional restoration of damaged, malfunctioning, or missing tissues. Tissue engineering is a promising approach for the regeneration of tissues, and this

Table 7.1 Basic features of different extracellular vesicles

Characteristic	Exosome	Microvesicle	Apoptotic body
Size (nm)	40–100 [25]	100–1000 [25]	50–5000 [28]
Morphology	Homogeneous (cup-shaped)	Heterogeneous	Heterogeneous
Parental cell condition	Physiology and pathologic conditions	Physiologic conditions or in response to stimuli	Apoptosis
Origin	Multivesicular body (MVB)	Plasma membrane	Programmed cell death
Formation mechanism	Endocytic pathway	Plasma membrane	Plasma membrane
Release pattern	Fusion of the membrane of MVBs with the plasma membrane; exocytosis of MVBs	Outward budding from the plasma membrane	Cell shrinkage and death; blebbing of the plasma membrane
Cargo	Lipids, proteins, RNAs, and similar to those in the parental cells	Lipids, proteins, RNAs	Cell organelles, lipids, proteins, RNAs, and DNA fragments
Markers	CD9, CD63, CD83, Alix, TSG101, GTPases	CD40 ligand, adenosine diphosphate ribosylation factor 6 (ARF6), several selectins and integrins	Thrombospondin, complement component C3b, histones

strategy often involves the use of mesenchymal stem cells (MSCs) due to their capacity to differentiate into multiple lineages and to modulate inflammation/immune responses [29]. The primary strategy has been to transplant MSCs at the site of injury [30]. However, accumulating evidence indicates that there is a lack of correlation between functional tissue regeneration and the differentiation of cell engraftment at the injury site [31]. It has become increasingly apparent that the secretory products of MSCs are primarily responsible for the observed regenerative effects [32]. These paracrine factors secreted by MSCs, including EVs and their enclosing bioactive molecules, are of major interest to discover new therapeutics that stimulate tissue regeneration.

EVs were initially regarded as a vehicle to transport unwanted compounds of cells to the extracellular milieu [10, 33]. It has subsequently been appreciated that membrane-bound EVs are composed of a lipid bilayer containing transmembrane proteins and enclosing cytosolic bioactive compounds, including proteins, nucleic acids, and lipids [34]. The primary role of EVs in cell–cell communication is to transfer various bioactive signaling molecules between the parent and the recipient cells. The precise biological function of EVs is a reflection of the parental cell from which they were derived and the local

microenvironment (e.g., inflammatory or hypoxic). EVs can transmit biological information by directly activating cell surface receptors on the recipient cells, fusing with recipient cell plasma membranes and delivering their functional cargoes, including proteins and RNAs, into the cytoplasm of the recipient cells [35]. As EVs can regulate the recipient cells at a posttranscriptional level, they have garnered significant attention due to the increasing evidence that posttranscriptional regulation plays a larger role than previously expected [36, 37]. Indeed, the regenerative effect of EVs has been validated in various tissues and organs, including the heart [38], lung [39], kidney [40], and brain [41].

Bone regeneration using cell-based therapies and tissue engineering strategies is one of the most widely researched fields in regenerative medicine. Bone regeneration is a highly orchestrated biological sequence of events, involving dynamic intercellular communication among immune cells, MSCs, bone-forming osteoblasts, bone-resorbing osteoclasts, osteocytes, and other cell types via extracellular factors, adhesion molecules, and signaling pathways [42, 43]. Much evidence has demonstrated the important roles of MSC-derived EVs in osteogenesis both *in vitro* and *in vivo*. MicroRNAs (miRNAs) are thought to be important posttranscriptional regulators of

osteogenesis and bone remodeling [44]. Being enclosed in the lipid membranes of EVs, miRNAs can avoid the decomposition of immune system and, therefore, exert their effects more efficiently [45]. Profiling data for the MSC-derived EVs have revealed that a series of miRNAs, such as miR-let-7a, miR-199b, miR-218, miR-148a, miR-135b, miR-203, miR-219, miR-299-5p, and miR-302b, are significantly upregulated during the osteogenic differentiation of MSCs [46, 47]. These data all demonstrated that MSC-derived EVs could promote bone regeneration by carrying specific miRNAs which have significant roles in osteoblast function and activity, possibly due to the activation of Wnt/ β -catenin [2] and PI3K/Akt signaling pathways [48]. These *in vitro* findings have led to further investigation and application of MSC-derived EVs *in vivo* [49–51], which proved that MSC-derived EVs could stimulate bone growth and accelerate fracture healing.

In turn, osteoblasts also secrete EVs and send messages back to MSCs, thus establishing a positive feedback of bone repair and regeneration. It has been reported that EVs released by osteoblasts at the mid- to late differentiation stage remarkably promoted osteogenic differentiation of MSCs [52, 53], which might be due to the activation of Wnt signaling [53]. Other *in vitro* experiments also demonstrated that EVs derived from MSCs at the late differentiation stage have the strongest pro-osteogenic ability [29, 46]. Consistently, miR-31, miR-221, and miR-144 that have inhibitory effect on osteogenic differentiation decrease substantially in the EVs derived from late differentiation stage of MSCs, whereas miR-21, miR-10b, and other miRNAs that contribute to osteogenesis is significantly upregulated. The cross talk between bone-forming osteoblasts and bone-resorbing osteoclasts plays crucial roles in bone homeostasis and bone remodeling. EVs derived from osteoblasts can be bound to osteoclasts, leading to osteoblast–osteoclast communication [54]. On the other hand, osteoclasts also deliver their EVs to osteoblasts and regulate osteoblast activity [55].

Osteocytes, the terminally differentiated cells, play multifunctional roles in the regulation of bone remodeling [56]. Sato and colleagues

demonstrated that MLO-Y4 cells, a murine osteocyte-like immortalized cell line, release miRNA-containing EVs [57]. Additionally, osteocyte ablation in the dentin matrix protein-1-driven diphtheria toxin receptor transgenic mice resulted in a decreased expression of osteocyte-derived EVs containing miRNAs [58]. This finding indicates that miRNA-containing EVs derived from osteocytes circulate systemically, which could allow for cell–cell communication between osteocytes and distant target cells.

The close relationship of the immune and skeletal systems, which share many of the same regulatory pathways, such as cytokines, transcription factors, and signaling cues – a relationship known as osteoimmunology, has attracted much attention recently [59]. The reciprocal interaction between immune cells and bone cells participates actively in the bone remodeling and regeneration process. During initial bone healing, resting macrophages (key immune regulators) are activated into pro-inflammatory M1 phenotype, which are found predominantly in the defect area [60]. And in addition to removing the necrotic cell debris, M1 macrophages secrete a repertoire of inflammatory and chemotactic mediators, such as IL-1 β , TNF- α , and CCL2, which initiate the recruitment of MSCs from their local niches [61]. Macrophage-derived pro-inflammatory cytokines and chemokines, together with growth factors such as TGF- β , BMPs, and VEGF, subsequently guide the proliferation, differentiation, and extracellular matrix production of the recruited MSCs [62] and ultimately lead to bone regeneration [60, 63].

Our recent study has shown that EVs derived from BMP2-stimulated macrophages have significant pro-osteogenic effect [64]. Other studies have also reported that dendritic cell-derived EVs are endocytosed by MSCs and promote their recruitment and migration [65], and monocyte-derived EVs can stimulate the osteogenic differentiation of MSCs [66]. MSCs reciprocally modulate the activation and function of macrophages in response to an inflammatory microenvironment [67–70]. Major findings reveal that stem cell-derived EVs can attenuate inflammation through polarizing macrophages toward the anti-inflammatory M2 phenotype [70, 71]. It has

been well established that MSCs can regulate the mobility and function of macrophages through producing various chemokines and other factors [72, 73]. When partially differentiated to osteoblasts in vitro, MSCs implanted to murine cranial defects can improve defect healing by inducing macrophage recruitment and activation through the secretion of VEGF [73]. Besides the cytokines, miRNAs secreted by MSCs also participate in the regulation of macrophages [74]. It has been demonstrated that miR-223 enriched in MSC-derived EVs can reduce levels of TNF- α , IL-1 β , and IL-6 secreted from macrophages in an inflammatory microenvironment [74].

Apart from the miRNAs mentioned above, other key proteins contained in EVs also actively mediate a series of signaling pathways and regulate bone regeneration, such as Ephrin A2 [75], Semaphorin 4D (Sema4D) [55], receptor activator of nuclear factor kappa-B ligand (RANKL) [54], transforming growth factor beta receptor II interacting protein 1 (TRIP-1) [76], and matrix metalloproteinase 9 (MMP9) [65].

7.3 Therapeutic Biomaterials Based on EVs for Bone Regeneration

Due to the characteristic of transferring their bioactive molecules from parent cells to recipient cells, EVs have attracted increasing attention as a delivery system, particularly as a new alternative for delivering protein therapeutics [22]. Taking into consideration the critical roles of MSCs and their products in tissue regeneration, MSC-derived EVs are particularly promising candidates for developing cell-free therapies for bone regeneration. Zhang and colleagues generated exosomes derived from human-induced pluripotent stem cell-derived mesenchymal stem cells (hiPS-MSC-Exos) which then blotted onto porous tricalcium phosphate (β -TCP) scaffolds [48]. These exosome- β -TCP combination scaffolds led to enhanced bone regeneration in a rat calvarial defect model compared to pure β -TCP scaffolds [48]. Further in vitro studies showed that there was an initial burst release of exosomes from the scaffolds which could be internalized by

human bone marrow-derived mesenchymal stem cells (hBMSCs) and could significantly enhance the osteogenic differentiation of hBMSCs by activating PI3K/Akt signaling pathway [48]. Another recent study has also utilized hiPSC-MSC-Exos+ β -TCP scaffolds to promote bone regeneration and angiogenesis in critical-sized calvarial defects in ovariectomized rats [77].

To exert the optimal biological efficacy of EVs by a slow-release system, poly(lactic-co-glycolic acid) (PLGA) scaffolds has been modified through a mussel-inspired immobilization strategy assisted by polydopamine (pDA) [78]. The cell-free system is comprised of human adipose-derived stem cell (hASC)-derived EVs, which could be released slowly and constantly from the PLGA/pDA scaffolds. The hASC-derived exosomes could be internalized by human bone marrow-derived mesenchymal stem cells (hBMSCs) and further promoted the proliferation, migration, and osteogenic differentiation capabilities of hBMSCs in vitro. When implanted into critical-sized mouse calvarial defects, the hASC-derived EV-integrated PLGA/pDA scaffolds significantly enhanced bone formation in 6 weeks, although the mechanism behind the EVs' effects was not clearly defined and needed further exploration [78].

Recently, three-dimensional (3D) printed scaffolds have attracted much attention for tissue engineering applications, owing to their precise design of shapes and sizes as well as abundant selection of components [79]. Polycaprolactone (PCL) is a biodegradable polyester with a low melting point of around 60 °C. PCL is easy to manufacture and has high mechanical strength and a low rate of degradation. However, PCL has a suboptimal cellular activity as it does not carry any biologically active molecules. To address these drawbacks, alginate is often used in combination with PCL due to its extracellular matrix-like structure and capability of encapsulating various bioactive molecules. By incorporating EVs derived from rat bone marrow MSCs into alginate-PCL 3D constructs, Xie and colleagues have demonstrated an enhanced vessel formation and bone regeneration in a nude mouse subcutaneous bone formation model both after 1 and 2 months of implantation [80]. Using combination

of poly(lactide) (PLA) 3D printed scaffolds and human gingival mesenchyme stem cell-derived EVs, Diomede and colleagues were also able to demonstrate significantly bone healing in a rat calvarial defect model after 6 weeks of implantation [81].

Apart from using synthetic materials, researchers also endeavor in applying natural/endogenous materials to deliver EVs for bone repair. Xie and colleagues have fabricated decalcified bone matrix (DBM) scaffolds from bovine limbs [82]. The scaffolds were then loaded with 20 μg of EVs derived from rat bone marrow MSCs. The EV-modified DBM scaffolds were implanted subcutaneously in nude mice and demonstrated superior pro-angiogenic and pro-osteogenic effects in vivo [82].

In addition, EVs released from immune cells like monocytes and macrophages, are implicated in several fundamental biological processes, such as the recruitment of inflammatory cells, neovascularization, coagulation, and regulation of MSC differentiation. Thus, they are also of vital importance in ensuring the appropriate inflammatory reaction after injury, which would boost tissue repair and regeneration. Our recent study has shown a positive regulatory effect of BMP2-stimulated macrophage-derived EVs on the osteogenic differentiation of MSCs. We generated titanium nanotubes by electrochemical anodization [83], which were further coated with poly(dopamine) [84] for the integration of the BMP2/macrophage-stimulated EVs. The encapsulation of EVs into titanium nanotubes dramatically increased the expression of early osteoblastic differentiation markers via activation of autophagic activity [64]. Table 7.2 below summarizes recent studies on EV-integrated biomaterials for bone regeneration as noted above.

7.4 Advantages/Limitations of EV Therapeutics

Cell-free approaches may be advantageous when risk factors associated with the usage of living cells, especially stem cells, are considered. These can be intrinsic factors relating to cell origin,

tumorigenic potential, cell differentiation, and proliferation capacity or extrinsic factors concerning cell handling, storage, and transport conditions, among others. Furthermore, it is important to consider that stem cell yield decreases with increased donor age and that age may negatively affect cell performance. EVs, on the other hand, bypass a series of issues that arise with stem cell therapy. EVs are generally easier to be manufactured, stored, and tested for optimal dosage and potency, all of which are more cost-efficient compared to stem cell expansion or collection from patients. By replacing the administration of living cells with their secreted EVs, many of the safety concerns and limitations associated with the transplantation of viable replicating cells could be mitigated. Another important feature of EVs is the encapsulation and protection of their contents from degradation in vivo, thereby potentially preventing some of the problems associated with small soluble molecules such as cytokines, growth factors, transcription factors, and RNAs, which can degrade rapidly.

While EVs exhibit several attractive features as a therapeutic agent, there are also potential limitations to be considered. EVs contain a mixture of biologically active molecules such as mRNAs, miRNAs, lncRNA, DNA, lipids, peptides, and vast array of proteins (including oncoproteins, tumor suppressors, transcriptional regulators, and splicing factors) [85], some of which seem to have beneficial effects, whereas others might have negative (e.g., pro-inflammatory) effects under certain conditions. Whether EVs will turn out to be superior to pro-angiogenic and/or pro-osteogenic drugs or purified recombinant growth factors and other peptides within the context of cell-free approaches to bone regeneration remains to be further investigated. Another major challenge for realizing EV-based therapeutics is a generally low productivity of EVs. For example, yield of exosomes is typically less than 1 μg exosomal protein from 1 mL of culture medium [86], whereas the useful dose of exosomes is approximately 10–100 μg exosomal protein/mouse [87, 88]. Therefore, scalable systems for the production of EVs to support large-scale commercially

Table 7.2 Recent studies on EV-integrated biomaterials for bone regeneration

Origin of EVs	Type of EVs	Biomaterials	In vitro evaluation	In vivo evaluation	Major findings
Human-induced pluripotent stem cell-derived mesenchymal stem cells (hiPS-MSCs) [48]	Exosomes (exos)	Tricalcium phosphate (β -TCP)	Isolation and identification of hiPS-MSC-Exos; exosome released from β -TCP; cell proliferation and migration; gene expression profiling and bioinformatics analysis; quantitative real-time PCR analysis (qRT-PCR) analysis of osteogenesis-related gene expressions; Western blot analysis; alkaline phosphatase (ALP) assay and Alizarin Red S (ARS) staining	Critical-sized rat calvarial defects implanted with: (1) β -TCP, (2) β -TCP + EVs (5×10^{11} particles/mL), and (3) β -TCP + EVs (1×10^{12} particles/mL); sequential fluorescent labeling; micro-CT analysis; histological and immunohistochemical analysis	The hiPS-MSCs-Exos-functionalized β -TCP scaffolds can effectively promote bone repair and regeneration with an increasing exosome concentration, which is likely due to the activation of the PI3K/Akt signaling pathway
Human-induced pluripotent stem cell-derived mesenchymal stem cells (hiPS-MSCs) [77]	Exosomes (exos)	Tricalcium phosphate (β -TCP)	Isolation and identification of hiPS-MSC-Exos; cell proliferation; qRT-PCR analysis of osteogenesis-related gene expressions; Western blot analysis; ALP assay and ARS staining	Critical-sized calvarial defects in ovariectomized rats implanted with (1) β -TCP, (2) β -TCP + 100 μ g EVs, and (3) β -TCP + 200 μ g EVs; sequential fluorescent labeling; micro-CT analysis; Microfil perfusion; histological and immunohistochemical analysis	The hiPS-MSCs-Exos-functionalized β -TCP scaffolds can promote angiogenesis and osteogenesis in an ovariectomized rat calvarial defect model with an increasing exosome concentration
Human adipose-derived stem cells (hASCs) [78]	Exosomes (exos)	Poly(lactic-co-glycolic acid) (PLGA) and polydopamine (pDA)	Isolation, purification, and identification of hASC-exos; exosome uptake assay; cell proliferation and migration; qRT-PCR analysis of osteogenesis-related gene expressions; ARS staining	Critical-sized mouse calvarial defects implanted with (1) PLGA, (2) PLGA/pDA, and (3) PLGA/pDA-Exo (250 μ g); micro-CT analysis; histological and immunohistochemical analysis	The hASCs-Exos-functionalized PLGA scaffolds can promote bone regeneration in mouse critical-sized calvarial defects

(continued)

Table 7.2 (continued)

Rat bone marrow-derived mesenchymal stem cell (rBMSCs) [80]	Microvesicles (MVs)	Alginate–polycaprolactone (PCL) 3D-printed scaffolds	Isolation and characterization of rBMSC-derived EVs and tube formation assay	Subcutaneous implantation in nude mice (1) BMSC–MV–alginate–PCL, (2) BMSC–alginate–PCL, (3) MV–alginate–PCL, and (4) alginate–PCL; micro-CT analysis; histological and immunohistochemical analysis	MV–alginate–PCL constructs enhance vessel formation and bone regeneration when combined with osteodifferentiated MSCs in a subcutaneous bone formation model in nude mice
Human gingival mesenchymal stem cell (hGMSCs) [81]	Heterogeneous population of EVs with diameters spanning from 100 to 1200 nm	Poly(lactide) (PLA) 3D-printed scaffolds	Isolation and characterization of hGMSC-derived EVs, qRT-PCR analysis of osteogenesis-related gene expressions, Western blot analysis, ARS staining	Critical-sized rat calvarial defects implanted with (1) 3-D PLA, (2) 3-D PLA + hGMSCs, (3) 3-D PLA + EVs, (4) 3-D PLA + EVs + hGMSCs; (5) 3-D PLA + polyethyleneimine (PEI)–EVs, and (6) 3-D PLA + PEI–EVs + hGMSCs; micro-CT analysis; histological and immunohistochemical analysis	The hGMSCs–EVs and PEI–EVs-functionalized PLA scaffolds can promote bone regeneration
Rat bone marrow-derived mesenchymal stem cell (rBMSCs) [82]	Heterogeneous population of EVs with diameters spanning from 100 to 1000 nm	Decalcified bone matrix scaffolds prepared from bovine limbs	Isolation and characterization of rBMSC-derived EVs, cell proliferation assay, scratch wound healing assay, tube formation assay, TUNEL assay, qRT-PCR analysis of osteogenesis-related gene expressions	Subcutaneous implantation in the nude mice, micro-CT analysis, histological and immunohistochemical analysis	EV-modified decalcified bone matrix (DBM) scaffolds promote bone regeneration by accelerating vascularization
Murine-derived macrophage cell line (RAW 264.7 cells) [64]	Exosomes (exos)	Titanium nanotubes	BMP2 stimulation, isolation and characterization of BMP2/macrophage-derived EVs, qRT-PCR analysis of osteogenesis-related gene expressions, Western blot analysis, immunofluorescence staining, ALP assay, cytokine secretion	N/A	The BMP2/macrophage-exos-functionalized titanium nanotubes promote osteogenic differentiation of activated autophagy during osteogenic differentiation of BMSCs by activating autophagy

viable manufacturing processes also need to be further developed. Although it has recently been demonstrated that tissue culture bioreactors can enhance exosome production (40-fold greater EVs/mL of culture medium) compared to conventional 2D culture conditions [89], it remains debatable whether the production of higher EV numbers will necessarily yield a higher-efficacy final product due to EV diversity and whether there is a possibility that only specific EV subtypes may represent the therapeutic agent [88].

7.5 Future Perspectives

Much excitement and promise has been garnered about the use of EVs in bone regenerative medicine, which offers the potential for safer products to cover a wider range of applications. Advances in data sharing, such as ExoCarta Database which continues to capture the genomic and proteomic data of EVs, will facilitate to determine which factors are most relevant to the functions of EVs. Also key to EV product translation will be advances in GMP supply and the production of clinical grade products, product characterization and potency assays, preclinical proof of efficacy, and the identification of target populations. Although some EV preparations are already being administered in the clinic, the regulatory road map for EV-based therapeutic product translation to clinical application will need to be carefully established. It is expected that the safety concerns for cell-free, EV-based clinical trials will be arguably milder compared to those that involve the direct use of stem cells due to the non-mutagenicity and non-oncogenicity of EVs [88].

Acknowledgements This work was supported by the National Health and Medical Research Council (NHMRC) Early Career Fellowship (Grant No. 1105035), the National Natural Science Foundation of China (NSFC) General Project (Grant No. 31771025), and the NSFC Young Scientists Fund (Grant No. 81700969).

References

1. Thery C, Witwer KW, Aikawa E et al (2018) Minimal information for studies of extracellular vesicles 2018 (MISEV2018): a position statement of the international society for extracellular vesicles and update of the MISEV2014 guidelines. *J Extracell Vesicles* 7(1):1535750
2. Chargaff E, West R (1946) The biological significance of the thromboplastic protein of blood. *J Biol Chem* 166(1):189–197
3. Wolf P (1967) The nature and significance of platelet products in human plasma. *Br J Haematol* 13(3):269–288
4. Anderson HC (1967) Electron microscopic studies of induced cartilage development and calcification. *J Cell Biol* 35(1):81–101
5. Bonucci E (1967) Fine structure of early cartilage calcification. *J Ultrastruct Res* 20(1):33–50
6. Trams EG, Lauter CJ, Salem N et al (1981) Exfoliation of membrane ecto-enzymes in the form of microvesicles. *Biochim Biophys Acta* 645(1):63–70
7. Taylor DD, Homesley HD, Doellgast GJ (1980) Binding of specific peroxidase-labeled antibody to placental-type phosphatase on tumor-derived membrane fragments. *Cancer Res* 40(11):4064–4069
8. Dvorak HF, Quay SC, Orenstein NS et al (1981) Tumor shedding and coagulation. *Science* 212(4497):923–924
9. Harding C, Heuser J, Stahl P (1983) Receptor-mediated endocytosis of transferrin and recycling of the transferrin receptor in rat reticulocytes. *J Cell Biol* 97(2):329–339
10. Pan BT, Johnstone RM (1983) Fate of the transferrin receptor during maturation of sheep reticulocytes in vitro: selective externalization of the receptor. *Cell* 33(3):967–978
11. Harding C, Heuser J, Stahl P (1984) Endocytosis and intracellular processing of transferrin and colloidal gold-transferrin in rat reticulocytes: demonstration of a pathway for receptor shedding. *Eur J Cell Biol* 35(2):256–263
12. Johnstone RM, Adam M, Hammond JR et al (1987) Vesicle formation during reticulocyte maturation. Association of plasma membrane activities with released vesicles (exosomes). *J Biol Chem* 262(19):9412–9420
13. Raposo G, Nijman HW, Stoorvogel W et al (1996) B lymphocytes secrete antigen-presenting vesicles. *J Exp Med* 183(3):1161–1172
14. Zitvogel L, Regnault A, Lozier A et al (1998) Eradication of established murine tumors using a novel cell-free vaccine: dendritic cell-derived exosomes. *Nat Med* 4(5):594–600

15. Thery C, Duban L, Segura E et al (2002) Indirect activation of naive CD4+ T cells by dendritic cell-derived exosomes. *Nat Immunol* 3(12):1156–1162
16. Skog J, Wurdinger T, van Rijn S et al (2008) Glioblastoma microvesicles transport RNA and proteins that promote tumour growth and provide diagnostic biomarkers. *Nat Cell Biol* 10(12):1470–1476
17. Park JE, Tan HS, Datta A et al (2010) Hypoxic tumor cell modulates its microenvironment to enhance angiogenic and metastatic potential by secretion of proteins and exosomes. *Mol Cell Proteomics* 9(6):1085–1099
18. Zomer A, Maynard C, Verweij FJ et al (2015) In vivo imaging reveals extracellular vesicle-mediated phenocopying of metastatic behavior. *Cell* 161(5):1046–1057
19. Lane RE, Korbie D, Hill MM et al (2018) Extracellular vesicles as circulating cancer biomarkers: opportunities and challenges. *Clin Transl Med* 7(1):14
20. Valadi H, Ekstrom K, Bossios A et al (2007) Exosome-mediated transfer of mRNAs and microRNAs is a novel mechanism of genetic exchange between cells. *Nat Cell Biol* 9(6):654–659
21. Ratajczak J, Miekus K, Kucia M et al (2006) Embryonic stem cell-derived microvesicles reprogram hematopoietic progenitors: evidence for horizontal transfer of mRNA and protein delivery. *Leukemia* 20(5):847–856
22. Cho E, Nam GH, Hong Y et al (2018) Comparison of exosomes and ferritin protein nanocages for the delivery of membrane protein therapeutics. *J Control Release* 279:326–335
23. Liu M, Sun Y, Zhang Q (2018) Emerging role of extracellular vesicles in bone remodeling. *J Dent Res* 97(8):859–868
24. Hao ZC, Lu J, Wang SZ et al (2017) Stem cell-derived exosomes: a promising strategy for fracture healing. *Cell Prolif* 50(5). <https://doi.org/10.1111/cpr.12359>
25. Raposo G, Stoorvogel W (2013) Extracellular vesicles: exosomes, microvesicles, and friends. *J Cell Biol* 200(4):373–383
26. Borges FT, Reis LA, Schor N (2013) Extracellular vesicles: structure, function, and potential clinical uses in renal diseases. *Braz J Med Biol Res* 46(10):824–830
27. Zhang Y, Chen X, Gueydan C et al (2018) Plasma membrane changes during programmed cell deaths. *Cell Res* 28(1):9–21
28. Hauser P, Wang S, Didenko VV (2017) Apoptotic bodies: selective detection in extracellular vesicles. *Methods Mol Biol* 1554:193–200
29. Wang X, Omar O, Vazirisani F et al (2018) Mesenchymal stem cell-derived exosomes have altered microRNA profiles and induce osteogenic differentiation depending on the stage of differentiation. *PLoS One* 13(2):e0193059
30. Squillaro T, Peluso G, Galderisi U (2016) Clinical trials with mesenchymal stem cells: an update. *Cell Transplant* 25(5):829–848
31. von Bahr L, Batsis I, Moll G et al (2012) Analysis of tissues following mesenchymal stromal cell therapy in humans indicates limited long-term engraftment and no ectopic tissue formation. *Stem Cell* 30(7):1575–1578
32. De Jong OG, Van Balkom BW, Schifferers RM et al (2014) Extracellular vesicles: potential roles in regenerative medicine. *Front Immunol* 5:608
33. Harding C, Stahl P (1983) Transferrin recycling in reticulocytes: pH and iron are important determinants of ligand binding and processing. *Biochem Biophys Res Commun* 113(2):650
34. Zaborowski MP, Balaj L, Breakefield XO et al (2015) Extracellular vesicles: composition, biological relevance, and methods of study. *Bioscience* 65(8):783–797
35. Maas SLN, Breakefield XO, Weaver AM (2017) Extracellular vesicles: unique intercellular delivery vehicles. *Trends Cell Biol* 27(3):172–188
36. He RZ, Luo DX, Mo YY (2019) Emerging roles of lncRNAs in the post-transcriptional regulation in cancer. *Genes Dis* 6(1):6–15
37. Wang W, Wang L, Ruan L et al (2018) Extracellular vesicles extracted from young donor serum attenuate inflammaging via partially rejuvenating aged T-cell immunotolerance. *FASEB J* 32(11):5899–5912
38. Agarwal U, George A, Bhutani S et al (2017) Experimental, systems, and computational approaches to understanding the MicroRNA-mediated reparative potential of cardiac progenitor cell-derived exosomes from pediatric patients. *Circ Res* 120(4):701–712
39. Tan JL, Lau SN, Leaw B et al (2018) Amnion epithelial cell-derived exosomes restrict lung injury and enhance endogenous lung repair. *Stem Cells Transl Med* 7(2):180–196
40. Bruno S, Tapparo M, Collino F et al (2017) Renal regenerative potential of different extracellular vesicle populations derived from bone marrow mesenchymal stromal cells. *Tissue Eng* 23(21–22):1262–1273
41. Patel NA, Moss LD, Lee JY et al (2018) Long noncoding RNA MALAT1 in exosomes drives regenerative function and modulates inflammation-linked networks following traumatic brain injury. *J Neuroinflammation* 15(1):204
42. Arvidson K, Abdallah BM, Applegate LA et al (2011) Bone regeneration and stem cells. *J Cell Mol Med* 15(4):718–746
43. Mori G, D’Amelio P, Faccio R et al (2013) The interplay between the bone and the immune system. *Clin Dev Immunol* 2013:720504
44. Martins M, Ribeiro D, Martins A et al (2016) Extracellular vesicles derived from osteogenically induced human bone marrow mesenchymal stem cells can modulate lineage commitment. *Stem Cell Rep* 6(3):284–291
45. Pegtel DM, Cosmopoulos K, Thorley-Lawson DA et al (2010) Functional delivery of viral miRNAs via exosomes. *Proc Natl Acad Sci U S A* 107(14):6328–6333

46. Xu JF, Yang GH, Pan XH et al (2014) Altered microRNA expression profile in exosomes during osteogenic differentiation of human bone marrow-derived mesenchymal stem cells. *PLoS One* 9(12):e114627
47. Wei J, Li H, Wang S, Li T et al (2014) Let-7 enhances osteogenesis and bone formation while repressing adipogenesis of human stromal/mesenchymal stem cells by regulating HMG2. *Stem Cells Dev* 23(13):1452–1463
48. Zhang J, Liu X, Li H et al (2016) Exosomes/tricalcium phosphate combination scaffolds can enhance bone regeneration by activating the PI3K/Akt signaling pathway. *Stem Cell Res Ther* 7(1):136
49. Otsuru S, Desbourdes L, Guess AJ et al (2018) Extracellular vesicles released from mesenchymal stromal cells stimulate bone growth in osteogenesis imperfecta. *Cytherapy* 20(1):62–73
50. Qin Y, Wang L, Gao Z et al (2016) Bone marrow stromal/stem cell-derived extracellular vesicles regulate osteoblast activity and differentiation in vitro and promote bone regeneration in vivo. *Sci Rep* 6:21961
51. Furuta T, Miyaki S, Ishitobi H et al (2016) Mesenchymal stem cell-derived exosomes promote fracture healing in a mouse model. *Stem Cells Transl Med* 5(12):1620–1630
52. Wei Y, Tang C, Zhang J et al (2019) Extracellular vesicles derived from the mid-to-late stage of osteoblast differentiation markedly enhance osteogenesis in vitro and in vivo. *Biochem Biophys Res Commun* 514(1):252–258
53. Cui Y, Luan J, Li H et al (2016) Exosomes derived from mineralizing osteoblasts promote ST2 cell osteogenic differentiation by alteration of microRNA expression. *FEBS Lett* 590(1):185–192
54. Deng L, Wang Y, Peng Y et al (2015) Osteoblast-derived microvesicles: a novel mechanism for communication between osteoblasts and osteoclasts. *Bone* 79:37–42
55. Li D, Liu J, Guo B et al (2016) Osteoclast-derived exosomal miR-214-3p inhibits osteoblastic bone formation. *Nat Commun* 7:10872
56. Bonewald LF (2002) Osteocytes: a proposed multifunctional bone cell. *J Musculoskelet Neuronal Interact* 2(3):239–241
57. Holliday LS, McHugh KP, Zuo J et al (2017) Exosomes: novel regulators of bone remodelling and potential therapeutic agents for orthodontics. *Orthod Craniofac Res* 20(Suppl 1):95–99
58. Qin Y, Peng Y, Zhao W et al (2017) Myostatin inhibits osteoblastic differentiation by suppressing osteocyte-derived exosomal microRNA-218: a novel mechanism in muscle-bone communication. *J Biol Chem* 292(26):11021–11033
59. Ponzetti M, Rucci N (2019) Updates on osteoimmunology: What's new on the cross-talk between bone and immune system. *Front Endocrinol (Lausanne)* 10:236
60. Schlundt C, El Khassawna T, Serra A et al (2018) Macrophages in bone fracture healing: their essential role in endochondral ossification. *Bone* 106:78–89
61. Wu AC, Raggatt LJ, Alexander KA et al (2013) Unraveling macrophage contributions to bone repair. *Bonekey Rep* 2:373
62. Tsiridis E, Upadhyay N, Giannoudis P (2007) Molecular aspects of fracture healing: which are the important molecules? *Injury* 38:S11–S25
63. Alexander KA, Chang MK, Maylin ER et al (2011) Osteal macrophages promote in vivo intramembranous bone healing in a mouse tibial injury model. *J Bone Miner Res* 26(7):1517–1532
64. Wei F, Li M, Crawford R et al (2019) Exosome-integrated titanium oxide nanotubes for targeted bone regeneration. *Acta Biomater* 86:480–492
65. Silva AM, Almeida MI, Teixeira JH et al (2017) Dendritic cell-derived extracellular vesicles mediate mesenchymal stem/stromal cell recruitment. *Sci Rep* 7(1):1667
66. Ekstrom K, Omar O, Graneli C et al (2013) Monocyte exosomes stimulate the osteogenic gene expression of mesenchymal stem cells. *PLoS One* 8(9):e75227
67. Zarychta-Wisniewska W, Burdzinska A, Kulesza A et al (2017) Bmp-12 activates tenogenic pathway in human adipose stem cells and affects their immunomodulatory and secretory properties. *BMC Cell Biol* 18(1):13
68. Kim H, Wang SY, Kwak G et al (2019) Exosome-guided phenotypic switch of M1 to M2 macrophages for cutaneous wound healing. *Adv Sci (Weinh)* 6(20):1900513
69. Pan Y, Hui X, Hoo RLC et al (2019) Adipocyte-secreted exosomal microRNA-34a inhibits M2 macrophage polarization to promote obesity-induced adipose inflammation. *J Clin Invest* 129(2):834–849
70. Zhao J, Li X, Hu J, Chen F et al (2019) Mesenchymal stromal cell-derived exosomes attenuate myocardial ischaemia-reperfusion injury through miR-182-regulated macrophage polarization. *Cardiovasc Res* 115(7):1205–1216
71. Zhao H, Shang Q, Pan Z et al (2018) Exosomes from adipose-derived stem cells attenuate adipose inflammation and obesity through polarizing M2 macrophages and beiging in white adipose tissue. *Diabetes* 67(2):235–247
72. Guilloton F, Caron G, Menard C et al (2012) Mesenchymal stromal cells orchestrate follicular lymphoma cell niche through the CCL2-dependent recruitment and polarization of monocytes. *Blood* 119(11):2556–2567
73. Zhou Y, Huang R, Fan W et al (2018) Mesenchymal stromal cells regulate the cell mobility and the immune response during osteogenesis through secretion of vascular endothelial growth factor a. *J Tissue Eng Regen Med* 12(1):e566–e578
74. Wang X, Gu H, Qin D et al (2015) Exosomal miR-223 contributes to mesenchymal stem cell-elicited cardioprotection in polymicrobial sepsis. *Sci Rep* 5:13721

75. Sun W, Zhao C, Li Y et al (2016) Osteoclast-derived microRNA-containing exosomes selectively inhibit osteoblast activity. *Cell Discov* 2:16015
76. Ramachandran A, Ravindran S, Huang CC et al (2016) TGF beta receptor II interacting protein-1, an intracellular protein has an extracellular role as a modulator of matrix mineralization. *Sci Rep* 6:37885
77. Qi X, Zhang J, Yuan H et al (2016) Exosomes secreted by human-induced pluripotent stem cell-derived mesenchymal stem cells repair critical-sized bone defects through enhanced angiogenesis and osteogenesis in osteoporotic rats. *Int J Biol Sci* 12(7):836–849
78. Li W, Liu Y, Zhang P et al (2018) Tissue-engineered bone immobilized with human adipose stem cell-derived exosomes promotes bone regeneration. *ACS Appl Mater Interfaces* 10(6):5240–5254
79. Derby B (2012) Printing and prototyping of tissues and scaffolds. *Science* 338(6109):921–926
80. Xie H, Wang Z, Zhang L et al (2016) Development of an angiogenesis-promoting microvesicle-alginate-polycaprolactone composite graft for bone tissue engineering applications. *Peer J* 4:e2040
81. Diomedea F, Gugliandolo A, Cardelli P et al (2018) Three-dimensional printed PLA scaffold and human gingival stem cell-derived extracellular vesicles: a new tool for bone defect repair. *Stem Cell Res Ther* 9(1):104
82. Xie H, Wang Z, Zhang L et al (2017) Extracellular vesicle-functionalized decalcified bone matrix scaffolds with enhanced pro-angiogenic and pro-bone regeneration activities. *Sci Rep* 7:45622
83. Fu Y, Mo A (2018) A review on the electrochemically self-organized titania nanotube arrays: synthesis, modifications, and biomedical applications. *Nanoscale Res Lett* 13(1):187
84. Yang Y, Li X, Qiu H et al (2018) Polydopamine modified TiO₂ nanotube arrays for long-term controlled elution of bivalirudin and improved hemocompatibility. *ACS Appl Mater Interfaces* 10(9):7649–7660
85. Szatanek R, Baran J, Siedlar M et al (2015) Isolation of extracellular vesicles: determining the correct approach (Review). *Int J Mol Med* 36(1):11–17
86. Yamashita T, Takahashi Y, Takakura Y (2018) Possibility of exosome-based therapeutics and challenges in production of exosomes eligible for therapeutic application. *Biol Pharm Bull* 41(6):835–842
87. Lv LL, Wu WJ, Feng Y et al (2018) Therapeutic application of extracellular vesicles in kidney disease: promises and challenges. *J Cell Mol Med* 22(2):728–737
88. Willis GR, Kourembanas S, Mitsialis SA (2017) Toward exosome-based therapeutics: isolation, heterogeneity, and fit-for-purpose potency. *Front Cardiovasc Med* 4:63
89. Watson DC, Bayik D, Srivatsan A et al (2016) Efficient production and enhanced tumor delivery of engineered extracellular vesicles. *Biomaterials* 105:195–205



In Vivo Evaluation of the Biocompatibility of Biomaterial Device

8

L. P. Frazão, J. Vieira de Castro, and Nuno M. Neves

Abstract

Biomaterials are widely used to produce devices for regenerative medicine. After its implantation, an interaction between the host immune system and the implanted biomaterial occurs, leading to biomaterial-specific cellular and tissue responses. These responses may include inflammatory, wound healing responses, immunological and foreign-body reactions, and even fibrous encapsulation of the implanted biomaterial device. In fact, the cellular and molecular events that regulate the success of the implant and tissue regeneration are played at the interface between the foreign body and the host inflammation, determined by innate and adaptive immune responses. This chapter focuses on host responses that must be taken into consideration in determining the biocompatibility of biomaterial devices when implanted in vivo of animal models.

Keywords

Biomaterial device · Biocompatibility · Animal models · Host reaction · Immune response · In vivo · Acute inflammation · Chronic inflammation · Humanized mouse models · Host response

8.1 Introduction

There are a great diversity of biomaterials proposed for regenerative medicine, such as tissue-engineered scaffolds that may contain allogeneic, autologous, or xenogeneic genetic materials, cells, synthetic or modified-natural materials [1]. A tissue-engineered implant can be a combination of biological components and biomaterials that creates a device aiming to restore or modify a tissue or organ function to its functional state. Thus, tissue-engineered devices with a biological component(s) require an expanded perspective and understanding of biocompatibility and biological response evaluation.

Biocompatibility is defined by the ability of a biomaterial or medical device to perform with an appropriate host response in a specific application. Its assessment is a measure of the magnitude and duration of the adverse alterations in homeostatic mechanisms that determine the host response and defines if the biomaterial device presents potential harm to the patient [1]. In fact,

Authors L. P. Frazão and J. Vieira de Castro have been equally contributed to this chapter.

L. P. Frazão · J. Vieira de Castro · N. M. Neves (✉)
I3B's – Research Institute on Biomaterials,
Biodegradables and Biomimetics of University of
Minho: 3Bs Research Group, Guimarães, Portugal
ICVS/3B's – PT Government Associate Laboratory,
Braga/Guimarães, Portugal

after biomaterial implantation, an interaction between the host immune system and implanted biomaterial occurs, resulting in a biomaterial-specific tissue response during a complex biological process, which needs to be characterized. The three major responses that must be considered for biocompatibility assessment are inflammation, wound healing, and immunological reactions or immunity. The response to injury may depend on numerous factors, including the extent of the injury, blood–material interactions, the loss of basement membrane structures, the extent or degree of cellular necrosis, provisional matrix formation, and the extent of the inflammatory response [1]. Additionally, the tissue or organ undergoing implantation may contribute significantly to the response. Thus, all these events, in turn, may affect the extent or degree of granulation tissue formation, foreign-body reaction (FBR), and fibrosis or fibrous capsule (scar) development (Fig. 8.1).

The idea of a passive material designed to diminish host response has changed. Currently, an ideal biomaterial is the one that triggers the desired immunological responses, enabling its integration and, consequently, tissue repair [2]. Basically, a balanced interplay between the host immune system and the biomaterial is desired. Invasive implantation methods (e.g., surgery) potentiate adverse host responses, which are determined by the biomaterial [3].

In vitro models have a limited capacity to recreate the complex in vivo environment, such as, the role of angiogenesis in the newly formed tissue, immune reaction to implanted biomaterials, and functional properties of the graft. So, in vivo models offer the whole picture of the host response to a biomaterial and are useful to predict the clinical behavior, safety, and biocompatibility of medical devices in humans. In vivo assays are a midway step between in vitro studies and human clinical trials [4–6].

8.2 The Immune Response

Following in vivo implantation, a host reaction is induced, determining the outcome of the integration and the biological performance of the implant. All implants develop cellular and tissue responses. Also biodegradable biomaterials and its degradation products result in surface changes that activate the immune system [7–9].

The human immune system has two different mechanisms: the innate immune system and the adaptive immune system. So, when a biomaterial is implanted in vivo, a nonspecific inflammatory response is elicited by the innate immune system. After the recognition of the foreign material, the adaptive immune system performs highly specific antigen responses and develops long-term memory. The innate immune system is composed of polymorphonuclear cells, mononuclear phagocyte cells (dendritic cells, monocytes, and macrophages), and lymphocytes (natural killer cells, gamma–delta T cells, and innate lymphoid cells), while the adaptive immune response involves B and T lymphocytes [10, 11] (Fig. 8.2).

The typical host reaction to an implant involves a mechanism that is similar to the early stages of wound healing [12]. However, the presence of an implanted device significantly alters the progression through the subsequent phases of repair [13]. Moreover, the extent of the immune response to a biomaterial is modulated by the characteristics of the material [14].

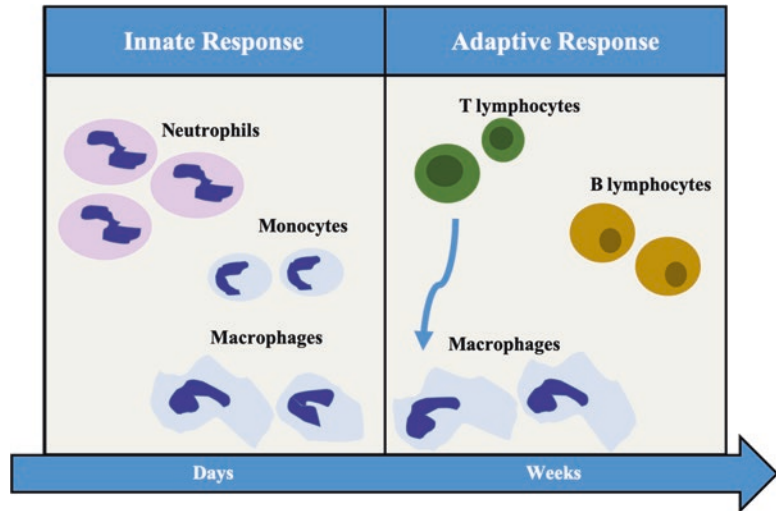
After the implantation of the biomaterial, an acute inflammatory response begins that in some circumstances can lead to a chronic inflammatory response to a FBR and to the deposition of a collagenous fibrous capsule around the implant (Fig. 8.1). Therefore, the efficacy of the biomaterial is affected by the extent and duration of the inflammatory process [6, 8].

The immune response to biomaterials implanted in vivo can be divided into four major



Fig. 8.1 Sequence of host reactions. (Adapted from Ref. [1])

Fig. 8.2 The two components of the human immune system that are involved in the reaction to a biomaterial implant



phases: (1) implantation, (2) blood–biomaterial interaction, (3) inflammation, and (4) tissue remodeling, which start at different times but can overlap with each other. All these four phases are discussed in more detailed below.

8.2.1 Implantation

There are basic responses of the body to implantation even in sham operations. The incision made to introduce the device into the body affects the vasculature, extracellular matrix, and eventually the local nerves [15]. The disruption of the host tissue homeostasis leads to local inflammation and wound healing [13, 15]. The response to injury associated with implantation of the device is essentially dependent on the size, surface area of the injury or implant, and anatomical site. Following injury, a normal wound healing process starts through overlapping phases of blood–biomaterial interactions, inflammation, proliferation, and tissue remodeling [6, 8, 13, 16]. Although the inflammatory response is initiated by the injury, it is mediated by the released chemicals from the plasma, cells, and injured tissue [8.31]. Normally, during the first several days after injury, the predominant cell type is the neutrophils, which are then replaced by monocytes that will differentiate into macrophages (Fig. 8.3).

8.2.2 Blood–Material Interactions: The Formation of the Provisional Matrix

Shortly (within minutes to hours) after biomaterial implantation, changes in the vascular flow and permeability occur [17]. Within a few seconds after the implantation, the blood from the damaged vessels surrounds the biomaterial. Therefore, the blood–material interactions begin spontaneously, and almost immediately, the host plasma components adsorption to the biomaterial’s surface occur. These components include lipids, sugars, ions, and proteins, such as albumin, fibrinogen, fibronectin, vitronectin, immune globulins, and a number of coagulation and complement factors [18–20] (Fig. 8.3).

Biomaterial device’s characteristics, such as surface energy, chemistry, topography, and roughness, are decisive determinants of the tissue reaction to the implants. It was demonstrated that those implants’ characteristics influenced the type, the amount, the composition, and the conformation changes of the adsorbed molecules [18, 21, 22]. Moreover, the composition of the layer of the adsorbed proteins (type of proteins, concentration, and conformation upon adsorption) is associated with the initiation of the coagulation cascade and the complement system, leading to the onset of inflammatory responses [19, 23–25]. From a wound-healing

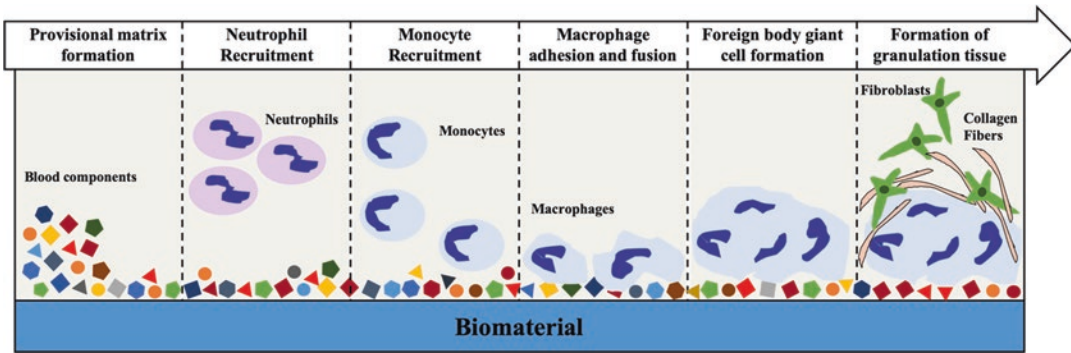


Fig. 8.3 Innate immune response to biomaterial implants: representation of the main cellular players in the interaction biomaterial–immune system. The main events from provisional matrix formation to formation of granulation tissue are represented

perspective, blood molecule deposition on a biomaterial surface is described as provisional matrix formation [1, 25, 26] (Fig. 8.3). However, the clot formation also defines the provisional matrix around the biomaterial implant [27, 28]. Blood coagulation associated with biomaterial implantation is a combination of contact activation, platelet adhesion and activation, and presence of leucocytes [29].

There are two pathways for contact activation of the coagulation cascade: the intrinsic (Hageman factor: factor XII or FXII as initiators) and the extrinsic pathway (tissue factor as initiator). For biomaterials, it has been described an activation of the intrinsic pathway after adsorption of FXII, kallikrein (KK), and high-molecular-weight kininogen (HMWK) as a cofactor [30]. In accordance, complement proteins activated upon contact with the biomaterial, synergistically support platelet adhesion, activation and recruitment of immune cells [7, 31–36]. Regarding the complement system, there are three different pathways that activate this system: the classical pathway, the alternative pathway, and the lectin (mannan-binding) pathway [37]. In biomaterials, it has been described that the complement system is mainly activated by the alternative pathway [36, 38]. However, this activation is related to biomaterials' surface properties, since it is associated with the adsorbed protein layer on biomaterials [31]. Moreover, it was shown that biomaterial surfaces with available OH and NH₂ groups had a greater activation of the comple-

ment system than biomaterial surfaces with available COOH [39]. Furthermore, the activation of the complement system leads to the activation of complement factors C3 and C5 that are fragmented into anaphylatoxins C3a and C5a, attracting leucocytes to the site of inflammation, increasing vascular flow and vascular permeability, extravasation of leucocytes, and chemotaxis. Additionally, some complement factors that opsonize bacteria that are also adsorbed to the biomaterial lead to the activation of monocytes and macrophages [7, 40].

In summary, due to the implantation of the biomaterial, there is development of the provisional matrix at the implant site. This provisional matrix is mainly composed of fibrin (produced by activation of the coagulative and thrombosis systems), activated platelets, inflammatory products, and cells, being also rich in cytokines, growth factors, and chemoattractants that are capable of recruiting cells of the innate immune system to the injury site [8, 25] (Fig. 8.3).

8.2.3 Inflammation

The inflammation process acts to contain, neutralize, dilute, or avoid contact with injurious agents or processes. It is defined as the reaction of vascularized living tissue to local injury. These processes initiate a cascade of several events to heal and regenerate the injured site [8].

Biomaterial device is a foreign object and, by definition, elicits an immune response. After the formation of the provisional matrix, an acute inflammatory response occurs followed by a chronic inflammatory response [8, 11, 16] (Fig. 8.3). The intensity and duration of these inflammatory responses are related not only to the extent of tissue damaged but also with the characteristics of the biomaterial device (composition, size, shape, topography, and chemical and physical properties) [1, 8, 16]. Moreover, some proteins that composed the provisional matrix, such as fibronectin and vitronectin, are important in the modulation of the inflammatory response to the biomaterial implant by enhancing cell adhesion. On the other hand, the fibrinogen and complement system are associated with the recruitment of the cellular components of the inflammatory system [41–43].

8.2.3.1 Acute Inflammation

Acute inflammation is the first line of defense of the immune system and a normal and necessary function of the innate immune system. This process is initiated by the presence of pathogens or by tissue damage, for example, through implantation of a biomaterial device [6, 8]. The acute inflammatory response is of relatively short duration, lasting from minutes to a few days. Persistence of the acute inflammation for more than 3 weeks usually indicates the presence of an infection. This response is mainly characterized by an exudation of fluid and plasma proteins (edema) and by the recruitment of polymorphonuclear leucocytes (PMNs), predominantly neutrophils. These cells migrate to the site of injury due to the increase of blood vessels permeability (associated with the activation of the complement system) and also due to the release of chemoattractants associated with the activation of complement factors C3 and C5, activated platelets, and fibrinopeptides (released after blood clotting) [3, 8, 44]. After recruitment, PMNs undergo activation through the release of danger signals by the injured cells at the implant site, such as “alarmins” (which include heat shock proteins, high-mobility group box 1, adenosine triphosphate (ATP), and uric acid) that are an endoge-

nous equivalent of pathogen-associated molecular patterns (PAMPs). Alarmins are recognized by pattern recognition receptors (PRRs), such as toll-like receptors (TLRs), scavenger receptors, and purinergic receptors [3, 45–49].

The main role of neutrophils in acute inflammation is to respond as the first line of cells to defend against invading pathogens (e.g., bacteria and fungi). They initiate a phagocytic response with the secretion of proteolytic enzymes and reactive oxygen species (ROS). PMNs adhere to the biomaterial surface by means of $\beta 2$ integrins in an attempt to destroy it. However, due to size disparity, phagocytosis does not occur, although, the destructive agents released by neutrophils may corrode the material surface [3, 44, 50–53]. Moreover, neutrophils release neutrophil extracellular traps (NETs) that have, as main functions, to trap pathogens and prevent the spread of infection. These networks are composed of granular proteins, neutrophil elastase, chromatin DNA, and histones. The altered release of NETs restrains the integration between the tissue and the biomaterial, since it leads to excessive production of a dense fibrotic matrix. In addition, it also degrades neutrophil-produced cytokines and chemokines that regulate the healing process. Furthermore, NETs released from neutrophils, unable to phagocytose a harmful stimulus, may be considered similar to the formation of foreign-body giant cells (FBGCs) (see subchapter 8.2.3.2) [54, 55].

PMNs have very short life spans (of hours to days) and rapidly disappear from the inflammation site. Usually, PMNs disappear from the implant site in the first 2 days after the biomaterial device implantation [3, 44, 50, 51]. When activated, PMNs secrete several immunoregulatory signals, such as, CX chemokine ligand 8 (CXCL 8) (the most prominent chemokine that primary target neutrophils), monocyte chemoattractant protein (MCP-1/CCL2), and macrophage inflammatory protein (MIP-1 β /CCL4), that will activate monocytes, macrophages, immature dendritic cells (DCs), and lymphocytes [3, 44, 56]. The progressive increase of these chemokines leads to monocyte infiltration at the implant site. Moreover, due to the lack of activating signals,

there is a suppression of neutrophils that undergo apoptosis and gradually disappear from the implantation site [8]. So, circulating monocytes that were attracted to the site of injury bind the fibrinogen deposited at the biomaterial provisional matrix. Thus, monocytes differentiate into the classical activated “M1” macrophages. These cells promote the inflammatory response by secreting various inflammatory cytokines and chemokines, such as, interleukin (IL) – 1 β , IL-6, tumor necrosis factor (TNF- α), IL-8/CXCL8, and also MCP-1/CCL2 and MIP-1/CCL4, that will promote the invasion of additional inflammatory cells. In an attempt to degrade the biomaterial and in accordance with what happened with leucocytes, macrophages also undergo frustrated phagocytosis by releasing potent oxygen and nitrogen radicals, as well as proteolytic enzymes. This may affect the surrounding tissue since the adjacent healthy cells are also getting damaged and destroyed, which can result in necrosis and present as a threat to patients. However, unlike PMNs, macrophages have longer life spans (from days to months), being the predominant cell type in both acute and chronic inflammation [1, 7, 43, 57–61].

8.2.3.2 Chronic Inflammation

Continuous inflammatory stimulus leads to chronic inflammation that generally does not last more than 2 weeks, and it is confined to the implantation site [6, 7, 59, 62]. This may be associated with the physiochemical characteristics of the biomaterial that leads to continuous opsonization and release of toxic degradation products. Moreover, it can also be associated with insufficient mechanical compliance or movement of the biomaterial at the implantation site [6].

Macrophages are one of the central cell types of the chronic inflammatory response [59, 62, 63]. Due to their large range of plasma membrane receptors, macrophages have a great plasticity and can change their physiology in response to environmental cues, inducing distinct cell populations with different functions [59, 62, 64]. Macrophages are divided into two major phenotypes: M1 and M2. While the M1 phenotype promotes pathogen killing and is related to the classical signs of active inflammation, M2 phe-

notype supports immunoregulation, tissue repair, and remodeling. These cells secrete anti-inflammatory cytokines, such as IL-10, and induce the migration and proliferation of fibroblasts [59, 62]. So, the adherent macrophages will eventually shift to the M2 phenotype. The overlapping events of the phenotypic M1 to M2 switch, together with the mechanisms of frustrated phagocytosis, result in macrophage membrane fusion to form a foreign-body giant cell (FBGC) [65].

FBGC formation (Fig. 8.3) represents and attempts to increase the cells' phagocytic or degradative capacities. It is also the hallmark of chronic inflammation [6, 65]. As previously described, the M1 macrophages secrete various inflammatory cytokines and chemokines that promote the invasion and activation of additional inflammatory cells, such as mast cells, basophils, and T-helper (Th) cells. These cells secrete IL-4 and IL-13 that have been considered as the main inducers of FBGC on implanted biomaterials, by upregulating mannose receptor on fusing macrophages [8, 65, 66]. Moreover, although the mechanism of macrophage fusion into FBGCs on the biomaterials is not fully understood, it has been proposed that it may depend on adhesion density and migration motility of the cells. Enough cells are needed for fusion to take place, and the attached macrophages have to migrate to meet each other and fuse [67]. So, it has been shown that the adsorbed proteins on the provisional matrix may influence FBGC formation. While all adsorbed proteins support initial monocyte adhesion, only vitronectin strongly promotes macrophage development and FBGC formation. Moreover, fibrinogen, plasma fibronectin, laminin, and collagens (associated with the adhesion of other cell types) do not support IL-4-induced FBGC formation. Additionally, β 1 integrins are dominant during monocyte activation to macrophages and during FBGC formation, while β 2 integrins are associated with initial monocyte adhesion [41]. Thus, FBGCs adhere to the surface of the biomaterial implant for a long time, forming a barrier between the tissue and the biomaterial. Due to its phagocytic activity, FBGCs secrete reactive oxygen species and other chemical agents, which may result in biomaterial dete-

rioration and eventually in the failure of the implanted devices [7].

Regarding lymphocytes and plasma cells, they are principally involved in immune reactions and are important mediators of antibody production and delayed hypersensitivity responses. Although it is known that T cells attached to the biomaterial surface and become activated through noncanonical pathways, little is known regarding immune responses and cell-mediated immunity directed to biomaterial implants [66]. During chronic inflammation, T lymphocytes, mainly CD4 helper T cells and their subsets (Th1 and Th2), modulate the pro- and/or anti-inflammatory responses, respectively, by producing the majority of cytokines [66]. The change in cytokine expression profile from Th1 to Th2 lymphocytes suggests that T lymphocytes are pivotal (together with the shift from M1 to M2 macrophage phenotype) in promoting the resolution of inflammation leading to tissue regeneration [11].

8.2.4 Tissue Remodulation

The formation of granulation tissue (Fig. 8.3) is the hallmark of healing inflammation, and it is initiated within 1 day after implantation of the biomaterial device. Its name was derived from the pink soft granular appearance on the surface of healing wounds. The granulation tissue is composed of macrophages, fibroblasts, and capillaries. So, the main histological feature of the granulation tissue is the proliferation of new small blood vessels and fibroblasts at the implant site. Depending on the extent of the injury, granulation tissue may be observed from day 3 to 5, after device implantation [1]. During this stage of healing, macrophages polarize toward M2 phenotype through a cross talk with a subpopulation of T cells defined as regulatory (Tregs). Tregs play an important role in tissue immune homeostasis and are able to switch the local immune response from inflammation to a pro-regenerative tissue repair cascade by the secretion of anti-inflammatory cytokines, such as, IL-10 [68].

M2 macrophages and FBGCs produce growth factors, such as, platelet-derived growth factor (PDGF), fibroblast growth factor, transforming

growth factor (TGF)- β 1, and vascular endothelial growth factor (VEGF), that stimulate fibroblasts, blood vessels formation, and regeneration of epithelial cells. Although there is a lack of information regarding the interaction and synergy between cytokines and growth factors released by activated cells, they are associated with the production of a wide variety of cells, with cell migration, differentiation, and tissue remodeling [1, 11, 43].

Through proliferation, maturation, and organization of endothelial cells into capillary tubes, small blood vessels are formed by budding or sprouting from preexisting vessels (neovascularization) [69]. Moreover, in an attempt to repair the damaged tissue, activated fibroblasts synthesize and deposit collagens and proteoglycans. In the early stages of granulation tissue, there is a predominance of proteoglycans. However, in the later stages, there is a prevalence of collagens (types I and III, being the type I the most abundant) around the biomaterial [1, 13, 70]. However, excessive collagen secretion (due to continuous stimulation form a pro-inflammatory environment) may lead to the formation of a fibrotic capsule around the biomaterial (greater ratio of collagen I/III is associated with a greater fibrotic tissue formation). This fibrous capsule isolates the biomaterial from the host tissues, leading to the failure of many implants, particularly the ones associated with drug release and sensors [71, 72]. Some activated fibroblasts can be differentiated into myofibroblasts, associated with an abundant expression of α -smooth muscle actin (α -SMA). These cells are responsible for wound contraction, promoting wound healing and scar formation [1, 73] (Fig. 8.3).

8.3 Animal Host Response Models and Implantation Site Characterization

Laboratory animal protection legislation assumes that, in specific conditions, it is morally acceptable to use animals for scientific purposes. However, most regulatory systems have the following general objectives: to keep the number of animals used to a minimum, to define legitimate

purposes for which laboratory animals may be used, to ensure the ability of all laboratory personnel and researchers, to avoid animal use when there are practicably available alternatives, to avoid unnecessary pain or distress to animals, to provide for the inspection of facilities and procedures, and to ensure public responsibility [74].

The choice of an appropriate animal model is intrinsically related to the specific goals of the experiment. Moreover, when choosing an animal model, it is important to take into account various aspects, such as the cost (e.g., the maintenance of smaller animal models is less costly than the maintenance of larger animals), the number of variables (e.g., a well-defined and well-described model may reduce random effects), the methodologies used to assess the sample collection and characterization, and the controls that should contain the clinical standard (or a material already in clinical use), an empty defect (to prove that the obtained results are related with the implantation of biomaterial), and if using cells, the material without cells [5].

Regardless of the effort of researchers to use the most adequate models for their experiments, it is difficult to draw valuable information due to the differences in model and reaction mechanisms in the implanted material surface properties. Thus, it is important to take into account the different types of host reactions that can be elicited after the implantation of biomaterials. After the initial primary acute inflammatory reaction, different scenarios can happen: (1) the implanted biomaterial does not degrade in the course of the inflammatory reaction and is surrounded by a fibrotic capsule and a foreign-body reaction is observed; (2) the biomaterial degrades in a relatively short time frame (while the inflammatory response is still being observed), and the degradation products are metabolically excreted by the host or may cause inflammation themselves; (3) the host does not surround the biomaterial with the fibrotic capsule, but is not able to degrade it, and thus two situations may occur: (i) the host immune system is activated into setting up a chronic reaction or (ii) the acute inflammation persists and a nonhealing wound appears at the implantation site [5].

The first approach to test a biomaterial *in vivo* is the ectopic model in small animals, commonly mice or rats. Ectopic models refer to studies where the implantation is done out of the intended final tissue. In contrast, orthotopic models refer to the implantations done in the tissue of interest. In the early phases of the research, ectopic models are preferred to orthotopic models due to the easier identification of the response and also of the effects, the technical abilities needed to perform them, and also because it is easier to compare results between a wealth of experiments reported in the literature. The most common ectopic models are the implantation in the subcutaneous, intramuscular and intraperitoneal sites. These locations are able to provide information about chronic or persistent acute inflammatory responses, particularly the chronic inflammatory response and regarding the integration of the biomaterial within the host tissue after long periods of implantation. Subcutaneous implantation is normally done in the dorsum of animals to prevent them from having access to the sutures, in order to maintain the biomaterials or cells in place. Intramuscular implantation, in small animals, is normally done in the hind limb, and the intraperitoneal implantation is performed in peritoneum (a body cavity) [4, 5]. Despite the intended final application of the biomaterials, the subcutaneous and intramuscular implantation models offer information about the direct effect of the biomaterial at the implant site, while intraperitoneal implantation provides data on the effect in the abdominal organs of the host, such as liver, kidney, spleen, mesenteric lymph nodes, and related adipose tissue [75–77], as an indication of the systemic influence of the biomaterials on the host. Moreover, intraperitoneal models are the most suitable for evaluating cell recruitment and activation status [77, 78] at short [19, 77, 79, 80] and long periods [77, 81] of reaction.

There are some differences in foreign-body response (FBR) related with the implantation site. For example, it was shown that the intraperitoneal site had higher levels of proangiogenic factors and lower levels of pro-inflammatory cytokines during the initial stage of the FBR, when compared with the subcutaneous

site. However, both sites led to fibrous encapsulation. This is associated with faster healing response that occurs in the peritoneal cavity compared to the dermis [82–84]. Moreover, the mouse strain also affects the FBR. It was shown that C57BL/6 strain is associated with a more robust FBR and with a fibrous encapsulation more similar to that of humans, when compared to BABL/c strain [85].

To study cell types and/or pathways that mediate FBR, genetically modified mouse models are frequently used. For example, it was shown that after biomaterial implantation in mice deficient in T cells [86], natural killer cells [87], or mast cells [87, 88], there was a normal formation of FBGCs and/or fibrous capsule formation, suggesting that those inflammatory cells are not essential for FBR [85]. Additionally, genetically modified mice/rats to not develop thymus must be used when it is necessary to conduct studies with allogeneic and xenogeneic cells with or without biomaterials. These immunocompromised animals are unable to produce mature T lymphocytes, key immune cells in graft or implant rejection [5].

Large animal models are generally used in orthotopic models due to easier comparison to man implantation. For example, sheep are usually used for the evaluation of heart valves. This is based on the rapid growth of these animals and also on the accelerated calcification, which has its clinical correlation in young and adolescent humans [6]. Moreover, pigs may be used to mimic pediatric and neonatal conditions due to its fast-growing ability [89, 90]. And due to its size and similar biological complexity with humans, pigs are largely used in wound healing studies, decreasing the number of animals needed [91].

Additionally, models as air pouches [92–94], cage implants [95, 96], or dorsal skinfold chambers [97] have also demonstrated consistent results concerning the interplay between direct and indirect material surface reactions. In fact, in the dorsal skinfold chamber, recruitment and accumulation of leukocytes were observed using intra-vital fluorescence and avoiding the killing of animals at different timepoints [97]. Moreover, the cage implant models are demonstrated to be

useful for identifying recruited and adherent cell types [96], macrophage fusion into FBGCs [95], and cytokine release [98] in response to implanted materials either in mice [98] or rats [95, 96]. On the contrary, host reaction evaluation should not be limited to the assessment of inflammatory reaction, particularly if the biomaterial is aimed to remain in the host for long periods and/or if it degrades during the implantation time. Therefore, the evaluation of the immune response should also be done before the implantation. An adequate method to assess in vivo immune stimulation by biomaterials is to do repetitive implants (rat subcutaneous [69] or intraperitoneal [54] model) and analyze the host–tissue response, immune cells, and antibody production [54, 69].

After the in vivo implantation of a biomaterial, it is important to characterize not only the associated biological processes, such as the adsorption of plasma proteins and immune cells, but also the mechanical, physical, and chemical properties of the device that may change over time [15].

Generally, the characterization of biological processes associated with in vivo implantation starts with a histological analysis in order to visualize and/or differentiate microscopic structures. This analysis is enhanced by the use of different staining that dye specific tissue components, such as connective tissue, elastic fibers, blood cells, and basement membrane. However, when the biological material is collected, it is necessary to assess some histopathological outcomes, such as herniations and/or adhesions.

The preparation of samples for histological analysis comprises five steps. The first step is the fixation of samples using chemical fixatives (the most used is 10% neutral buffered formalin). Sample fixation will avoid tissue degradation and maintain cellular structures and subcellular components. In the second step, the sample must be dehydrated, normally using a sequence of increasing concentrations of ethanol. The aim of this step is to remove the water from the tissue, replacing it with a hard matrix (generally molten paraffin wax), allowing the cut of thin sections (typically of 5 μm). So, xylene is used to remove ethanol from the sample, and then molten paraffin

wax infiltrates in the tissue to replace xylene. The third step consists in the external embedding of the material. Samples are placed in molds with an embedding liquid, such as agar, gelatin, or wax. These liquids are then hardened. The most common method used for biological tissues is the formalin-fixed paraffin-embedded (PPFE) tissues because it allows samples to be stored indefinitely at room temperature and also because of the recovery of nucleic acids (DNA and RNA) in the samples. Sample sectioning and mounting on a glass microscope slide is the fourth step. Sample sections can be cut in different directions, such as vertical (longitudinal sections, by cutting perpendicularly to the surface of the tissue), horizontal (transverse sections), or transversely. The last step deals with section staining, since biological tissues have little inherent contrast in light or electron microscope [99].

Eosin and hematoxylin (E&H) is the most frequently used histological staining. Eosin is an acid dye that stains the cytoplasm pink, and hematoxylin is a basic dye that stains the nuclei dark blue/black due to the affinity to nucleic acids. Moreover, muscle fibers appear in deep red, red blood cells (RBCs) in orange red, and fibrin in deep pink. This staining is widely used to analyze foreign-body response, allowing the identification of capsule formation, FBGCs, and macrophages [13]. Additionally, it can also be used to identify the formation of new tissue. Other histological stainings may be used depending on the goals of the study. For example, Masson's trichrome staining is commonly used for connective tissue: staining cartilage and collagen fibers in blue or green, muscle fibers in red, nuclei in black, cytoplasm in red or pink, and RBCs in red [100].

In accordance with the purpose of the study, immunostaining may be necessary to be performed. Immunostaining is an antibody-based method enabling to detect a specific protein in a sample and may be performed in fresh tissue or in histological sections mounted in glass microscope slides after antigen retrieval. In each histology section, different parameters must be evaluated, such as the number (expression) of inflammatory cells (neutrophils, plasma cells, lymphocytes, and macrophages), FBGCs, the

severity of necrosis, the extent of neovascularization, fibrosis, and fatty infiltration [101–103].

8.4 Humanized Mouse Models

Currently, there are no set standards that recapitulate the human immune response for preclinical evaluations, often leading to poor or unexpected outcomes in human recipients. One major challenge is that the commonly used animal models in these preclinical studies, such as the wild-type or immunodeficient murine models, provide a limited representation of the human immune response. In fact, it is known that human immune cells have several unique characteristics and interactions that are not observed in murine cells [104–106]. One method that is used to address this challenge is the use of humanized immune system mouse model. Humanized mouse model are created by the implantation of human tissue (e.g., cells or genes) into mouse, which will allow these animals to produce functional human cells and gene products *in vivo*. These types of mice have been advantageous in the studies of human diseases involving human-immune cell interactions, such as, infectious diseases [107], oncology [108], testing for potential graft rejection [109], and therapeutic toxicity [110]. Regarding the biomaterial field, the humanized mice can be a powerful tool that provides a potential platform for improving our understanding and tailoring our biomaterials for safer and more effective interactions with the human immune response. Humanized mice are classified as chimeric mice that were transgenically or surgically modified by the integration of human cells, tissue, and/or genes to generate models of human biological responses. The generation of humanized mice producing human immune cells stems from the discovery of genetic mutations creating immunodeficient mouse lines that allow for the engraftment of multiple human-derived tissues and cells. In fact, particular practices and selections have a greater reconstitution of the human immune response, which leads to the numerous versions of humanized mice [111].

The first model of humanized mice involved the engraftment of human peripheral blood

lymphocyte in SCID mice (Hu-PBL-SCID) by the injection of mature human peripheral lymphocytes [112]. Additionally, a human SCID-repopulating cell NOD-SCID (Hu-SRC-NOD-SCID) mice was also developed by intravenous injection of human CD34+ cells derived from fetal liver, cord blood, bone marrow, or G-CSF cytokine-mobilized peripheral blood mononuclear cells [113]. In order to overcome some limitations observed in the first model, including (1) the engrafted human T and B cells, which are present only for a limited period of time; (2) the human T cells that interacted with the host MHC molecules, inducing a xenogeneic graft-versus-host disease response; and (3) the development of T cell, which is limited due to the lack of human thymic tissue in the host animal [114], the SCID-Human (SCID-Hu) model was developed. In this humanized mice model, there is a co-implantation of human fetal thymus and liver under the kidney capsule of SCID mice [115]. These mice developed autologous thymic educated and human leukocyte antigen- (HLA-) restricted T cells *in vivo*, making it an excellent model for HIV studies [116]. However, the level of hematopoietic lineage cells was low, and the functionality of the human immune system was poor [117]. Thus, the bone marrow, liver, thymus (BLT) humanized mouse was developed being a modification of the SCID-Hu model. This model is generated by the co-implantation of human fetal liver and thymus under the kidney capsule along with the intravenous injection of the autologous human CD34+ cells, with the maturation occurring in the implanted autologous thymic tissues, resulting in a long-term and systematic repopulation of multiple lineages of hematopoietic cells in the mouse [118]. Additionally, human T cells are developed with a human HLA-restricted T cell. However, it was demonstrated in the long-term studies that BLT humanized mice are susceptible to thymic lymphoma, giving them a short life span and limiting long-term studies [119]. Thus, issues with thymic lymphoma development can be mitigated by the use of NOD-SCID IL2R γ (null) (NSG) host mouse [120].

Regarding *in vivo* biomaterial assessment, the humanized mouse model generated by human

thymus implantation and intravenous transfusion of human CD34+ fetal liver cells were used to evaluate the immune response of decellularized cardiac extracellular matrix (ECM) hydrogels [121]. Humanized mice have also been used for the biocompatibility assessment of cellular grafts (human embryonic stem cell allografts) that can also be useful for biomaterial assessment as a delivery vehicle for cellular therapies [122]. In addition, recent studies have demonstrated the power of humanized mice in evaluating the immunogenicity of cells derived from human-induced pluripotent stem cells [123]. Thus, the humanized mouse model could be further used to assess the potential benefits or complications that can occur when stem cells are used in synergy with the biomaterials; therefore, additional modifications to the standard models can also provide insight into specific patient populations of interest. In fact, these mice models allow for more personalized immune assessments and therapy developments to be validated in patient populations susceptible to unexpected immune responses.

In summary, although humanized mouse models do provide an improved representation of the human immune response, there are some limitations that should be considered, demonstrating that further research is needed to improve and expand the capabilities of humanized mice as representative models of the human immune response. Nevertheless, humanized mice models can provide a critical tool for a more effective and safe translation of novel therapies in the rapidly developing biomaterial field.

8.5 Conclusions and Future Perspectives

Tissue-engineered devices are combinations of biological–biomaterial in which some components of tissue have been combined with a biomaterial to create a device for the regeneration of tissue or organ function. The development of new biomaterials requires an in-depth understanding of the biological responses to implanted biomaterials.

The inflammatory response is the first step of wound healing but is also the underlying reason for the failure of many implanted scaffolds. However, the immune system remains the most significant critical issue for the development of tissue engineering. Once a biomaterial device is implanted, a sequence of events takes place leading to the formation of FBGCs at the biomaterial–tissue interface. However, the type of cellular and tissue response to the implant is dependent on the nature of the implanted biomaterials. It is known that several immune cell subpopulations and immune-modulating factors are involved in the different phases of healing; however, the impact of material properties on immune activation and through which mechanisms this activation occurs still need to be fully elucidated. In fact, it is of great importance to understand the process of the innate immune inflammation by which neutrophils and monocytes or macrophages can be activated by biomaterials devices. Additionally, it is important to clarify why some macrophages shift from an inflammatory to an anti-inflammatory phenotype in certain types of tissues, while a distinct population of anti-inflammatory macrophages is mobilized in others.

The increasing knowledge and awareness deriving from biological systems and new structural, chemical, and physical understandings of human-derived biomaterials, together with advances in the synthesis of new biomaterials, will open the way to a new and more sophisticated device designs and scaffolding technology. The future of this field will continue to grow and evolve with the collaborative development of tissue-engineered products that offer simple solutions to complex problems. Nevertheless, we should also be interested in knowing what the safety of immune-engineered biomaterials and their long-term efficacy will be.

References

1. Anderson JM (2019) Biocompatibility and bioreponse to biomaterials. In: Atala A, Lanza R, Mikos AG, Nerem R (eds) *Principles of regenerative medicine*, 3rd edn. Elsevier, London, pp 675–694

2. Vasconcelos DP, Águas AP, Barbosa MA et al (2019) The inflammasome in host response to biomaterials : bridging inflammation and tissue regeneration. *Acta Biomater* 83:1–12
3. Christo SN, Diener KR, Bachhuka A et al (2015) Innate immunity and biomaterials at the nexus : friends or foes. *Biomed Res Int* 2015:342304
4. Saleh LS, Bryant SJ (2017) In vitro and in vivo models for assessing the host response to biomaterials. *Drug Discov Today Dis Model* 24:13–21
5. Costa-Pinto A, Santos TC, Neves NM et al (2016) Testing natural biomaterials in animal models. In: Neves NM, Reis RL (eds) *Biomaterials from nature for advanced devices and therapies*, 1st edn. Wiley, Hoboken, pp 562–579
6. Anderson JM (2001) Biological responses to materials. *Annu Rev Mater Res* 31:81–110
7. Sheikh Z, Brooks PJ, Barzilay O et al (2015) Macrophages, foreign body giant cells and their response to implantable biomaterials. *Materials* 8(9):5671–5701
8. Anderson JM, Rodriguez A, Chang DT (2008) Foreign body reaction to biomaterials. *Semin Immunol* 20(2):86–100
9. Salgado AJ, Coutinho OP, Reis RL et al (2007) In vivo response to starch-based scaffolds designed for bone tissue engineering applications. *J Biomed Mater Res* 80(4):983–989
10. Delves PJ, Martin SJ, Burton DR et al (2011) *Roitt's essential immunology*, 12th edn. Wiley-Blackwell, Hoboken
11. Mariani E, Lisignoli G, Maria R et al (2019) Biomaterials: foreign bodies or tuners for the immune response? *Int J Mol Sci* 20(3):636
12. Santos TC, Reis RL, Marques AP (2016) Can host reaction animal models be used to predict and modulate skin regeneration? *J Tissue Eng Regen Med* 11(8):2295–2303
13. Major MR, Wong VW, Nelson ER et al (2015) The foreign body response: at the interface of surgery and bioengineering. *Plast Reconstr Surg* 135(5):1489–1498
14. Ma PX (2008) Biomimetic materials for tissue engineering. *Adv Drug Deliv Rev* 60(2):184–198
15. Hasirci V, Hasirci N (2018) *Fundamentals of biomaterials*. Springer, New York
16. Gretchen SS, Fetz AE, Radic MZ et al (2017) An overview of the role of neutrophils in innate immunity, inflammation and host-biomaterial integration. *Regen Biomater* 4(1):55–68
17. Weissman G, Smoles JE, Korchak HM (1980) Release of inflammatory mediators from stimulates neutrophils. *N Engl J Med* 303:27–34
18. Wilson CJ, Clegg RE, Ph D et al (2005) Mediation of biomaterial – cell interactions by adsorbed proteins: a review. *Tissue Eng* 11(1–2):1–18
19. Tang BL, Eaton JW (1993) Fibrin (ogen) mediates acute inflammatory responses to biomaterials. *J Exp Med* 178(6):2147–2156

20. Vroman L, Adams AL, Fischer GC et al (1980) Interaction of high molecular weight kininogen, factor XII, and fibrinogen in pPlasma at interfaces. *Blood* 55(1):156–159
21. Kim YK, Que R, Wang SW et al (2014) Modification of biomaterials with a self protein inhibits the macrophage response. *Adv Healthc Mater* 3(7):989–994
22. Milleret V, Buzzi S, Gehrig P et al (2015) Protein adsorption steers blood contact activation on engineered cobalt chromium alloy oxide layers. *Acta Biomater* 24:343–351
23. Markiewski MM, Nilsson B, Ekdahl KN et al (2007) Complement and coagulation: strangers or partners in crime? *Trends Immunol* 28(4):184–192
24. Jenney CR, Anderson JM (2000) Adsorbed IgG: a potent adhesive substrate for human macrophages. *J Biomed Mater Res* 50(3):281–290
25. Gorbet MB, Sefton MV (2004) Biomaterial-associated thrombosis: roles of coagulation factors, complement, platelets and leukocytes. *Biomaterials* 25(26):5681–5703
26. Ekdahl KN, Lambris JD, Elwing H et al (2011) Innate immunity activation on biomaterial surfaces: a mechanistic model and coping strategies. *Adv Drug Deliv Rev* 63(12):1042–1050
27. Chiumiento A, Lamponi S, Barbucci R (2007) Role of fibrinogen conformation in platelet activation. *Biomacromolecules* 8(2):523–531
28. Wu Y, Simonovsky FI, Ratner BD, Horbett TA (2005) The role of adsorbed fibrinogen in platelet adhesion to polyurethane surfaces: a comparison of surface hydrophobicity, protein adsorption, monoclonal antibody binding, and platelet adhesion. *J Biomed Mater Res* 74(4):722–738
29. Hong J, Ekdahl KN, Reynolds H et al (1999) A new in vitro model to study interaction between whole blood and biomaterials: studies of platelet and coagulation activation and the effect of aspirin. *Biomaterials* 20(7):603–611
30. Zhou G, Groth T (2018) Host responses to biomaterials and anti-inflammatory design — a brief review. *Macromol Biosci* 18(8):e1800112
31. Andersson J, Nilsson K, Lambris JD et al (2005) Binding of C3 fragments on top of adsorbed plasma proteins during complement activation on a model biomaterial surface. *Biomaterials* 26(13):1477–1485
32. Flick MJ, Du X, Witte DP et al (2004) Leukocyte engagement of fibrin (ogen) via the integrin receptor α M β 2/Mac-1 is critical for host inflammatory response in vivo. *J Clin Invest* 113(11):1596–1606
33. Nilsson B, Nilsson K, Eirik T et al (2007) The role of complement in biomaterial-induced inflammation. *Mol Immunol* 44(1–3):82–94
34. Szaba FM, Smiley ST (2002) Roles for thrombin and fibrin (ogen) in cytokine/chemokine production and macrophage adhesion in vivo. *Blood* 99(3):1053–1059
35. Li M, Peake PW, Charlesworth JA et al (2007) Complement activation contributes to leukocyte recruitment and neuropathic pain following peripheral nerve injury in rats. *Eur J Neurosci* 26(12):3486–3500
36. Hed J, Johansson M, Lindroth M (1984) Complement activation according to the alternate pathway by glass and plastic surfaces and its role in neutrophil adhesion. *Immunol Lett* 8(6):295–299
37. Sarma JV, Ward PA (2011) The complement system. *Cell Tissue Res* 343(1):227–235
38. Lhotta K, Wurzner R, Kronenberg F et al (1998) Rapid activation of the complement system by cuprophane depends on complement component C4. *Kidney Int* 53(4):1044–1051
39. Chenoweth DE (1987) Complement activation in extracorporeal circuits. *Ann N Y Acad Sci* 516:306–313
40. Becker EL (1972) The relationship of the chemotactic behavior of the complement-derived factors, C3a, C5a, and C567, and a bacterial chemotactic factor to their ability to activate the proesterase 1 of rabbit polymorphonuclear leukocytes. *J Exp Med* 135(2):376–387
41. McNally AK, Jones JA et al (2008) Vitronectin is a critical protein adhesion substrate for IL-4-induced foreign body giant cell formation. *J Biomed Mater Res* 86(2):535–543
42. Keselowsky BG, Bridges AW, Burns KL et al (2007) Role of plasma fibronectin in the foreign body response to biomaterials. *Biomaterials* 28(25):3626–3631
43. Shen M, Garcia I, Maier RV et al (2004) Effects of adsorbed proteins and surface chemistry on foreign body giant cell formation, tumor necrosis factor alpha release and procoagulant activity of monocytes. *J Biomed Mater Res* 70(4):533–541
44. Franz S, Rammelt S, Scharnweber D et al (2011) Biomaterials immune responses to implants—a review of the implications for the design of immunomodulatory biomaterials. *Biomaterials* 32(28):6692–6709
45. Akira S, Uematsu S, Takeuchi O (2006) Pathogen recognition and innate immunity. *Cell* 124(4):783–801
46. Bianchi ME (2007) DAMPs, PAMPs and alarmins : all we need to know about danger. *J Leucoc Biol* 81(1):1–5
47. Grandjean-laquerriere A, Tabary O, Jacquot J et al (2007) Involvement of toll-like receptor 4 in the inflammatory reaction induced by hydroxyapatite particles. *Biomaterials* 28(3):400–404
48. De Oliveira S, López-muñoz A, Candel S et al (2014) ATP modulates acute inflammation in vivo through dual oxidase 1 – derived H₂O₂ production and NF- κ B activation. *J Immunol* 192(12):5710–5719
49. Lee J, Jackman JG, Kwun J et al (2017) Nucleic acid scavenging microfiber mesh inhibits trauma-induced inflammation and thrombosis. *Biomaterials* 120:94–102

50. Wright HL, Moots RJ, Bucknall RC et al (2010) Neutrophil function in inflammation and inflammatory diseases. *Rheumatology* 49(9):1618–1631
51. Labow RS, Meek E, Santerre JP (2001) Neutrophil-mediated biodegradation of medical implant materials. *J Cell Physiol* 186(1):95–103
52. Nimeri G, Ohman L, Elwing H et al (2002) The influence of plasma proteins and platelets on oxygen radical production and F-actin distribution in neutrophils adhering to polymer surfaces. *Biomaterials* 23(8):1785–1795
53. Nimeri G, Majeed M, Elwing H et al (2003) Oxygen radical production in neutrophils interacting with platelets and surface-immobilized plasma proteins : role of tyrosine phosphorylation. *J Biomed Mater Res* 67(2):439–447
54. Branzk N, Lubojemska A, Hardison SE et al (2015) Europe PMC funders group neutrophils sense microbial size and selectively release neutrophil extracellular traps in response to large pathogens. *Nat Immunol* 15(11):1017–1025
55. Hahn J, Schauer C, Czegley C et al (2018) Aggregated neutrophil extracellular traps resolve inflammation by proteolysis of cytokines and chemokines and protection from antiproteases. *FASEB J* 33(1):1401–1414
56. Yamashiro S, Kamohara H, Wang J et al (2001) Phenotypic and functional change of cytokine-activated neutrophils: inflammatory neutrophils are heterogeneous and enhance adaptive immune responses. *J Leucoc Biol* 69(5):698–704
57. Altieri DC, Mannucci PM, Capitanio AM (1986) Binding of fibrinogen to human monocytes. *J Clin Invest* 78(4):968–976
58. Mesure L, De Visscher G, Vranken I et al (2010) Gene expression study of monocytes/macrophages during early foreign body reaction and identification of potential precursors of myofibroblasts. *PLoS One* 5(9):e12949
59. Badylak SF, Gilbert TW (2008) Immune response to biologic scaffold materials. *Semin Immunol* 20(2):109–116
60. Lynn AD, Kyriakides TR, Bryant SJ (2009) Characterization of the in vitro macrophage response and in vivo host response to poly (ethylene glycol)-based hydrogels. *J Biomed Mater Res Part A* 93(3):941–953
61. Zhao Q, Topham N, Anderson JM (1991) Foreign-body giant cells and polyurethane biostability : in vivo correlation of cell adhesion and surface cracking. *J Biomed Mater Res* 25(2):177–183
62. Mantovani A, Vecchi A, Allavena P (2014) ScienceDirect pharmacological modulation of monocytes and macrophages. *Curr Opin Pharmacol* 17:38–44
63. Wynn TA, Ph D, Barron L, Ph D (2010) Macrophages: master regulators of inflammation and fibrosis. *Semin Liver Dis* 30(3):245–257
64. Taylor PR, Martinez-Pomares L, Stacey M et al (2005) Macrophage receptors and immune recognition. *Annu Rev Immunol* 23:901–944
65. Mosser DM, Edwards JP (2008) Exploring the full spectrum of macrophage activation. *Nat Rev Immunol* 8(12):958–969
66. Brodbeck WG, Macewan M, Colton E et al (2005) Lymphocytes and the foreign body response : lymphocyte enhancement of macrophage adhesion and fusion. *J Biomed Mater Res A* 74(2):222–229
67. Helming L, Gordon S (2007) Macrophage fusion induced by IL-4 alternative activation is a multistage process involving multiple target molecules. *Eur J Immunol* 37(1):33–42
68. Arpaia N, Green JA, Moltedo B et al (2015) A distinct function of regulatory t cells in tissue protection. *Cell* 162(5):1078–1089
69. Browder T, Folkman J, Pirie-shepherd S (2000) The hemostatic system as a regulator of angiogenesis. *J Biol Chem* 275(3):1521–1524
70. Ward WK (2008) A review of the foreign-body response to subcutaneously-implanted devices: the role of macrophages and cytokines in biofouling and fibrosis. *J Diabetes Sci Technol* 2(5):768–777
71. Ratner BD (2002) Reducing capsular thickness and enhancing angiogenesis around implant drug release systems. *J Control Release* 78(1–3):211–218
72. Diegelmann RF, Evans MC (2004) Wound healing: an overview of acute, fibrotic and delayed healing. *Front Biosci* 9:283–289
73. Rockey DC, Bell D, Hill JA (2015) Fibrosis—a common pathway to organ injury and failure. *N Engl J Med* 372(1):1138–1149
74. Van Zutphen LFM, Baumans V, Beynen AC (2001) Principles of laboratory animal science, revised edition, 1st edn. Elsevier, New York
75. Azab AK, Doviner V, Orkin B et al (2007) Biocompatibility evaluation of crosslinked chitosan hydrogels after subcutaneous and intraperitoneal implantation in the rat. *J Biomed Mater Res A* 83(2):414–422
76. De Souza R, Zahedi P, Allen CJ et al (2009) Biocompatibility of injectable chitosan-phospholipid implant systems. *Biomaterials* 30(23–24):3818–3824
77. Tomazic-Jezic VJ, Merritt K, Umbreit TH (2001) Significance of the type and the size of biomaterial particles on phagocytosis and tissue distribution. *J Biomed Mater Res* 55(4):523–529
78. Bajaj G, Van Alstine WG, Yeo Y (2012) Zwitterionic chitosan derivative, a new bBiocompatible pharmaceutical excipient, prevents endotoxin-mediated cytokine release. *PLoS One* 7(1):e30899
79. Lozano FS, García-Criado FJ, Fresnadillo MJ et al (2002) Systemic inflammatory response induced by dacron graft and modulation by antimicrobial agents: experimental study. *J Surg Res* 107(1):7–13
80. Busuttill SJ, Ploplis VA, Castellino FJ et al (2004) A central role for plasminogen in the inflammatory

- response to biomaterials. *J Thromb Haemostasis* 2(10):1798–1805
81. Schlosser M, Wilhelm L, Urban G et al (2002) Immunogenicity of polymeric implants: long-term antibody response against polyester (Dacron) following the implantation of vascular prostheses into LEW.1A rats. *J Biomed Mater Res* 61(3):450–457
82. Skokos EA, Charokopos A, Khan K et al (2011) Lack of TNF- α -induced MMP-9 production and abnormal E-cadherin redistribution associated with compromised fusion in MCP-1-null macrophages. *Am J Pathol* 178(5):2311–2321
83. Kyriakides TR, Foster MJ, Keeney GE et al (2004) The CC chemokine ligand, CCL2/MCP1, participates in macrophage fusion and foreign body giant cell formation. *Am J Pathol* 165(2):2157–2166
84. Mendes JB, Campos PP, Ferreira MAND et al (2007) Host response to sponge implants differs between subcutaneous and intraperitoneal sites in mice. *J Biomed Mater Res B Appl Biomater* 83(2):408–415
85. King A, Sandler S, Andersson A (2001) The effect of host factors and capsule composition on the cellular overgrowth on implanted alginate capsules. *J Biomed Mater Res* 57(3):374–383
86. Rodriguez A, MacEwan SR, Meyerson H et al (2009) The foreign body reaction in T-cell-deficient mice. *J Biomed Mater Res A* 90(1):106–113
87. Yang J, Jao B, McNally AK et al (2014) In vivo quantitative and qualitative assessment of foreign body giant cell formation on biomaterials in mice deficient in natural killer lymphocyte subsets, mast cells, or the interleukin-4 receptor α and in severe combined immunodeficient mice. *J Biomed Mater Res A* 102(6):2017–2023
88. Avula MN, Rao AN, McGill LD et al (2014) Foreign body response to subcutaneous biomaterial implants in a mast cell-deficient Kitw-Sh murine model. *Acta Biomater* 10(5):1856–1863
89. Gonzalez R, Hill SJ, Mattar SG et al (2011) Absorbable versus nonabsorbable mesh repair of congenital diaphragmatic hernias in a growing animal model. *J Laparoendosc Adv Surg Tech* 21(5):449–454
90. Roth WJ, Kissinger CB, McCain RR et al (2013) Assessment of juvenile pigs to serve as human pediatric surrogates for preclinical formulation pharmacokinetic testing. *AAPS J* 15:763–774
91. Seaton M, Hocking A, Gibran NS (2015) Porcine models of cutaneous wound healing. *ILAR J* 56(1):127–138
92. Krause TJ, Robertson FM, Greco RS (1993) Measurement of intracellular hydrogen peroxide induced by biomaterials implanted in a rodent air pouch. *J Biomed Mater Res* 27(1):65–69
93. Hooper KA, Nickolas TL, Yurkow EJ et al (2000) Characterization of the inflammatory response to biomaterials using a rodent air pouch model. *J Biomed Mater Res* 50(3):365–374
94. Wooley PH, Morren R, Andary J et al (2002) Inflammatory responses to orthopaedic biomaterials in the murine air pouch. *Biomaterials* 23(2):517–526
95. Kao WJ, Lee D (2001) In vivo modulation of host response and macrophage behavior by polymer networks grafted with fibronectin-derived biomimetic oligopeptides: the role of RGD and PHSRN domains. *Biomaterials* 22(21):2901–2909
96. Brodbeck WG, Patel J, Voskerician G et al (2002) Biomaterial adherent macrophage apoptosis is increased by hydrophilic and anionic substrates in vivo. *PNAS* 99(16):10287–10292
97. Laschke MW, Haufel JM, Thorlacijs H et al (2005) New experimental approach to study host tissue response to surgical mesh materials in vivo. *J Biomed Mater Res A* 74(4):696–704
98. Brodbeck WG, Voskerician G, Ziats NP et al (2003) In vivo leukocyte cytokine mRNA responses to biomaterials are dependent on surface chemistry. *J Biomed Mater Res A* 64(2):320–329
99. Pawlina W (2016) *Histology – text and atlas*, 7th edn. Wolters Kluwer Health, Philadelphia
100. Correia RC, Santos TC, Pirraco RP et al (2017) In vivo osteogenic differentiation of stem cells inside compartmentalized capsules loaded with co-cultured endothelial cells. *Acta Biomater* 15:483–494
101. Popa EG, Carvalho PP, Dias AF et al (2014) Evaluation of the in vitro and in vivo biocompatibility of carrageenan-based hydrogels. *Soc Biomater* 102(11):4087–4097
102. Marques AP, Reis RL, Hunt JA (2005) An in vivo study of the host response to starch-based polymers and composites subcutaneously implanted in rats. *Macromol Biosci* 5:775–785
103. Rodrigues MT, Gomes ME, Viegas CA et al (2011) Tissue-engineered constructs based on SPCL scaffolds cultured with goat marrow cells: functionality in femoral defects. *J Tissue Eng Regen Med* 5(1):41–49
104. Spiller KL, Wrona EA, Romero-Torres S et al (2016) Differential gene expression in human, murine, and cell line-derived macrophages upon polarization. *Exp Cell Res* 347(1):1–13
105. Siegers GM, Swamy M, Fernández-Malavé E et al (2007) Different composition of the human and the mouse $\gamma\delta$ T cell receptor explains different phenotypes of CD3 γ and CD3 δ immunodeficiencies. *J Exp Med* 204(11):2537–2544
106. Mestas J, Hughes CCW (2004) Of mice and not men: differences between mouse and human immunology. *J Immunol* 172(5):2731–2738
107. Rodríguez E, Ip WH, Kolbe V et al (2017) Humanized mice reproduce acute and persistent human adenovirus infection. *J Infect Dis* 215(1):70–79
108. Jespersen H, Lindberg MF, Donia M et al (2017) Clinical responses to adoptive T-cell transfer can be modeled in an autologous immune-humanized mouse model. *Nat Commun* 8:707

109. Rong Z, Wang M, Hu Z et al (2014) An effective approach to prevent immune rejection of human ESC-derived allografts. *Cell Stem Cell* 14(1):121–130
110. Nishimura T, Hu Y, Wu M et al (2012) Using chimeric mice with humanized livers to predict human drug metabolism and a drug-drug interaction. *J Pharmacol Exp Ther* 344(2):388–396
111. Walsh NC, Kenney LL, Jangalwe S et al (2017) Humanized mouse models of clinical disease. *Annu Rev Pathol* 12:187–215
112. Duchosal MA, Eming SA, McConahey PJ et al (1992) The hu-PBL-SCID mouse model. Long-term human serologic evolution associated with the xenogeneic transfer of human peripheral blood leukocytes into SCID mice. *Cell Immunol* 139(2):468–477
113. Greiner DL, Hesselton RA, Shultz LD (1998) SCID mouse models of human stem cell engraftment. *Stem Cells* 16(3):166–177
114. Legrand N, Weijer K, Spits H (2014) Experimental models to study development and function of the human immune system in vivo. *J Immunol* 176(4):2053–2058
115. McCune JM (1996) Development and applications of the SCID-hu mouse model. *Semin Immunol* 8(4):187–196
116. Denton PW, García JV (2011) Humanized mouse models of HIV infection. *AIDS Rev* 13(3):135–148
117. Shultz LD, Brehm MA, Garcia-Martinez JV et al (2012) Humanized mice for immune system investigation: progress, promise and challenges. *Nat Rev Immunol* 12(11):786–798
118. Wege AK, Melkus MW, Denton PW et al (2008) Functional and phenotypic characterization of the humanized BLT mouse model. *Curr Top Microbiol Immunol* 324:149–165
119. Shultz LD, Schweitzer PA, Christianson SW et al (1995) Multiple defects in innate and adaptive immunologic function in NOD/LtSz-scid mice. *J Immunol* 154(1):180–191
120. Shultz LD, Lyons BL, Burzenski LM et al (2005) Human lymphoid and myeloid cell development in NOD/LtSz-scid IL2R gamma null mice engrafted with mobilized human hematopoietic stem cells. *J Immunol* 174(10):6477–6489
121. Wang RM, Johnson TD, He J et al (2017) Humanized mouse model for assessing the human immune response to xenogeneic and allogeneic decellularized biomaterials. *Biomaterials* 129:98–110
122. He J, Rong Z, Fu X, Xu Y (2017) A safety checkpoint to eliminate cancer risk of the immune evasive cells derived from human embryonic stem cells. *Stem Cells* 35(5):1154–1161
123. Zhao T, Zhang Z, Westenskow PD et al (2015) Humanized mice reveal differential immunogenicity of cells derived from autologous induced pluripotent stem cells. *Cell Stem Cell* 17(3):353–359



Biocompatibility of Materials for Biomedical Engineering

9

Yu-Chang Tyan, Ming-Hui Yang,
Chin-Chuan Chang, and Tze-Wen Chung

Abstract

In the tissue engineering research field, nanobio-materials highlight the impact of novel bioactive materials in both current applications and their potentials in future progress for tissue engineering and regenerative medicine. Tissue engineering is a well-investigated and challenging biomedical field, with promising perspectives to improve and support quality of life for the patient. To assess the response of those *extracellular matrices* (ECMs), induced by biomedical materials, this review will focus on cell response to natural biomaterials for biocompatibility.

Authors Yu-Chang Tyan and Chin-Chuan Chang have equally contributed to this chapter.

Y.-C. Tyan

Department of Medical Imaging and Radiological Sciences, Kaohsiung Medical University, Kaohsiung, Taiwan

Center for Cancer Research, Kaohsiung Medical University, Kaohsiung, Taiwan

Graduate Institute of Medicine, College of Medicine, Kaohsiung Medical University, Kaohsiung, Taiwan

Institute of Medical Science and Technology, National Sun Yat-sen University, Kaohsiung, Taiwan

Department of Medical Research, Kaohsiung Medical University Hospital, Kaohsiung, Taiwan

Research Center for Environmental Medicine, Kaohsiung Medical University, Kaohsiung, Taiwan

Keywords

Biocompatible · Bioactive · Tissue engineering · Extracellular matrix · Cell/tissue reaction · Nanoparticle · Hyaluronic acid · Silk fibroin · Chitosan · Cell-biomaterial interaction

M.-H. Yang

Department of Medical Education and Research, Kaohsiung Veterans General Hospital, Kaohsiung, Taiwan

Master Program in Clinical Pharmacogenomics and Pharmacoproteomics, College of Pharmacy, Taipei Medical University, Taipei, Taiwan

National Mosquito-Borne Diseases Control Research Center, National Health Research Institutes, Zhunan, Taiwan

C.-C. Chang

Department of Nuclear Medicine, Kaohsiung Medical University Hospital, Kaohsiung, Taiwan

Graduate Institute of Clinical Medicine, Kaohsiung Medical University, Kaohsiung, Taiwan

Neuroscience Research Center, Kaohsiung Medical University, Kaohsiung, Taiwan

T.-W. Chung (✉)

Department of Biomedical Engineering, National Yang-Ming University, Taipei, Taiwan

Center for Advanced Pharmaceutical Science and Drug Delivery, National Yang-Ming University, Taipei, Taiwan

e-mail: twchung@ym.edu.tw

9.1 Introduction

A biomaterial has been formally defined as a systemically and pharmacologically inert substance designed to be implanted in or associated with life systems by the Clemson University Advisory Board for Biomaterials [1]. Other definitions include “non-living materials for medical devices that are designed to interact with the biological systems” [2], “synthetic and natural source materials in contact with tissues, blood and biological fluids, and intended for use in prosthetics, diagnosis, treatment or storage applications without adversely affecting the organisms and their components” [3], as well as “any combination of substances, drugs or substances of synthetic or natural in origin, which may be used at any time, as a whole or as a part of a system of treating, enhancing or replacing any tissue, organ or function of the body” [4].

Biomedical materials can be roughly classified into several types by the tissue response. One is a bioinert biomaterial which once placed in the human body has minimal interaction with its surrounding tissue. Another is a bioactive biomaterial that interacts with the surrounding bones when placed in a human body and, in some cases, even with soft tissues. The other is a bio-absorbable biomaterial that starts to dissolve when placed in a human body and is slowly replaced by propelling tissue such as bone. Since more substances are treated as biomaterials, it becomes important to distinguish suitable ones from unfit products or materials which have not been thoroughly evaluated. Materials which can be used as a biomaterial need to meet several strict restrictions. First, a biological material must be biocompatible. It should not cause any adverse reaction in the body, and vice versa. In addition, it should be nontoxic and non-carcinogenic. Also, the biomaterial should have sufficient physical and mechanical properties to be used as an enhancement or replacement for a designated part or function in the human body.

When the material is placed into the human body, the tissue reacts to the implant in a variety

of ways dependent upon the type of material. The composition of the material and the surrounding environment determines the properties to be considered.

As the medical devices/medical materials are implanted into the organism, they may induce nontoxic reactions or severe inflammation. If the surrounding tissues grow normally and the implanted organism survives, biocompatibility has been achieved.

The biggest problem in the development of biomedical materials is the cell/tissue reactions such as blood coagulation, immune response, carcinogenicity caused by long-term material contact to the human body, as well as the decrease of mechanical strength and cytotoxic substances released by degradation and abrasion. Thus, the primary part in the development of biomedical materials is evaluation to minimize the host reaction.

9.2 Biocompatibility Assessment Test Planning

Biocompatibility of biomaterials is a term widely used in science, but there still exists a lot of uncertainty about what it practically means and the mechanisms of the phenomena that collectively constitute biocompatibility. By definition, it is a measurement of the compatibility of the device with the biological system. The aim of conducting biocompatibility tests is to determine the suitability of the device for human use and to check if the use of the device may induce any potentially harmful physiological effects.

The biocompatibility assessment is mainly to determine potential toxins. When the materials are used for medical equipment, these toxins may be released after exposure to the human body and may cause damage or disease. In addition to the beneficial tissue responses and the clinically relevant properties of the biological materials, cytotoxicity, stimulatory response, allergic test, implantation effects, genotoxicity, carcinogenicity, and biodegradability are considered to be the components of biocompatibility.

9.2.1 Cytotoxicity

The cytotoxicity tests are *in vitro* tests in mammalian cells which are a useful initial step in determining the potential toxicity of biomaterials. Those biomaterials are used to contact test cells *in vitro* with different contact methods, and then the biological parameters of the cells are tested for the biological response of the medical devices, materials, or their extracts. Thus, the cellular toxicity studies play an important role in the successful development of the minimal to no toxicity biomaterial preparation. The definition of cytotoxicity may contain a wide and vague interpretation. Sometimes acute toxicity is also considered for inclusion [5]. For an *in vitro* cell culture system where the substance is interfered with cell attachment, it may significantly alter morphology, adversely affect cell growth rate, or cause cell death. Thus, it is considered to be cytotoxic [6]. Examples of basic metabolic functions shared by all cells include maintenance of cell mitochondrial activity, membrane integrity, and protein synthesis [7]. Due to the metabolic rate, different organs may contain different levels of activity. It is speculated that in some cases, mammalian target organ toxicity reflects the underlying cytotoxicity of chemicals assigned to affected organs [7].

9.2.2 Stimulatory Response

The stimulatory response tests are assessed for the biomaterials, medical devices, and their extracts at appropriate implant sites (skin, eye, mucosa, etc.) to evaluate the irritation. Those test methods were selected for the special signal pathways to determine the irritation after exposure or contact to medical equipment, materials, and their extracts. The stimulatory response is a dose (or concentration)-response relationship in which low concentrations of other toxic substances result in an increase in one or more biological responses.

Recent research in the field of biomaterials has shown that the functional porous biomateri-

als in regenerative medicine have the ability to activate the immune system, even in the absence of other immune stimuli, or the potential to reduce the need for the replacement of damaged tissue. Some research results suggest that these reactions may be influenced by the physicochemical properties of the material [8]. Although it has been repeatedly suggested that stimulatory effects should be included in the default model of toxicology, they are not even used as secondary models in risk assessment [9].

9.2.3 Allergic Test

Allergic contact inflammation is acquired through previous sensitization with a foreign substance. Allergic tests are used in appropriate experimental models to assess contact allergies or allergenic reactions caused by biomaterials, medical devices, and/or their extracts. Any exposure to trace amount of potential eluate may cause allergic or sensitizing reactions. Exposures may induce allergic reactions, which are caused by the complex cellular activation and the humoral immune mechanisms. If the biomaterial is suitable for intradermal injection, it is recommended to maximize the test. The closed-patch test is the non-extractable selection test, or when the extract or material may be applied topically [10].

9.2.4 Implantation Effects

Biomaterial implantation may induce edema formation and focal hemorrhage that cause the enrichment of protein interstitial fluid. Within a few seconds of implantation, the protein interacts with the surface of biomaterial and over time forms as a proteinaceous coating. The evaluation of the host response to implanted biomaterials is usually focused on the tissue response at the site of implantation. A broader perspective reveals various possible and actual systemic effects of carcinogenic, metabolic, immunological, and bacterial properties [11].

For the implantation effect, the acute systemic toxicity evaluation and systemic effects are required for all devices which have direct or indirect contact with blood. Also, the hemocompatibility needs to be considered for biomaterials. For medical devices that are exposed to blood (regardless of exposure time), it is recommended to consider hemolytic, immunological (complementary activity), and thrombogenicity tests. Indirect blood contact with medical equipment is generally not required for complement activity and *in vivo* thrombogenicity testing.

9.2.5 Genotoxicity

If the biomaterials are indicated by the chemistry and/or composition or if *in vitro* test results indicate potential genotoxicity, the *in vivo* genotoxicity tests are required. If the result of the injury is a substance that causes a sudden change in the cytogenetic gene or a chromosomal abnormality, the concentration of a mutagenic substance (mutagenic substance or mutagen) may need to be increased for carcinogenicity. For the genotoxicity tests, at least three *in vitro* assays should be required and two of them should be done in mammalian cells. For the initial *in vitro* assays, it should include the three kinds of genotoxic effects: DNA destruction, gene mutations, and chromosomal aberrations [12].

9.2.6 Carcinogenicity

Reproductive and developmental toxicity testing uses rodents and rabbits as test animals to assess such toxicity before, during, and after lactation to provide an understanding of the product's fertility, embryo toxicity, and neonatal and maternal lactation and the possibility of the malformations of causing teratogenesis. Usually, the carcinogenicity tests should be considered when the data from other experiment suggest a tendency of tumor formation. The conventional tests for carcinogenicity and chronic toxicity should be planned in a single experimental design in which

the long-term rodent carcinogenicity bioassay requires 2 years [13].

9.2.7 Biodegradability

The degradation of biomaterials is always a serious issue for the medical device whether it is to prevent the degradation of implantable devices or to predict the amount of degradation of tissue engineering scaffolds or drug-releasing elements. In recent years, polymer science has been developed tremendously. Researchers have made some major discoveries and advances in this research field. It resulted in a new era of polymer science, especially biodegradable polymers. The suitability of polymers for biomedical applications depends on its biocompatibility, degradation process, and non-immunogenicity. Biodegradable polymers play an important role in therapeutics and drug delivery, which is advantageous in the tissue engineering [14].

Biodegradation tests are used to determine the biodegradability of a product in a given or intended use environment. Biodegradation testing of plastics is usually carried out under the conditions close to commercial composting; liquid biodegradation tests are carried out in representative aquatic systems. The US Food and Drug Administration recommends that when biodegradable designs are used, live biodegradability tests are performed on applicable animal models.

9.3 Traditional Biomaterials

Metal is the most diffusely used biomaterial for load-bearing implants. While many metals and their alloys are used in medical device applications, the most widely used are stainless steel, commercial pure titanium and titanium alloys, and cobalt-based alloys. The biocompatibility of the metal implant is very worrying because these implants may corrode when exposed to the *in vivo* environment [15]. The consequence of corrosion is the disintegration of the implant material itself, which may weaken the implant

and cause harmful effects of corrosion products on surrounding tissues and organs [16].

The motivations for using ceramics are (1) their inertness in the living body, (2) their ability to be shaped into various shapes and pores, (3) their high compressive strength, and (4) their excellent wear characteristics in some cases. Ceramics have traditionally been widely used as dental restorative materials. However, the poor fracture toughness of ceramics has severely limited their application in load-bearing uses. Thus, compared to metals and polymers, ceramic use in other fields of biomedicine is not so extensive.

There are a large number of polymeric materials that have been used as part of an implant or implant system. The main advantages of polymer biomaterials compared to metal or ceramic materials are their ease of manufacture to produce various shapes (latex, film, sheet, fiber, etc.), ease of secondary processing, reasonable cost, and the availability of required physical and mechanical properties. Their applications include facial prosthesis, artificial blood vessels and heart valves, catheters, tracheal tubes, hip and knee joint replacement, and artificial liver, heart, bladder, kidney, and pancreas.

The biologically derived materials are proteins and polysaccharides extracted from the extracellular matrix of an organism or human source. These materials also may be characteristically bioactive and biodegradable, which can be induced to improve human compatibility with contact tissue regeneration. Those materials can also be used as cosmetic medicine fillers or artificial skin. However, most of those materials also lack mechanical strength. These types of biomedical materials can also be combined with other composite materials to increase compatibility with the human body.

The term “composite” in composite biomaterials generally retains several materials in which the different phases are separated at a level greater than the atomic scale, wherein properties such as elastic modulus are significantly different compared to the properties of the homogeneous material. Composite materials have unique properties and are generally stronger than any single materials from which they are made. Moreover,

composite materials are widely used in artificial joints, where their combination of low density/weight and high strength makes them ideal materials for those clinical applications.

9.4 Natural Materials

At present, biomedical materials are generally divided into four categories, which included metals, ceramics, polymer materials, and biological materials. However, the biodegradable materials, another class of advance materials, are receiving increasing attention. For example, the absorbable suture materials are used to hold the wound together but resorb in the body and make the wound heal and gain strength with natural growth. Certain wound dressings and ceramic bone reinforcements promote tissue growth by providing a stent. The scaffold material can be or not absorbed over a period of time, but in each case, the native tissue has grown into space and then restored to natural function. Another application of biodegradable materials is used for drug delivery. When these materials are placed in the body and the drug is released upon degradation of the material, certain drugs can be chemically bonded to the biodegradable material to provide the local persistence of the drug during a predictable period of time.

Except the synthetic materials mentioned above, several natural biomaterials derived from animals or plants are being considered for use as biomaterials that deserve discussion. Natural biomaterials do not usually cause the toxic problems, which are often induced by synthetic materials. Besides, they can carry specific protein binding sites and induce other biochemical signal pathways that may contribute to the tissue healing or integration. The natural materials include collagen, coral, chitin (from insects and crustaceans), keratin (from hair), organism, hyaluronic acid, alginic acid, and cellulose. In the following article, we will focus on several polymer biomaterials that more and more researchers have investigated in recent years such as hyaluronic acid (HA), chitosan (CS), silk fibroin (SF), collagen, alginate,

and some polymeric micelles. The advantages and disadvantages of the natural materials are listed in Table 9.1.

The schematic representation of some possible signaling pathways activated by HA, CS, and SF which may regulate metabolism of proliferating cells is shown in Fig. 9.1. The cell-biomaterial interaction may activate PI3K/AKT1/mTOR pathway, which is responsible for cell proliferation and is required for cell survival. When GSK3B binds to APP and SPARC, the PI3K/AKT1/mTOR pathway can also be stimulated by GSK3B. The hypothesis of the mTOR pathway is that it acts as the primary switch for cell catabo-

lism and anabolism, thereby determining cell growth and proliferation. For most cells, the PI3K/AKT/mTOR signal is activated by mutations in the pathway components and the activation of upstream signaling molecules, resulting in deregulation of proliferation, resistance to apoptosis, and alteration of metabolic properties of transformed cells [17].

9.4.1 Hyaluronic Acid

HA polymers, the poly-disaccharides composed of D-glucuronic acid and D-N-acetylglucosamine, can range from 5000 to 20,000,000 daltons and are one of the major components of extracellular matrix in connective tissues [18, 19]. HA appears relatively late in the evolution because its presence in organisms is usually observed after the appearance of chordate [20]. HA is in nearly all human tissues and also in other vertebrates; however, it is not found in fungi, plants, and insects [21].

HA interacts with extracellular molecules to form a complex extracellular matrix (ECM) and is involved in regulating of cell growth, differentiation, and migration. It is recognized by cell surface receptors, which include CD44, receptor for *hyaluronic acid-mediated* motility (RHAMM), and some Toll-like receptors. Binding of HA to these cell membrane receptors may result in activation of intracellular signaling pathways or cell uptake of cellular HA. Recently, HA has been shown to be one of the key regulators of various human tumors influencing cell proliferation rates, altering cell motility, controlling malignancy, and mediating angiogenesis [22, 23]. In many different types of tumors, the HA receptors, such as CD44 and RHAMM, are highly expressed and activated, which may promote cell infiltration and tumor malignancy [24, 25].

HA has been reported as a significant factor in a wide range of medical and biological material fields, such as reactive oxygen species, angiogenesis, cancer, lung injury, liver injury, kidney injury, brain injury, diabetes, leukocyte trafficking, and immune regulation [26, 27]. It also plays important roles in neural proliferation, differentiation, migration, survival, and cell signaling

Table 9.1 The advantages and disadvantages of the natural materials

	Advantages	Disadvantages
Hyaluronic acid	Highly flexible Non-allergenic and non-inflammatory properties Viscoelastic, muco-adhesive, and hydrophilic	Skin dependent Extremely drying Stomach discomfort
Chitosan	Nontoxic, biocompatible, and biodegradable properties Chemo-attraction characteristic	Insoluble in organic solvents Lacking thermoplastic properties
Silk fibroin	Low immunogenicity Non-thrombogenicity Anti-inflammatory properties	Fragility after insolubilization
Polymeric micelles	Longer half-life Lower adverse toxicity	Dissociate very slowly High cost of preparation Deformation and disassembly
Collagen	Resorbable Nontoxic with minimal immune response	Possibly cause alteration of cell behavior Possibly undergo contraction
Alginate	Biodegradable Nontoxic and non-inflammatory properties Controllable porosity	Weakness Poor cell adhesion

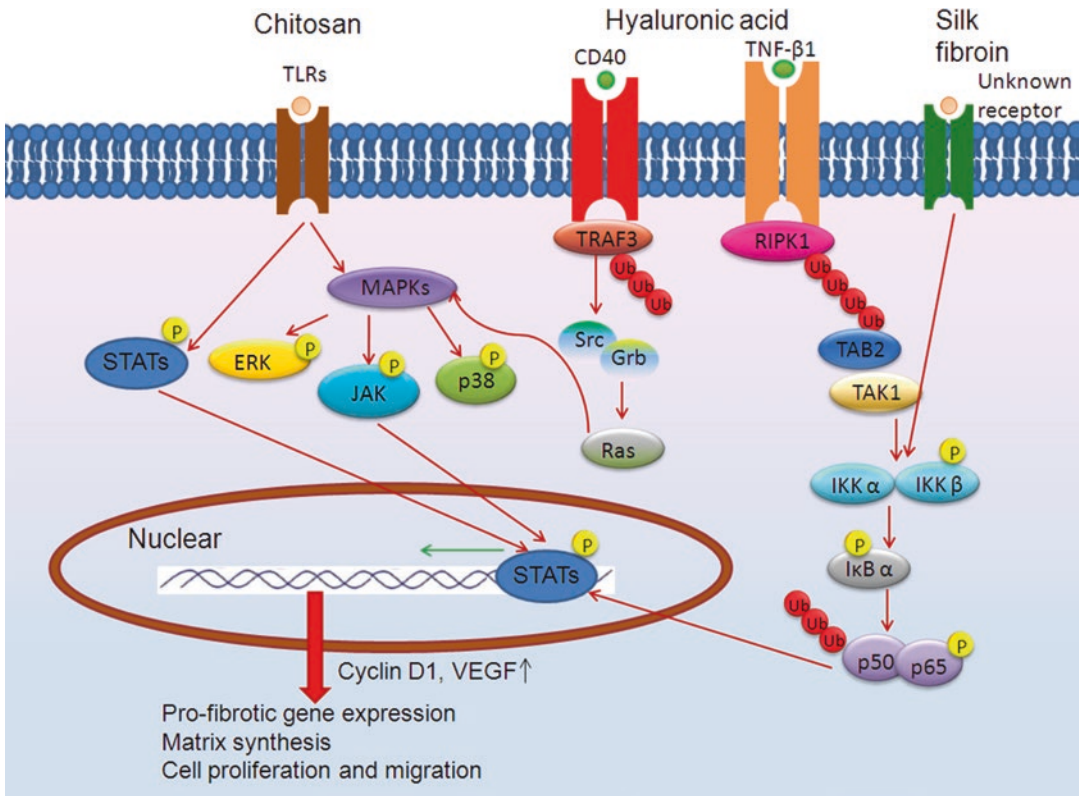


Fig. 9.1 Schematic representation of some possible signaling pathways activated by HA, CS, and SF which may regulate metabolism of proliferating cells

[28]. HA is highly flexible and therefore has different shapes and configurations which may affect its mechanical and molecular signaling functions and makes it as an ideal choice for a variety of biomedical applications [29–31]. For medical applications, HA is exploited for several products, including viscoelastic supplementation, drug delivery, ophthalmic surgery, tissue regeneration, and embryo protection. Several different levels of HA biomaterial products have been created with properties including durability and controlled therapeutic properties. Unlike other materials (such as CS derivatives), there are several advantages for the biomaterials and scaffolds made by HA, particularly the non-allergenic and non-inflammatory properties. Thus, HA has become the most adaptive biopolymer, which is mainly involved in tissue regeneration and medicine, including ophthalmology, dermatology, and orthopedics [32–34].

HA is an important raw material in the research of biomaterials. It is widely used as a filler, hydrogel material, cell carrier, and drug delivery system in surgical applications. The ease of separation and production and extensive biological activity make HA as a very attractive target for the system development of therapeutic biomaterial.

The excellent viscoelasticity, muco-adhesiveness, and hydrophilicity of HA make it useful in a variety of drug delivery applications. It can be used for topical and parenteral administration. For topical use, HA forms as a film on the surface of the skin or on the cornea that protects the drug carried by the HA and forms a reservoir for slow release of the drug, which can increase drug retention and efficiency. Since HA is essentially a polyanion under physiological conditions, it is widely used in coatings using polymeric charging properties. Typically, the coating is designed to induce a

favorable response from cells introduced onto the surrounding tissue of the implant [35]. For example, growth factors are important for regulating cellular processes, such as angiogenesis [36]. For tissue regeneration, ideal growth factor delivery should be continuous.

HA is critical for brain development, especially for the postnatal brain in areas near the lateral ventricle where stem cells are located [37, 38]. It is reported to be an important factor in a wide range of medical and biological fields such as reactive oxygen species; angiogenesis; cancer, lung, liver, kidney, and brain damage; diabetes and leukocyte trafficking; and immune regulation [39, 40]. It also plays an important role in neural proliferation, differentiation, migration, and survival and cell signaling [41]. HA-induced signal transduction is dependent on cell surface receptor interactions, and upon intravenous injection, HA targets specific receptors, including cluster determinant 44 (CD44) and Toll-like receptor 4 (TLR4) [42]. Thus, HA selectively delivers the drug to areas where these receptors are elevated [30, 43–45]. The non-immunogenic properties of HA are beneficial in parenteral/pulmonary drug delivery systems to achieve stable release or prolonged maintenance of various agents. The direct binding of HA to cytotoxic drugs such as paclitaxel, doxorubicin, and butyric acid can be internalized by cancer cells through receptor-mediated endocytosis, releasing active drugs and restoring their natural cytotoxicity [46]. In the central nervous system, the level of HA expression is elevated at the site of injury. High molecular weight HA is digested by hyaluronidase into smaller fragments; these products activate downstream signal transduction, regulate progenitor cell differentiation and proliferation, and promote nerve repair [44]. It also has the advantage of being a scaffolding material and can be combined with a binder peptide or other ECM component to provide cell attachment. Previous studies have shown that a combination scaffold consisting of fibrin with HA and laminin provides biomaterial properties to enable cells to polymerize. This mimics the natural tissues of the brain and supports the differentiation of human neural stem/progenitor cells (hNSPC) function [47]. Currently, HA-based biomaterials are used to regulate cell differentiation and bind

growth factors or ECM components for tissue engineering purposes for tissue repair [48]. In the future, there is reason to expect development of more HA derivatives for regenerative medicine, especially immunomodulation, angiogenesis, nerve regeneration and HA-containing hybrid materials.

9.4.2 Chitosan

Chitosan (CS), a biocompatible and biodegradable polymer, is the most abundant ingredient in the shell of krill, lobster, crawfish, shrimp, and crab. It is a modified natural carbohydrate polymer prepared by the partial N-deacetylation of chitin composed of β -(1 \rightarrow 4)-linked D-glucosamine residues, obtained by partial N-deacetylation of chitin (primary unit: 2-deoxy-2-(acetyl-amino) glucose). Thus, chitosan is usually not a homopolymer of D-glucosamine but a copolymer containing less than 40% N-acetyl-D-glucosamine residues. This polyaminosaccharide polymer and its derivatives have polycationic properties, due to the presence of large numerous amino groupings [49, 50], excellent chemical and biological properties, and nontoxicity and biocompatibility, making them very attractive for applications in many areas such as biology, chemistry, pharmaceuticals, medicine, agriculture, food, and environment (water and waste treatment) [51, 52]. CS has amino/acetamido groups along with both primary and secondary hydroxyl functional reactive groups at C-2, C-3, and C-6 positions, respectively. The arrangement and distribution of these functional groups are the major factors affecting to the structural, physical, and chemical properties of CS [53, 54]. Due to its unique biological effect, CS has received extensive attention as a biomedical material for anti-obesity [55], anti-hypertensive [56], anti-bacterial [57], anti-tumor [58], anti-inflammatory [59], and anti-oxidant [60] properties.

CS has been proposed for the development of hemodialysis and blood oxygenators, membranes and fibers for skin substitutes, wound dressings, and suture materials, for immobilization of enzymes and cells for binding to bile and fatty acids, and as a carrier for drug or gene delivery

[61, 62]. CS has a chemo-attraction characteristic that promotes the wound healing process or a high capacity that forms a complex with inorganic and biochemical substances for tissue engineering in bone regeneration [54, 63]. It also has the ability to activate complement and coagulation systems in blood [64], although it is suitable for applications involving blood contact such as hemodialysis membranes. CS-based biomaterials show great potential in a variety of biotechnological applications. Although chitosan is suitable for medical applications and involves blood contact, such as hemodialysis membranes, chitosan promotes surface-induced thrombosis and embolism; it is also a bioactive carbohydrate polymer that may be used for tissue engineering and gene or drug delivery. However, none of them are totally free of shortcomings. For example, CS is water-insoluble, which is the most important limiting factor for its use in biological systems. CS also prevents the absorption of the required vitamins and minerals. People who are allergic to shellfish may also be at risk.

Due to its low water solubility, being insoluble in organic solvents, and lacking thermoplastic properties, CS has limited use in some areas. Chemical modification may be useful to solve these problems. Grafting is a modification technique in which a polymer is covalently bonded to the backbone of the parent polymer (matrix). This method changes the surface characteristics, while the modified product retains the overall properties of the parent polymer. Due to its covalent nature, the grafting can reduce the absorption and delivers long-term chemical stability. In recent years, the chemical modification of polysaccharides has received more and more attention, opening up prospects for the application of these modified macromolecules in different fields [65, 66]. In the modification process, graft polymerization is a promising strategy for introducing various functional groups into polymers [67]. Chung et al. have also reported that grafting of CS as a scaffold onto polycaprolactone (PCL) can increase the growth rate of fibroblasts or PC12 cells in the biomaterials of a neurocatheter [68, 69]. With the rapid development of nanotechnology in medical research, various polymer-

based multifunctional nanoparticles (NPs) have been developed and are generally used to simultaneously diagnose and treat serious diseases such as cancer or malignant tumors [70–72]. Carbohydrate-based biodegradable polymers are often used to prepare nano-formulations. They are more favored than synthetic polymers, due to the biocompatibility, negligible toxicity, adequate stability, and high potential for functionalization and modification [73–75]. CS nanoparticles prepared by ion gel technology were first reported [76]. The positive charge of CS makes it possible to target negatively charged cell surfaces and receptors expressed by various cancer cells and cancer stem cell-like cells such as CD44. High uptake of CS-coated NPs by cancer cells has been reported to have induced the cytotoxicity six times higher than free doxorubicin [77]. Recent development in CS-based nano-systems multi-functionalized with agent has demonstrated that CS is a versatile polymer for targeted imaging and therapy.

9.4.3 Silk Fibroin

Silk fibroin (SF) is an insoluble fibrous polymer protein with a large hydrophobic domain, which is composed of anti-parallel β -sheets that can be easily purified into silk-based biomaterials without sericin. It can be from the larvae of *Bombyx mandarina* and *Bombyx mori*, the moths such as *Antheraea*, *Cricula*, *Samia*, and *Gonometa*, silkworm cocoons (such as *Nephila clavipes*) or spiders. SF is the essential component of the fabric mesh [78]. The primary structure of SF is characterized by a natural block copolymer comprising a hydrophobic block of a short side chain amino acid which has a repeat sequence, such as glycine and alanine, and mainly by a repeating amino acid sequence $(\text{Gly-Ser-Gly-Ala-Gly-Ala})_n$ composition. The original state consists of two major proteins, sericin and fibroin, which are coated with two layers of silk fibroin, called brins [79]. SF is a highly biocompatible material due to its low immunity, non-thrombogenic or anti-inflammatory response, cell adhesion, cellular response and regeneration characteristics, and favorable bio-

reactive properties [79–81]. SF-based biomaterials have been studied in the form of foams, fibers, hydrogels, granules, and scaffolds, as well as the application of vascular, neurological, cutaneous, bone, and cartilage tissue regeneration [82–87]. There are several additional properties of SF that have been mentioned. Falini et al. reported its strong affinity to polysaccharides [88]. Altman et al. reported its mechanical properties which include high strength with flexibility [89]. Yeo et al. reported its swelling properties which are dependent on solution pH [90]. These dynamic properties of the SF microstructure make it as a unique candidate for controlled and sustained gene or drug delivery [80, 81]. Due to its new understanding of processing and mechanical strength, elasticity, biocompatibility, and controllable biodegradability, SF has been used in several other fields of biomedical science [80]. Previously, *in vivo* and *in vitro* studies indicated that the serine-coated natural silk fibers could up-regulate inflammatory cytokines with increasing concentrations of sericin [91]. However, when the sericin coating was removed, the thrombogenic and inflammatory response of SF was eliminated [79]. Thus, SF protein polymers with sericin removed have better biomedical applications. These characteristics of SF are particularly useful for tissue engineering.

The nanoparticle is small enough to penetrate small capillaries, allowing enhanced cells to uptake the encapsulated drug or therapeutic molecule. The biocompatibility and controlled degradation of SF make it as an ideal candidate for nanoscale drug delivery carriers. The SF nanoparticle delivery platform allows for the preparation of therapeutic agents for the delivery of nutraceuticals, drugs, genes, siRNAs, peptides, antigens, and other agents, such as vaccines for prophylactic care, cancer, AIDS, mad cow disease, and Alzheimer's disease. The SF biopolymer nanoparticle may also induce and activate CD44 to enhance cell adhesion and proliferation [92].

Another application of SF is to improve the biocompatibility of quantum dots (QDs). The synthesis, characterization, and application of SF-coated semiconductor nanocrystals (also known as QD) in cell systems were reported [93, 94]. Coating QD with SF provides a biological

and biocompatible alternative to traditional fluorescent labels for *in vitro* and *in vivo* cell imaging applications. Cell and tissue imaging of SF-QD nanoparticles reveals cell surface markers, intracellular tracking, and tumor markers.

9.4.4 Collagen

Collagen, a protein which consists of various amino acids, plays an important role on strength of tissues and is widely found in mammals. Because collagen is also one of the structural proteins which is very important in extracellular matrices of animals, the applications associated with a variety of biomaterials are designed to create temporary scaffolding to support new tissue formations [95, 96]. A classic collagen molecule consists of three intertwined peptide chains forming a helical structure similar to a typical staircase. These peptide molecules are brought together to form collagen fibers of different length, thickness, and interlacing pattern. Some collagen molecules are formed as a rope-like structure, while other collagen molecules will form a mesh or network [96–99]. It is reported that purified collagen in the form of powder or solution may increase the ratio reactions of insoluble matter by additive or photocross-linking reactions.

Collagen can be absorbed into the body which produces minimal immune response, excellent cell attachment and biological interactions. Collagen can also be processed into a variety of forms, including porous sponges, gels, and flakes, and can be chemically cross-linked with many reagents to enhance its strength or alternatively change its rate of degradation. The biomedical applications of collagen include various types of surgery, cosmetic and drug delivery, and also tissue engineering of multiple tissues to replicate the function and healing of natural tissues.

Crosslinking low cytotoxic collagen in solution using different methods, such as the presence of vitamin E [96], melanin [97], glutaraldehyde, or methylene sulfonate [99–101], showed useful information to overcome aging and complex degradation of collagen. In fact, there are at least 15 different types of collagen with different structure,

function, and other characteristics. The main form used in biomedical applications is type I collagen, a rope-forming collagen that can be found almost anywhere in the body, including bone and skin.

However, there are some disadvantages of using collagen as a cellular substrate. Depending on how the collagen is processed, collagen may cause changes in cell behaviors (e.g., changes in growth or movement), inappropriate mechanical properties, or contraction (shrinkage). Since the interaction of cells with collagen is easy, cells can be actually pulled and recombined with collagen fibers. Interestingly, collagen can easily be combined with other organisms or synthetic materials to improve its mechanical properties or to change the ways of cell behaviors.

9.4.5 Alginate

Alginate is a linear natural anionic hetero-polysaccharide that is extracted from natural brown algae, seaweed, the bacterial genera *Pseudomonas* and *Azotobacter*, and marine algae, which is composed of β -(1–4) linked D-mannuronic acid and α -L-guluronic acid units and has useful properties for the chemical, food, medical, and agricultural industries. Degradation of alginate with alginate lyase is the key process for the production of unsaturated oligo-alginate and monosaccharide 4-deoxy-1-erythro-5-hexoseulose uronic acid [102]. Alginate lyases belonging to the polysaccharide lyase family have been found and isolated in organisms thriving in various environments.

The most common usage of alginate in biomedicine is for a cell-compatible hydrogel. Alginate may form as the strong hydrogels in the presence of divalent cations (such as Ca^{2+}) that interact with the carboxylic groups present in the alginate backbone to form ionic cross-links [103]. Similar to chitosan, alginate is easily processed in water and indicated as fairly nontoxic and non-inflammatory.

In some countries, alginate has been approved for use in wound dressing and food. It is biodegradable, has a controlled porosity, and can be attached to other bioactive molecules. Alginate is

not a preferred biological material because it lacks cell binding motif and exhibits poor cell adherence [103]. To overcome these limitations, mixing with other materials including the natural polymers such as agarose and chitosan can enhance the strength and cell behavior of alginate.

9.4.6 Polymeric Micelles

Polyesters are synthetic polymers with repeating ester linkages in the main polymer chain. A number of types of polyesters have been developed for biomedical applications in tissue engineering and drug delivery systems, such as poly(lactic acid) (PLA), poly(glycolic acid) (PGA), and poly(ϵ -caprolactone) (PCL), etc. Therapeutic effects for cancer drugs are complicated, but traditional drug delivery strategies still need improvement. Recently, polymeric micelles are having attention because their structural and functional aspects are similar to those of biological transport systems [104–106]. Micelles are self-assembled from aqueous amphiphilic block copolymers, which contain a hydrophobic core and a hydrophilic shell. Hydrophobic nuclei are typically spherical in nanoscales (10–100 nm) and can be used as nano-containers for the effective loading of hydrophobic drugs or agents [104, 105, 107]. Polyester micelles can be loaded with more than one type of bioactive compounds in a hydrophobic core; they are usually shielded with poly(ethylene glycol) (PEG) to amplify the effects of biocompatibility, stability, and stealth. Advantages of polyester micelles are longer half-life of the biologically active compound during circulation, lower adverse toxicity, and, most importantly, elevated amount of drug delivered specifically for the disease site (a.k.a. increasing the targeting ability).

Delivery systems are the main applications of polyester in drugs [108]. It has been reported that due to impaired lymphatic drainage of the tumor, polyester micelles may use such distinguishing characteristic to be accumulated in the tumor [108], and this procedure is generally considered as “passive targeting” [109]. Some polyester micelles have been modified to specifically inter-

act with highly expressed cancer cell surface receptors to enhance the targeting ability [109].

In addition, polyester micelles are also designed to have stimuli-responsive functions, such as pH and enzyme response, to control the release of cargo in tumors and to improve the specificity of drug delivery [110]. With advances in nanobiotechnology and molecular imaging technology, some probes and contrast agents are modified to the polyester micelles for tumor diagnosis, image-guided therapy, and therapeutic diagnosis [111]. However, since no functional groups can directly interact with the growth factors, nor can the growth factor can be easily attached to the surface of synthetic polymers, it has been proposed to modify the PLGA surface by a multilayer polyelectrolyte system formed by HA and CS [112]. The biochemical properties of natural materials provide a means to interact with growth factors and cytokines and propose more use of natural materials in various drug delivery systems.

9.5 Conclusions

Cell and tissue engineering includes the functional studies of cell mechanics and cell signaling; mechanical transduction; biosystems engineering and computational biology; nanotechnology, microfluidics, bioMEMS, and gene chips; functional tissue engineering and biomaterials; tissue structure functions; and cell-matrix interactions. Biomaterials interfaced with biological systems are used to deliver drugs safely and efficiently; to prevent, detect, and treat diseases; to help the body heal; and to design the functional tissues outside of the body to replace organs. Biomedical materials, in addition to being a filling material, have become important topics in regenerative medicine in recent years. The transition has been from permissive to promotion of biomaterials that are no longer bioinert but bioactive.

Tissue engineering has become a key therapeutic tool for the treatment of damaged or diseased organs. Despite this, there is still a need to overcome major challenges, particularly to construct tissues with high cell densities and to prevent post-

transplant inflammation. Understanding the interactions between cells and materials is important for developing new materials for biological applications. Recognizing micro-environmental cues which affect cell phenotype and function will help the general understanding of cell interaction and provide a direct method of engineering artificial tissue for medical applications.

Biomaterials play an important role in regenerative medicine, tissue engineering, and drug delivery. Polymer-based biomaterials have been developed from natural and synthetic sources. Polysaccharides and proteins are recognized as natural polymeric biomaterials that have found many applications in tissue regeneration. CS is one of the best polysaccharides with excellent biocompatibility and biodegradability. It consists of multifunctional groups, making it a potential candidate for future biomaterial development for cell function and differentiation into tissue engineering. Poly-disaccharide-based biomaterials, such as HA, have been obtained from animal sources and explored in tissue regeneration. Although proteins are highly biocompatible, SF may degrade rapidly and have low mechanical strength, resulting in a lack of structural support during tissue development. Polymeric biomaterials are also formed by homo-polymerization or copolymer reaction polymerization of one or more monomers to form non-biodegradable [113, 114] and biodegradable materials [115]. Structure, molecular chain length, and stereochemistry can be tailored by changing chemical and physical parameters during synthesis. There is a need to continually work in this area to design more potential biomaterials in the future.

The most common problem in the implantation of biomedical materials is that the body cannot successfully repair itself. This condition causes a foreign matter reaction over a long period of time and drives the formation of a capsule coating. Several studies have indicated that the surface of biomedical materials has been modified mainly by polymer coating and biologically derived materials which may reduce the initiation of cellular immune responses *in vitro* and promote tissue regeneration.

A modification method utilizing bio-sourced materials can enhance cell differentiation and proliferation in cell experiments. In past experiments, it has been confirmed that modification of the surface by bio-derived material can easily induce cell activation of *multiple signaling pathways* to cause cell differentiation and proliferation.

Due to the difference in external biomaterials, it may affect the signal transmission mediated by cell surface integrin and cause different results of cell growth, DNA synthesis, and cell migration and differentiation. In this way, by changing the surface of the biomedical material attached to the cell and then changing the signal transmission by the integrin in the cell to affect the cell behavior, it will be a good application and operation of the cell for biomedical materials and biomedical engineering.

Acknowledgments The authors thank S. Sheldon (Medical Technologist, American Society of Clinical Pathology, retired, MT, ASCP) of Oklahoma University Medical Center Edmond for fruitful discussions and editorial assistance. This work was supported by Research Grants NHRI-108A1-MRCO-0419192 from the National Health Research Institutes; MOST-107-2320-B-037-003, MOST-104-2221-E-10-004-MY3, and MOST-107-2221-E-010-005-MY3 from the Ministry of Science and Technology (MOST); AS-KPQ-105-TPP from Taiwan Protein Project; NSYSUKMU106-P011 from NSYSU-KMU Research Project; and KMU-TC108A04 from Kaohsiung Medical University Research Center Grant and the Research Center for Environmental Medicine, Kaohsiung Medical University, Kaohsiung, Taiwan, from The Featured Areas Research Center Program within the framework of the Higher Education Sprout Project by the Ministry of Education (MOE) in Taiwan.

References

- Black J (1982) The education of the biomaterialist: report of a survey. *J Biomed Mater Res* 16(2):159–167
- Buddy D, Ratner (2004) *Biomaterials science: an introduction to materials in medicine*. Saint Louis, Elsevier
- Bronzino JD (1999) *Biomedical engineering handbook*, 2nd edn. CRC Press, Boca Raton
- Helmus MN, Gibbons DF, Cebon D (2008) Biocompatibility: meeting a key functional requirement of next-generation medical devices. *Toxicol Pathol* 36(1):70–80
- Al N, Moravec RA, Riss TL (2008) Update on in vitro cytotoxicity assays for drug development. *Expert Opin Drug Discovery* 3(6):655–669
- Horvath S (1980) Cytotoxicity of drugs and diverse chemical agents to cell cultures. *Toxicology* 16(1):59–66
- Bondesson I, Ekwall B, Hellberg S et al (1989) MEIC-A new international multicenter project to evaluate the relevance to human toxicity of in vitro cytotoxicity tests. *Cell Biol Toxicol* 5(3):331–347
- Andorko JJ, Jewell CM (2017) Designing biomaterials with immunomodulatory properties for tissue engineering and regenerative medicine. *Bioeng Translat Med* 2(2):139–155
- Calabrese EJ (2005) Hormetic dose-response relationships in immunology: occurrence, quantitative features of the dose response, mechanistic foundations, and clinical implications. *Crit Rev Toxicol* 35(2–3):89–295
- Fage SW, Muris J, Jakobsen S et al (2016) Titanium: a review on exposure, release, penetration, allergy, epidemiology, and clinical reactivity. *Contact Dermatitis* 74(6):323–345
- Blac J (1984) Systemic effects of biomaterials. *Biomaterials* 5(1):11–18
- Bolognesi C, Castoldi AF, Crebelli R et al (2017) Genotoxicity testing approaches for the safety assessment of substances used in food contact materials prior to their authorization in the European Union. *Environ Mol Mutagen* 58(5):361–374
- Watson AY, Bates RR, Kennedy D (eds) (1998) *Air pollution, the automobile, and public health*. National Academies Press, Washington
- Soni S, Gupta H, Kumar N et al (2010) Biodegradable biomaterials. *Recent Pat Biomed Eng* 3(1):30–40
- Amadeh A, Ebadpour R (2013) Effect of cobalt content on wear and corrosion behaviors of electrodeposited Ni-Co/WC nano-composite coatings. *J Nanosci Nanotechnol* 13(2):1360–1363
- Kamachi Mudali U, Sridhar TM, Raj B (2003) Corrosion of bio implants. *Sadhana* 28:601–637
- Yang MH, Chen KC, Chiang PW et al (2016) Proteomic profiling of neuroblastoma cells adhesion on hyaluronic acid-based surface for neural tissue engineering. *Biomed Res Int* 2016:1–13
- Sugahara K, Schwartz NB, Dorfman A (1979) Biosynthesis of hyaluronic acid by streptococcus. *J Biol Chem* 254(14):6252–6261
- Takechi K, Kinoshita M, Yasueda S (2003) Hyaluronic acid: separation and biological implications. *J Chromatogr B* 797(1–2):347–355
- Vigetti D, Karousou E, Viola M et al (2014) Hyaluronan: biosynthesis and signaling. *Biochim Biophys Acta* 1840(8):2452–2459
- Kogan G, Soltes L, Stern R, Gemeiner P (2007) Hyaluronic acid: a natural biopolymer with a broad range of biomedical and industrial applications. *Biotechnol Lett* 29(1):17–25
- Toole BP, Zoltan-Jones A, Misra S et al (2005) Hyaluronan: a critical component of epithelial-mes-

- enchymal and epithelial-carcinoma transitions. *Cells Tissues Organs* 179(1–2):66–72
23. Itano N, Sawai T, Atsumi F et al (2004) Selective expression and functional characteristics of three mammalian hyaluronan synthases in oncogenic malignant transformation. *J Biol Chem* 279(18):18679–18687
 24. Sironen RK, Tammi M, Tammi R et al (2011) Hyaluronan in human malignancies. *Exp Cell Res* 317(4):383–391
 25. Bharadwaj AG, Kovar JL, Loughman E et al (2009) Spontaneous metastasis of prostate cancer is promoted by excess hyaluronan synthesis and processing. *Am J Pathol* 174(3):1027–1036
 26. Jiang D, Liang J, Noble PW (2007) Hyaluronan in tissue injury and repair. *Annu Rev Cell Dev Biol* 23:435–461
 27. Liang J, Jiang D, Noble PW (2016) Hyaluronan as a therapeutic target in human diseases. *Adv Drug Deliv Rev* 97:186–203
 28. Sherman LS, Matsumoto S, Su W et al (2015) Hyaluronan synthesis, catabolism, and signaling in neurodegenerative diseases. *Int J Cell Biol* 2015:368584
 29. Toole BP (2004) Hyaluronan: from extracellular glue to pericellular cue. *Nat Rev Cancer* 4(7):528
 30. Girish KS, Kemparaju K (2007) The magic glue hyaluronan and its eraser hyaluronidase: a biological overview. *Life Sci* 80(21):1921–1943
 31. James R, Kesturu G, Balian G et al (2008) Tendon: biology, biomechanics, repair, growth factors, and evolving treatment options. *J Hand Surg [Am]* 33(1):102–112
 32. Prestwich GD (2011) Hyaluronic acid-based clinical biomaterials derived for cell and molecule delivery in regenerative medicine. *J Control Release* 155(2):193–199
 33. Allison DD, Grande-Allen KJ (2006) Hyaluronan: a powerful tissue engineering tool. *Tissue Eng* 12(8):2131–2140
 34. Morra M (2005) Engineering of biomaterials surfaces by hyaluronan. *Biomacromolecules* 6(3):1205–1223
 35. Müller S, Koenig G, Charpiot A et al (2008) VEGF-functionalized polyelectrolyte multilayers as pro-angiogenic prosthetic coatings. *Adv Funct Mater* 18(12):1767–1775
 36. Tabata Y (2003) Tissue regeneration based on growth factor release. *Tissue Eng* 9(4, Suppl 1):5–15
 37. Preston M, Sherman LS (2012) Neural stem cell niches: roles for the hyaluronan-based extracellular matrix. *Front Biosci (Schol Ed)* 3:1165–1179
 38. Margolis RU, Margolis RK, Chang LB et al (1975) Glycosaminoglycans of brain during development. *Biochemistry* 14(1):85–88
 39. Jiang D, Liang J, Noble PW (2007) Hyaluronan in tissue injury and repair. *Annu Rev Cell Dev Biol* 23:435–461
 40. Liang J, Jiang D, Noble PW (2016) Hyaluronan as a therapeutic target in human diseases. *Adv Drug Deliv Rev* 97:186–203
 41. Sherman LS, Matsumoto S, Su W et al (2015) Hyaluronan synthesis, catabolism, and signaling in neurodegenerative diseases. *Int J Cell Biol* 2015:368584
 42. Solis MA, Chen YH, Wong TY et al (2012) Hyaluronan regulates cell behavior: a potential niche matrix for stem cells. *Biochem Res Int* 2012:346972
 43. Liao YH, Jones SA, Forbes B et al (2005) Hyaluronan: pharmaceutical characterization and drug delivery. *Drug Deliv* 12(6):327–342
 44. Yadav AK, Mishra P, Agrawal GP (2008) An insight on hyaluronic acid in drug targeting and drug delivery. *J Drug Target* 16(2):91–107
 45. Oh EJ, Park K, Kim KS et al (2010) Target specific and long-acting delivery of protein, peptide, and nucleotide therapeutics using hyaluronic acid derivatives. *J Control Release* 141(1):2–12
 46. Luo Y, Ziebell MR, Prestwich GD (2000) A hyaluronic acid-taxol antitumor bioconjugate targeted to cancer cells. *Biomacromolecules* 1(2):208–218
 47. Arulmoli J, Wright HJ, Phan DT et al (2016) Combination scaffolds of salmon fibrin, hyaluronic acid, and laminin for human neural stem cell and vascular tissue engineering. *Acta Biomater* 43:122–138
 48. Moshayedi P, Carmichael ST (2013) Hyaluronan, neural stem cells and tissue reconstruction after acute ischemic stroke. *Biomater* 3(1):e23863
 49. Alves NM, Mano JF (2008) Chitosan derivatives obtained by chemical modifications for biomedical and environmental applications. *Int J Biol Macromol* 43(5):401–414
 50. Anitha A, Maya S, Deepa N et al (2011) Efficient water soluble O-carboxymethyl chitosan nanocarrier for the delivery of curcumin to cancer cells. *Carbohydr Polym* 83(2):452–461
 51. Yao K, Li J, Yao F, Yin Y (eds) (2011) Chitosan-based hydrogels: functions and applications. CRC Press, London
 52. Kashyap PL, Xiang X, Heiden P (2015) Chitosan nanoparticle based delivery systems for sustainable agriculture. *Int J Biol Macromol* 77:36–51
 53. Younes I, Rinaudo M (2015) Chitin and chitosan preparation from marine sources. Structure, properties and applications. *Mar Drugs* 13(3):1133–1174
 54. Muzzarelli RAA (2009) Chitins and chitosans for the repair of wounded skin, nerve, cartilage and bone. *Carbohydr Polym* 76(2):167–182
 55. Pan H, Fu C, Huang L et al (2018) Anti-obesity effect of chitosan oligosaccharide capsules (COSCs) in obese rats by ameliorating leptin resistance and adipogenesis. *Mar Drugs* 16(6):198
 56. Auwal SM, Zarei M, Tan CP et al (2017) Improved in vivo efficacy of anti-hypertensive biopeptides encapsulated in chitosan nanoparticles fabricated by ionotropic gelation on spontaneously hypertensive rats. *Nano* 7(12):421
 57. Shahzad S, Yar M, Siddiqi SA et al (2015) Chitosan-based electrospun nanofibrous mats, hydrogels and cast films: novel anti-bacterial wound dressing matrices. *J Mater Sci Mater Med* 26(3):136

58. Ravi H, Kurrey N, Manabe Y et al (2018) Polymeric chitosan-glycolipid nanocarriers for an effective delivery of marine carotenoid fucoxanthin for induction of apoptosis in human colon cancer cells (Caco-2 cells). *Mater Sci Eng C Mater Biol Appl* 91:785–795
59. Paramasivan S, Jones D, Baker L et al (2014) The use of chitosan-dextran gel shows anti-inflammatory, antibiofilm, and antiproliferative properties in fibroblast cell culture. *Am J Rhinol Allergy* 28(5):361–365
60. Guo M, Ma Y, Wang C et al (2015) Synthesis, antioxidant activity, and biodegradability of a novel recombinant polysaccharide derived from chitosan and lactose. *Carbohydr Polym* 118:218–223
61. Krishna Rao KSV, Vijaya Kumar Naidu B, Subha MCS et al (2006) Novel chitosan-based pH-sensitive interpenetrating network microgels for the controlled release of cefadroxil. *Carbohydr Polym* 66(3):333–344
62. Kandra P, Challa MM, Jyothi HK (2012) Efficient use of shrimp waste: present and future trends. *Appl Microbiol Biotechnol* 93(1):17–29
63. Muzzarelli RAA (2011) Chitosan composites with inorganics, morphogenetic proteins and stem cells, for bone regeneration. *Carbohydr Polym* 83(4):1433–1445
64. Zhang J, Xia W, Liu P et al (2010) Chitosan modification and pharmaceutical/biomedical applications. *Mar Drugs* 8(7):1962–1987
65. Cumpstey I (2013) Chemical modification of polysaccharides. *ISRN Org Chem* 2013:417672
66. Pillay V, Seedat A, Choonara YE et al (2013) A review of polymeric refabrication techniques to modify polymer properties for biomedical and drug delivery applications. *AAPS Pharm Sci Tech* 14(2):692–711
67. Jayakumar R, Prabakaran M, Reis RL et al (2005) Graft copolymerized chitosan—present status and applications. *Carbohydr Polym* 62(2):142–158
68. Chung TW, Wang SS, Wang YZ et al (2009) Enhancing growth and proliferation of human gingival fibroblasts on chitosan grafted poly(*ε*-caprolactone) films is influenced by nano-roughness chitosan surfaces. *J Mater Sci Mater Med* 20(1):397–404
69. Chung TW, Yang MC, Tseng CC et al (2011) Promoting regeneration of peripheral nerves in vivo using new PCL-NGF/Tirofiban nerve conduits. *Biomaterials* 32(3):734–743
70. Adeli M, Kalantari M, Parsamanesh M et al (2011) Synthesis of new hybrid nanomaterials: promising systems for cancer therapy. *Nanomedicine* 7(6):806–817
71. Chandra S, Barick KC, Bahadur D (2011) Oxide and hybrid nanostructures for therapeutic applications. *Adv Drug Deliv Rev* 63(14–15):1267–1281
72. Barar J, Omid Y (2014) Surface modified multi-functional nanomedicines for simultaneous imaging and therapy of cancer. *Bioimpacts* 4(1):3
73. Liu Z, Jiao Y, Wang Y et al (2008) Polysaccharides-based nanoparticles as drug delivery systems. *Adv Drug Deliv Rev* 60(15):1650–1662
74. Prabakaran M (2015) Chitosan-based nanoparticles for tumor-targeted drug delivery. *Int J Biol Macromol* 72:1313–1322
75. Saravanakumar G, Jo DG, Park JH (2012) Polysaccharide-based nanoparticles: a versatile platform for drug delivery and biomedical imaging. *Curr Med Chem* 19(19):3212–3229
76. Calvo P, Remunan-Lopez C, Vila-Jato JL et al (1997) Chitosan and chitosan/ethylene oxide-propylene oxide block copolymer nanoparticles as novel carriers for proteins and vaccines. *Pharm Res* 14(10):1431–1436
77. Rao W, Wang H, Han J et al (2015) Chitosan-decorated doxorubicin-encapsulated nanoparticle targets and eliminates tumor reinitiating cancer stem-like cells. *ACS Nano* 9(6):5725–5740
78. Kaplan DL, Adams WW, Farmer B et al (1994) In: Kaplan DL, Adams WW, Farmer B, Viney C (eds) *Silk polymers materials science and biotechnology*. American Chemical Society, Washington DC
79. Santin M, Motta A, Freddi G et al (1999) In vitro evaluation of the inflammatory potential of the silk fibroin. *J Biomed Mater Res* 46(3):382–389
80. Ha SW, Tonelli AE, Hudson SM (2005) Structural studies of bombyx mori silk fibroin during regeneration from solutions and wet fiber spinning. *Biomacromolecules* 6(3):1722–1731
81. Yang MH, Chung TW, Lu YS, et al (2015) Activation of the ubiquitin proteasome pathway by silk fibroin modified chitosan nanoparticles in hepatic cancer cells. *Int J Mol Sci*. 16(1):1657–76
82. Um IC, Kweon HY, Park YH et al (2001) Structural characteristics and properties of the regenerated silk fibroin prepared from formic acid. *Int J Biol Macromol* 29(2):91–97
83. Zhang X, Reagan MR, Kaplan DL (2009) Electrospun silk biomaterial scaffolds for regenerative medicine. *Adv Drug Deliv Rev* 61(12):988–1006
84. Guziewicz N, Best A, Perez-Ramirez B et al (2011) Lyophilized silk fibroin hydrogels for the sustained local delivery of therapeutic monoclonal antibodies. *Biomaterials* 32(10):2642–2650
85. Soffer L, Wang X, Zhang X et al (2008) Silk-based electrospun tubular scaffolds for tissue-engineered vascular grafts. *J Biomater Sci Polym Ed* 19(5):653–664
86. Yang Y, Chen X, Ding F et al (2007) Biocompatibility evaluation of silk fibroin with peripheral nerve tissues and cells in vitro. *Biomaterials* 28(9):1643–1652
87. Li C, Vepari C, Jin HJ, Kim HJ et al (2006) Electrospun silk-BMP-2 scaffolds for bone tissue engineering. *Biomaterials* 27(16):3115–3124
88. Falini G, Weiner S, Addadi L (2003) Chitin-silk fibroin interactions: relevance to calcium carbonate formation in invertebrates. *Calcif Tissue Int* 72(5):548–554

89. Altman GH, Diaz F, Jakuba C et al (2003) Silk-based biomaterials. *Biomaterials* 24(3):401–416
90. Yeo JH, Lee KG, Lee YW et al (2003) Simple preparation and characteristics of silk fibroin microsphere. *Eur Polym J* 39(6):1195–1199
91. Aramwit P, Kanokpanont S, De-Eknamkul W et al (2009) Monitoring of inflammatory mediators induced by silk sericin. *J Biosci Bioeng* 107(5):556–561
92. Yang MH, Yuan SS, Chung TW et al (2014) Characterization of silk fibroin modified surface: a proteomic view of cellular response proteins induced by biomaterials. *Biomed Res Int* 2014:209469
93. Nathwani BB, Jaffari M, Juriani AR et al (2009) Fabrication and characterization of silk-fibroin-coated quantum dots. *IEEE Trans Nanobioscience* 8(1):72–77
94. Chang SQ, Dai YD, Kang B et al (2009) Gamma-radiation synthesis of silk fibroin coated CdSe quantum dots and their biocompatibility and photostability in living cells. *J Nanosci Nanotechnol* 9(10):5693–5700
95. Ito Y, Kajihara M, Imanishi Y (1991) Materials for enhancing cell adhesion by immobilization of cell-adhesive peptide. *J Biomed Mater Res* 25(11):1325–1337
96. Torikai A, Shibata H (1999) Effect of ultraviolet radiation on photo-degradation of collagen. *J Appl Polym Sci* 73:1259–1265
97. Bellincampi LD, Dunn MG (1997) Effect of cross-linking method on collagen fiber-fibroblast interactions. *J Appl Polym Sci* 63:1493–1498
98. Sionkowska A (1999) Photochemical transformations in collagen in the presence of melanin. *J Photochem Photobiol A Chem* 124:91–94
99. Sionkowska A, Kaminska A (1999) Thermal helix-coil transition in UV irradiated collagen from rat tail tendon. *Int J Biol Macromol* 24:337–340
100. Barbani N, Giusti P, Lazzeri L et al (1995) Bioartificial materials based on collagen :1. Collagen cross-linking with gaseous glutaraldehyde. *J Biomater Sci Polym Ed* 7(6):461–469
101. Friess W, Lee G (1996) Basic thermo-analytical studies of insoluble collagen matrices. *Biomaterials* 17(23):2289–2294
102. Larsen B, Salem DM, Sallam MA et al (2003) Characterization of the alginates from algae harvested at the Egyptian Red Sea coast. *Carbohydr Res* 338(22):2325–2336
103. Lee KY, Mooney DJ (2012) Alginate: properties and biomedical applications. *Prog Polym Sci* 37(1):106–126
104. Torchilin VP (2001) Structure and design of polymeric surfactant-based drug delivery systems. *J Control Release* 73(2–3):137–172
105. Torchilin VP (2002) PEG-based micelles as carriers of contrast agents for different imaging modalities. *Adv Drug Deliv Rev* 54(2):235–252
106. Park YJ, Lee JY, Chang YS et al (2002) Radioisotope carrying polyethylene oxide-polycaprolactone copolymer micelles for targetable bone imaging. *Biomaterials* 23(3):873–879
107. Lavasanifar A, Samuel J, Kwon GS (2002) Poly(ethylene oxide)-block-poly(L-amino acid) micelles for drug delivery. *Adv Drug Deliv Rev* 54(2):169–190
108. Matsumura Y, Maeda H (1986) A new concept for macromolecular therapeutics in cancer chemotherapy: mechanism of tumorotropic accumulation of proteins and the antitumor agent smancs. *Cancer Res* 46(12):6387–6392
109. Cheng CJ, Tietjen GT, Saucier-Sawyer JK et al (2015) A holistic approach to targeting disease with polymeric nanoparticles. *Nat Rev Drug Discov* 14(4):239–247
110. Grossen P, Witzigmann D, Sieber S et al (2017) PEG-PCL-based nanomedicines: a biodegradable drug delivery system and its application. *J Control Release* 260:46–60
111. Nottelet B, Darcos V, Coudane J (2015) Aliphatic polyesters for medical imaging and theranostic applications. *Eur J Pharm Biopharm* 97(Pt B):350–370
112. Go DP, Gras SL, Mitra D et al (2011) Multilayered microspheres for the controlled release of growth factors in tissue engineering. *Biomacromolecules* 12(5):1494–1503
113. Tare RS, Khan F, Tourniaire G et al (2009) A microarray approach to the identification of polyurethanes for the isolation of human skeletal progenitor cells and augmentation of skeletal cell growth. *Biomaterials* 30(6):1045–1055
114. Medine CN, Lucendo-Villarin B, Storck C et al (2013) Developing high-fidelity hepatotoxicity models from pluripotent stem cells. *Stem Cells Transl Med* 2(7):505–509
115. Khan F, Valere S, Fuhrmann S et al (2013) Synthesis and cellular compatibility of multi-block biodegradable poly(ϵ -caprolactone)-based polyurethanes. *J Mater Chem B* 1(20):2590–2600



Regulation of Stem Cell Functions by Micro-Patterned Structures

10

Guoping Chen and Naoki Kawazoe

Abstract

Micro-patterned surfaces have been broadly used to control the morphology of stem cells for investigation of the influence of physio-chemical and biological cues on stem cell functions. Different structures of micro-patterned surfaces can be prepared by photolithography through designing the photomask features. Cell spreading area, geometry, aspect ratio, and alignment can be regulated by the micro-patterned structures. Their influences on adipogenic, osteogenic, and smooth muscle differentiation of the human bone marrow-derived mesenchymal stem cells are compared and investigated in details. Variation of cell morphology can trigger rearrangement of cytoskeleton, generating cytoskeletal mechanical stimulation and consequently inducing differentiation of mesenchymal stem cells into different lineages. This chapter summarizes the latest development of regulation of mesenchymal stem cell morphology by micro-patterns and the influence on the behaviors and differentiation of the mesenchymal stem cells.

Keywords

Micro-patterned surface · Mesenchymal stem cell · Cell morphology · Cell function · Differentiation

10.1 Introduction

Manipulation of stem cell functions is important for tissue engineering and regenerative medicine. Various types of stem cells, such as, embryonic stem cells, induced pluripotent stem cells, and mesenchymal stem cells, have been established and isolated for tissue engineering and regenerative medicine. In particular, mesenchymal stem cells (MSCs) have attracted plenty of interest due to their easy availability and high potential for regeneration of bone, cartilage, and many other tissues [1]. They can be harvested in many tissues, such as, bone marrow, adipose tissue, and dental pulp, and are capable to differentiate into osteoblasts, adipocytes, chondrocytes, myoblasts, and tenocytes [2]. They have been even reported to differentiate into cell types other than mesenchymal tissues [3]. Controlling of the differentiation of stem cells to an expected lineage is pivotal for the regeneration of functional tissues or organs. The cells exist in their respective in vivo microenvironments that are important for the maintenance of cell functions and metabolism. The microenvironments include biological

G. Chen (✉) · N. Kawazoe
Research Center for Functional Materials, National
Institute for Materials Science,
Tsukuba, Ibaraki, Japan
e-mail: Guoping.CHEN@nims.go.jp

and physicochemical cues to dictate cell migration, adhesion, proliferation, differentiation, and secretion of extracellular matrix secretion. Biological cues, such as, cell–cell interaction and cell–ECM interaction, and physicochemical cues, such as, chemical moiety, electrostatic properties, size, shape, stiffness, roughness, and topography, have been widely studied to elucidate their influence on cell behaviors, especially on the differentiation of stem cells [4, 5].

In the recent years, the importance of cell morphology in the regulation of MSC functions and behavior has been revealed through various micro structured micro-structured and nano-structured substrates [6, 7]. By seeding the cells on micro-structured and nano-structured surfaces, the morphology of the cells is easily regulated and the influence of cell morphology on the MSC functions and behavior is evaluated [8]. A number of micro- and nano-patterning methods have been developed to control the surface structures of the cell culture biomaterials and scaffolds to explore the influence of the cell microenvironments on cell migration, proliferation, polarization, and differentiation [5, 9–12]. The micro- and nano- patterned surface can not only regulate cell morphology but also separate each of the parameters to allow analysis of the independent influence of individual parameter.

We have used a photolithographic method by using a photoreactive polymer polyvinyl alcohol (PVA) to prepare a few types of micro-patterns and nano–micro hybrid patterns to control physicochemical cues and cell–cell interaction during the cell culture. PVA is a cell adhesion-repellent polymer. The PVA-micro-patterned surfaces are stable and useful for long-term culture. The PVA-micro-patterned surfaces have been used for investigating the influence of cell spreading area (size), cell geometry, aspect ratio, surface charge, cell density, cell–cell interaction, and cell protrusion on the adipogenic, chondrogenic, osteogenic, and myogenic differentiation of the human bone marrow-derived MSCs [13–25]. The latest results are summarized and discussed in this chapter by focusing on the parameter of cell spreading area, geometry, aspect ratio, and align-

ment and their influences on adipogenic, osteogenic, and smooth muscle differentiation of the human bone marrow-derived MSCs.

10.2 Design and Preparation and of Micro-Patterned Surfaces

Ultraviolet photolithography is used for preparation of PVA-micro-patterned surfaces. The photoreactive PVA is firstly synthesized by introducing azidophenyl groups in the hydroxyl side groups of the PVA [13]. The photoreactive PVA is subsequently coated on cell-culture polystyrene plates that are cut from cell-culture flasks or dishes, which support cell adhesion. After drying off the coated photoreactive PVA layer in the dark, the surfaces are covered with a photomask and irradiated with UV light. UV light can pass through the transparent areas on the photomask, and the azidophenyl groups in the photoreactive PVA under the transparent areas are activated to generate azido radicals. The azido radicals react with the surrounding molecules to make the PVA molecules under the transparent areas to be intermolecularly and intramolecularly cross-linked and grafted on the polystyrene surfaces. The black areas on the photomask are nontransparent for the UV light and the photoreactive PVA molecules under the nontransparent areas remain unreactive, which can be removed by washing. Finally, the UV irradiated polystyrene plates are washed with water to remove the unreacted PVA, and the micro-patterned surfaces are generated.

The micro-patterns can be controlled by designing the photomasks. A few types of photomasks having size difference micro-pattern (Fig. 10.1a), shape difference micro-pattern (Fig. 10.1b), and aspect ratio micropattern (Fig. 10.1c) are used to prepare the micro-patterned surfaces [19]. The prepared micro-patterns have a feature of polystyrene microdots surrounded with the PVA. The polystyrene microdot regions can support cell adhesion similar to that of the cell-culture polystyrene plate. The surrounding PVA can inhibit protein adsorp-

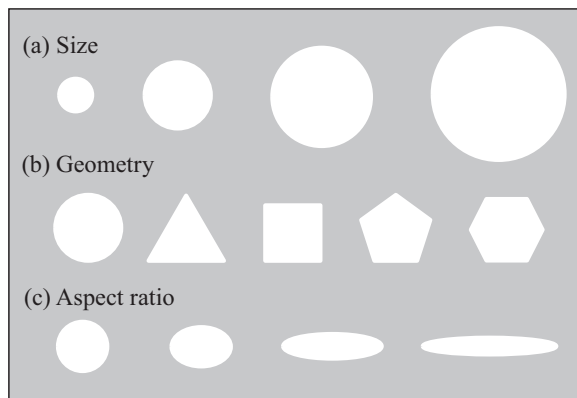


Fig. 10.1 Illustration of PVA-micro-patterned polystyrene surfaces. The micro-patterns have different sizes (a), geometries (b), and aspect ratios (c). The diameters of circle micro-patterns in (a) are 20, 40, 60, and 80 μm . The circle, triangle, square, pentagon, and hexagon

micro-patterns in (b) have the same surface area of $1134 \mu\text{m}^2$. The ellipse micro-patterns in (c) have the same surface area of $706 \mu\text{m}^2$ but different aspect ratios of 1.0, 1.5, 4.0, and 8.0.

tion and cell adhesion. To facilitate the cell adhesion on the polystyrene regions, the micro-patterned surfaces can be coated with cell adhesion proteins, such as, fibronectin, laminin, collagen, and vitronectin. The thickness of the PVA-grafted layer can be controlled by the amount of the coated photoreactive PVA. Usually, a thickness of 40–70 nm of the PVA is grafted, which is thick enough to inhibit protein adsorption and cell adhesion. When cells are cultured on the micro-patterned surfaces, they only adhere on the polystyrene regions forming micro-patterned cells according to the underlying micro-patterns.

Micro-nano hybrid patterns of nanogrooves and microstripes are designed and prepared to control cell alignment and elongation [23]. The hybrid patterns are prepared by introducing the PVA microstripes on the PS nanogrooves through UV lithography and nanoimprinting method (Fig. 10.2). The PVA microstripes are controlled to be parallelly or orthogonally oriented to the PS nanogrooves. At first, PS nanogrooved substrates are fabricated by a nanoimprinting method. A nano-textured polydimethylsiloxane (PDMS) mold having nanogrooves with a ridge depth of 400 nm, a ridge width of 800 nm, and a spacing distance of 800 nm is prepared after casting on a prefabricated silicon master and cured at 60 °C. One drop of a 3 (w/v) % PS toluene solution is dropped on polyethylene terephthalate

(PET) substrate ($1 \times 1 \text{ cm}^2$) and directly pressed by the nanostructured PDMS mold at constant pressure (10 kPa). PDMS mold is peeled off after air-drying for 12 hours to prepare the nanogrooved PS substrate (PS nanogrooves). The PS nanogrooves are treated with oxygen plasma to improve the cell adhesion property of the PS. Subsequently, the photoreactive PVA is coated on the PS nanogrooves and dried overnight at room temperature in the dark. A photomask containing microstripes with various equal width and spacing (50/50 μm , 100/100 μm , and 200/200 μm) is covered on the photoreactive PVA-coated PS nanogrooves during UV irradiation. The microstripes of photomask are parallel or orthogonally oriented along the PS nanogrooves to obtain the different micro-nano hybrid pattern surfaces. The PVA microstripes on the PS nanogrooves are obtained after washing with water. Finally, to promote cell adhesion during the cell culture experiments, the micro-nano hybrid pattern surfaces are coated with fibronectin.

Stripe micro-patterns with different stripe widths are prepared to control cell alignment [18]. The photoreactive PVA is coated on polystyrene plates ($5.5 \times 2.5 \text{ cm}$) and air-dried at room temperature in the dark. The plates are covered with a predesigned photomask and irradiated with UV light. After irradiation, the

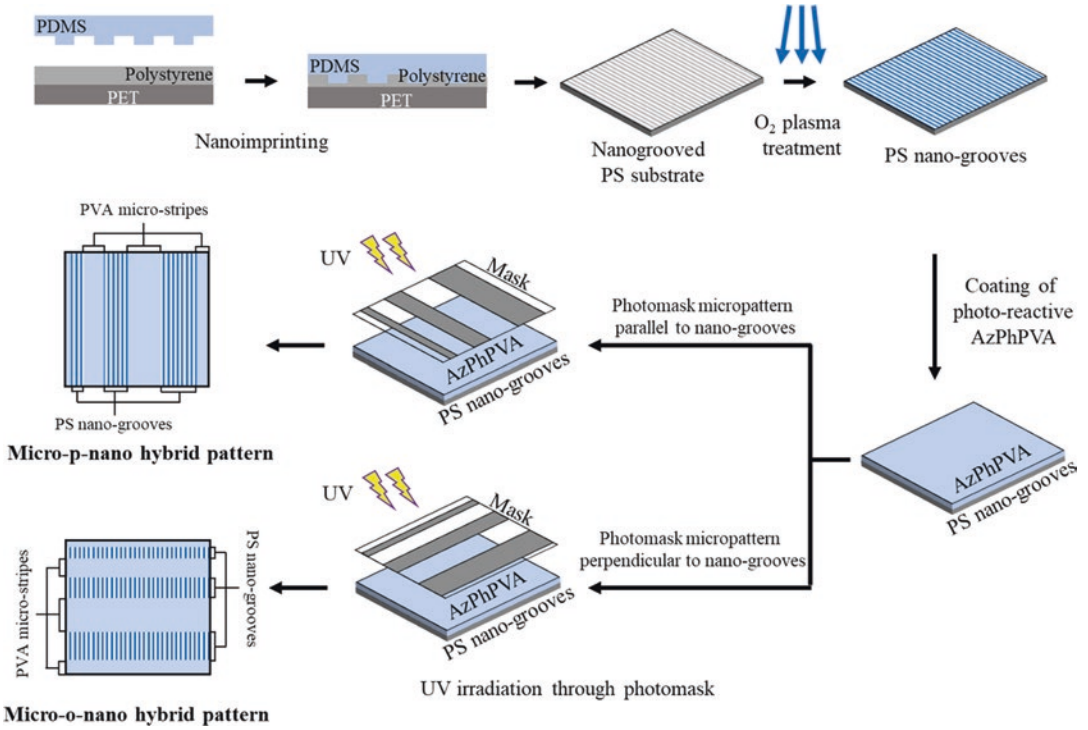


Fig. 10.2 Preparation scheme of micro–nano hybrid patterns through nanoimprinting and UV lithography. (Reproduced from Ref. [23] with permission),

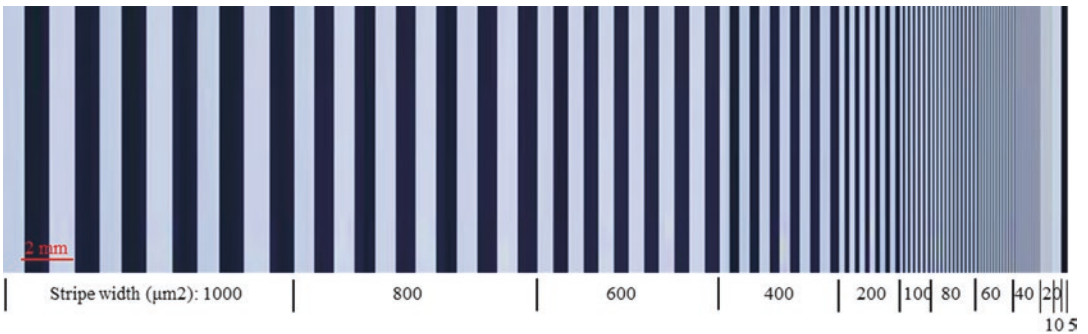


Fig. 10.3 Phase-contrast micrograph of stripe micro-pattern photomask. The designed width is 5, 10, 20, 40, 60, 80, 100, 200, 400, 600, 800, and 1000 μm, in order. (Reproduced from Ref. [18] with permission)

plates are washed with water. The photomask consists of UV-nontransparent dark stripe areas and UV-transparent light stripe areas with different widths of 5, 10, 20, 40, 60, 80, 100, 200, 400, 600, 800, and 1000 μm (Fig. 10.3).

10.3 Regulation of Single Stem Cell Morphology and Its Influence on Stemness of Stem Cells

The most attractive properties of stem cells are multi-potency and self-renewal. These properties make them versatile and promising cell source

for regenerative medicine and tissue engineering. In vivo, stem cells are generally quiescent under homeostasis but capable to undergo activation upon stimulation. The quiescent state contributes to stem cell maintenance. Stem cells may lose their pluripotency during in vitro expansion culture, which limits their application in clinical use. Stem cells change their morphology during in vitro cell expansion culture. Investigation of cell morphology variation on the stemness maintenance of stem cells is important to disclose details of the interaction between stem cells and biomaterials. The micro-patterns shown in Fig. 10.1 are used for culture of the MSCs to regulate their cell size (spreading area), geometry, and aspect ratio at single cell level. The influence of cell size, geometry, and aspect ratio on stemness maintenance of the MSCs is compared [19].

At first, the human bone marrow-derived MSCs are purified by using clonal culture to obtain homogeneous cell mass. The initial state of the purified MSCs is checked by immunofluorescence staining. The MSCs express the surface markers of CD73, CD105, CD44, CD106, and STRO-1, while do not express CD11b, CD19, CD34, and CD45 [26–28]. These surface markers are used for the MSCs characterization. And then, the purified homogeneous MSCs are used for culture on the micro-patterns in the low-glucose DMEM medium supplemented with 10% FBS. Before seeding on the micro-patterns, the MSCs are treated with serum-free low-glucose DMEM medium (starvation) for 24 hours to obtain the cells at G0/G1-enriched state. The starved MSCs are seeded and cultured on the micro-patterns. The MSCs attach onto the micro-patterned surfaces, and their morphologies are controlled by the underlying micro-patterns. Single MSC arrays with different spreading areas (size), geometries, and aspect ratios are formed.

The staining of F-actin filaments and nuclei shows that MSCs occupy the microdots of the micro-patterns and have different spreading areas, geometries, and aspect ratios (Fig. 10.4). The F-actin structure of single MSCs is influenced by the spreading area (Fig. 10.4a). The circular cells with large spreading area assemble their actin filaments in both radial and concentric

directions of the circle. With the decrease of the spreading area, the radial filaments gradually disappear and the concentric filaments only assemble at the cell periphery. The MSCs having different geometries show similar actin organization (Fig. 10.4b). These cells predominately assemble their actin filaments at the periphery of the cells, and the formed stress fibers stretch along the edges of the micro-patterns, while no ordered filament structure is found at the central region of cells. Aspect ratio also shows obvious influence on the F-actin structures. Unlike in the circular cells, actin filaments in the elongated cells are paralleled along the long axis of the cell and span over the nucleus (Fig. 10.4c). Not only the cytoskeleton, the nuclear geometry is also elongated dramatically with the increase of the aspect ratio and orient toward the direction of long cell axis.

After the MSCs are cultured on the micro-patterns for 2 weeks, the stemness of MSCs is analyzed by the expression of surface markers of CD44, CD73, CD105, CD106, and STRO-1. The expression of CD44, CD73, CD105, CD106, and STRO-1 gradually decreases with the increase of the spreading area [19]. The MSCs cultured on the micro-patterns having different geometries expressed in similar levels of CD44, CD73, CD105, CD106, and STRO-1. The expression of CD44, CD73, CD105, CD106, and STRO-1 slightly declines with the increase of the aspect ratio. Round cells exhibit significantly higher expression of CD44, CD73, CD105, and CD106 compared to the cells with the aspect ratio of eight or four. The results indicate that the size and aspect ratio of a single cell can affect the stemness of the MSCs, while shape shows no influence on stemness of the MSCs when cell spreading area and aspect ratio are the same. Small size and low aspect ratio are good for the maintenance of MSCs stemness.

Cell nuclear activity and cell mechanics are considered to be related with the stemness maintenance of the MSCs. The cell nuclear activity analysis experiment shows that the spreading area has a significant influence on the nuclear activity. With the increase of spreading area, more active nuclei are detected on the

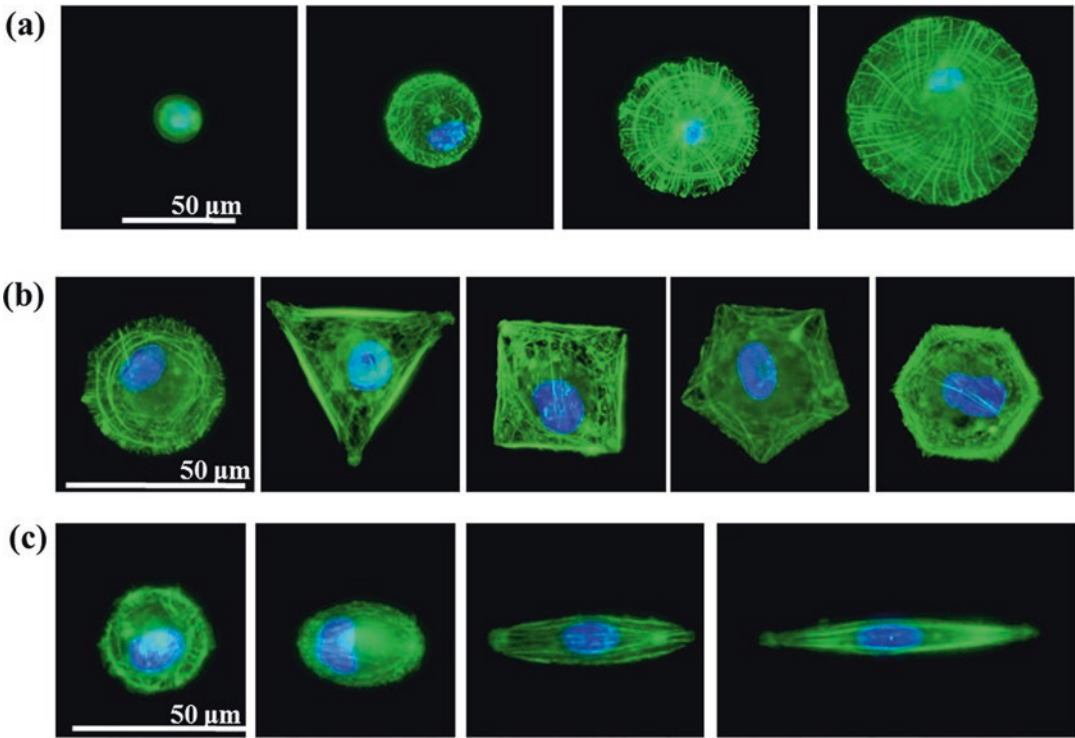


Fig. 10.4 F-actin staining of MSCs cultured on micro-patterns with various spreading areas (a), geometries (b), and aspect ratios (c). The diameters of circle micro-patterns in (a) are 20, 40, 60, and 80 μm . The circle, triangle, square, pentagon, and hexagon micro-patterns in

(b) have the same surface area of $1134 \mu\text{m}^2$. The ellipse micro-patterns in (c) have the same surface area of $706 \mu\text{m}^2$ but different aspect ratios of 1.0, 1.5, 4.0, and 8.0. (Reproduced from Ref. [19] with permission)

micro-patterns. However, the cells having different geometries but the same spreading area and aspect ratio do not show significant difference of nuclear activity. The elongation of the cells with the same spreading area resulted in gradual enhancement of nuclear activity. Cell mechanics measured by atomic force microscopy (AFM) nanoindentation indicates that Young's modulus of the MSCs increase with the increase of the spreading area and aspect ratio, while the MSCs having different geometries show similar Young's modulus [19].

These results indicate that the influence of spreading area, geometry, and aspect ratio of MSCs on their expression level of stem cell surface markers is accompanied with different nuclear activities, cytoskeletal structures, and nanomechanics. The micro-patterns should

directly affect cytoskeletal structures. The resulting cytoskeletal structure can determine cellular nanomechanics, nuclear activity, and stemness of MSCs. Large spreading area and high aspect ratio lead cells to a stressed state with active nuclear synthesis and, therefore, result in low expression of stem cell surface markers. When spreading area is limited, changes in cell geometries do not influence cell elasticity and nuclear activity. Ordered cytoskeletal structure results in high cell elasticity and nuclear activity and decreases the expression of surface markers indicating partial loss of multi-potency. The MSCs with disrupted cytoskeletal structure exhibit low nanomechanical properties and remain in a quiescent state which promotes stem cell phenotype.

10.4 Influence of Cell Size, Geometry, and Aspect Ratio on Adipogenic and Osteogenic Differentiation of MSCs

Cells encounter many topographical features of extracellular matrices from protein folding to collagen banding in vivo, so interactions exist between cells and nanoscale or microscale features. Traditionally, the expansion and differentiation of stem cells are mainly conducted in biological medium consisting of growth factors and cytokines. Except the influence of biological cues on stem cell functions, the influence of physical cues, such as, cell spreading area (cell size), geometry, and aspect ratio, needs to be considered because spreading area has been reported to affect cell behaviors and functions [29, 30]. During traditional cell culture, the process of cell spreading is often accompanied by a change in cell shape and aspect ratio. The area of cell spreading, cell shape, and aspect ratio are diverse among cells, and the heterogeneity within a cell population is complex. It has been difficult to discriminate the influence of cell spreading area, geometry, and aspect ratio on cell functions by traditional cell culture method. Therefore, changing of one of the three parameters (cell spreading area, geometry, and aspect ratio) of a large number of individual cells, while keeping another two parameters unchanged, is extremely important to investigate the independent influence of cell spreading area, geometry, and aspect ratio on cell functions.

Micro-patterns are useful to separate the cell spreading area, geometry, and aspect ratio. The cell spreading area, geometry, and aspect ratio can be well controlled by the PVA micro-patterns as shown in Fig. 10.3. To investigate the influence of cell spreading area on adipogenic and osteogenic differentiation of MSCs, PVA circle micro-patterns having a diameter of 40, 60, and 80 μm are used for culture of MSCs [14]. After 6 hours of culture, the MSCs adhere on the cell-adhesive circular polystyrene micro-patterns, and the MSCs on nonadhesive PVA regions are removed by a medium change. The MSCs are cultured on

the micro-patterns in adipogenic induction medium for 7 days. Lipid vacuoles are observed in some MSCs on the micro-patterns. The lipid vacuoles are stained with Oil Red O. The cells with positive Oil Red O staining are counted, and the probability of adipogenesis is calculated. The results show the probability of MSC adipogenesis being dependent on the degree of cell spreading area. The percentage of MSCs undergoing adipogenic differentiation is $45.3 \pm 3.4\%$, $26.3 \pm 3.4\%$, and $14.7 \pm 4.2\%$ for 40, 60, and 80 μm circles, respectively and $12.4 \pm 2.0\%$ for the bare polystyrene surface (non-patterned). The probability of adipogenic differentiation of MSCs decreases as the degree of cell spreading increases.

Osteogenic differentiation of MSCs on the micro-patterns is evaluated by culturing MSCs on the micro-patterns in the osteogenic induction medium for 7 and 21 days [14]. Osteogenic differentiation is evaluated by ALP staining. The percentage of MSCs undergoing osteogenic differentiation is $13.0 \pm 2.2\%$, $28.3 \pm 3.0\%$, and $41.2 \pm 1.9\%$ on micro-patterns with 40, 60, and 80 μm circles, respectively and $54.6 \pm 4.2\%$ on the bare polystyrene surface (non-patterned) after 7 days of osteogenic induction culture. The probability of osteogenic differentiation of MSCs increases as the degree of cell spreading is enhanced. After the osteogenic induction culture for 21 days, the percentage of MSCs undergoing osteogenic differentiation are $17.5 \pm 3.5\%$, $40.2 \pm 3.8\%$, and $53.9 \pm 5.4\%$ on the micro-patterns with 40, 60, and 80 μm circles, respectively and $86.0 \pm 3.0\%$ on the bare polystyrene surface (non-patterned). Although the trend of the probability of osteogenic differentiation at 21 days is similar to that at 7 days, more MSCs undergo osteogenic differentiation after long-term culture. These results indicate that cell spreading facilitates osteogenic differentiation of MSCs.

To investigate the influence of cell geometry on adipogenic differentiation of MSCs, PVA micro-patterns of regular triangle, pentagon, hexagon, square, and circle having the same surface area of $1134 \mu\text{m}^2$ are used for the culture of MSCs [13]. After culture in adipogenic induction

medium for 7 days, Oil Red O staining shows the percentage of adipogenic differentiation of MSCs is $35.7 \pm 1.4\%$, $33.9 \pm 5.5\%$, $35.8 \pm 4.7\%$, $43.0 \pm 2.5\%$, and $42.9 \pm 6.3\%$ on the triangular, square, pentagonal, hexagonal, and circular micro-patterns, respectively. Although the MSCs with hexagonal and circular shapes shows slightly higher potential for adipogenesis, there is no significant difference among the different cellular shapes. However, the percentage of adipogenic differentiation of MSCs on a non-patterned surface is significantly lower than that on the micro-patterns.

The five types of geometric micro-patterns (triangle, square, pentagon, hexagon, and circle) have varying degrees of roundness, but all are symmetrical and small for cell spreading. Based on the formation of lipid vacuole, no significant difference in the adipogenic differentiation of MSCs is detected among these five geometric micro-patterns. However, MSCs show significantly higher potential for adipogenic differentiation on these micro-patterns than on the non-patterned polystyrene surface.

It has been reported that cytoskeletal organization in the cells is important to the commitment of MSCs [31]. Generally, the assembly of cytoskeleton correlates with intracellular contractility. Large cell spreading and increased contractility favor osteogenic differentiation, while small cell spreading and low contractility favor adipogenic differentiation. The MSCs cultured on the triangular, square, pentagonal, hexagonal, and circular micro-patterns in the control medium show similar patterns of actin filaments. Although actin filaments are thicker and denser at the edges than in the interior regions of the micro-patterns, asymmetrical concentrations of actin filaments are not shown in either edge of the geometries, and no predominated alignment of the actin filaments emerges inside the micro-pattern geometry. After culture in the adipogenic induction medium for 1 week, the actin cytoskeleton undergo remodeling and the differentiated cells show faint actin filaments. The similarity and symmetry of cytoskeletal structures may implicate the similar low level of intracellular contractility in the cells cultured on the five

micro-patterns and may partially cause the parallel potential of adipogenic differentiation of the MSCs on the micro-patterns.

10.5 Discrimination of Cell Elongation and Aspect Ratio and Their Influence on Adipogenic and Osteogenic Differentiation of MSCs

Cell elongation has been demonstrated to be critical in regulating cell proliferation, reprogramming, stemness, and differentiation [6, 7, 19, 32]. Additionally, unified cell alignment is effective in muscle, liver, and blood vessel generation [33–36]. However, manipulation of cell alignment has always been accompanied with change of cell elongation in the previous works [37, 38]. It is still not clear whether cell alignment and elongation have different roles in regulation of cell functions. To investigate the influence of cell alignment and elongation on cell functions, micro- and nano-patterned surfaces have been widely used. However, by using micro-patterns or nano-structured surfaces, cell elongation is always positively correlated with the state of cell alignment. Cell alignment and elongation cannot be separately controlled. Therefore, to discriminate the influence of cell alignment and elongation, micro–nano hybrid patterns of different structures as shown in Fig. 10.2 are designed and prepared to control cell alignment and elongation independently [23].

Two types of micro–nano hybrid patterns are prepared: one is the PVA microstripes parallelly oriented to the PS nanogrooves (micro-p-nano), and the other one is the PVA microstripes orthogonally oriented to the PS nanogrooves (micro-o-nano). MSCs are cultured on the micro-p-nano and micro-o-nano hybrid patterns. Staining of actin filaments and nuclei of the MSCs after 1 day culture show the cells spread and have different morphology on the hybrid patterns (Fig. 10.5a). The cells adhere on the PS nanogrooves and are constrained within the PVA microstripe spacing. The cells align more

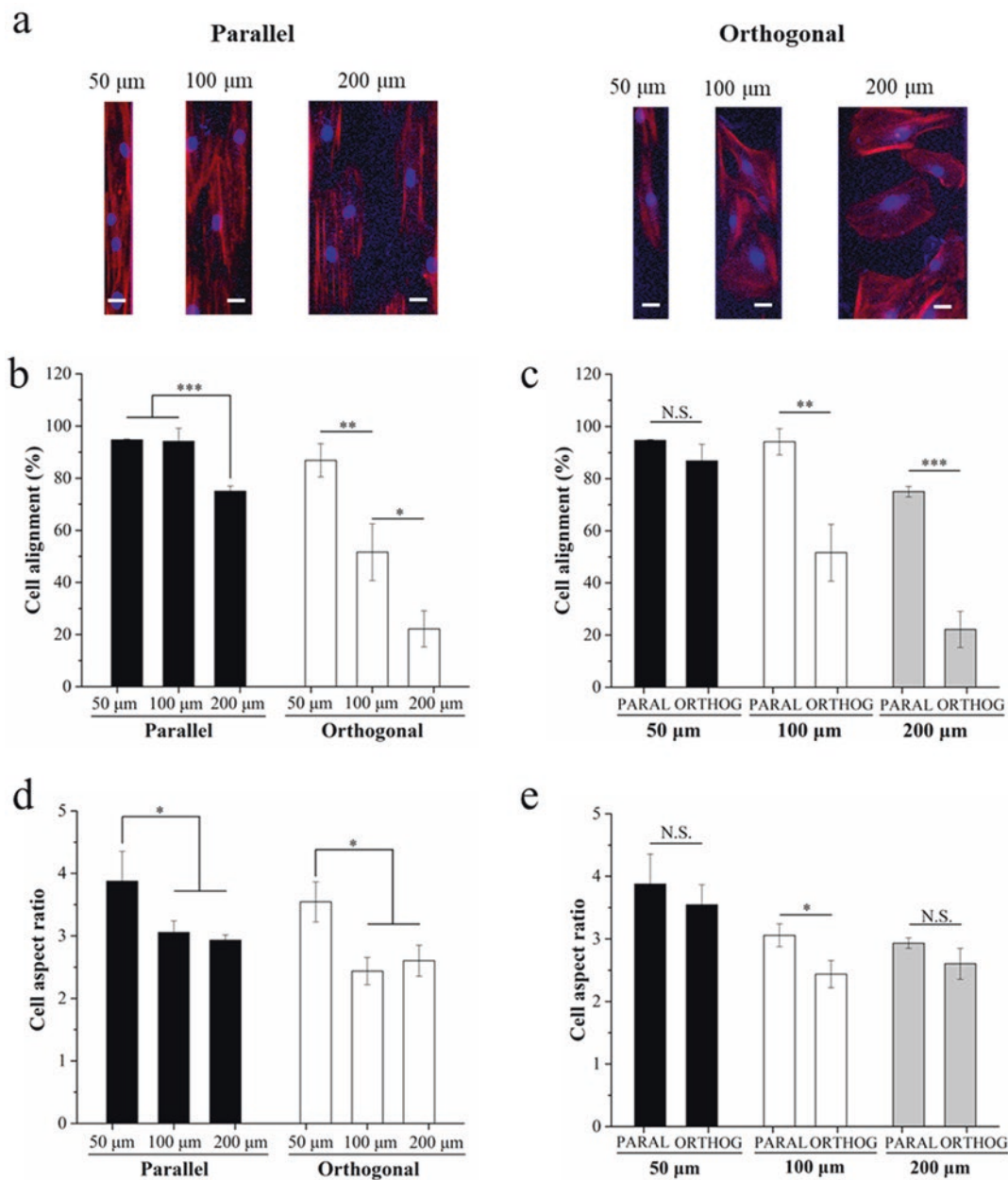


Fig. 10.5 Morphological characterization of hMSCs after 1 day culture on micro–nano hybrid patterns. (a) Representative fluorescence images of actin (red) and nuclei (blue) stained MSCs (a). Percentage of aligned

MSCs to the total cells (b, c). Aspect ratio (elongation) of MSCs (d, e). Data are presented as means ± SDs (n = 3). **p* < 0.05, ***p* < 0.01, ****p* < 0.001. Scale bar: 25 μm. (Reproduced from Ref. [23] with permission)

regularly on the narrow and parallel hybrid patterns than on the wide and orthogonal hybrid patterns.

The cell alignment and elongation on the hybrid patterns are compared (Fig. 10.5b–d). Both the PVA microstripe spacing and PS nanogroove orientation affect the cell alignment

(Fig. 10.5b, c). When the PS nanogroove orientation was fixed at parallel or orthogonal direction, the PVA microstripe spacing shows significant effect on the cell alignment (Fig. 10.5b). The cells show the highest alignment percentage when the PVA microstripe spacing is 50 μm , while the lowest when the PVA microstripe spacing is 200 μm . The cell alignment percentage on the micro-o-nano hybrid patterns increases significantly with the decrease of the PVA microstripe spacing. The cell alignment percentage on the micro-p-nano hybrid patterns having the PVA microstripe spacing of 50 and 100 μm is almost the same. When the PVA microstripe spacing is fixed (Fig. 10.5c), the influence of nanogroove orientation on the cell alignment relies on the PVA microstripe spacing. At a spacing of 50 μm , cell alignment is almost the same regardless of the orientation of the nanogrooves. When the PVA microstripe spacing is 100 or 200 μm , the aligned cell percentage on the micro-p-nano hybrid patterns is significantly higher than that on the micro-o-nano hybrid patterns.

The cell elongation on the micro-nano hybrid patterns having PVA microstripe spacing of 50 μm is higher than that on the micro-nano hybrid patterns having PVA microstripe spacing of 100 or 200 μm (Fig. 10.5d). The cell elongation on the micro-nano hybrid patterns having PVA microstripe spacing of 100 or 200 μm is almost the same. When PVA microstripe spacing is fixed at 50 or 200 μm , the cell elongation on the micro-p-nano hybrid patterns and micro-o-nano hybrid patterns has no significant difference (Fig. 10.5e). When the PVA microstripe spacing is 100 μm , the cell elongation on the micro-p-nano hybrid patterns is significantly higher than that on the micro-o-nano hybrid patterns.

The cell alignment and aspect ratio results indicate that both cell alignment percentage and elongation are dominantly controlled by the PVA micro-pattern spacing when the PVA microstripe spacing is narrow (50 μm). The cell alignment becomes more random and the cell elongation decreases as the spacing of PVA stripes increases, and the effects from PS nanogroove orientation come into play. When the PVA

microstripe spacing is 50 μm , the cells on both the micro-p-nano hybrid patterns and micro-o-nano hybrid patterns have the same level of high alignment and high aspect ratio. At the PVA microstripe spacing of 100 μm , the cells on the micro-p-nano hybrid patterns have significantly higher alignment and higher aspect ratio than those on the micro-o-nano hybrid patterns. When the PVA microstripe spacing increases to 200 μm , the cells on the micro-p-nano hybrid pattern and micro-o-nano hybrid pattern have significantly different alignments but the same level of elongation. Cell alignment and elongation can be separately controlled by the spacing of the PVA micro-stripes and orientation of the PS nano-grooves.

After the MSCs are cultured on the micro-nano hybrid patterns in adipogenic induction medium for 2 weeks, the cells are stained with Oil Red O to evaluate adipogenic differentiation potential. When the micro-nano hybrid patterns having the same parallel or orthogonal orientation but different PVA micro-stripe spacing are compared, adipogenic differentiation potential of MSCs is dependent on both the PVA microstripe spacing and PS nanogroove orientation. On the parallelly oriented micro-p-nano hybrid patterns, the adipogenic differentiation level of the MSCs on the PVA microstripe spacing of 50 μm is the lowest. On the orthogonally orientated micro-o-nano hybrid patterns, the MSCs have similar level of adipogenic differentiation level regardless of the PVA microstripe spacing. On the other hand, when the PVA microstripe spacing is fixed at 50 or 100 μm , adipogenic differentiation level on the micro-p-nano hybrid pattern is significantly lower than that on the micro-o-nano hybrid pattern. When the PVA microstripe spacing is fixed at 200 μm , the adipogenic differentiation level had no significant difference. The results indicate that the orthogonal orientation of the PS nanogrooves and the wide PVA microstripe spacing are beneficial to adipogenic differentiation, while the narrow PVA microstripe spacing and parallel orientation of the PS nanogrooves have inhibitory effect on the adipogenic differentiation. The adipogenic differentiation level of the hMSCs on the micro-nano hybrid patterns has

no evident relationship with either the cell alignment or cell aspect ratio, although high cell alignment and high aspect ratio inhibit the adipogenic differentiation of the hMSCs on the parallelly oriented micro-p-nano hybrid patterns having PVA microstripes of 50 μm .

After the MSCs are cultured in the osteogenic induction medium for 2 weeks, ALP staining is conducted and used to evaluate osteogenic differentiation. By comparing micro-nano hybrid patterns having the same parallel or orthogonal orientation but with different PVA microstripe spacings, the MSCs show the highest osteogenic differentiation level when the PVA microstripe spacing is 50 μm . The osteogenic differentiation level decreases when the PVA microstripe spacing increases. The osteogenic differentiation level of the hMSCs on the micro-nano hybrid patterns having PVA microstripe spacing of 100 and 200 μm has no significant difference. However, when the PVA microstripe spacing is fixed at 50 or 200 μm , the osteogenic differentiation level of the hMSCs on the micro-o-nano and micro-p-nano hybrid patterns has no significant difference. The orientation of the PS nanogrooves shows no influence on the osteogenic differentiation of the hMSCs. On the micro-nano hybrid pattern having PVA microstripe spacing of 100 μm , the parallelly oriented PS nano-grooves show significantly higher promotive effect on the osteogenic differentiation than the orthogonally oriented PS nanogrooves. These results indicate that both the PVA microstripe spacing and PS nanogroove orientation can influence osteogenic differentiation. The narrow PVA microstripe spacing and parallel orientation of the PS nanogrooves have promotive effect, while wide PVA microstripe spacing and orthogonal orientation of the PS nano-grooves have inhibitory effect on the osteogenic differentiation of the hMSCs. When the cell alignment and aspect ratio parameters and osteogenic differentiation data are compared, it is clear that osteogenic differentiation level of hMSCs on micronano hybrid patterns has the same trend as that of cell aspect ratio. However, the changing trend of cell alignment is different from that of osteogenic differentiation level. In particular, when cell alignment is low,

difference between the changing trends of cell alignment and osteogenic differentiation becomes evident. The cell alignment on the micronano hybrid patterns having the same orientation of the PS nanogrooves but with different PVA microstripe spacings of 100 and 200 μm or the same PVA micro-stripe spacing of 200 μm but with different orientations of PS nanogrooves is significantly different; osteogenic differentiation level has no significant difference. It can be concluded that osteogenic differentiation of the hMSCs is dominantly regulated by the cell elongation, although cell alignment has some influence. High elongation promotes osteogenic differentiation.

Preparation of PS and PVA micro-nano hybrid patterns through nanoimprinting and photolithography provides a useful method to control cell alignment and elongation and to investigate their influence on osteogenic and adipogenic differentiation of hMSCs. Cell alignment and elongation are simultaneously regulated by changing the PVA microstripe spacing and orientation of PS nanogrooves of micro-nano hybrid patterns. On micro-nano hybrid patterns, the cell alignment and elongation show different influences on the hMSCs differentiation. The osteogenic differentiation of the MSCs is dominantly regulated by cell elongation. The adipogenic differentiation level of the hMSCs on the micro-nano hybrid patterns has no evident relationship with either cell alignment or cell elongation.

10.6 Influence of Micro-Pattern Width on MSCs Differentiation to Vascular Smooth Muscle Cells

Vascular smooth muscle cells (SMCs) perform a crucial function in angiogenesis, mechanical support of vessels, and blood pressure control [39]. To successfully construct tissue-engineered blood vessels, regeneration of functional SMC layer is required. Smooth muscle cells can differentiate into a variety of cell types including myocytes [2]. Biological cues, such as transforming growth factor beta-1 (TGF- β 1), are generally

used for differentiation of MSC into SMC phenotype [40, 41]. Except biological cues, physical cues and their combination have been widely investigated for smooth muscle cell differentiation of the MSCs [42]. Usage of micro-patterning technique to regulate cell alignment is considered an effective way for SMC differentiation [43–45].

The stripe micro-patterns prepared with photo-mask shown in Fig. 10.3 are used for culture of MSCs to investigate the micro-pattern width on smooth muscle cell differentiation of MSCs [18]. The width of cell-adhesive polystyrene stripes is 5, 10, 20, 40, 60, 80, 100, 200, 400, 600, 800, and 1000 μm . The alternate PVA stripes have the same width as that of polystyrene stripes. The MSCs are cultured on the micro-patterns in DMED-supplemented 10% fetal bovine serum for 1 day. To induce smooth muscle cell differentiation, the medium is changed to myogenic differentiation medium consisting of MesenPRO RS™ medium supplemented with TGF β 1. After culture for 7 days in the differentiation medium, the cells proliferate and occupy the spaces in the stripes areas (Fig. 10.6). The cells show better orientation along the narrow stripes than cells on the wide stripes. The cell distribution and alignment are quantified using phase-contrast images of the MSCs on the micro-patterns. The cell alignment on the stripes having widths of 5 and 10 μm is not measured because the cell number on these stripes

is few. The degree of alignment is defined as the angle formed with the axis of the stripes. The cell alignment angle is calculated, and the cell orientation on different widths of the stripes is quantified after the 7 days of culture in the differentiation medium. For the cells on the non-patterned region, the orientation is randomly distributed from 0° to 90°. On the other hand, the cell orientation on the micro-patterns shows a well-restricted way. The MSCs show much higher degree of alignment on the small width stripes (20, 40, and 60 μm) than on the big width stripes (80, 100, 200, 400, 600, 800, and 1000 μm) after the 7 days of culture. The results indicate that micro-patterns can guide MSCs to spread in the direction of the micro-pattern stripes and restrict cell spreading in the perpendicular direction. The cell alignment analysis reveals that the cells orient in parallel to the narrow micro-pattern stripes, suggesting that the cells are able to sense the surface topography. The width of micro-pattern stripes is shown to be important for all alignments. Narrow micro-pattern stripes have a stronger effect on cell alignment than the wide micro-pattern stripes.

Differentiation of MSCs to SMC is evaluated by immunofluorescence staining of SMA and calponin, which are early and mid-SMC markers, respectively [46]. After 7 days of culture in the differentiation medium, most of the MSCs are stained positively for SMA and calponin on all the

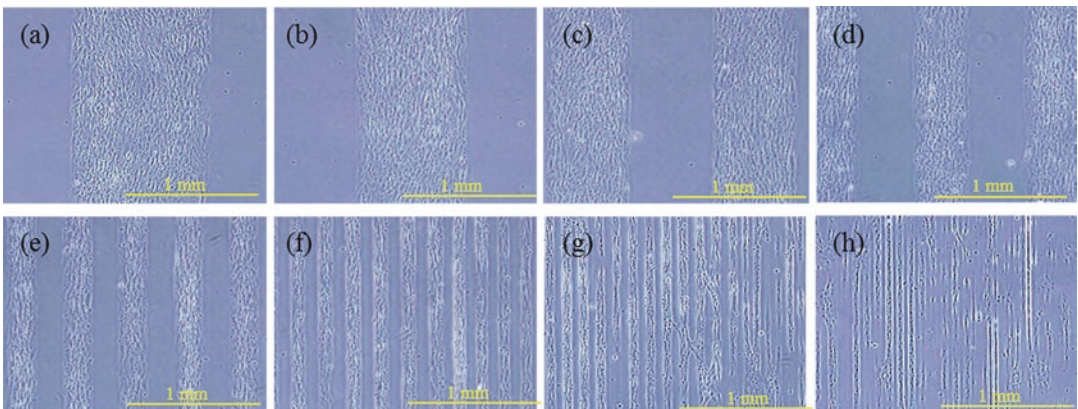


Fig. 10.6 Phase-contrast photographs of MSCs cultured on micro-pattern stripes having different widths of 1000 μm (a), 800 μm (b), 600 μm (c), 400 μm (d), 200 μm

(e), 100/80 μm (f), 60/40 μm (g), and 40/20/10/5 μm (h) in differentiation medium for 1 day. (Reproduced from Ref. [18] with permission)

micro-pattern stripes. Compared to non-patterned region, a higher expression of calponin and SMA in cells on the narrow micro-patterns with a stripe width ranging from 200 μm to 20 μm is observed. However, there is no significant difference of calponin and SMA expression in cells on the wide micro-pattern stripes (400, 600, 800, and 1000 μm) and the non-patterned surface. The influence of micro-pattern width on the SMC differentiation of the hMSCs is compared by calculating the percentage of cells positively stained for calponin and SMA on the different micro-pattern stripes. Eighty five to ninety seven percent of MSCs cultured on the narrow micro-patterns with a stripe width ranging from 200 μm to 20 μm undergo SMC differentiation, which is significantly higher than that of MSCs cultured on the wide micro-patterns with a stripe width ranging from 400 to 1000 μm . The narrow stripe micro-patterns promote cell alignment and facilitate SMC differentiation of hMSCs.

The results indicate that micro-pattern stripe width has an obvious effect on the orientation and SMC differentiation of MSCs. Narrow stripes limit cell spreading in perpendicular direction and allow cells to spread in the direction of stripes. As a result, small alignment angles are observed among the narrow micro-pattern stripes. Compared with the cells on the non-pattern region, the MSCs cultured on the narrow stripes ranging from 200 μm to 20 μm show a significantly higher expression of the SMC marker proteins, SMA, and calponin after the 7 days of culture in differentiation medium. The influence of stripe width on the VSMC differentiation of hMSCs is correlated with the cell alignment.

10.7 Summary

Various micro-patterns having different sizes, geometries, aspect ratios, nano–micro hybrid structures, and stripe widths are prepared by using photoreactive PVA through UV photolithograph. The micro-patterns are used for culture of MSCs to investigate the influence of cell morphology on stemness maintenance, adipogenic, osteogenic, and muscle smooth differentiation of

the MSCs. Single cell and multiple cell arrays having controlled cell morphology are realized by using the micro-patterns. Comparison of the behaviors and differentiation of MSCs on these single and multiple cell arrays discloses some useful information of the influences of these physiochemical cues on the commitment of MSCs. MSCs with small spreading area and low aspect ratio are more quiescent and softer than their large and elongated counterpart, and they show higher potential to maintain the multipotency of stem cells. Large cell spreading and increased contractility favor osteogenic differentiation, while small cell spreading and low contractility favor adipogenic differentiation. MSCs cultured on triangular, square, pentagonal, hexagonal, and circular micro-patterns show similar level of differentiation potential. Culture of MSCs on the nano–micro hybrid patterns shows that osteogenic differentiation is dominated by cell elongation, while adipogenic differentiation is influenced by neither cell alignment nor cell elongation. The width of micro-pattern stripes has obvious effect on cell orientation, morphology, and smooth muscle differentiation of MSCs. MSCs have high degree of orientation when being cultured on narrow micro-pattern stripes. Higher expression of calponin and smooth muscle actin is observed among the narrow micro-patterns ranging from 200 μm to 20 μm , compared to the non-patterned area and wide micro-pattern areas, which show similar levels of expression. The results should provide very useful information for stem cell research and regenerative medicine.

Acknowledgements This work was supported by JSPS KAKENHI Grant Number 18K19947, 18K19945 and 19H04475.

References

1. Cook D, Genever P (2013) Regulation of mesenchymal stem cell differentiation. In: Hime G, Abud H (eds) Transcriptional and translational regulation of stem cells, *Advances in experimental medicine and biology*, vol 786. Springer, Dordrecht, pp 213–229

2. Pittenger MF, Mackay AM, Beck SC et al (1999) Multilineage potential of adult human mesenchymal stem cells. *Science* 284:143–147
3. Jiang YH, Jahagirdar BN, Reinhardt RL et al (2002) Pluripotency of mesenchymal stem cells derived from adult marrow. *Nature* 418:41–49
4. Lane SW, Williams DA, Watt FM (2014) Modulating the stem cell niche for tissue regeneration. *Nat Biotechnol* 32:795–803
5. Thery M (2010) Micro-patterning as a tool to decipher cell morphogenesis and functions. *J Cell Sci* 123:4201–4213
6. Versaevael M, Grevesse T, Gabriele S (2012) Spatial coordination between cell and nuclear shape within micro-patterned endothelial cells. *Nat Commun* 3:671–681
7. Downing TL, Soto J, Morez C (2013) Biophysical regulation of epigenetic state and cell reprogramming. *Nat Mater* 12:1154–1162
8. Ermis M, Antmen E, Hasirci V (2018) Micro and nanofabrication methods to control cell-substrate interactions and cell behavior: a review from the tissue engineering perspective. *Bioact Mater* 3:355–369
9. Lim JY, Donahue HJ (2007) Cell sensing and response to micro- and nanostructured surfaces produced by chemical and topographic patterning. *Tissue Eng* 13:1879–1891
10. Jiang XY, Bruzewicz DA, Wong AP et al (2005) Directing cell migration with asymmetric micro-patterns. *Proc Natl Acad Sci U S A* 102:975–978
11. Thakar RG, Cheng Q, Patel S et al (2009) Cell-shape regulation of smooth muscle cell proliferation. *Biophys J* 96:3423–3432
12. Thery M, Racine V, Piel M et al (2006) Anisotropy of cell adhesive microenvironment governs cell internal organization and orientation of polarity. *Proc Natl Acad Sci U S A* 103:19771–19776
13. Song W, Lu H, Kawazoe N et al (2011) Adipogenic differentiation of individual mesenchymal stem cell on different geometric micro-patterns. *Langmuir* 27:6155–6162
14. Song W, Kawazoe N, Chen G (2011) Dependence of spreading and differentiation of mesenchymal stem cells on micro-patterned surface area. *J Nanomater* 2011:9
15. Song W, Wang X, Lu H et al (2012) Exploring adipogenic differentiation of a single stem cell on poly(acrylic acid) and polystyrene micro-patterns. *Soft Matter* 8:8429–8437
16. Wang X, Song W, Kawazoe N et al (2013) The osteogenic differentiation of mesenchymal stem cells by controlled cell-cell interaction on micro-patterned surfaces. *J Biomed Mater Res A* 101:3388–3395
17. Wang X, Song W, Kawazoe N et al (2013) Influence of cell protrusion and spreading on adipogenic differentiation of mesenchymal stem cells on micro-patterned surfaces. *Soft Matter* 9:4160–4166
18. Nakamoto T, Wang X, Kawazoe NP et al (2014) Influence of micro-pattern width on differentiation of human mesenchymal stem cells to vascular smooth muscle cells. *Colloid Surf B-Biointerfaces* 122:316–323
19. Wang X, Nakamoto T, Dulinska-Molak I et al (2016) Regulating the stemness of mesenchymal stem cells by tuning micro-pattern features. *J Mater Chem B* 4:37–45
20. Wang X, Hu X, Kawazoe N et al (2016) Manipulating cell nanomechanics using micro-patterns. *Adv Funct Mater* 26:7634–7643
21. Wang X, Hu X, Dulińska-Molak I et al (2016) Discriminating the independent influence of cell adhesion and spreading area on stem cell fate determination using micro-patterned surfaces. *Sci Rep* 6:28708
22. Wang X, Hu XH, Li J et al (2016) Influence of cell size on cellular uptake of gold nanoparticles. *Biomater Sci* 4:970–978
23. Yang Y, Wang X, Huang T et al (2018) Regulation of mesenchymal stem cell functions by micro-nano hybrid patterned surfaces. *J Mater Chem B* 6:5424–5434
24. Yang Y, Wang X, Wang Y et al (2019) Influence of cell spreading area on the osteogenic commitment and phenotype maintenance of mesenchymal stem cells. *Sci Rep* 9:6891
25. Yang Y, Wang X, Hu X et al (2019) Influence of cell morphology on mesenchymal stem cell transfection. *ACS Appl Mater Interfaces* 11:1932–1941
26. Denitsa D, Florian H, Matthias S (2008) Mesenchymal stem cells and their cell surface receptors. *Curr Rheumatol Rev* 4:155–160
27. Majumdar MK, Keane-Moore M, Buyaner D et al (2003) Characterization and functionality of cell surface molecules on human mesenchymal stem cells. *J Biomed Sci* 10:228–241
28. Dominici M, Le Blanc K, Mueller I et al (2006) Minimal criteria for defining multipotent mesenchymal stromal cells. The International Society for Cellular Therapy position statement. *Cytotherapy* 8:315–317
29. Bhadriraju K, Hansen LK (2002) Extracellular matrix- and cytoskeleton-dependent changes in cell shape and stiffness. *Exp Cell Res* 278:92–100
30. Szabo E, Feng TS, Dziak E et al (2009) Cell adhesion and spreading affect adipogenesis from embryonic stem cells: the role of calreticulin. *Stem Cells* 27:2092–2102
31. Falconnet D, Csucs G, Grandin HM et al (2006) Surface engineering approaches to micro-patterned surfaces for cell-based assays. *Biomaterials* 27:3044–3063
32. Zhang D, Sun MB, Lee JM et al (2016) Cell shape and the presentation of adhesion ligands guide smooth muscle myogenesis. *J Biomed Mater Res A* 104:1212–1220
33. Zhao Y, Zeng HS, Nam J et al (2009) Fabrication of skeletal muscle constructs by topographic activation of cell alignment. *Biotechnol Bioeng* 102:624–631

34. Wang PY, Yu HT, Tsai WB (2010) Modulation of alignment and differentiation of skeletal myoblasts by submicron ridges/grooves surface structure. *Biotechnol Bioeng* 106:285–294
35. Hoehme S, Brulport M, Bauer A et al (2010) Prediction and validation of cell alignment along microvessels as order principle to restore tissue architecture in liver regeneration. *Proc Natl Acad Sci U S A* 107:10371–10376
36. Xu CY, Inai R, Kotaki M et al (2004) Aligned biodegradable nanofibrous structure: a potential scaffold for blood vessel engineering. *Biomaterials* 25:877–886
37. Aubin H, Nichol JW, Hutson CB et al (2010) Directed 3D cell alignment and elongation in microengineered hydrogels. *Biomaterials* 31:6941–6951
38. Wang PY, Yu J, Lin JH et al (2011) Modulation of alignment, elongation and contraction of cardiomyocytes through a combination of nanotopography and rigidity of substrates. *Acta Biomater* 7:3285–3293
39. Owens GK, Kumar MS, Wamhoff BR (2004) Molecular regulation of vascular smooth muscle cell differentiation in development and disease. *Physiol Rev* 84:767–801
40. Park JS, Chu JS, Tsou AD et al (2011) The effect of matrix stiffness on the differentiation of mesenchymal stem cells in response to TGF- β . *Biomaterials* 32:3921–3930
41. Floren M, Bonani W, Dharmarajan A et al (2016) Human mesenchymal stem cells cultured on silk hydrogels with variable stiffness and growth factor differentiate into mature smooth muscle cell phenotype. *Acta Biomater* 31:156–166
42. Parandakh A, Anbarlou A, Tafazzoli-Shadpour M et al (2019) Substrate topography interacts with substrate stiffness and culture time to regulate mechanical properties and smooth muscle differentiation of mesenchymal stem cells. *Colloids Surf B Biointerfaces* 173:194–201
43. Huang NF, Lee RJ, Li S (2010) Engineering of aligned skeletal muscle by micro-patterning. *Am J Transl Res* 2:43–55
44. Tay CY, Pal M, Yu HY et al (2011) Bio-inspired micro-patterned platform to steer stem cell differentiation. *Small* 7:1416–1421
45. Khetan S, Burdick JA (2010) Patterning network structure to spatially control cellular remodeling and stem cell fate within 3-dimensional hydrogels. *Biomaterials* 31:8228–8234
46. Solway J, Seltzer J, Samaha FF et al (1995) Structure and expression of a smooth-muscle cell-specific gene, SM22 α . *J Biol Chem* 270:13460–13469

Part IV

Nano-Intelligent Biocomposites for Regenerative Medicine



Natural Polyphenols as Modulators of the Fibrillization of Islet Amyloid Polypeptide

11

Ana R. Araújo, Rui L. Reis, and Ricardo A. Pires

Abstract

Diabetes mellitus type 2 (type-2 diabetes) is a metabolic disorder characterized by the increased blood glucose concentration and insulin resistance in peripheral tissues (e.g., muscles and adipose tissue). The initiation of the pathological cascade of events that lead to type-2 diabetes has been subject of debate; however, it has been commonly accepted that the oversecretion of human islet amyloid polypeptide (hIAPP, a hormone co-secreted with insulin) by the pancreatic β -cells is the main trigger of type-2 diabetes. In fact, 90% of the type-2 diabetes patients present hIAPP deposits in the extracellular space of the β -cells. These hIAPP supramolecular arrangements (both fibrillar and oligomeric) have been reported to be the origin of cytotoxicity, which leads to β -cell dysfunction through a

series of different mechanisms, including the interaction of hIAPP oligomers with the cell membrane that leads to the influx of Ca^{2+} and increase in the cellular oxidative stress, among others. This overview shows the importance of developing type-2 diabetes treatment strategies able to (1) remodel of the secondary structure of cytotoxic hIAPP oligomers entrapping them into off-pathway nontoxic species and (2) reestablish physiological levels of oxidative stress. Natural polyphenols are a class of antioxidant compounds that are able to perform both functions. Herein we review the published literature of the most studied polyphenols, in particular for their ability to remodel the hIAPP aggregation pathway, to rescue the *in vitro* pancreatic β -cell viability and function, as well as to perform under a complex biological environment, i.e., *in vivo* animal models and clinical trials. Overall, natural polyphenols are able to control the cytotoxic hIAPP aggregation and minimize hIAPP-mediated cellular dysfunction and can be considered as important lead compounds for the treatment of type-2 diabetes.

A. R. Araújo · R. L. Reis · R. A. Pires (✉)
3B's Research Group, I3Bs – Research Institute on Biomaterials, Biodegradables and Biomimetics, Headquarters of the European Institute of Excellence on Tissue Engineering and Regenerative Medicine, University of Minho, Guimarães, Portugal

ICVS/3B's–PT Government Associate Laboratory, Braga/Guimarães, Portugal

The Discoveries Centre for Regenerative and Precision Medicine, Headquarters at University of Minho, Guimarães, Portugal
e-mail: rpirez@i3bs.uminho.pt

Keywords

Diabetes mellitus type 2 · Islet amyloid polypeptide · Amylin · Amyloid · Protein aggregation · Natural polyphenols

11.1 Introduction

Diabetes mellitus type 2 (type-2 diabetes) is a metabolic condition associated with the deficient release of insulin into the bloodstream after a glucose intake stimulus, as well as peripheral insulin resistance, where the muscles, liver, and adipose tissue present an impaired response to insulin [1]. Its prevalence is increasing due to lifestyle and eating habits, namely, sedentary behaviors and the increasing prevalence of high-calorie diets [2]. For several years, that type-2 diabetes has been considered a major public health concern. The complications associated with type-2 diabetes start to appear at the prediabetic stage, described as a “metabolic condition characterized by insulin resistance and primary or secondary beta cell dysfunction which increases the risk of development type 2 diabetes” [3]. Even at this stage, there is an increased risk of developing cardiovascular diseases [3], renal failure [4], among other clinical complications.

Considering the European population above 25 years old, it is accounted that 60 million people have diabetes. This incidence corresponds to approximately 10% of men and approximately 9% of women [2]. Moreover, about 40% of the population above 40 years old is at a prediabetic condition [3], while the most recent estimations indicate that approximately 50% of the European population will suffer from hyperglycemia or type-2 diabetes during their lifetime [5]. It is also relevant to note that, worldwide, every year, there are 3.4 million deaths related to diabetes, while the World Health Organization (WHO) estimates that this number can double by 2030 [2] and that the type-2 diabetes cases can reach 600 million by 2035. These estimations are at the basis of the urgency to control type-2 diabetes and its incidence in the population, as well as to study its causes and develop efficient treatment strategies [6].

Type-2 diabetes is associated with the deficient ability of the body to maintain normoglycemia. In general, healthy individuals process carbohydrates through the digestive system leading to the formation of glucose, which is transferred into the bloodstream through different glucose transporters. The increased concentra-

tion of glucose in the blood induces the secretion of insulin by the pancreatic β -cells. The systemic release of insulin leads to the lowering of the concentration of glucose in the blood through two main mechanisms, namely: (1) it induces the uptake of glucose by the liver, as well as its transformation into glycogen – which acts as a glucose reservoir; (2) it stimulates the peripheral tissues, e.g., muscle cells and adipocytes, to uptake and store glucose which can be latter used as a locally available energy source (in the case of the muscles) or as a long-term energy storage (in the case of the adipocytes) [4].

The secretion of insulin by the β -cells is accompanied by the release of a hormone designated by islet amyloid polypeptide (hIAPP) or amylin, under a ratio of 50:1 (insulin/hIAPP). Both insulin and hIAPP are co-stored in the secretory granules and are released into the bloodstream at the same time [7]. While the activity and physiological relevance of insulin are known, the biological relevance of hIAPP is still under debate. However, it has been reported that hIAPP bioactivity is exerted in a number of interrelated ways, namely: (1) the reduction of gastric emptying [4, 8] that leads to the increased feeling of satiety and the subsequent reduction of food intake; (2) the inhibition of the release of glucose from the liver by suppressing the production of glucagon [8], contributing to the achievement of normoglycemia; (3) the modulation of the activity of neuropeptide Y [9] a strong feeding stimulant; and (4) the counterbalancing of insulin activity, as well as glycogen synthesis [10]. In general, all these bioactivities are important mechanisms used by the body to control the intake of carbohydrates or to maintain normoglycemia, acting in the digestive system, in the blood, and in the brain [4].

Despite its important physiological role, hIAPP is a peptide that is highly prone to aggregate and form extracellular deposits in the pancreas of both diabetic and nondiabetic individuals. However, while nondiabetic patients present immunoreactivity toward non-aggregated forms of hIAPP, this is not the case for type-2 diabetes patients. In this latter case, immunoreactivity toward non-aggregated forms of hIAPP is lower

[1], and hIAPP deposits are observed in approximately 90% of the cases [11, 12]. These observations support the pivotal role of hIAPP in the pathophysiology of type-2 diabetes.

11.2 The Role of hIAPP in Diabetes Mellitus Type 2

It is clear the importance of hIAPP in controlling food intake by triggering the feeling of satiety. When physiological levels of hIAPP are not enough to reduce the ingestion of carbohydrates during meals, the pancreas increased the secretion of insulin and hIAPP to levels that may lead to pathological consequences. In fact, hIAPP deposits in the pancreas of type-2 diabetes patients were initially identified by Opie [13] more than 100 years ago. The presence of these deposits (of hIAPP in a fibrillar form) in more than 90% of the type-2 diabetes cases led to the initial assumption that the fibrillar hIAPP was one of the triggers of this condition [11, 12, 14]. This was based on a series of studies, reporting the toxicity of hIAPP fibers toward the pancreatic β -cells [11, 15], which leads to their reduced activity and lower capacity to secrete insulin, compromising the ability of the body to reduce the glucose levels in the bloodstream after the ingestion and processing of carbohydrates by the digestive system. Further evolution of this condition leads to the death of β -cells, which may lead to the significantly lower capacity of the pancreas to release suitable levels of insulin into the bloodstream. As a consequence, the body is not able to maintain normoglycemia, leading to long-term high levels of glucose in the blood.

This general overview is still valid; however, the reason behind hIAPP cytotoxicity toward β -cells has been extensively studied during the last years, leading to significant updates on its mechanisms. In fact, several studies indicate that the fibrillar forms of hIAPP are less cytotoxic, while its oligomeric forms have been reported as the most cytotoxic for several reasons, such as the following: (1) they are highly mobile and able to diffuse through the cellular environment, both extra- and intracellularly [16, 17]; (2) they pres-

ent a dynamic secondary structure, allowing the formation of cytotoxic supramolecular conformations [18]; (3) they are able to interact with membrane lipids and generate pores that increase ionic fluxes that compromise intracellular ionic homeostasis [11, 12, 19–21]; and (4) higher-order hIAPP assemblies are able to interact strongly with the cell membrane, leading to its disruption and compromising cellular integrity [11, 12, 20]. In addition, ongoing studies report the interaction of hIAPP on its different supramolecular arrangements with proteins [22] and cell receptors [23] perturbing a series of cellular cascades. As an example, we can refer the known interaction between oligomeric hIAPP and NLRP3 inflammasome [22], which leads to the expression of $IL1\beta$, an inflammatory mediator, known to be activated in type-2 diabetes. It is also relevant to note that there is an increasing body of evidences that link type-2 diabetes and Alzheimer's disease (AD) [17, 24], more specifically: (1) hIAPP has been detected in the brain of AD patients, which, occasionally are detected mixed with the $A\beta_{42}$ deposits characteristic of AD [25], and (2) it is known that oligomeric hIAPP interacts with AMY_R and TRPV4 receptors leading to calcium imbalance and membrane disruption, although under mechanisms that are still not completely clear [6].

11.3 Mechanism of hIAPP Aggregation and Its Cytotoxicity

Protein/peptide aggregation has been associated with the pathophysiology of a series of amyloid-based diseases, including neurodegenerative disorders [26], retinal amyloidosis [27], and type-2 diabetes [13], among others. Observations of cytotoxicity when fibrils and aggregates were present in the cellular environment led researchers to believe that the main drivers of toxicity were mature fibrils [11, 15]; however, this view has not been confirmed by experimental evidence. In fact, nowadays, it is commonly accepted that the intermediate oligomeric structures are the ones that are at the basis of cytotoxicity and

trigger pathological pathways in the cellular environment [28]. This view increases the importance of a clear understanding of the mechanisms at the basis of fibril/aggregate formation, including the supramolecular organization of oligomers, their stability, and the way they interact with the cellular components.

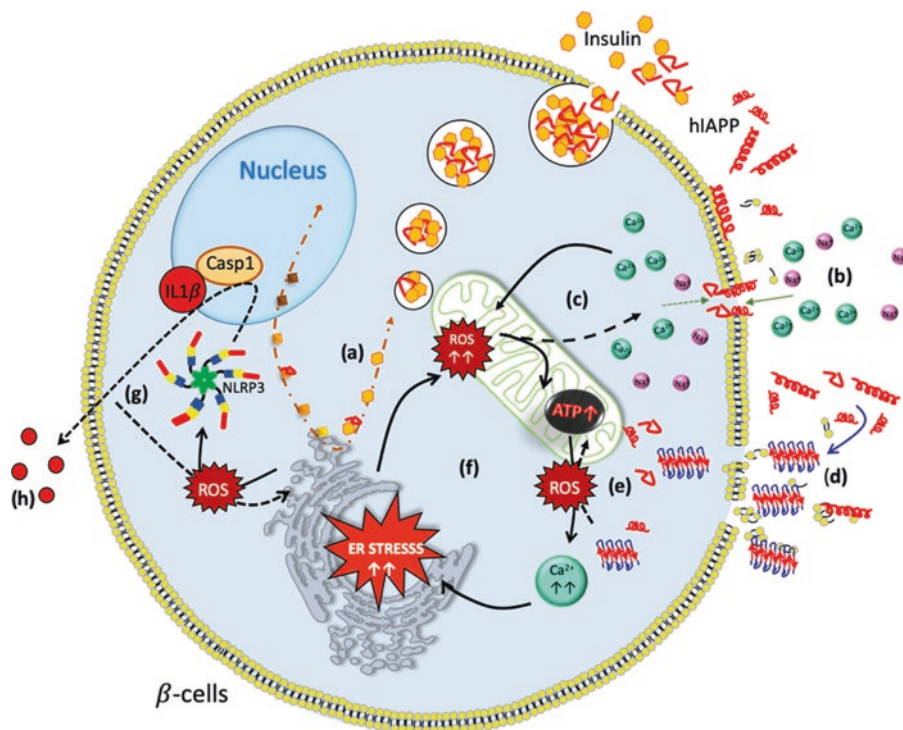
In general, the fibrillogenesis of amyloids present common features that are independent of the peptide/protein, and hIAPP is not an exception. Usually the fibril formation process is divided into three main stages: (1) lag phase, (2) exponential growth, and (3) saturation phase [7, 20]. During the lag phase, monomeric peptide/protein units interact between themselves forming low-order unstructured assemblies (i.e., oligomeric and protofibrillar structures). In the second phase (exponential growth), these peptide/protein oligomers/protofibrils are converted into β -sheet-rich structures, and they grow into higher-order fibrils through self-assembling mechanisms; in the last saturation phase, the assembled fibers reach thermodynamic stability, and their disruption is more difficult.

As previously described, hIAPP has been linked to the onset of type-2 diabetes, where it is believed to contribute to β -cell dysfunction, through different pathways (Scheme 11.1) [7], such as the generation of membrane pores (a), partial membrane disruption (b and d), induction of oxidative stress (c, e, and f), promotion of apoptosis (g and h), etc. hIAPP is a 37 amino acid peptide, which presents three potential β -strand regions [18–23, 24–29, 32–37], suggesting that intramolecular β sheets can be easily formed [29]. It has been recently reported that hIAPP loses its biofunctional character due to thermodynamic instability. In general, this transformation is linked with perturbations of the peptide micro-environment, i.e., temperature, metal ions, pH, nucleation-independent pathway, and ionic strength [30]. Under these conditions, the peptide suffers high structural reorganization, exposing hydrophobic groups and their chain amides to its outer surface, promoting new intermolecular interactions generating oligomeric structures. The conformational change of the peptide secondary structure is concentration-dependent and

driven by hydrogen bonding and hydrophobic effects. Since this process is dynamic, and the fact that there is a continuous flux of newly synthesized hIAPP, the aggregation of a variety of thermodynamically unstable structures increases in a time-dependent manner (lag phase of aggregation). At this stage, these oligomers are able to interact with cellular organelles and biomolecules perturbing normal cellular function. These toxic oligomeric species, if not completely cleared by the cellular machinery, induce deficits in the activity of different biomolecules/pathways, such as molecular chaperones, ubiquitin-proteasome, and heat shock proteins, which are able to control the formation and modulate the elimination of pathological pre-fibrillar and fibrillar assemblies. These supramolecular forms of hIAPP lead to the reduction of β -cell mass due to their cytotoxicity. These hIAPP oligomers, as well as pre-formed fibrils [31, 32], are the ones described to promote disruption of cellular membranes (plasma and organelles) by uptake of the lipid molecules during fibrillogenesis into protofibril units or by acting as nonselective ion channels that disrupt membrane permeability and promote a misregulation of the metal ion homeostasis (see Scheme 11.1). These mechanisms compromise the integrity of the cell and its normal function, leading to the dysfunction of the cellular machinery and cell death [33].

The subsequent hIAPP fibrillization occurs at the exponential growth phase and is characterized by the remodeling of the oligomers' secondary structure into cross- β -sheet organization and continuous aggregation of the oligomers/monomers into unidirectionally ordered fibrillar structures maintained together by hydrogen bonding [31, 34]. These mature fibers are believed to be less toxic because they reached a thermodynamically stable aggregated state (saturation phase) [35].

An assessment of the supramolecular organization of the initial hIAPP's monomeric/oligomeric states (described above as highly toxic and that trigger fibril formation) has been performed by several groups, using NMR, CD, and diffusion measurements [36, 37]. The reported results showed that hIAPP in a monomeric form adopts a highly dynamic metastable state which presents



Scheme 11.1 Schematic illustration of some of the different mechanisms reported in the literature by which extracellular hIAPP supramolecular species interfere with pancreatic β -cell functions: (a) insulin/hIAPP synthesized in the endoplasmic reticulum (ER) and further transported by the secretory granules onto the surface of the cell's basement membrane; (b) formation of nonspecific membrane pores mediated by hIAPP oligomers leading to the

(c) intracellular accumulation of ions (i.e., Ca^{2+}); (d) lipid membrane disruption promoted by hIAPP toxic species, (e, f) leading to an increased oxidative stress, ATP imbalance, and uncontrolled generation of ROS, which trigger the activation of inflammatory response through the (g and h) NLRP3 inflammasome, which ultimately leads to pyroptosis and cell death

a predominant unfolded random coil globular form [38]. This metastable form is less compact than an unfolded protein, lacking the well-packed core, which is at the basis of their high propensity to aggregate and form higher-order assemblies, i.e., oligomers rich in β -sheets [36]. The β -sheet formation mechanism is controlled by nucleation through the buildup of a small population of energetically unfavorable oligomers that initiate the supramolecular assembly and subsequent nanofiber formation. This initial formation of oligomers is followed by secondary nucleation which accelerates fiber growth. Each generated hIAPP nanofiber is used as a new substrate for secondary nucleation and elongation. This process can be boosted by the presence of hIAPP micelles, since aggregation appears to nucleate

within the micelle from the central region of the peptide (residues 20–29, which are considered to be the fibrillating core sequence of hIAPP at physiological conditions) [39]. The mature fibers, formed during these events, present twisted, left-handed chirality and constant periodicity. Atomic force microscopy (AFM) evaluation of hIAPP nanofibers has been used to perform quantitative nanomechanical measurements, showing that the twisted conformation represents a decrease in local stiffness compared to the multi-stranded ribbon (a helical hollow structure is the final stage of a fibrillation process characterized by a stable thermodynamic state). As shown here, the aggregation pathway of IAPP has been extensively studied leading to a better understanding of the supramolecular organization of

its monomers, oligomers, and nanofibers. Their correlation with cytotoxicity is currently under investigation, and it is expected new insights on the biophysical interactions responsible for the cytotoxic mechanisms that lead to cell death, e.g., membrane disruption, etc.

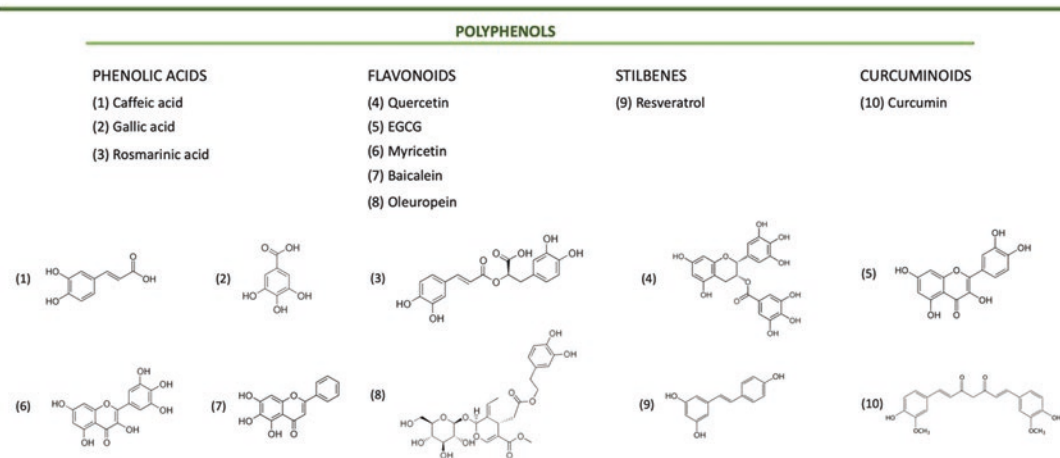
11.4 Modulation of hIAPP Aggregation by Natural Compounds

Pathological hIAPP aggregation into cytotoxic soluble oligomers and/or fibrillar deposits has been considered a hallmark of type-2 diabetes. The remodeling of these misfolded states has been targeted as a treatment approach or a way to control the evolution of type-2 diabetes, in a similar fashion as for other amyloidogenic peptides/proteins responsible for several other disorders [40–43]. In general, peptide/protein misfolding (including hIAPP) has been linked to increased oxidative stress, imbalance of Ca^{2+} homeostasis, mitochondria dysfunction, and transcriptional deregulation. These phenomena can occur independently or concurrently, and it is still under debate if they are the cause or the consequence of the presence of thermodynamically unstable peptide/protein species [44, 45].

The progression of type-2 diabetes is complex, involving different mechanisms that lead to difficulties in identifying effective disease targets. However, different natural compounds are known to inhibit protein aggregation while also presenting antioxidant and anti-inflammatory activities, a multifunctionality relevant for type-2 diabetes [41, 46–49]. In fact, results obtained using several cohorts highlight the benefit of a diet rich in vegetables and fruits in reducing the risk of age-associated amyloid-based disorders [49, 50]. In addition, the ingestion of a wider variety of these compounds improves glucose tolerance and decreases the risk of type-2 diabetes [51]. Thus, the daily ingestions of fruits and red wine (due to the presence of resveratrol), olive oil (rich in oleuropein), spices and herbs (especially the ones that include curcumin, caffeic acid, rosmarinic acid), and tea (that present epigallocatechin gallate (EGCG) and myricetin in their composition) are examples of dietary components that are rich in bioactive species and that have been reported to have a positive impact on type-2 diabetes [52–55].

There is a wide range of natural compounds [56, 57] (including flavonoids, anthraquinones, phenolic acids, stilbenes; see Scheme 11.2) reported in the literature to be able to remodel the hIAPP secondary structure into nontoxic species

NATURAL COMPOUNDS



Scheme 11.2 Classification of the most studied natural polyphenols that are able to inhibit or remodel the hIAPP supramolecular organization

[47, 52, 58–61] and to contribute to control several hallmarks of type-2 diabetes, namely, reduction of the cellular oxidative stress and inflammatory cascade, and to contribute to maintain Ca^{2+} homeostasis, among others [43, 52, 62, 63].

11.4.1 Chemical Inhibition of the hIAPP Aggregation and Modulation of Its Secondary Structure

The exact mechanisms by which natural compounds interact with the different amyloidogenic peptides/proteins are not fully understood and are still a subject of intense research. However, it is known that polyphenols interfere with the aggregation pathway contributing to the reduction of the concentration of toxic oligomers; inhibit fibril elongation; promote the disassembling of preformed fibrils; inhibit amyloid-membrane interactions, which have been reported to be responsible for membrane disruption and for the formation of pores that increase Ca^{2+} transport [43, 64]; as well as contribute to the scavenging of reactive oxygen species (ROS) produced during hIAPP misfolding and/or aggregation [47, 65].

The formation of supramolecular assemblies of amyloid fibers is commonly detected by the fluorescent dye thioflavin T (ThT) – which changes its fluorescence spectrum when bound to the cross- β -sheets of different amyloids [66]. The establishment of this method to monitor amyloid fibril formation (as well as of Congo red, used as an histological stain for amyloids) contributed to the unraveling of the different steps of amyloids' aggregation, as well as to the discovery of a number of natural compounds that are able to interfere with β -sheet-based protein/peptide aggregation. ThT and Congo red have been used to identify the fibrillization of a series of peptides, including A β 40/42 and hIAPP [67]. However, despite the ability of Congo red to bind to the amyloid fibrils, it can also interfere with the aggregation process of several peptides/proteins promoting the formation of oligomers [68]. In the ThT case, it has been demonstrated its capacity to form micelles that specifically bind to

the cross- β -sheet of the amyloid fibers, changing its emission spectra by increasing the emission wavelength of the formed amyloid-ThT complexes [41, 66]. ThT enables a high-throughput analysis using multi-well plates, with real-time characterization of the aggregation kinetics. Moreover, the intensity of the fluorescent signal is considered to be proportional to the concentration of the β -sheet-rich amyloid fibers [66]. Following the variation of the time constant of the typical sigmoidal aggregation curve, it is possible to evaluate the impact of the addition of an inhibitor in the fibrillization kinetics. ThT fluorescence is one of the most widely used techniques to evaluate peptide/protein aggregation; however, it presents some significant disadvantages: (1) it is an indirect method; (2) it has been reported that only parallel β -sheet arrangements can be detected [69]. Given these limitations, it is usually used in association with other methodologies, namely, advanced microscopic techniques, such as transmission electron microscopy (TEM) and atomic force microscopy (AFM). In addition, it has been increasingly common the use of molecular in silico simulations (MD) and NMR predictions to complement the discussions based on results obtained by ThT and microscopic techniques.

In the specific case of hIAPP, it has been reported the ability of natural compounds (such as EGCG, resveratrol, curcumin, oleuropein, among others [52, 54, 55, 70]) to bind to intermediate oligomeric forms, as well to monomers and mature fibrils through non-covalent interactions, e.g., π - π stacking. Therefore, the aromatic component of these natural moieties, e.g., EGCG present two galloyl units in their structure, is an important chemical feature that is at the center of their interference in the β -sheet peptide assembly blocking the growth of the hIAPP fiber or remodeling its supramolecular structure. In addition to π - π stacking, it has been also reported that electrostatic, van der Waals, and solvophobic forces may be also present, fostering weak but important non-covalent interactions between the aromatic part of the natural molecules and the hIAPP hydrophobic regions present both at its backbone and on its side chains [48]. The synergistic effect

of all these forces perturbs the hIAPP's thermodynamic state interfering with its hydrophobic sequence, leading to a disruption of its secondary structure. Finally, the hydroxyl groups present in *ortho* or *para* positions of several polyphenols are fundamental for redox reactions which may have a critical role in their ability to present antioxidant characteristics [47, 71].

All the abovementioned non-covalent interactions have been reported to participate in the perturbation of the hIAPP secondary structure. However, it has been also described that the interference promoted by natural polyphenols may also be driven by hydrogen bonding with the peptide backbone (during the elongation process) and by nonspecific hydrophobic effects with the hIAPP's side chains. As mentioned before, these interactions favor a remodeling of the peptide's secondary structure, likely by decreasing the concentration of cross- β -sheets generating off-

pathway oligomers unable to bind to ThT [41]. This type of remodeling usually leads to a reduction of cytotoxicity, which is in agreement with reports showing that the small early forming oligomers of misfolded hIAPP (thermodynamically unstable) are the main drivers of toxicity and not the larger mature fibers. Thus, having small molecules able to inhibit the formation of cytotoxic oligomers, early in the lag phase, constitutes a promising strategy to minimize cellular damage (through the remodeling of these on-pathway oligomers into off-pathway oligomers) [52] that has been observed by TEM/AFM (example presented in Fig. 11.1) [72].

In addition to the previously listed covalent and non-covalent interactions between the natural molecules and hIAPP, it has been also reported the covalent interactions between the nucleophilic thiols (from the peptide side chain) and amines (from the peptide bonds, as well as the

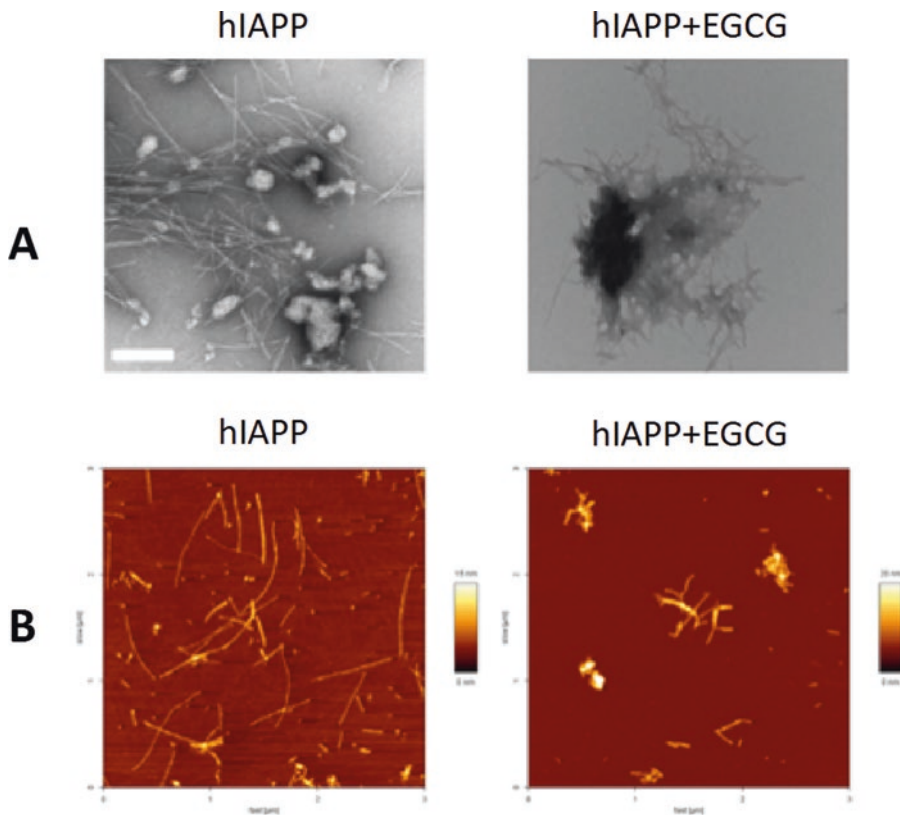


Fig. 11.1 hIAPP fibril formation studied using TEM (a) and AFM (b) in the absence (left) and presence (right) of EGCG. The white bar represents 200 nm [72]

terminal amines) with the electrophilic carbonyls from the o-quinone intermediates and/or aldehyde moieties from the natural polyphenols, leading to a stabilization of hIAPP into non-cytotoxic forms [73, 74].

MD simulation analysis performed by Rao et al. [75] confirmed that curcumin interacts with hIAPP mainly through π - π stacking. The results from MD simulations complemented the Daval et al. [76] data showing that the two phenyl rings of curcumin interact with Val18, Lis16, and Hist14 of the hIAPP sequence by a combination of π - π stacking and hydrophobic effects, as well as hydrogen bonding from the opposite strands of the cross- β spine [52]. In addition, the interplay near His18 is also critical, since several reports note that Hist18 plays a key role in controlling the toxicity of the peptide, by modulating the interactions of hIAPP with the phospholipid membrane at the initial stages of aggregation [21]. Porat et al. [70] confirmed these results by showing that hIAPP oligomeric forms are stabilized by curcumin, through the same mechanism, which inhibits the supramolecular assembly of hIAPP into high-order nanofibers. They also showed that curcumin can intercalate within the hydrophobic core of the peptide, including its interaction with the amino acid residues Leu12, Leu27, Phe5, Phe23, and Tyr37 from the hIAPP sequence [6]. The same type of studies using EGCG showed that hydrophobic interactions between EGCG and hIAPP are at the basis of the inhibition of its aggregation. In addition, it has been shown that the hIAPP disulfide bridge (between Cys2 and Cys7), the presence of free amine groups, or the availability of the tyrosine side chain is not always required for EGCG to inhibit the hIAPP aggregation [77]. In addition to curcumin and EGCG, it is reported that rutin (a polyphenol that comprises quercetin-3-O-rutinoside) and quercetin are able to interact with the amyloidogenic region in hIAPP and suppress β -sheet formation, remodeling the peptide secondary structure into α -helix. This is achieved by the interaction of the polycyclic quercetin group and its metabolites [78]. Moreover, resveratrol presents the same type of activity toward hIAPP, where its two aromatic rings promote strong

aromatic-hydrophobic interactions with the side chain of Arg11 and Arg31 of hIAPP, while its hydroxyl groups participate in hydrogen bonding interactions with the peptide's side chain, as well as the amine groups of several residues [79].

As previously referred, the stabilization of hIAPP by natural compounds can be also promoted by covalent bonding [80]. In this case, polyphenols are able to react with hIAPP through an o-quinone bond mechanism, where the polyphenol is autoxidized into the quinone form and, in turn, forms covalent complexes with hIAPP. EGCG [70] and baicalein [81] are two examples of o-quinone mediated covalent mechanisms based on the oxidation of their galloyl moieties where its activity is enhanced upon oxidation when compared with the freshly prepared form. Myricetin and quercetin are, likewise, also able to form covalent bonds through a similar mechanism, generating o-quinone-Lys adducts, which are responsible for their anti-amyloid activity [73].

All these types of interactions define a large variability of the structural characteristics of the aggregates formed in the presence of polyphenols. Importantly, the time dependence of the aggregation pathway also contributes to increase this variability, as the same polyphenol might contribute with distinct interactions depending on the aggregation state of the peptide. In fact, it has been reported that the particular activity of EGCG is dependent on the time point of the hIAPP aggregation at which it is added. Thus, when it is mixed during the end of the lag phase, small non-fibrillar aggregates with some amorphous content are typically formed. If it is added to the early stages of the nucleation process, the pre-formed β -sheet-containing species are remolded to smaller, thinner aggregates which have a minimal β -sheet character, demonstrating that EGCG may not completely reverse fibrillation into the monomeric state, but it may promote off-pathway oligomers. Finally, when EGCG is mixed with the preformed fibers, the ThT signal is not completely reverted into the initial baseline, which indicates that the nonfibrillar small aggregates formed from the disruption of the hIAPP fibers are morphologically distinct from the aggregates formed

when EGCG is added at the early stages of hIAPP aggregation, supporting its capacity to form non-cytotoxic off-pathway oligomers at early stages of aggregation [60].

11.4.2 Biological Impact of the Modulation of IAPP Aggregation

The ability to remodel the hIAPP supramolecular structure is imperative to be able to rescue cell viability. However, adequate therapeutic approaches can also target the recovery of the normal function of the cell machinery that is affected by the activity of the toxic hIAPP species. It has been reported different perturbations in different cellular processes, namely, dysfunction of the mitochondria and endoplasmic reticulum (ER), driven by alterations in the intracellular redox state; increase in cell membrane permeability, promoting Ca^{2+} imbalance due to the ion pore formation; and membrane disruption promoted by the interaction between the membrane lipids and hIAPP.

The ER is the organelle where protein folding occurs, such as insulin/IAPP. Accumulation of misfolded hIAPP in the ER alters its homeostasis and leads to the unfolded protein response (UPR), an adaptive cellular mechanism, which reduces this overload; however, the continued activation of the UPR has been reported to promote pancreatic β -cell death [82]. The hIAPP accumulation in the cellular environment leads to the activation of autophagy, a protective mechanism against the proteotoxic effect stimulated by the increased aggregate-prone activity of hIAPP [83]. However, the presence of cytotoxic hIAPP aggregates may already increase the enzymatic antioxidant defenses through a RAGE-Nox1-mediated pathway (by glucose auto-oxidation with the production of advanced glycation end products – AGEs) and enhance the signaling of the mechanistic target of rapamycin complex 1 (mTORC1, a natural inhibitor of autophagy) creating a dangerous imbalance [84]. In fact, Hernandez et al. [83] have shown that the hyperactivation of mTORC1 signaling is due to the increased ROS activity

observed in hIAPP-overexpressing cells, which causes a blockage in the mitophagic flux (an autophagic process of damaged and dysfunctional mitochondria). This limited ability to recycle the damaged cellular organelles results in an accumulation of fissioned mitochondria [85]. Under these conditions, a high level of mitochondrial oxidative phosphorylation occurs, and the flow of electrons from the mitochondrial electron transport chain is captured by molecular oxygen and generates ROS. These ROS damage the different components of the mitochondria (e.g., proteins, DNA, its membrane lipids, etc.) and release them in the cytosol. These mitochondrial elements are signaled as danger-associated molecular patterns (DAMPs) by cytosolic pattern recognition receptors, such as inflammasomes. Finally, these inflammasomes (NLRP3) initiate a pyroptotic cascade through cleavage of procaspase-1 into an active form of caspase-1, which produces the inflammatory cytokine interleukin-1 β (an important mediator of the inflammatory response). This biochemical cascade generates nitric oxide radicals (NO \bullet) which react with O_2^- increasing ROS levels and lately inducing inflammation and cell death by pyroptosis [85]. Many other sources of ROS contributing to type-2 diabetes have been described, namely, the overexposure to angiotensin II, which increases NADPH oxidase activity, leading to the production of O_2^- and to the excessive production of ROS [84]. Therefore, the peroxidation of the mitochondria's lipid membrane due to its interaction with hIAPP is a possible trigger of a significant ROS imbalance and one of the contributors to the signaling for β -cell apoptosis.

It has been proposed that once the insulin/hIAPP secretory granules reach the cell's basement membrane and release its content into the extracellular space, hIAPP is converted from a disorder partial α -helical conformation into β -sheet-rich oligomers that interact with the cells' lipid membrane (Scheme 11.1) [86]. As previously mentioned, the hydrophobic and membrane-permeable on-pathway hIAPP oligomers represent the most toxic species [60]. These hIAPP species act in the cell membrane through a detergent-like mechanism, i.e., hIAPP causes

large-scale defects in the lipid bilayer (especially in the presence of anionic lipids), resulting in membrane thinning and fragmentation, accompanied by increased membrane conductance [86].

Therefore, the hIAPP-mediated formation of nonspecific pores, as well as lipid membrane disruption, allows the influx of ions (e.g., Ca^{2+}), which leads to their accumulation at the intracellular space. To restore Ca^{2+} homeostasis, cellular control mechanisms (at the mitochondria and ER) induce an increment of ATP production, and this compensation leads to an additional increment on the intracellular concentration of ROS (as previously described) [87]. The continuing accumulation of ROS in the cellular space contributes to an oxidative environment, which leads to pancreatic β -cell death. In fact, a recent work on the mild exposure of pancreatic cell line to toxic hIAPP oligomers results in a trigger of the antioxidant defenses in a response to transient levels of oxidative stress [88]. Therefore, under this particular cellular environment, which presents increased levels of oxidative stress and the formation of toxic hIAPP species, the use of antioxidant natural polyphenols for the treatment or modulation of type-2 diabetes can be regarded as an interesting multifunctional strategy able to reduce hIAPP toxicity through the inhibition of the formation of on-pathway oligomers, as well as reduce cellular oxidative stress through their antioxidant activity, leading to the restoration of the concentration of intracellular ROS to healthy physiological levels.

EGCG is one of the natural polyphenols more widely studied for its ability to modulate hIAPP cytotoxicity. Different *in vitro* studies have shown that it is able to inhibit the formation of hIAPP β -sheets reducing its cytotoxicity toward pancreatic β -cells [59, 72]. In fact, it has been shown that, in the presence of EGCG and negatively charged lipid bilayers, hIAPP aggregates faster. A possible explanation for this observation is the interaction of EGCG with the lipid bilayer that leads to its insertion in the upper lipid chain region, as well as to the decrease on the packing of the lipids. In a similar fashion, resveratrol has been proposed to interact strongly with the exposed hydrophobic regions of soluble hIAPP,

masking these sites and blocking the interaction between hIAPP and the lipid bilayer. Molecular simulation studies are consistent with these findings, showing that resveratrol is able to inhibit hIAPP fibril elongation on the surface of the cell's basement membrane by altering the secondary structure of hIAPP to an α -helix conformation while blocking the structural transitions (i.e., formation to β -sheet conformations) required for further aggregation [60]. This type of interactions, as the ones described here for hIAPP and EGCG/resveratrol, is not universal when other amyloids are considered. In addition, the efficacy against amyloid aggregation in solution is not a guarantee of activity against membrane-mediated aggregation or pore formation. EGCG and resveratrol present surprisingly different activities in the modulation of hIAPP-induced cellular damage: while EGCG presents a higher capacity to reduce the cytotoxicity of amyloidogenic peptides and modulate their secondary structure, in the specific case of hIAPP, resveratrol is more efficient than EGCG in reducing the cytotoxicity of its oligomers toward pancreatic β -cells [89]. It has been also shown that pancreatic β -cells that overexpress hIAPP benefit from the presence of resveratrol through the (1) reduction of TSC2 nitration levels, a marker of oxidative stress; (2) ameliorated MTORC1 activation, a signaling pathway to suppress the autophagy system, important for the clearance of misfolded proteins; and (3) enhanced MAP1LC3 lipidation levels, which indicates the restoration of autophagy degradation system and recovery of intracellular homeostasis [83].

In addition to EGCG and resveratrol, there are other natural compounds that have been evaluated for their ability to act in the pathological mechanisms that lead to hIAPP cytotoxicity and type-2 diabetes. In the case of myricetin, it has been shown that it is able to lower hIAPP fibrillization with similar outcomes as EGCG. It has been also shown that it enhances early pore formation; however, in latter stages, it suppresses fibril growth on the surface of the lipid membrane [60]. Curcumin has been also reported to protect pancreatic β -cells against hIAPP toxicity; however, curcumin itself becomes cytotoxic at micro-

molar concentrations. In fact, despite the ability of curcumin to inhibit hIAPP aggregation and the capacity to partially protect INS cells from exogenous hIAPP toxicity, it has been shown that due to its cytotoxicity, it is unlikely to be therapeutically useful for controlling type-2 diabetes [76]. Oleuropein is another natural polyphenol able to remodel hIAPP secondary structure during its aggregation pathway, avoiding the formation of toxic oligomeric forms, consistently preventing hIAPP cytotoxicity on RIN-5F pancreatic β -cells. The mechanism of its protective role is reported to be the interference on the interaction between the cell basement membrane and hIAPP cytotoxic species, which occurs exclusively through the interaction of oleuropein and the cell membrane, as shown by fluorescence microscopy and synthetic lipid vesicle permeabilization studies [55]. Finally, quercetin [64] and baicalein [81] have been also reported to reduce the hIAPP-induced cytotoxicity toward INS-1 β -cells in a dose-dependent manner through an antioxidant mechanism and remodeling of the hIAPP secondary structure.

In this section, we gave a brief overview of some of the most studied natural polyphenols able to inhibit or modulate the hIAPP aggregation while controlling the subsequent biochemical cascade of events that lead to pancreatic β -cell dysfunction/death. However, many other natural polyphenols have been proposed as direct inhibitors of hIAPP aggregation, as well as of other aggregation-prone peptides and proteins, such as A β 42 or alpha-synuclein related to AD and Parkinson disease, respectively [40, 90].

11.4.3 In Vivo Evaluation Studies

The reported biophysical studies are based on *in vitro* reductionist approaches that not always can be translated to the *in vivo* setting. However, the *in vitro* cell culture experiments report the ability of several natural polyphenols to ameliorate the hallmarks of type-2 diabetes, leading to their evaluation under different animal models. These *in vivo* studies typically use transgenic mice, whose pancreatic β -cells overexpress

hIAPP. This is an essential requirement because the ability for IAPP to aggregate *in vitro* is species dependent. For example, the cat and human IAPP sequences oligomerize and form fibrils in a timeframe of hours, while others, such as the rat/mice and pig sequences, have low propensity to form amyloid aggregates [91]. These hIAPP transgenic animals (e.g., tg-mice) are able to present several type-2 diabetes features, namely, high blood glucose, reduced levels of insulin in the blood, high glucagon levels, and hIAPP fibrillar deposits [92].

The described animal model has been used to evaluate the ability of different polyphenols to modulate the reported type-2 diabetes hallmarks. In this context, EGCG is one of the most studied natural polyphenols due to its previously described *in vitro* ability to rescue pancreatic β -cell dysfunction and death, upon exposure to cytotoxic levels of hIAPP [93, 94]. Franko et al. [72] showed that the *in vivo* administration of EGCG reduced fibril formation in nondiabetic tg-mice. However, no significant changes were observed in the deposition of hIAPP aggregates in the pancreas of diabetic tg-mice animals, after treatment with EGCG during 3 weeks, which might be related with the EGCG low dose. The authors speculate that in diabetic tg-mice, it might be necessary higher doses of EGCG to achieve an effective reduction of hIAPP aggregation in the pancreas. Additional *in vivo* studies report the ability of different natural polyphenols (e.g., rutin, quercetin, and resveratrol) to modulate insulin resistance, oxidative stress, or pancreatic β -cell mass. The oral administration of rutin conducted on hemizygous hIAPP tg-mice doubled their long-term survival, prevented the loss of bodyweight (reducing the severity of the disease), and delayed the increment of blood glucose, reflecting a decrease in the rate of the progression of the disease [78]. In another study, quercetin improved enzymatic markers for oxidative stress, decreased lipid peroxidation, lowered plasma glucose and glycated hemoglobin, and finally reduced oxidative stress in streptozotocin-induced diabetic rats [62]. Resveratrol has been also tested, and it was able to improve the glucose tolerance in diabetic mice,

with a significant increase in both the pancreas weight and β -cell mass. It is also able to reduce oxidative stress, through the modulation of 8-OHdG levels (a marker for ROS), accompanied by a significant decrease on islet fibrosis [95, 96].

The reported *in vivo* studies confirm the ability of natural polyphenols to modulate the hallmarks of type-2 diabetes and control the progression of the disease. Moreover, there are an increasing number of studies that consistently link type-2 diabetes (and hIAPP) with AD. In fact, *in vitro* studies have shown that modifications in the hIAPP C-terminal or the reduction of its C2-C7 disulfide bond decreases its biological activity and the formation of toxic on-pathway oligomers [34]. Such oligomers are known to form deposits in peripheral organs in type-2 diabetes patients, in particular in the brain of patients that present both type-2 diabetes and AD. These findings may lead in the near future to the publication of a significant number of *in vivo* studies to evaluate the link between type-2 diabetes (or hIAPP) and AD, as well as to better understand the role of hIAPP in brain functions, such as controlling appetite and cognition [97].

11.4.4 Clinical Trials Using Natural Compounds

There are a series of *in vivo* studies that evaluate the ability of natural polyphenols to modulate the hallmarks of type-2 diabetes with important positive outcomes; however, their translation into clinical trials has been limited. The human clinical studies reported until now are mainly focused on EGCG, which has been shown to present beneficial effects on type-2 diabetes, through the recovery of normoglycemia (i.e., maintenance of physiological levels of blood glucose) and hemoglobin levels; however these observations were not universal, i.e., some trials present contradictory outcomes [47]. Resveratrol, one of the main polyphenols in red wine, has been also evaluated on its ability to modulate endothelial function in patients with type-2 diabetes [43]. Clinical trials to test the efficacy of quercetin to lower blood glucose and blood vessel function in type-2 diabetes

have been also conducted [64]. Most of the clinical trials performed until now are based on the ability of the compounds to ameliorate the markers of type-2 diabetes, e.g., blood glucose levels, etc.; however, the source of this outcomes is usually not evaluated in detail. In this context, it is missing clinical results that link the modulation of the disease progression with the ability to inhibit the aggregation/oligomerization of hIAPP in the pancreas of type-2 diabetes patients. In contrast to type-2 diabetes, there are a significant number of clinical trials testing the ability of natural polyphenols to improve the clinical outcome of other amyloid-based disorders (e.g., AD). In fact for the AD case, it has been evaluated under clinical trials the ability of natural polyphenols (e.g., EGCG, resveratrol, curcumin, among others) to inhibit the aggregation of amyloid- β and Tau [48].

11.5 Conclusions

Type-2 diabetes is a multifactorial disease characterized by the deposition of misfolded hIAPP in the pancreas, high blood glucose levels, impaired glucose tolerance, and increased stress on pancreatic islets, among other hallmarks. It is relevant to point out that, while contributing to the development of type-2 diabetes, misfolded oligomeric hIAPP species may also be involved in the onset and progression of AD and cardiovascular diseases. The central role of hIAPP in the type-2 diabetes has been suggested by a vast number of studies, making it an important target for the development of drugs able to control the progression of the disease. In this context, natural polyphenols are well-tolerated compounds, which are widely available in different foods used in the human diet. Some of them have been proven to present antidiabetic activity. In fact, polyphenols, in addition to their anti-hyperglycemic effects, are also antioxidant and anti-inflammatory molecules, which are able to ameliorate glucose metabolism and β -cell function and reduce insulin resistance. Importantly, they are able to remodel hIAPP supramolecular assemblies and reduce the cytotoxicity of on-pathway oligomers toward pancreatic β -cells.

The use of natural polyphenols is a promising therapeutic approach to control type-2 diabetes due to the presence of phenolic rings, which are at the basis of their ability to inhibit hIAPP oligomerization. In addition, it is important to highlight the fact that the hIAPP-polyphenol complexes are able to prevent different pathological events, in the intracellular environment of the pancreatic β -cells, such as decreasing the ROS imbalance, preventing the mitochondria and ER dysfunction, and reduction of the inflammatory cascade (Table 11.1). In addition, it is relevant to note that the antioxidant properties of the polyphenol (ROS scavenging) have been associated with the reduced risk of developing type-2 diabetes; however further research to clarify the mechanisms behind this observation is required.

Most of the bioactivities of natural polyphenols and their interaction with hIAPP have been confirmed under *in vitro* studies. However, it is still lacking a more extensive number of *in vivo* studies to be able to further clarify the ability of these compounds to act under complex biological environments. Finally, there is a clear lack of clinical trials (with individuals diagnosed with prediabetes and type-2 diabetes) to be able to evaluate

and clarify the specific mechanisms of action of the natural polyphenols. Other important points to consider are as follows: the bioactivities are dependent on the type and class of polyphenol; there is a clear dose-dependent activity which might hinder their use in the type-2 diabetes context; and it has been proposed the use of polyphenol-rich diet in type-2 diabetes patients; however, it is important to evaluate their bioavailability following dietary intake to evaluate about the suitability of this approach. Finally, several reports show that the activity of natural polyphenols in the aggregation of hIAPP and their ability to control the progression of the disease are dependent on the stage at which the administration starts, *i.e.*, early versus late stages of the disease. Overall, natural polyphenols have demonstrated benefits in controlling the progression of type-2 diabetes; however, the translation from the *in vitro* studies to *in vivo* and clinical trials has not been straightforward. A significant number of new studies closer to the clinical practice are expected in the near future to complement the positive *in vitro* experimental evidences and to evaluate if these compounds are able to perform under complex biological environments.

Table 11.1 Comparison of the bioactivity of different natural compounds for distinct type-2 diabetes-related targets under chemical, biological, *in vivo*, and clinical assessments

Classification	Compounds	Activity/outcome	Methods/target	References
Chemical	EGCG Oleuropein Resveratrol Curcumin	Remodeling of the hIAPP's supramolecular assemblies; disruption of hIAPP secondary structure	Remodeling of the supramolecular assembly; ThT assay; AFM; TEM; CD	[47, 52, 54, 55, 60, 70–74]
Biological	EGCG Oleuropein Resveratrol Curcumin	Improves enzymatic antioxidant defenses; inhibition of ROS imbalance; ameliorate inflammatory cascade; improves autophagy homeostasis	Antioxidant imbalance; RAGE-Nox1-mediated pathway; inflammasomes (NLRP3) initiate a pyroptotic cascade; rapamycin complex 1 (mTORC1)	[55, 59, 60, 64, 72, 76, 81, 85, 90]
<i>In vivo</i>	EGCG Rutin Quercetin Resveratrol	Reduction of hIAPP intermediate species formation; modulate insulin resistance, oxidative stress, or pancreatic β -cell mass: Decreased lipid peroxidation, lowered plasma glucose and glycated hemoglobin, and reduced oxidative stress	Diabetic tg-mice: monitor weight and glucose; postmortem analysis; RAGE-Nox1-mediated pathway; rapamycin complex 1 (mTORC1); inflammasomes (NLRP3) – pyroptotic cascade	[62, 72, 78, 94–97]
Clinical studies	EGCG Resveratrol Quercetin	Recovery of normoglycemia and hemoglobin levels; modulation of the endothelial function; lower blood glucose and blood vessel function	Clinical observations	[43, 47, 48, 64]

Acknowledgments The authors acknowledge the financial support from the European Commission's H2020 program, under grant agreements H2020-WIDESPR EAD-2014-668983-FORECAST and H2020-WIDE SPREAD-01-2016-2017-739572-THE DISCOVERIES CTR. ARA acknowledges Norte2020, NORTE-08-5369-FSE-000037, for her PhD grant.

References

1. Westermark P, Wilander E, Westermark GT, Johnson KH (1987) Islet amyloid polypeptide-like immunoreactivity in the islet B-cells of Type-2 (non-insulin-dependent) diabetic and nondiabetic individuals. *Diabetologia* 30:887–892
2. WHO Regional office for Europe (2019) Data and statistics. <http://www.euro.who.int/en/health-topics/noncommunicable-diseases/diabetes/data-and-statistics>. Accessed 12 Dec 2019
3. Valensi P, Schwarz EH, Hall M et al (2005) Pre-diabetes essential action: a European perspective. *Diabetes Metab* 31:606–620
4. Pillay K, Govender P (2013) Amylin uncovered: a review on the polypeptide responsible for type II diabetes. *Biomed Res Int* 2013:826706
5. Schwarz PEH, Lindström J, Kissimova-Scarbeck K et al (2008) The European perspective of type 2 diabetes prevention: diabetes in Europe – prevention using lifestyle, physical activity and nutritional intervention (DE-PLAN) project. *Exp Clin Endocrinol Diabetes* 116:167–172
6. Grizzanti J, Corrigan R, Servizi S et al (2019) Amylin signaling in diabetes and Alzheimer's disease: therapy or pathology? *J Neurol Neuromed* 4:12–19
7. Abedini A, Plesner A, Cao P et al (2016) Time-resolved studies define the nature of toxic IAPP intermediates, providing insight for anti-amyloidosis therapeutics. *elife* 5:e12977
8. Kruger DF, Gatcomb PM, Owen SK (1999) Clinical implications of amylin and amylin deficiency. *Diabetes Educ* 25:389–397
9. Morris MJ, Nguyen T (2001) Does neuropeptide Y contribute to the anorectic action of amylin? *Peptides* 22:541–546
10. Pithadia A, Brender JR, Fierke CA (2016) Inhibition of IAPP aggregation and toxicity by natural products and derivatives. *J Diabetes Res* 2016:2046327
11. Hoppener JWM, Ahren B, Lips CJM (2000) Islet amyloid and type 2 diabetes mellitus. *New Engl J Med* 343:411–419
12. Milardi D, Sciacca MFM, Randazzo L et al (2014) The role of calcium, lipid membranes and islet amyloid polypeptide in the onset of type 2 diabetes: innocent bystanders or partners in a crime? *Front Endocrinol* 5:216
13. Opie EL (1901) On the relation of chronic interstitial pancreatitis to the islands of Langerhans and to diabetes mellitus. *J Exp Med* 5:397–428
14. Verchere CB, D'Alessio DA, Palmiter RD et al (1996) Islet amyloid formation associated with hyperglycemia in transgenic mice with pancreatic beta cell expression of human islet amyloid polypeptide. *Nat Acad Sci* 93:3492–3496
15. Lorenzo A, Razzaboni B, Weir GC et al (1994) Pancreatic-islet cell toxicity of amylin associated with Type-2 diabetes-mellitus. *Nature* 368:756–760
16. Gurlo T, Ryazantsev S, Huang CJ et al (2010) Evidence for proteotoxicity in beta cells in Type 2 diabetes toxic islet amyloid polypeptide oligomers form intracellularly in the secretory pathway. *Am J Pathol* 176:861–869
17. Despa F, DeCarli C (2013) Amylin: what might be its role in Alzheimer's disease and how could this affect therapy? *Expert Rev Proteomics* 10:403–405
18. Miller K, Zerze GH, Mittal J (2013) Molecular simulations indicate marked differences in the structure of amylin mutants, correlated with known aggregation propensity. *J Phys Chem B* 117:16066–16075
19. Anguiano M, Nowak RJ, Lansbury PT (2002) Protofibrillar islet amyloid polypeptide permeabilizes synthetic vesicles by a pore-like mechanism that may be relevant to type II diabetes. *Biochemistry* 41:11338–11343
20. Scalisi S, Sciacca MF, Zhavnerko G et al (2010) Self-assembling pathway of HiApp fibrils within lipid bilayers. *Chembiochem* 11:1856–1859
21. Brender JR, Hartman K, Reid KR et al (2008) A single mutation in the nonamyloidogenic region of islet amyloid polypeptide greatly reduces toxicity. *Biochemistry* 47:12680–12688
22. Masters SL, Dunne A, Subramanian SL et al (2010) Activation of the NLRP3 inflammasome by islet amyloid polypeptide provides a mechanism for enhanced IL-1 beta in type 2 diabetes. *Nat Immunol* 11:897
23. Westermark P, Andersson A, Westermark GT (2011) Islet amyloid polypeptide, islet amyloid, and diabetes mellitus. *Physiol Rev* 91:795–826
24. de la Monte SM, Wade JD (2008) Alzheimer's disease is type 3 diabetes – evidence reviewed. *J Diabetes Sci Technol* 2:1101–1113
25. Jackson K, Barisone GA, Diaz E et al (2013) Amylin deposition in the brain: a second amyloid in Alzheimer disease? *Ann Neurol* 74:517–526
26. Alzheimer A (1907) Über eine eigenartige Erkrankung der Hirnrinde. *Zentralbl Nerven Psych* 64:146–148
27. Gupta V, Gupta VB, Chitranshi N et al (2016) One protein, multiple pathologies: multifaceted involvement of amyloid beta in neurodegenerative disorders of the brain and retina. *Cell Mol Life Sci* 73:4279–4297
28. Aguzzi A, O'Connor T (2010) Protein aggregation diseases: pathogenicity and therapeutic perspectives. *Nat Rev Drug Discov* 9:237–248
29. Jaikaran ETAS, Higham CE, Serpell LC et al (2001) Identification of a novel human islet amyloid polypeptide beta-sheet domain and factors influencing fibrillogenesis. *J Mol Biol* 308:515–525

30. Hirakura Y, Kagan BL (2001) Pore formation by beta-2-microglobulin: a mechanism for the pathogenesis of dialysis associated amyloidosis. *Amyloid* 8:94–100
31. Eisele YS, Monteiro C, Fearn C et al (2015) Targeting protein aggregation for the treatment of degenerative diseases. *Nat Rev Drug Discov* 14:759–780
32. Quist A, Doudevski I, Lin H et al (2005) Amyloid ion channels: a common structural link for protein-misfolding disease. *PNAS* 102:10427–10432
33. Powers ET, Balch WE (2013) Diversity in the origins of proteostasis networks – a driver for protein function in evolution. *Nat Rev Mol Cell Biol* 14:237–248
34. DeToma AS, Salamekh S, Ramamoorthy A et al (2012) Misfolded proteins in Alzheimer's disease and type II diabetes. *Chem Soc Rev* 41:608–621
35. Dobson CM (2003) Protein folding and misfolding. *Nature* 426:884–890
36. Soong R, Brender JR, Macdonald PM et al (2009) Association of highly compact type II diabetes related islet amyloid polypeptide intermediate species at physiological temperature revealed by diffusion NMR spectroscopy. *ACS* 131:7079–7085
37. Yonemoto IT, Kroon GJA, Dyson HJ et al (2008) Amylin proprotein processing generates progressively more amyloidogenic peptides that initially sample the helical state. *Biochemistry* 47:9900–9910
38. Chaffotte AF, Guijarro JI, Guillou Y et al (1997) The “pre-molten globule,” a new intermediate in protein folding. *J Protein Chem* 16:433–439
39. Zhang S, Andreasen M, Nielsen JT et al (2013) Coexistence of ribbon and helical fibrils originating from hIAPP(20–29) revealed by quantitative nanomechanical atomic force microscopy. *PNAS* 110:2798–2803
40. Bieschke J, Russ J, Friedrich RP et al (2010) EGCG remodels mature alpha-synuclein and amyloid-beta fibrils and reduces cellular toxicity. *PNAS* 107:7710–7715
41. Giorgetti S, Greco C, Tortora P et al (2018) Targeting amyloid aggregation: an overview of strategies and mechanisms. *Int J Mol Sci* 19:2677
42. Porat Y, Abramowitz A, Gazit E (2005) Inhibition of amyloid fibril formation by polyphenols: structural similarity and aromatic interactions as a common inhibition mechanism. *Chem Biol Drug Des* 67:27–37
43. Sgarbossa A (2012) Natural biomolecules and protein aggregation: emerging strategies against amyloidogenesis. *Int J Mol Sci* 13:17121–17137
44. Stefani M, Dobson CM (2003) Protein aggregation and aggregate toxicity: new insights into protein folding, misfolding diseases and biological evolution. *J Mol Med* 81:678–699
45. Moreira PI, Santos MS, Moreno A et al (2002) Effect of amyloid beta-peptide on permeability transition pore: a comparative study. *J Neurosci Res* 69:257–267
46. Sequeira IR, Poppitt SD (2017) Unfolding novel mechanisms of polyphenol flavonoids for better glycaemic control: targeting pancreatic islet amyloid polypeptide (IAPP). *Nutrients* 9(7):788
47. Molino S, Dossena M, Buonocore D et al (2016) Polyphenols in dementia: from molecular basis to clinical trials. *Life Sci* 161:69–77
48. Cheng B, Gong H, Xiao H et al (2013) Inhibiting toxic aggregation of amyloidogenic proteins: a therapeutic strategy for protein misfolding diseases. *Biochim Biophys Acta* 1830:4860–4871
49. Quideau S, Deffieux D, Douat-Casassus C et al (2011) Plant polyphenols: chemical properties, biological activities, and synthesis. *Angew Chem Int Ed Eng* 50:586–621
50. Crozier A, Jaganath IB, Clifford MN (2009) Dietary phenolics: chemistry, bioavailability and effects on health. *Nat Prod Rep* 26:1001–1043
51. Cooper AJ, Sharp SJ, Lentjes MA et al (2012) A prospective study of the association between quantity and variety of fruit and vegetable intake and incident type 2 diabetes. *Diabetes Care* 35:1293–1300
52. Nedumpully-Govindan P, Kakinen A, Pilkington EH et al (2016) Stabilizing off-pathway oligomers by polyphenol nanoassemblies for IAPP aggregation inhibition. *Sci Rep* 6:19463
53. Stefani M, Rigacci S (2014) Beneficial properties of natural phenols: highlight on protection against pathological conditions associated with amyloid aggregation. *Biofactors* 40:482–493
54. Ngoungoure VL, Schluesener J, Moundipa PF et al (2015) Natural polyphenols binding to amyloid: a broad class of compounds to treat different human amyloid diseases. *Mol Nutr Food Res* 59:8–20
55. Rigacci S, Guidotti V, Bucciantini M et al (2010) Oleuropein aglycon prevents cytotoxic amyloid aggregation of human amylin. *J Nutr Biochem* 21:726–735
56. Velander P, Wu L, Henderson F et al (2017) Natural product-based amyloid inhibitors. *Biochem Pharmacol* 139:40–55
57. Zhang H, Tsao R (2016) Dietary polyphenols, oxidative stress and antioxidant and anti-inflammatory effects. *Curr Opin Food Sci* 8:33–42
58. Cao P, Raleigh DP (2012) Analysis of the inhibition and remodeling of islet amyloid polypeptide amyloid fibers by flavanols. *Biochemistry* 51:2670–2683
59. Meng F, Abedini A, Plesner A et al (2010) The flavanol (-)-epigallocatechin 3-gallate inhibits amyloid formation by islet amyloid polypeptide, disaggregates amyloid fibrils, and protects cultured cells against IAPP-induced toxicity. *Biochemistry* 49:8127–8133
60. Pithadia A, Brender JR, Fierke CA et al (2016) Inhibition of IAPP aggregation and toxicity by natural products and derivatives. *J Diabetes Res* 2016:2046327
61. Young LM, Cao P, Raleigh DP et al (2013) Ion mobility spectrometry-mass spectrometry defines the oligo-

- meric intermediates in amylin amyloid formation and the mode of action of inhibitors. *J Am Chem Soc* 136:660–670
62. Coskun O, Kanter M, Korkmaz A et al (2005) Quercetin, a flavonoid antioxidant, prevents and protects streptozotocin-induced oxidative stress and beta-cell damage in rat pancreas. *Pharmacol Res* 51:117–123
 63. Jiang P, Li W, Shea JE et al (2011) Resveratrol inhibits the formation of multiple-layered beta-sheet oligomers of the human islet amyloid polypeptide segment 22–27. *Biophys J* 100:550–1558
 64. López L, Varea O, Navarro S et al (2016) Benzofuranone, quercetin, and folic acid inhibit amylin aggregation. *Int J Mol Sci* 17:964
 65. Gazit E (2002) A possible role for pi-stacking in the self-assembly of amyloid fibrils. *FASEB J* 16:77–83
 66. Khurana R, Coleman C, Lonescu-Zanetti C et al (2005) Mechanism of thioflavin T binding to amyloid fibrils. *J Struct Biol* 151:229–238
 67. Vassar PS, Culling CF (1959) Fluorescent stains, with special reference to amyloid and connective tissues. *Arch Pathol* 68:487–498
 68. Khurana R, Uversky VN, Nielsen L et al (2001) Is Congo red an amyloid-specific dye? *J Biol Chem* 276:22715–22721
 69. Abeyawardhane DL, Fernández RD, Murgas CJ et al (2018) Iron redox chemistry promotes antiparallel oligomerization of alpha-synuclein. *J Am Chem Soc* 140:5028–5032
 70. Porat Y, Abramowitz A, Gazit E (2006) Inhibition of amyloid fibril formation by polyphenols: structural similarity and aromatic interactions as a common inhibition mechanism. *Chem Biol Drug Des* 67:27–37
 71. Bagli E, Goussia A, Moschos MM et al (2016) Natural compounds and neuroprotection: mechanisms of action and novel delivery systems. *In Vivo* 30:535–547
 72. Franko A, Camargo DCR, Böddrich A et al (2018) Epigallocatechin gallate (EGCG) reduces the intensity of pancreatic amyloid fibrils in human islet amyloid polypeptide (hIAPP) transgenic mice. *Sci Rep* 8:1116
 73. Sato M, Murakami K, Uno M et al (2013) Site-specific inhibitory mechanism for amyloid beta42 aggregation by catechol-type flavonoids targeting the Lys residues. *J Biol Chem* 288:23212–23224
 74. Tanaka T, Matsuo Y, Kouno I (2010) Chemistry of secondary polyphenols produced during processing of tea and selected foods. *Int J Mol Sci* 11:14–40
 75. Rao PP, Mohamed T, Teckwani K et al (2015) Curcumin binding to beta amyloid: a computational study. *Chem Biol Drug Des* 86:813–820
 76. Daval M, Bedrood S, Gurlo T et al (2010) The effect of curcumin on human islet amyloid polypeptide misfolding and toxicity. *Amyloid* 17:118–128
 77. Mo Y, Lei J, Sun Y et al (2016) Conformational ensemble of hIAPP dimer: insight into the molecular mechanism by which a green tea extract inhibits hIAPP aggregation. *Sci Rep* 6:33076
 78. Aitken JF, Loomes KM, Riba-garcia I et al (2017) Rutin suppresses human-amylin/hIAPP misfolding and oligomer formation in-vitro, and ameliorates diabetes and its impacts in human-amylin/hIAPP transgenic mice. *Biochem Biophys Res Commun* 482:625–631
 79. Wang Q, Ning L, Niu Y et al (2014) Molecular mechanism of the inhibition and remodeling of human islet amyloid polypeptide (hIAPP1–37) oligomer by resveratrol from molecular dynamics simulation. *J Phys Chem B* 119:15–24
 80. Gersch M, Kreuzer J, Sieber SA (2012) Electrophilic natural products and their biological targets. *Nat Prod Rep* 29:659–682
 81. Velander P, Wu L, Ray WK et al (2016) Amylin amyloid inhibition by flavonoid baicalein: key roles of its vicinal dihydroxyl groups of the catechol moiety. *Biochemistry* 55:4255–4258
 82. Herbert TP, Laybutt DR (2016) A reevaluation of the role of the unfolded protein response in islet dysfunction: maladaptation or a failure to adapt? *Diabetes* 65:1472–1480
 83. Hernandez MG, Aguilar AG, Burillo J et al (2018) Pancreatic beta cells overexpressing hIAPP impaired mitophagy and unbalanced mitochondrial dynamics. *Cell Death Dis* 9:481
 84. Borch E, Bargelli V, Guidotti V et al (2014) Mild exposure of RIN-5F beta-cells to human islet amyloid polypeptide aggregates upregulates antioxidant enzymes via NADPH oxidase-RAGE: an hormetic stimulus. *Redox Biol* 2:114–122
 85. Volpe CMO, Villar-Delfino PH, dos Anjos PMF et al (2018) Cellular death, reactive oxygen species (ROS) and diabetic complications. *Cell Death Dis* 9:119
 86. Gao M, Winter R (2015) The effects of lipid membranes, crowding and osmolytes on the aggregation, and fibrillation propensity of human IAPP. *J Diabetes Res* 2015:849017
 87. Sciacca MFM, Monaco I, La Rosa C et al (2018) The active role of Ca(2+) ions in Abeta-mediated membrane damage. *Chem Commun* 54:3629–3631
 88. Wu L, Velander P, Liu D et al (2017) Olive component oleuropein promotes beta-cell insulin secretion and protects beta-cells from amylin amyloid-induced cytotoxicity. *Biochemist* 56:5035–5039
 89. Lolicato F, Raudino A, Milardi D et al (2015) Resveratrol interferes with the aggregation of membrane-bound human-IAPP: a molecular dynamics study. *Eur J Med Chem* 92:876–881
 90. Wobst HJ, Sharma A, Diamond MI et al (2015) The green tea polyphenol (-)-epigallocatechin gallate prevents the aggregation of tau protein into toxic

- oligomers at substoichiometric ratios. *FEBS Lett* 589:77–83
91. Chakraborty S, Chatterjee B, Basu S (2012) A mechanistic insight into the amyloidogenic structure of hIAPP peptide revealed from sequence analysis and molecular dynamics simulation. *Biophys Chem* 168–169:1–9
 92. Janson J, Soeller WC, Roche PC et al (1996) Spontaneous diabetes mellitus in transgenic mice expressing human islet amyloid polypeptide. *PNAS* 93:7283–7288
 93. Ortsater H, Grankvist N, Wolfram S et al (2012) Diet supplementation with green tea extract epigallocatechin gallate prevents progression to glucose intolerance in db/db mice. *Nutr Metab* 9:11
 94. Zhang Z, Ding Y, Dai X et al (2011) Epigallocatechin-3-gallate protects pro-inflammatory cytokine induced injuries in insulin-producing cells through the mitochondrial pathway. *Eur J Pharmacol* 670:311–316
 95. Szkudelski T, Szkudelska K (2011) Anti-diabetic effects of resveratrol. *Ann N Y Acad Sci* 1215:34–39
 96. Lee YE, Kim JW, Lee EM et al (2012) Chronic resveratrol treatment protects pancreatic islets against oxidative stress in db/db mice. *PLoS One* 7:e50412
 97. Schultz N, Janelidze S, Byman E et al (2019) Levels of islet amyloid polypeptide in cerebrospinal fluid and plasma from patients with Alzheimer's disease. *PLoS One* 14:e0218561



Recent Advances of Biphasic Calcium Phosphate Bioceramics for Bone Tissue Regeneration

12

Sung Eun Kim and Kyeongsoon Park

Abstract

Biphasic calcium phosphate bioceramics consist of an intimate mixture of hydroxyapatite (HA) and beta-tricalcium phosphate (β -TCP) in varying ratios. Due to their biocompatibility, osteoconductivity, and safety in in vitro, in vivo, and clinical models, they have become promising bone substitute biomaterials and are recommended for use as alternatives for or as additives in bone tissue regeneration in various orthopedic and dental applications. Many studies have demonstrated the potential uses of BCP bioceramics as scaffolds for tissue engineering. Here, we highlight the recent advances in the uses of BCP bioceramics and functionalized BCPs for bone tissue regeneration.

Keywords

Marked BCP · Injectable BCP/polymer · Osteoinductive growth factors · Drug delivery · Osseointegration

12.1 Introduction

Bone tissue regeneration is a complex and well-orchestrated process of biological events of bone induction and conduction to optimize skeletal repair and restore skeletal function [1]. Currently, autografts and allografts are commonly performed and are considered as the gold standard for bone replacement surgery. However, their clinical applications are still challenging due to several disadvantages, such as the limited supply of donor bone graft, a secondary trauma for autograft, and the immune reactions against the allograft [2].

Synthetic or natural bioceramics with properties similar to native bone have been developed as alternatives to autografts or allografts for bone replacement. The most common bioceramics are calcium phosphate (CaP)-based biomaterials, including hydroxyapatite (HA), α - and β -tricalcium phosphates (α -TCP, β -TCP), octacalcium phosphate (OCP), amorphous calcium phosphate (ACP), and biphasic calcium phosphates (BCP) [3, 4]. Due to their biocompatibility, safety, availability, low morbidity, and cost-effectiveness over autografts and allografts,

S. E. Kim

Department of Orthopedic Surgery and Rare Diseases Institute, Korea University Medical College, Korea University Guro Hospital, Seoul, Republic of Korea
e-mail: sekim10@korea.ac.kr

K. Park (✉)

Department of Systems Biotechnology, Chung-Ang University, Anseong-si, Gyeonggi-do, Republic of Korea
e-mail: kspark1223@cau.ac.kr

these CaP bioceramics are commonly used for medical and dental applications, such as treatment of bone defects and fracture, joint replacement, dental implants, and periodontal therapy [5].

BCPs consist of a more stable hydroxyapatite [HA, $\text{Ca}_{10}(\text{PO}_4)_6(\text{OH})_2$] and a more soluble beta-tricalcium phosphate [β -TCP, $\text{Ca}_3(\text{PO}_4)_2$] in different proportions. Among the CaP biomaterials, BCPs have significant advantages over other CaP materials. Variations in the HA/ β -TCP ratio can modulate their bioactivity and balance between resorption and solubilization which guarantees the stability of the biomaterials while promoting bone ingrowth [6]. However, their inherent brittleness is not suitable in load-bearing bone applications [7]. Despite their brittleness, depending on the ratio of HA and β -TCP, various BCP ceramics can be obtained for the application to large bone defects as well as customized pieces [8]. Additionally, owing to their suitable degradation rates and chemical similarity to the mineral phase of the bone, they have common clinical applications in the fields of dental and orthopedic surgery [6, 9, 10]. Previous studies have shown that BCP-based materials have osteoconductive properties in a specific HA/ β -TCP ratio, leading to enhanced osteoblast proliferation and osteogenic differentiation [11–14]. In addition to osteoconductivity, BCP-based materials have osteoinductivity, that is, the property of graft materials in which it induces de novo bone formation with biomimetic substances such as bone morphogenic proteins (BMPs). Indeed, recent study suggested that the optimization of the material characteristics can endow biomaterials with osteoinductive ability [15]. Indeed, the researchers showed that BCP (30% HA and 70% β -TCP) promoted much greater expression of BMP-2 and showed higher osteoinductivity in vivo than BCP (70% HA and 30% β -TCP), pure β -TCP, and HA [15]. However, BCP-based scaffolds still have a limitation toward new bone formation due to their lack of intrinsic osteoinductivity.

To enlarge the application of BCPs in bone tissue regeneration, many researches have focused on the development of the functionalized BCP scaffolds by combining with various polymers

and adding bioactive factors. In this chapter, we describe the characteristics of BCPs and marketed BCP products. Also, we review the latest advances in the study of various functionalized BCPs for enhancing bone tissue regeneration.

12.2 Characteristics of BCPs

BCPs are composed of two phases such as a more stable HA and a more soluble β -TCP in different ratios. As a first phase, HA is ideal material for bone substitute and is commonly used because of its similarity to the mineral phase of the bone and better mechanical properties. However, the bioresorption of a more stable HA is slower than other CaP such as TCP. These non-resorbable and bioinert properties of HA lead to incomplete remodeling of the bone [16]. Thus, HA is usually combined with other bioresorbable bone phases at an appropriate ratio because its bioresorption rates can be controlled by the HA/TCP ratio. As a second phase, β -TCP is generally selected because it has a higher chemical stability and biodegradation rate [17]. The composite BCP ceramics, comprising a mixture of HA with good osteoconductivity and β -TCP with high resorption, proved to be highly biocompatible with good osteoconductive properties in specific ratios of HA/ β -TCP [11, 18]. By manipulating the HA/ β -TCP composition ratios, it is possible to optimize the biodegradation rate of BCPs [19]. Therefore, biodegradation kinetics of BCPs depends on the types of chemical phases (HA/ β -TCP) and their percentage ratios, where the higher the TCP ratio, the higher is the biodegradation of the BCPs. The biodegradation process of BCPs is also influenced by several other factors. For instance, a lower porosity and surface area or a higher crystallinity and larger particle sizes exhibited a slower biodegradation rate [6, 20]. Importantly, the higher biodegradation of BCPs facilitates an increase of calcium (Ca^{2+}) and phosphate (HPO_4^{2-} , PO_4^{3-}) ion concentration in the vicinity of the bone cells. This results in osteogenic differentiation and the subsequent mineralization of extracellular matrix (ECM) in the newly generated bone [21–23].

12.3 Marketed BCP Products

Due to these characteristics, many BCP bone substitute products, with suitable composition ratios of HA and TCP, are commercially available for various orthopedic and maxillofacial applications, as summarized in a previous review article [6]. Some of the marketed BCP products are as follows. For alternative autogenous bone grafts, Graftys BCP® (Latin American Solutions (LAS), Brazil) has been marketed in several forms such as granules, sticks, cylinders, and wedges. This product is a micro-, meso-, and macro-porous two-phase CaP ceramic consisting of 60% HA and 40% β -TCP, which facilitates long-term volume stability by decelerating the overall resorption capabilities and promoting a more stable and uniform bone growth [24]. Bicara™ (60% HA and 40% β -TCP, Wiltrom Co., Ltd.) shows good biocompatibility in vivo without side effects such as abnormal inflammation at implantation sites. Although complete absorption and replacement were not observed after 6 months of implantation, new bone regeneration was seen to occur effectively on the surface of the periphery in the specimens with the use of Bicara™. Another synthetic BCP, OSOPIA (>90% TCP and <10% HA), is manufactured by NextGen Biomaterials (London, UK) and is much closer to biologically derived bone grafts than the standard synthetic materials [25]. OSOPIA features higher bone ingrowth rates than BCP grafts and a more controlled cellular-induced resorption pattern compared to standard TCP materials [26].

Based on these results, most studies have reported that, regardless of the HA/ β -TCP ratio, BCP scaffolds generally enhance the rate and quality of bone tissue regeneration compared to empty control groups. In this regard, the various types of BCP bioceramics are considered as the best materials for bone tissue regeneration because they possess the inorganic phase of the bone ECM with mineral composition similar to that of natural bone. It has been reported that only BCPs with HA/ β -TCP ratios of 65/35, 60/40, and 50/50 have been successfully applied in human clinical trials [27–29]. For an example, Artzi et al. reported that the combination of BCP (50%

HA and 50% β -TCP) with particulate autogenous bone chips in a 1 to 1 ratio showed osteoconductive properties and promoted newly formed bone [27]. More recently, clinical trials have been studied to compare the new bone formation of two BCPs (B1, 60.28% HA and 39.72% β -TCP; B2, 78.21% HA and 21.79% β -TCP) and BoneCeramic (61% HA and 39% β -TCP) in fresh dental sockets after 6 months [30]. In this study, the B1 group showed the greatest amount of newly formed bone compared to other groups after 6 months. Although BCPs have shown biocompatibility, osteoconductivity, and new bone formation, currently, there is no general agreement on an ideal HA/ β -TCP ratio for BCPs in clinical applications. Therefore, various HA/ β -TCP ratios have been evaluated by researchers to determine the best ratio for optimum bone regeneration.

12.4 Injectable BCPs/Polymer Scaffolds

Porous scaffolds provide the structural support for cell adhesion, proliferation, and differentiation. They have been used as substrates for promoting new bone formation at the defect through surgical procedures [31, 32]. From a clinical perspective, injectable scaffold systems are one of the best options for bone tissue regeneration of irregular-shaped bone defects.

Porous microspheres have been used as vehicles for sustained drug or protein delivery due to their inherently small size, small volume, large surface area, and high drug loading efficiency [33]. Recently, Song and coworkers developed an injectable BCP (60% HA and 40% β -TCP)/porous microsphere scaffold system through the surface immobilization of BCP nanoparticles modified with heparin on porous poly(lactic-co-glycolic acid) (PLGA) microspheres modified with positively charged L-lysine via electrostatic interactions [34]. Although this system showed enhanced ALP activity, calcium deposition, and expression of osteogenic differentiation genes (i.e., osteocalcin and osteopontin), only in vitro

results of this study were not enough to demonstrate its enhanced osteogenesis effects.

Poly(methyl methacrylate) (PMMA) bone cement has been used in bone defects caused by osteoporosis due to its excellent mechanical properties [35, 36]. However, its bioinertness and non-degradation have limited its extensive application in bone regeneration. To enhance its biological activity, HA could be incorporated into PMMA bone cement [37]. Although the formulation of HA/PMMA bone cement has some advantages, such as the excellent mechanical properties and injectability, it still has some limitations due to the slow biodegradation of HA *in vivo*, consequently leading to a weakening of the interfacial integration between host bone tissue and cement [38]. Recently, Quan et al. fabricated a series of bioactive BCP (40%)/PMMA bone cements containing different BCP contents (up to 40%) to achieve an adjustable resorption rate and to accelerate osteogenesis *in vivo* [39]. The increase of β -TCP content (30%, 50%, and 70% of β -TCP per BCP contents) in BCP/PMMA cements induced more mineralization and was seen to promote cell adhesion, proliferation, and differentiation of rat bone marrow mesenchymal stem cells (rBMSCs) and osteogenesis. Furthermore, micro-computed tomography and histological studies have demonstrated that the growth rate of new bone was accelerated by increasing the β -TCP content in such BCP/PMMA cements.

Multichannel BCP granule (MCG, 60% HA and 40% β -TCP) is also an appropriate bone graft material due to its unique morphology, optimal porosity with interconnected pores, good mechanical strength, biocompatibility, osteoconductivity, and biodegradability [40]. Additionally, its porous structure is much like the osteon of a natural bone and allows bone cells to attach, migrate, and proliferate in the defect site [41, 42]. However, its low weight and repellent nature make it difficult to handle them in clinical applications. To solve this problem, MCGs are mixed with a material that can hold them by its cohesive force and induce bone formation at the defect site. As one of the main ECM components, hyaluronic acid (HA) has been previously evaluated in conjunction with CaP granules for improving

injectability and stimulating bone regeneration due to its non-toxicity, non-immunogenicity, viscosity, and good biodegradability, as well as for its wound healing and drug delivery capabilities [43–46]. Recently, the addition of HA to MCG (0.7 mm, 60% HA and 40% β -TCP) resulted in injectable granules and allowed for their easy handling during the implantation [47]. Without a significant change in porosity, the injectable HA/MCG exhibited greater cell viability and proliferation *in vitro*, as well as better *in vivo* bone tissue growth at critical sized defects after 4 weeks of implantation compared to MCG alone.

Calcium phosphate cement (CPC) with biocompatibility and osteoconductivity is considered as the most promising injectable filler material due to its identical composition to the mineral part of the bone [48]. However, the lack of interconnected porosity and inadequate pore size distribution in CPC cements may adversely affect bone growth. To improve biocompatibility, CPC has been incorporated with sucrose granules and/or different amounts of NaHCO_3 and Na_2HPO_4 to achieve the desired size distribution and interconnected pores [49]. Additionally, to promote cell adhesion and differentiation through specific interactions with ligands and adhered cells, collagen has been adsorbed onto the surface of these bioceramics because it is a major component of bone ECM [50–52]. Moreover, to further accelerate tissue regeneration, a potent osteoinductive growth factor, such as bone morphogenetic protein-2 (BMP-2), is also incorporated into bioceramics [53]. Recently, Lee et al. developed an advanced injectable CPC bone cement system by incorporating 15% of the functionalized MCGs (60% HA and 40% β -TCP) with collagen coating and BMP-2 loaded into CPC to enhance bone tissue regeneration [40]. The incorporation of the functionalized MCGs into CPC achieved a sustained BMP-2 release for 1 month, as well as implant degradation behavior, resulting in boosted bone tissue growth as compared to CPC matrix alone, in a rabbit femur head defect model after 2 and 4 weeks of implantation.

12.5 Functionalized BCPs with Bioactive Molecules

12.5.1 Functionalized BCPs for the Delivery of Osteoinductive Growth Factors

As described above, BCP-based scaffolds have gained attention in the fields of dental and orthopedic surgery due to their excellent biocompatibility and biodegradability. However, BCP-based scaffolds alone are not sufficient to stimulate adequate revascularization, cellular reconstitution, or osteogenesis. Many researchers have tried to incorporate bioceramics into polymer scaffolds to improve bioactivity [54], but due to the lack of bioactive signaling molecules, bare BCP or bare BCP/polymer scaffold systems are not effective in promoting cell proliferation, osteogenic differentiation, and tissue regeneration. In particular, BCPs/polymer composite scaffolds do not have appropriate pore structures and interconnectivity for cell accommodation [55]. Therefore, a combination of an appropriate scaffold and bioactive molecules has been suggested which play an extensive role in the stimulation of cell growth, migration, differentiation, and angiogenesis [56–58].

Among the osteoinductive factors, BMP-2 has been widely used in bone tissue engineering because of its superior osteoinductive activity, which stimulates the gene expression of osteogenic markers such as osteocalcin, osteopontin, bone sialoprotein, and alkaline phosphatase during osteoblast differentiation *in vitro* [59, 60]. To enhance bone tissue regeneration *in vivo*, several growth factors containing BCP ceramics were evaluated in animal models. Cho et al. found that BMP-2-loaded BCP (20% HA and 80% β -TCP) effectively induced new bone formation in the rat calvarial defect model [61]. Although new bone formation in 10 μ g and 20 μ g BMP-2/BCP groups was seen to be greater at 8 weeks than at 2 weeks, a statistically significant difference depending on the BMP-2 dose was not observed. On the other hand, bone replacement via alloplast needs to be accompanied by ample vascularization since it is one of the most important prerequisites for bone

healing [62]. Recently, Arisan and coworkers showed that vascular endothelial growth factor (VEGF)-incorporated BCP (60% HA and 40% β -TCP) alloplast enhanced early-term new bone formation in femoral defect models [63]. However, although VEGF seemed to significantly contribute to recovery and osteogenesis in the early stages of bone defect healing, the new bone of the VEGF/BCP alloplast did not show a statistically significant difference compared to that of bare BCP alloplast. Based on these results, it was evident that the simple mixing and incorporation of growth factors into BCP ceramics may not significantly improve new bone formation *in vivo*. It may be possible that the growth factors were not released to the defect in a sustained manner due to the short retention of growth factors *in vivo*. When they are loaded into BCP scaffolds by soaking, all of growth factors are rapidly released at once and disappear completely within 2 days of scaffold implantation [64]. Due to the short *in vivo* half-life of growth factors such as BMP-2, clinicians tried using a large dose of BMP-2. However, a high loading amount of BMP-2 onto a defect site may cause side effects like bone overgrowth and may also illicit an immune response [65].

To overcome these limitations, gradually degradable scaffolds with a sustained release of bioactive molecules are necessary to reduce the dose for clinical applications as well as to induce successful bone formation. By simply mixing BCP nanoparticles with heparin-alendronate (Hep-ALN), Kim and Park modified the surface of the BCPs (60% HA and 40% β -TCP) through the intense interactions between the phosphate groups of ALN and the calcium ions of BCP [66]. This modification prevents the BCPs from forming large particles due to the repulsion of negatively charged heparin molecules. Additionally, Hep-ALN/BCPs extended the release profile of osteoinductive BMP-2 up to 30 days in a sustained manner, as a result of the strong electrostatic interactions between Hep and BMP-2. This sustained release of BMP-2 from BCPs promoted the *in vitro* osteogenic differentiation of human adipose-derived stem cells (hADSCs) and the *in vivo* bone tissue regeneration in a rat calvarial defect model. This proposed simple bio-functionalization tech-

nique is applicable to CaP-based bioceramics and has potential in bone tissue engineering via the effective and sustained delivery of osteoinductive growth factors. As another example, Lee et al. recently developed a new 3D scaffold system with the sustained release of dual growth factors such as BMP-2 and VEGF [67], since dual delivery of BMP-2 and VEGF exhibited a better and more efficient bone regeneration than that of single growth factor delivery [68, 69]. The new 3D scaffold system (BNBV) was prepared by loading a sponge BCP (25% of nano-sized BCP powder) scaffold with 0.5% nano-cellulose (NC) containing BMP-2 and VEGF. This system resulted in the sustained release of the dual growth factors over a period of 30 days. This sustained release of the BNBV system better induced the cell attachment, proliferation, and differentiation of the rat bone marrow mesenchymal stem cells (rBMSCs) as compared to scaffold systems loaded with single growth factor. The use of cellulose in scaffolds, with its high density of hydroxyl groups, facilitates the immobilization of cell adhesive proteins [70]. BNBV scaffolds showed a higher amount of bone formation than BCP scaffolds, suggesting that the released dual growth factors from scaffolds resulted in accelerated bone healing mechanism. In particular, an increase in vasculature of the newly deposited bone and connective tissue inside the pores demonstrated the angiogenic effect of the released VEGF. As a chemoattractant, VEGF promoted differentiation of osteoblasts and thereby promoted BMP-2-induced bone formation [71, 72]. Therefore, stem cell-loaded BNBV scaffolds increased the extent of bone and vessel formation in the orthotopic site at 4 weeks.

Healing of bone defects is based on various biological cascade processes such as the recruitment and activation of cell lineages, regulation by molecular mediators (i.e., chemokines, growth factors, and cytokines), and cooperation in a cascade of events to fill the gap of bone fractures [73]. Considering the complicated bone healing cascade depends on a wide range of growth factors, it has been suggested that incorporation of various growth factors would be a more rational approach compared to using a specific growth factor for bone tissue engineering [74]. For more efficient

bone repair, platelet-rich plasma (PRP) is a promising alternative approach because it contains various growth factors, including platelet-derived growth factor (PDGF), transforming growth factor- β (TGF- β), epidermal growth factor (EGF), insulin growth factor (IGF), and VEGF [75, 76]. Although PRP can be used alone, the combination of PRP with scaffolds containing polymers and ceramics has been suggested to enhance bone healing process. Previous studies have reported that the combination of PRP with various biomaterials and cell sources showed positive effects on bone regeneration [77] and led to improved osteogenesis in ADSCs [78]. Recently, Chen et al. developed the thermo-gelling hydrogel scaffold by incorporating PRP and BCPs (60% HA and 40% β -TCP) in the thermo-gelling hydrogel, hyaluronic acid-*g*-chitosan-*g*-poly(N-isopropylacrylamide) (HA-CPN) [79]. This thermo-gelling HA-CPN/PRP/BCP hydrogel scaffold exhibited highly efficient cell proliferation and enhanced osteogenic differentiation. In vitro results revealed that PRP/BCP boosts osteoblastic differentiation and ECM mineralization of ADSCs in a HA-CPN scaffold. Additionally, in vivo CT and histological analyses confirmed that ADSCs and HA-CPN/PRP/BCP system showed successful bone formation in a rabbit calvarial defect model. Taken together, combining osteoinductive PRP and osteoconductive BCP with a HA-CPN hydrogel system could promote the osteogenesis of ADSCs for bone tissue engineering.

12.5.2 Functionalized BCPs for the Delivery of Small Molecular Drugs

As mentioned previously, osteoinductive growth factors have been incorporated in appropriate BCP scaffolds to render scaffolds with good osteoinductivity. However, the most commonly used osteoinductive proteins, including BMPs and TGF- β , can readily lose their bioactivity during the preparation of these scaffolds [80]. To minimize denaturation and to maintain their bioactivity, growth factors are usually incorporated into BCP scaffolds by physical adsorption.

However, the initial burst release of physically adsorbed growth factors is inevitable and cannot be retained in vivo at the implantation site for a long period [81]. Alternatively, osteoinductive small molecular drugs have drawn much attention for incorporation in scaffolds for bone tissue engineering due to their relatively high stability even in tough chemical environments [82].

Alendronate (ALN) can effectively inhibit bone resorption and induce osteogenic differentiation of osteoblasts, BMSCs, and ADSCs [83–85]. However, due to its high hydrophilic property, its oral bioavailability is only about 0.9%–1.8% [86]. Many researchers have tried to find appropriate delivery carriers that can provide an osteoconductive matrix for implantation at the bone repair sites [87, 88]. Song et al. prepared BCP (60% HA and 40% β -TCP) scaffolds that maintained ALN concentrations at the repair site long enough to allow the bone-forming cells to migrate to the defect site, proliferate, and differentiate in response to ALN [89]. This ALN/BCP scaffold significantly enhanced osteogenesis and mineralization in vitro, and the locally delivered ALN might affect the remodeling of newly regenerated bone in vivo, thus promoting osteogenesis in a rat tibia defect model.

Dexamethasone (DEX) is one of the low-molecular weight osteoinductive factors for bone tissue regeneration [82]. DEX and HA nanoparticles were hybridized with gelatin and poly(L-lactide) (PLLA) to construct a HA/DEX/PLLA/gelatin composite scaffold by the electrospinning technique [90]. However, the problem of initial burst release and a short release period of DEX still needed to be solved. Recently, composite scaffold systems of collagen and DEX-loaded BCP nanoparticles were prepared for a sustained release of DEX, together with the calcium and phosphorous ions [91]. DEX-loaded BCP nanoparticles were homogeneously distributed on the walls of the collagen scaffolds, enhancing the mechanical properties and roughness of the scaffolds. The sustained and prolonged release of DEX from the scaffolds was achieved for up to 35 days. This scaffold system, with good biocompatibility, enhanced the osteogenic differentiation of human BMSCs in vitro depending on the concentration of DEX, by increasing ALP activity and gene expres-

sion of *ALP*, runt-related transcription factor-2 (*RUNX2*), bone sialoprotein 2 (*IBSP*), and *BMP-2* both in vitro and in vivo. Furthermore, the scaffold increased the concentration of collagen I and osteocalcin in the in vivo environment.

12.5.3 Functionalized BCPs for Immunomodulation

Osseointegration is a direct contact between bone and the implanted biomaterials. During the osseointegration process, inflammation and immune reactions can be observed at the implanted sites [92, 93]. Although TGF- β 1 plays many important roles in regeneration processes, it is mostly related to the increased production of fibrotic tissue [94, 95]. Therefore, recent studies suggested that the inhibition of TGF- β 1 is an alternative strategy for enhancing osseointegration around medical implants by preventing several fibrotic reactions [96–98]. Among TGF- β 1 inhibitors, it has been known that P144 (TGF- β 1 inhibitor peptide) blocks the binding of TGF- β 1 with its receptor [99–101]. Previous results showed that P144-biofunctionalized CP-Ti surfaces reduced fibrotic differentiation and increased osteoblastic differentiation [96]. Also, the inhibiting TGF- β 1 can prevent the formation of fibrotic tissues or induce osseointegration around the implanted biomaterials [97, 98]. In a recent study, Gil group demonstrated that P144-biofunctionalized BCPs (60% HA and 40% β -TCP) in the hemimandibles of beagle dogs after tooth extraction maintained a stable membranous bone formation and showed the constant presence of vascular structures in the alveolar space compared to bare BCPs [102]. These results suggested that immunomodulation using TGF- β 1 inhibitor peptide can be an alternative strategy for enhancing osseointegration of the implanted biomaterials.

12.6 Conclusion

In summary, due to the excellent biocompatibility, biodegradability, bioactivity, safety, and cost-effectiveness over autografts and allografts, BCP

Table 12.1 Various types of BCPs and functionalized BCPs for bone tissue regeneration

Types of BCPs	Ratio of HA to β -TCP	Bioactive factors	References
Nano-BCP/porous PLGA microspheres	60:40	–	[34]
BCP/PMMA	30:70, 50:50, 70:30	–	[39]
Multichannel BCP (MCG)	60:40	–	[40–42]
Hyaluronic acid (HA)/MCG	60:40	–	[47]
Collagen/MCG/CPC	60:40	BMP-2	[40]
BCP	20:80	BMP-2	[61]
BCP alloplast	60:40	VEGF	[63]
Heparinized BCP	60:40	–	[66]
3D scaffold containing nano-BCP/ nano-cellulose	60:40	BMP-2, VEGF	[67–69]
HA-CPN/BCP	60:40	PRP	[79]
BCP	60:40	Alendronate	[89]
Collagen/Nano BCP	60:40	Dexamethasone	[91]
BCP	60:40	P144 (TGF- β 1 inhibitor peptide)	[102]

scaffolds ranging from nanoparticles to granules are very attractive biomaterials with preclinical and clinical applications for bone tissue engineering. Although BCP scaffolds have good osteoconductivity, bare BCP scaffolds alone are not enough to significantly improve osteogenic differentiation in vitro and new bone formation in vivo. As summarized in Table 12.1, to achieve more effective bone tissue regeneration, osteoinductive molecules, including growth factors or small molecular drugs, have been combined with BCP scaffolds or BCP/hydrogel polymer systems. By combining these bioactive molecules with BCPs or BCP/hydrogel polymer scaffolds, their initial burst release and short retention time in vitro and in vivo could be overcome, thereby promoting cell proliferation, osteogenic differentiation, and new bone tissue regeneration. However, efforts are still required to find the optimal BCP-based scaffolds with the most effective clinical outcomes.

Acknowledgments This research was supported by the Bio and Medical Technology Development Program of the NRF funded by the Korean government, MSIP (NRF-2017M3A9B3063640).

References

1. Cho TJ, Gerstenfeld LC, Einhorn TA (2002) Differential temporal expression of members of the transforming growth factor beta superfamily during murine fracture healing. *J Bone Miner Res* 17(3):513–520
2. Petite H, Viateau V, Bensaid W et al (2000) Tissue-engineered bone regeneration. *Nat Biotechnol* 18(9):959–963
3. Dorozhkin SV (2010) Bioceramics of calcium orthophosphates. *Biomaterials* 31(7):1465–1485
4. Carrodeguas RG, De Aza S (2011) Alpha-Tricalcium phosphate: synthesis, properties and biomedical applications. *Acta Biomater* 7(10):3536–3546
5. Best SM, Porter AE, Thian ES et al (2008) Bioceramics: past, present and for the future. *J Eur Ceram Soc* 28(7):1319–1327
6. Ebrahimi M, Botelho MG, Dorozhkin SV (2017) Biphasic calcium phosphates bioceramics (HA/TCP): concept, physicochemical properties and the impact of standardization of study protocols in biomaterials research. *Mater Sci Eng C Mater Biol Appl* 71:1293–1312
7. Rezwan K, Chen QZ, Blaker JJ et al (2006) Biodegradable and bioactive porous polymer/inorganic composite scaffolds for bone tissue engineering. *Biomaterials* 27(18):3413–3431
8. Daculsi G, LeGeros RZ, Heughebaert M et al (1990) Formation of carbonate-apatite crystals after implantation of calcium phosphate ceramics. *Calcif Tissue Int* 46(1):20–27
9. Mercier P, Bellavance F, Cholewa J et al (1996) Long-term stability of atrophic ridges reconstructed with hydroxylapatite: a prospective study. *J Oral Maxillofac Surg* 54(8):960–968

10. Fuerst M, Niggemeyer O, Lammers L et al (2009) Articular cartilage mineralization in osteoarthritis of the hip. *BMC Musculoskelet Disord* 10:166
11. Fellah BH, Gauthier O, Weiss P et al (2008) Osteogenicity of biphasic calcium phosphate ceramics and bone autograft in a goat model. *Biomaterials* 29(9):1177–1188
12. Zhang Y, Xiang Q, Dong S et al (2010) Fabrication and characterization of a recombinant fibronectin/cadherin bio-inspired ceramic surface and its influence on adhesion and ossification in vitro. *Acta Biomater* 6(3):776–785
13. Roohani-Esfahani SI, Nouri-Khorasani S, Lu Z et al (2010) The influence hydroxyapatite nanoparticle shape and size on the properties of biphasic calcium phosphate scaffolds coated with hydroxyapatite-PCL composites. *Biomaterials* 31(21):5498–5509
14. Chen JP, Tsai MJ, Liao HT (2013) Incorporation of biphasic calcium phosphate microparticles in injectable thermoresponsive hydrogel modulates bone cell proliferation and differentiation. *Colloids Surf B: Biointerfaces* 110:120–129
15. Tang Z, Li X, Tan Y et al (2018) The material and biological characteristics of osteoinductive calcium phosphate ceramics. *Regen Biomater* 5(1):43–59
16. Caroline Victoria E, Gnanam FD (2002) Synthesis and characterization of biphasic calcium phosphate. *Trends Biomater Artif Organs* 16(1):12–14
17. Jensen SS, Broggin N, Hjorting-Hansen E et al (2006) Bone healing and graft resorption of autograft, anorganic bovine bone and beta-tricalcium phosphate. A histologic and histomorphometric study in the mandibles of minipigs. *Clin Oral Implants Res* 17(3):237–243
18. Lee JH, Jung UW, Kim CS et al (2008) Histologic and clinical evaluation for maxillary sinus augmentation using macroporous biphasic calcium phosphate in human. *Clin Oral Implants Res* 19(8):767–771
19. Daculsi G, LeGeros RZ, Nery E et al (1989) Transformation of biphasic calcium phosphate ceramics in vivo: ultrastructural and physicochemical characterization. *J Biomed Mater Res* 23(8):883–894
20. Radin SR, Ducheyne P (1994) Effect of bioactive ceramic composition and structure on in vitro behavior. III. Porous versus dense ceramics. *J Biomed Mater Res* 28(11):1303–1309
21. Maeno S, Niki Y, Matsumoto H et al (2005) The effect of calcium ion concentration on osteoblast viability, proliferation and differentiation in monolayer and 3D culture. *Biomaterials* 26(23):4847–4855
22. Titorencu I, Jinga V, Constantinescu E et al (2007) Proliferation, differentiation and characterization of osteoblasts from human BM mesenchymal cells. *Cytotherapy* 9(7):682–696
23. Khoshniat S, Bourguine A, Julien M et al (2011) Phosphate-dependent stimulation of MGP and OPN expression in osteoblasts via the ERK1/2 pathway is modulated by calcium. *Bone* 48(4):894–902
24. Puttini IDO, Poli PP, Maiorana C et al (2019) Evaluation of osteoconduction of biphasic calcium phosphate ceramic in the calvaria of rats: microscopic and histometric analysis. *J Funct Biomater* 10:7
25. Yuan H, Fernandes H, Habibovic P et al (2010) Osteoinductive ceramics as a synthetic alternative to autologous bone grafting. *Proc Natl Acad Sci U S A* 107(31):13614–13619
26. LeGeros RZ, Lin S, Rohanizadeh R et al (2003) Biphasic calcium phosphate bioceramics: preparation, properties and applications. *J Mater Sci Mater Med* 14(3):201–209
27. Artzi Z, Weinreb M, Carmeli G et al (2008) Histomorphometric assessment of bone formation in sinus augmentation utilizing a combination of autogenous and hydroxyapatite/biphasic tricalcium phosphate graft materials: at 6 and 9 months in humans. *Clin Oral Implants Res* 19(7):686–692
28. Friedmann A, Dard M, Kleber BM et al (2009) Ridge augmentation and maxillary sinus grafting with a biphasic calcium phosphate: histologic and histomorphometric observations. *Clin Oral Implants Res* 20(7):708–714
29. Rouvillain JL, Lavalley F, Pascal-Mousellard H et al (2009) Clinical, radiological and histological evaluation of biphasic calcium phosphate bioceramic wedges filling medial high tibial valgisation osteotomies. *Knee* 16(5):392–397
30. Uzeda MJ, de Brito Resende RF, Sartoretto SC et al (2017) Randomized clinical trial for the biological evaluation of two nanostructured biphasic calcium phosphate biomaterials as a bone substitute. *Clin Implant Dent Relat Res* 19(5):802–811
31. Antonov EN, Bagratashvili VN, Whitaker MJ et al (2004) Three-dimensional bioactive and biodegradable scaffolds fabricated by surface-selective laser sintering. *Adv Mater* 17(3):327–330
32. Bettinger CJ, Weinberg EJ, Kulig KM et al (2005) Three-dimensional microfluidic tissue-engineering scaffolds using a flexible biodegradable polymer. *Adv Mater* 18(2):165–169
33. Freiberg S, Zhu XX (2004) Polymer microspheres for controlled drug release. *Int J Pharm* 282(1–2):1–18
34. Shim KS, Kim SE, Yun YP et al (2017) Biphasic Calcium Phosphate (BCP)-immobilized porous poly (d,l-lactic-co-glycolic acid) microspheres enhance osteogenic activities of osteoblasts. *Polymers* 9(7):297
35. Yan D, Duan L, Li J et al (2011) Comparative study of percutaneous vertebroplasty and kyphoplasty in the treatment of osteoporotic vertebral compression fractures. *Arch Orthop Trauma Surg* 131(5):645–650
36. Griza S, Ueki MM, Souza DH et al (2013) Thermally induced strains and total shrinkage of the polymethyl-methacrylate cement in simplified models of total hip arthroplasty. *J Mech Behav Biomed Mater* 18:29–36

37. Tamimi F, Sheikh Z, Barralet J (2012) Dicalcium phosphate cements: brushite and monetite. *Acta Biomater* 8(2):474–487
38. Boulter JM, Pilet P, Gauthier O, Verron E (2017) Biphasic calcium phosphate ceramics for bone reconstruction: a review of biological response. *Acta Biomater* 53:1–12
39. Zhang X, Kang T, Liang PY et al (2018) Biological activity of an injectable biphasic calcium phosphate/PMMA bone cement for induced osteogenesis in rabbit model. *Macromol Biosci* 18:1700331
40. Lee GH, Makkar P, Paul K et al (2017) Incorporation of BMP-2 loaded collagen conjugated BCP granules in calcium phosphate cement based injectable bone substitutes for improved bone regeneration. *Mater Sci Eng C Mater Biol Appl* 77:713–724
41. Kim YH, Jyoti MA, Youn MH et al (2010) In vitro and in vivo evaluation of a macro porous beta-TCP granule-shaped bone substitute fabricated by the fibrous monolithic process. *Biomed Mater* 5(3):35007
42. Sarkar SK, Lee BY, Padalhin AR et al (2016) Brushite-based calcium phosphate cement with multichannel hydroxyapatite granule loading for improved bone regeneration. *J Biomater Appl* 30(6):823–837
43. Allison DD, Grande-Allen KJ (2006) Hyaluronan: a powerful tissue engineering tool. *Tissue Eng* 12(8):2131–2140
44. Price RD, Myers S, Leigh IM et al (2005) The role of hyaluronic acid in wound healing: assessment of clinical evidence. *Am J Clin Dermatol* 6(6):393–402
45. Suzuki K, Anada T, Miyazaki T et al (2014) Effect of addition of hyaluronic acids on the osteoconductivity and biodegradability of synthetic octacalcium phosphate. *Acta Biomater* 10(1):531–543
46. Chazono M, Tanaka T, Komaki H et al (2004) Bone formation and bioresorption after implantation of injectable beta-tricalcium phosphate granules-hyaluronate complex in rabbit bone defects. *J Biomed Mater Res A* 70(4):542–549
47. Taz M, Makkar P, Imran KM et al (2019) Bone regeneration of multichannel biphasic calcium phosphate granules supplemented with hyaluronic acid. *Mater Sci Eng C Mater Biol Appl* 99:1058–1066
48. Ko CL, Chen JC, Hung CC et al (2014) Biphasic products of dicalcium phosphate-rich cement with injectability and nondispersibility. *Mater Sci Eng C Mater Biol Appl* 39:40–46
49. Takagi S, Chow LC (2001) Formation of macropores in calcium phosphate cement implants. *J Mater Sci Mater Med* 12(2):135–139
50. Friess W (1998) Collagen-biomaterial for drug delivery. *Eur J Pharm Biopharm* 45(2):113–136
51. Ferreira AM, Gentile P, Chiono V et al (2012) Collagen for bone tissue regeneration. *Acta Biomater* 8(9):3191–3200
52. Ou KL, Chung RJ, Tsai FY et al (2011) Effect of collagen on the mechanical properties of hydroxyapatite coatings. *J Mech Behav Biomed Mater* 4(4):618–624
53. Hunziker EB, Enggist L, Kuffer A et al (2012) Osseointegration: the slow delivery of BMP-2 enhances osteoinductivity. *Bone* 51(1):98–106
54. Xu Y, Wu J, Wang H et al (2013) Fabrication of electrospun poly(L-lactide-co-epsilon-caprolactone)/collagen nanoyarn network as a novel, three-dimensional, macroporous, aligned scaffold for tendon tissue engineering. *Tissue Eng Part C Methods* 19(12):925–936
55. Le Nihouannen D, Guehenec LL, Rouillon T et al (2006) Micro-architecture of calcium phosphate granules and fibrin glue composites for bone tissue engineering. *Biomaterials* 27(13):2716–2722
56. Heckman JD, Ehler W, Brooks BP et al (1999) Bone morphogenetic protein but not transforming growth factor-beta enhances bone formation in canine diaphyseal nonunions implanted with a biodegradable composite polymer. *J Bone Joint Surg Am* 81(12):1717–1729
57. Street J, Bao M, deGuzman L et al (2002) Vascular endothelial growth factor stimulates bone repair by promoting angiogenesis and bone turnover. *Proc Natl Acad Sci U S A* 99(15):9656–9661
58. Wozney JM (2002) Overview of bone morphogenetic proteins. *Spine* 27(16 Suppl 1):S2–S8
59. Karageorgiou V, Meinel L, Hofmann S et al (2004) Bone morphogenetic protein-2 decorated silk fibroin films induce osteogenic differentiation of human bone marrow stromal cells. *J Biomed Mater Res A* 71(3):528–537
60. Liu Y, Enggist L, Kuffer AF et al (2007) The influence of BMP-2 and its mode of delivery on the osteoconductivity of implant surfaces during the early phase of osseointegration. *Biomaterials* 28(16):2677–2686
61. Jang JW, Yun JH, Lee KI et al (2012) Osteoinductive activity of biphasic calcium phosphate with different rhBMP-2 doses in rats. *Oral Surg Oral Med Oral Pathol Oral Radiol* 113(4):480–487
62. Honkanen R, Pulkkinen P, Jarvinen R et al (1996) Does lactose intolerance predispose to low bone density? A population-based study of perimenopausal Finnish women. *Bone* 19(1):23–28
63. Bedeloglu E, Ersanli S, Arisan V (2017) Vascular endothelial growth factor and biphasic calcium phosphate in the endosseous healing of femoral defects: an experimental rat study. *J Dent Sci* 12(1):7–13
64. Kanematsu A, Yamamoto S, Ozeki M et al (2004) Collagenous matrices as release carriers of exogenous growth factors. *Biomaterials* 25(18):4513–4520
65. Ma Z, Kotaki M, Inai R et al (2005) Potential of nanofiber matrix as tissue-engineering scaffolds. *Tissue Eng* 11(1–2):101–109
66. Shim KS, Kim HJ, Kim SE et al (2018) Simple surface biofunctionalization of biphasic calcium phosphates for improving osteogenic activity and bone tissue regeneration. *J Ind Eng Chem* 68:220–228

67. Sukul M, Nguyen TB, Min YK et al (2015) Effect of local sustainable release of BMP2-VEGF from nano-cellulose loaded in sponge biphasic calcium phosphate on bone regeneration. *Tissue Eng A* 21(11–12):1822–1836
68. Patel ZS, Young S, Tabata Y et al (2008) Dual delivery of an angiogenic and an osteogenic growth factor for bone regeneration in a critical size defect model. *Bone* 43(5):931–940
69. Kempen DH, Lu L, Heijink A et al (2009) Effect of local sequential VEGF and BMP-2 delivery on ectopic and orthotopic bone regeneration. *Biomaterials* 30(14):2816–2825
70. Noiset O, Schneider YJ, Marchand-Brynaert J (1999) Fibronectin adsorption or/and covalent grafting on chemically modified PEEK film surfaces. *J Biomater Sci Polym Ed* 10(6):657–677
71. Deckers MM, Karperien M, van der Bent C et al (2000) Expression of vascular endothelial growth factors and their receptors during osteoblast differentiation. *Endocrinology* 141(5):1667–1674
72. Midy V, Plouet J (1994) Vasculotropin/vascular endothelial growth factor induces differentiation in cultured osteoblasts. *Biochem Biophys Res Commun* 199(1):380–386
73. Frost HM (1989) The biology of fracture healing. An overview for clinicians. Part I. *Clin Orthop Relat Res* 248:283–293
74. Su J, Xu H, Sun J et al (2013) Dual delivery of BMP-2 and bFGF from a new nano-composite scaffold, loaded with vascular stents for large-size mandibular defect regeneration. *Int J Mol Sci* 14(6):12714–12728
75. Marx RE (2004) Platelet-rich plasma: evidence to support its use. *J Oral Maxillofac Surg* 62(4):489–496
76. Liao HT, Marra KG, Rubin JP (2014) Application of platelet-rich plasma and platelet-rich fibrin in fat grafting: basic science and literature review. *Tissue Eng B Rev* 20(4):267–276
77. Feng L, Chang W, Tian B et al (2017) Bone regeneration combining platelet rich plasma with engineered bone tissue. *J Biomater Tissue Eng* 7:841–847
78. Liao HT, Chen JP, Lee MY (2013) Bone tissue engineering with adipose-derived stem cells in bioactive composites of laser-sintered porous polycaprolactone scaffolds and platelet-rich plasma. *Materials (Basel)* 6(11):4911–4929
79. Liao HT, Tsai MJ, Brahmayya M et al (2018) Bone regeneration using adipose-derived stem cells in injectable thermo-gelling hydrogel scaffold containing platelet-rich plasma and biphasic calcium phosphate. *Int J Mol Sci* 19:2537
80. Ripamonti U, Parak R, Klar RM et al (2016) The synergistic induction of bone formation by the osteogenic proteins of the TGF-beta supergene family. *Biomaterials* 104:279–296
81. Ziegler J, Mayr-Wohlfart U, Kessler S et al (2002) Adsorption and release properties of growth factors from biodegradable implants. *J Biomed Mater Res* 59(3):422–428
82. Chou JW, Decarie D, Dumont RJ et al (2001) Stability of dexamethasone in extemporaneously prepared oral suspensions. *Can J Hosp Pharm* 54:97–103
83. Inoue Y, Hisa I, Seino S et al (2010) Alendronate induces mineralization in mouse osteoblastic MC3T3-E1 cells: regulation of mineralization-related genes. *Exp Clin Endocrinol Diabetes* 118(10):719–723
84. von Knoch F, Jaquiere C, Kowalsky M et al (2005) Effects of bisphosphonates on proliferation and osteoblast differentiation of human bone marrow stromal cells. *Biomaterials* 26(34):6941–6949
85. Wang CZ, Chen SM, Chen CH et al (2010) The effect of the local delivery of alendronate on human adipose-derived stem cell-based bone regeneration. *Biomaterials* 31(33):8674–8683
86. Porras AG, Holland SD, Gertz BJ (1999) Pharmacokinetics of alendronate. *Clin Pharmacokinet* 36(5):315–328
87. Moon HJ, Yun YP, Han CW et al (2011) Effect of heparin and alendronate coating on titanium surfaces on inhibition of osteoclast and enhancement of osteoblast function. *Biochem Biophys Res Commun* 413(2):194–200
88. Kim CW, Yun YP, Lee HJ et al (2010) In situ fabrication of alendronate-loaded calcium phosphate microspheres: controlled release for inhibition of osteoclastogenesis. *J Control Release* 147(1):45–53
89. Park KW, Yun YP, Kim SE et al (2015) The effect of alendronate loaded biphasic calcium phosphate scaffolds on bone regeneration in a rat tibial defect model. *Int J Mol Sci* 16:26738–26753
90. Amjadian S, Seyedjafari E, Zeynali B et al (2016) The synergistic effect of nano-hydroxyapatite and dexamethasone in the fibrous delivery system of gelatin and poly(L-lactide) on the osteogenesis of mesenchymal stem cells. *Int J Pharm* 507(1–2):1–11
91. Chen Y, Kawazoe N, Chen G (2018) Preparation of dexamethasone-loaded biphasic calcium phosphate nanoparticles/collagen porous composite scaffolds for bone tissue engineering. *Acta Biomater* 67:341–353
92. Cornelini R, Rubini C, Fioroni M et al (2003) Transforming growth factor-beta 1 expression in the peri-implant soft tissues of healthy and failing dental implants. *J Periodontol* 74(4):446–450
93. Sadowska JM, Wei F, Guo J et al (2018) Effect of nano-structural properties of biomimetic hydroxyapatite on osteoimmunomodulation. *Biomaterials* 181:318–332
94. Santiago B, Gutierrez-Canas I, Dotor J et al (2005) Topical application of a peptide inhibitor of transforming growth factor-beta1 ameliorates bleomycin-induced skin fibrosis. *J Invest Dermatol* 125(3):450–455
95. Janssens K, ten Dijke P, Janssens S et al (2005) Transforming growth factor-beta1 to the bone. *Endocr Rev* 26(6):743–774

96. Sevilla P, Cirera A, Dotor J et al (2018) In vitro cell response on CP-Ti surfaces functionalized with TGF-beta1 inhibitory peptides. *J Mater Sci Mater Med* 29(6):73
97. Filvaroff E, Erlebacher A, Ye J et al (1999) Inhibition of TGF-beta receptor signaling in osteoblasts leads to decreased bone remodeling and increased trabecular bone mass. *Development* 126(19):4267–4279
98. Shen ZJ, Kim SK, Jun DY et al (2007) Antisense targeting of TGF-beta1 augments BMP-induced upregulation of osteopontin, type I collagen and Cbfa1 in human Saos-2 cells. *Exp Cell Res* 313(7):1415–1425
99. Ezquerro IJ, Lasarte JJ, Dotor J et al (2003) A synthetic peptide from transforming growth factor beta type III receptor inhibits liver fibrogenesis in rats with carbon tetrachloride liver injury. *Cytokine* 22(1–2):12–20
100. Vicent S, Luis-Ravelo D, Anton I et al (2008) A novel lung cancer signature mediates metastatic bone colonization by a dual mechanism. *Cancer Res* 68(7):2275–2285
101. Serrati S, Margheri F, Pucci M et al (2009) TGFbeta1 antagonistic peptides inhibit TGFbeta1-dependent angiogenesis. *Biochem Pharmacol* 77(5):813–825
102. Cirera A, Manzanares MC, Sevilla P et al (2019) Biofunctionalization with a TGFβ-1 inhibitor peptide in the osseointegration of synthetic bone grafts: an in vivo study in beagle dogs. *Materials* 12:3168



Surface-Modifying Polymers for Blood-Contacting Polymeric Biomaterials

Chung-Man Lim, Mei-Xian Li, and Yoon Ki Joung

Abstract

Bulk blending is considered as one of the most effective and straightforward ways to improve the hemo-compatibility of blood-contacting polymeric biomaterials among many surface modification methods. Zwitterionic structure-, glycocalyx-like structure-, and heparin-like structure-based oligomers have been synthesized as additives and blended with base polymers to improve the blood compatibility of base polymers. Fluorinated end- and side-functionalized oligomers could promote the migration of functionalized groups to the surface of biomedical polymers without changing their bulk properties, and it highly depends on the number and concentration of functional groups. Moreover, oligomers having both zwitterion and fluorine are receiving considerable attention due to their desirable phase

separation, which can avoid undesired protein adsorption and platelet adhesion. The surface analysis of the surface-modified materials is usually investigated by analytical tools such as contact angle measurement, atomic force microscopy (AFM), and X-ray photoelectron spectroscopy (XPS). Blood compatibility is mainly evaluated via platelet adhesion and protein adsorption test, and the result showed a significant decrease in the amount of undesirable adsorption. These analyses indicated that surface modification using bulk blending technique effectively improves blood compatibility of polymeric biomaterials.

Keywords

Surface modification · Bulk blending · Additives · Oligomers · Blood-contact · Hemo-compatibility · Biocompatibility · Protein · Adsorption · Polymers · Biomaterials · Zwitterion · Fluorine

C.-M. Lim · M.-X. Li
Center for Biomaterials, Biomedical Research
Institute, Korea Institute of Science and Technology
(KIST), Seoul, Republic of Korea

Y. K. Joung (✉)
Center for Biomaterials, Biomedical Research
Institute, Korea Institute of Science and Technology
(KIST), Seoul, Republic of Korea

Division of Bio-Medical Science and Technology,
Korea University of Science and Technology (UST),
Deajeon, Republic of Korea
e-mail: ykjoung@kist.re.kr

13.1 Blood-Contacting Medical Devices

Thrombosis is the most critical issue of blood-contacting medical devices, which often leads to device failure, patient morbidity, and patient mortality [1–4]. A large number of polymeric

biomaterials (e.g., intravascular catheters, coronary artery and vascular stents, blood-loop circuits, prosthetic heart valves, and artificial kidneys) have been used for a variety of blood-contacting and extracorporeal devices due to their suitable biocompatibility and mechanical properties [5]. However, their hemo-compatibility should be improved for wider range of applications. The interaction of implanted blood-contacting polymeric biomaterials with the blood is very complicated and requires broad knowledge of several fields of research in order to understand it correctly.

When an artificial polymeric device contacts with the blood, in the first step toward thrombus formation, plasma proteins rapidly adsorb on the surface of device to form a layer of adherent proteins [6–8]. Both adherent platelets and adsorbed proteins induce the complement activation and attract some immune cells such as white blood cells, allowing the immune system to identify the implanted material surface as incidental harmful effects and secrete inflammatory chemokines to promote inflammation. Furthermore, adhered platelets are aggregated on the device surface via the coagulation cascade. As a result, interactions between the blood and an implanted material contribute gradually to the complications of thromboembolism, which can impair device function and cause fatal complications [9]. Using this process, researchers measured the blood compatibility by quantifying the platelets and proteins adsorbed on the surface of polymeric biomaterials.

Considerable attention has been given to the surface modification of biomedical polymers to address the need, which is divided into three methods: non-covalent coating, grafting, and bulk blending [10–13]. Coating technologies include physical networking through intermolecular interactions, plasma deposition technologies, layer-by-layer technologies, Langmuir-Blodgett techniques, and dip coatings [14–18]. Grafting methods are divided into “grafting from” for surface-initiated polymerization and “grafting to” for immobilizing the pre-synthesized polymer [19]. These include UV-induced grafting, chain growth grafting using

reverse addition-fragmentation chain transfer (RAFT) and atom transfer radical polymerization (ATRP), and graft-to-surface methods using crosslinking and dipping [20–23]. Although non-covalent coating and grafting methods have been widely applied for improving blood compatibility of blood-contacting polymers, some drawbacks such as low adhesion stability for surface coatings and complex process for grafting method have been raised.

Surface modification by bulk blending is more effective and simpler way. This can be achieved by only blending bio-functional materials with base polymers. The blending of oligomers with these base polymers has benefits of combining oligomers with base polymers at different ratios to obtain optimum properties. This method is also highly productive and efficient, as it does not require subsequent manufacturing steps, unlike other surface modifications. In addition, this has non-leaching advantage as compared to other technologies with leaching concern.

13.2 Non-fluorinated Oligomers as Surface-Modifying Polymers

13.2.1 Zwitterionic Oligomers

Zwitterion is a substance that has both positive and negative charges within a molecule and has received much attention in the biomaterial fields due to its anti-biofouling and antithrombotic effects. Studies employing zwitterionic monomers, such as phosphorylcholine (PC), carboxyl betaine (CB), and sulfobetaine (SB), have demonstrated that electrostatic interaction with water molecules induces a hydration layer on the surface of a material, which reduces cell adhesion and protein absorption [26–29]. This process greatly contributes to the enhancement of hemo-compatible property (Fig. 13.1).

Especially, Ishihara et al. first designed biomembrane mimetic PC group, i.e., 2-methacryloyloxyethyl phosphorylcholine (MPC). The low molecular weight MPC-based poly(2-methacryloyloxyethyl phosphorylcho-

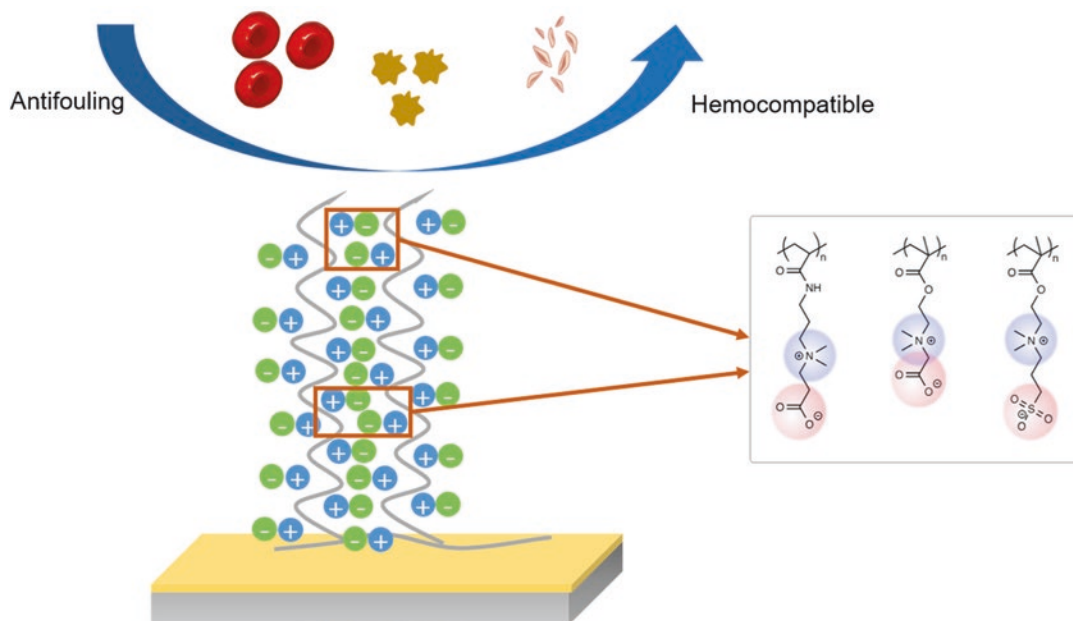


Fig. 13.1 Illustration of zwitterionic polymer structure and their effects

line-*co*-methacryloyloxyethyl butyl urethane) (PMBU) and polysulfone (PSf) have been blended to prepare protein-adsorption-resistant biodegradable porous membrane [30]. Surface characterization by X-ray photoelectron spectroscopy (XPS) showed that the surface of PSf/PMBU blended membrane contains MPC units. Furthermore, the hemo-compatibility of PSf membrane was significantly improved by the MPC group. A large amount of proteins adsorbed on the surface of PSf, but the amount drastically decreased on the surface of PSf/PMBU. The permeability after protein adsorption was also improved. In the case of original membrane, the permeability for cytochrome C decreased by 35%. On the other hand, the permeability of PSf/PMBU membrane was maintained. The organized layer of adsorbed proteins leads to a reduction in permeability of the membrane via adhesion of platelets and their activation. These problems would be solved by adding PMBU as the interaction between the membrane and the protein becomes weak. The water contact angle of the surface decreased as the composition of MPC polymer increased because of its strong hydrophilicity. The hydrophilicity is one of the

important factors for preventing protein adsorption in hemodialysis membrane.

Poly(lactide-*co*-glycolide) (PLGA) has been researched in biomaterials fields for its biodegradability and non-toxicity [31]. However, inflammatory responses should be discussed further, and oligomers of poly(2-methacryloyloxyethyl phosphorylcholine-*co*-2-ethylhexyl methacrylate) (PMEH) have been blended with PLGA [32]. PLGA/PMEH blended membranes were synthesized using a solvent casting method to impart both anti-biofouling nature and anti-inflammatory property to base polymer. Thermal properties were analyzed via a differential scanning calorimeter (DSC), and the results showed that PLGA and PMEH were mixed homogeneously. XPS analysis revealed that the MPC units exist on the surface of the PLGA/PMEH membrane and the concentration of MPC units observed at the surface increased as the concentration of mixed PMEH increased. In addition, on the PLGA/PMEH membrane, NIH-3 T3 mouse fibroblast cells were cultured for 2 days. The number of adherent cells decreased with an increase of the concentration of the PMEH. The amount of interleukin-1b (IL-1b) mRNA (inflammatory cytokine

expressed from adhered human promyelocytic leukemia cells) on the PMEHA blended membranes was also significantly lower than that on PLGA membrane with no difference in the number of human promyelocytic leukemia cells.

Low molecular weight MPC oligomers blended with a novel cellulose acetate (CA) membrane were achieved to improve blood compatibility for filtration system [33]. MPC-based copolymers were synthesized from MPC and *n*-butyl methacrylate (MPC/*n*-butyl methacrylate=30/70 molar ratio; PMB30), and a porous structure was prepared by a phase inversion method. The permeability and mechanical properties of the blended membrane could be controlled by tuning reaction conditions including solvent evaporation time and the composition of the solvent. XPS analysis confirmed that the MPC units are present on the surface of the blended membrane. Water contact angle measurement showed that surface hydrophilicity increased by the addition of PMB30. This also indicates that the MPC units exist on the surface of the blended membrane. Furthermore, the CA/PMB30 blended membranes showed excellent hemo-compatibility due to the zwitterionic property of MPC units such as promoting the hydration on the surface. Protein adsorption resistance of the blended membrane surface dramatically improved against immunoglobulin G (IgG), fibrinogen (Fg), and albumin when compared to the original membrane.

Another zwitterionic structure is CB, and polysulfone (PSF)-modified ultrafiltration (UF) membranes were prepared via surface zwitterionization from a PSF-based block copolymer additive containing poly(*N,N*-dimethylamino-2-ethylmethacrylate) (PDMAEMA) blocks [34]. Triblock copolymers (PDMAEMA-*b*-PSF-*b*-PDMAEMA) were synthesized using condensation polymerization and atom transfer radical polymerization (ATRP). This copolymer was blended with PSF resin to form membranes by phase inversion process. The PDMAEMA chains on the surface of the membrane were transformed into zwitterionic poly(carboxybetaine methacrylate) (PCBMA) by quaternizing the membrane with 3-bromopropionic acid (3-BPA) for 12, 24,

and 48 h. The hydrophilicity measured with water contact angle increased with an increase of the copolymer additive concentration in the membrane and quaternization time. The filtration experiments such as membrane permeation and separation tests and membrane anti-fouling test showed that fouling resistance of the modified membrane was noticeably improved. Platelet adhesion also decreased due to these properties, which means that the blood compatibility is significantly enhanced.

In addition, poloxamers and polyurethanes (PUs) with zwitterionic additives including PC and SB group have been synthesized to be oligomers that are likely to be used in polymer blends to improve the blood compatibility of the base polymer [35–37].

13.2.2 Other Oligomers

Several oligomers with other chemical structures, with or without charged structures, mimicked the function of biomacromolecules such as glycocalyx and heparin structures. The glycosylated molecules are located in the outer region of the cell membrane, and certain interactions such as cell-cell recognition are affected by these molecules [38]. Biomimetic glycocalyx-like structures also prevent nonspecific attachment of cells and other undesirable molecules by steric repulsion [39, 40]. Low molecular weight poly(ethylene oxide-propylene oxide-ethylene oxide) (PEO-PPO-PEO) triblock copolymers activated by amino acid and tripeptide of arginine-glycine-aspartic acid (RGD) derivatives were synthesized via the methyl sulfonyl chloride method [41]. PDL-LA was blended with the ligand-tethered poloxamer derivatives, and the surface of modified PDL-LA film was characterized by ATF-FTIR, XPS, and contact angle. The results of ATR-FTIR and XPS confirmed PEO enrichment on the surface and self-segregation behavior of tethered PEO-PPO-PEO copolymer where PPO groups are entangled with PDL-LA surface and PEO groups locate an outer layer. The hydrophilicity of all the modified surfaces increased due to hydrophilic PEO chains on the surface of PDL-LA film. The chondrocyte

attachment on the poloxamer-modified film was less than that on unmodified film due to the steric repulsion effect of PEO chains against cells and proteins. However, the chondrocyte attachment dramatically increased after covalent binding of amino acid sequences such as RGD to the ends of PEO groups to induce specific cell interactions. Furthermore, the growth of chondrocyte was promoted on the surface of PEO-PPO-PEO amino acid and RGD-combined PDL-LA films, and it could be a potential for tissue engineering and various biomedical applications.

Another promising approach is the synthesis of antithrombotic macromolecules with heparin-like structures [42–44]. Sulfonated poly(styrene-*co*-acrylic acid)-*b*-poly(vinyl pyrrolidone)-*b*-poly(styrene-*co*-acrylic acid) (P(St-*co*-AA)-*b*-PVP-*b*-P(St-*co*-AA)) low molecular weight copolymer was synthesized via reversible addition-fragmentation chain transfer (RAFT) polymerization, and it was blended with polyethersulfone (PES) in *N,N*-dimethylacetamide (DMAC) to manufacture membrane using a liquid-liquid phase separation method [45]. GPC results showed that the polydispersity index (PDI) was well distributed within the theoretical range, which confirmed the advantages of the RAFT polymerization. It was observed with scanning electron microscopy (SEM) and atomic force microscopy (AFM) that more pores were produced in the membrane and the surface was roughened with the increased concentration of the additives. The grooves and fine pores are due to the tendency of the copolymer to migrate to the water/polymer interface. The presence of additives on the surface was further confirmed by FTIR and XPS analysis. It was found that blood coagulation was prolonged in the modified membrane compared to the PES membrane. Moreover, it was also found that platelet adhesion reduced when the content of additive increased in the modified surface. The mechanism has been described to be abundant on the membrane surface and dependent on the presence of anionic or polar groups (SO₃H, OH, and COOH) mimicking the anticoagulant properties of heparin. These polar groups also contributed to imparting hydrophilicity to the surface.

13.3 Fluorinated Oligomers as Surface-modifying Polymers

Numerous studies related to the surface modification of polymeric blood-contacting medical devices have been conducted to improve anti-thrombotic and anti-fouling properties [46]. One of the strategies is to blend a base polymer with a surface modifier, such as surface-modifying macromolecules (SMMs) and surface-modifying additives (SMAs), which spontaneously adsorb to the surface during the processing.

Polyurethanes (PUs) are one of the widely used polymers for medical devices such as catheters [47, 48], membranes [49, 50], and vascular grafts [51, 52] due to their excellent mechanical properties, tailored stability, and relatively good biocompatibility [53]. However, many existing commercial PUs have a recognized limit for long-term implants due to inherent thrombogenic and inflammatory characters, and the biodegradation of PUs from the surface into the bulk materials [54]. Therefore, the most effective and simple strategy is to improve the biocompatibility of the base polymer by blending with surface-modifying additives. In this section, we will mainly introduce some surface modifiers functionalized with fluorine (Fig. 13.2).

13.3.1 End-Functionalized Fluorinated Oligomers

The form of fluorinated oligomers affects blood compatibility of the base polymer for a medical device. Generally, end-functionalized fluorinated oligomers have good blood compatibility with low denaturing of coagulation proteins due to their inherent compatibility with the base polymer for devices and free mobility of the terminal fluorinate groups [55–58]. In order to give uniform coverage of the diffusion of copolymers from bulk to surface, end-functionalized fluorinated surface-modifying oligomers have been widely used as additives due to low polarity and high hydrophobicity of fluorinated segments. The end-functionalized oligomeric additives can be

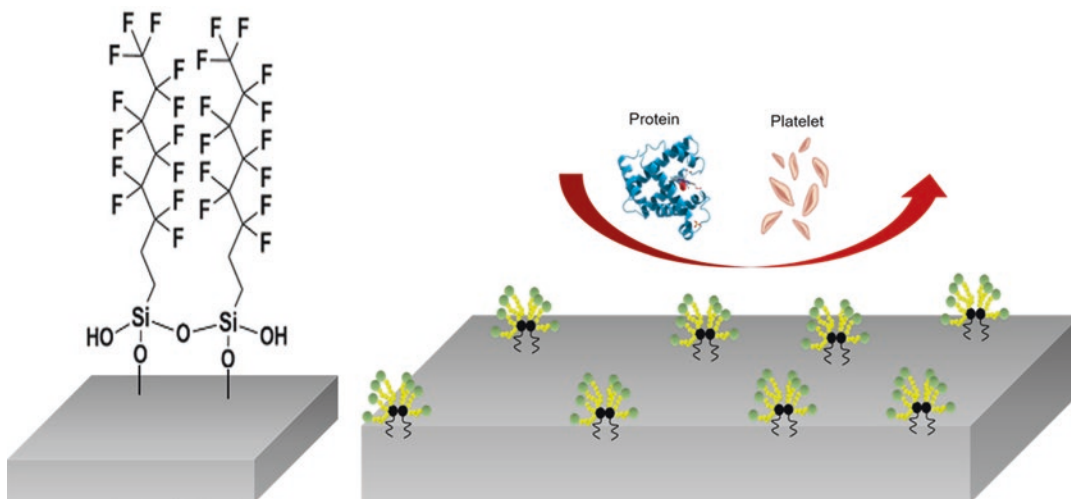


Fig. 13.2 Schematic illustration of fluorinated polymer structure and their effects

divided into mono-end-functionalized fluorinated oligomers [59, 60] and multi-end-functionalized fluorinated additives based on both ATRP and ring opening polymerization (ROP) reactions [61].

Tang et al. [62] developed two types of fluorinated SMMs using polypropylene oxide (PPO) and poly(tetramethylene oxide) (PTMO), which could migrate to the upper surface of the base material, and then these SMMs were blended with base PU polymer, respectively. The results showed that many fluorine groups were enriched at the surface of the polymer; thereby the surface became more hydrophobic, and fibrinogen adsorption and enzyme-induced biodegradation of PU were reduced, resulting in the improvement of the blood compatibility of PUs in vivo. Although mono-end-functionalized fluorinated additives show promising blood compatible property, it is still challenging to control the hydrophobicity of the surface for classical linear FPU because fluorinated hard segments are restricted to migration to the surface of base polymer [63]. Therefore, a number of studies related to multi-end-functionalized fluorinated additives have been investigated.

Li and coworkers [64] designed and synthesized fluorinated phospholipid end-functionalized PUs as additives using diphenylmethane diisocyanate and 1,4-butanediol as hard segments;

poly(tetramethylene glycol), polypropylene glycol, polycarbonate diols, and polyethylene glycol as soft segments, respectively; and amino-functionalized hybrid hydrocarbon/fluorocarbon double-chain phospholipid as an end-capper. The results showed that the surfaces could effectively suppress fibrinogen adsorption and enhance blood compatibility of existing medical PUs. In addition, it is demonstrated that the surface properties were strongly dependent on the number of fluoroalkyl (CF_n) groups [61, 65]. Generally, higher number of CF_n groups leads to an increasing static water contact angle (WCA) of PLA-, PS-, PVP-, and PMMA-based polymers [66–68]. However, the improvement in properties of end-functionalized PUs prepared by fluorinated alcohol was not evident compared to hydrogenated PUs due to the less content of fluorine and lower molecular weight of fluorinated alcohols [69].

13.3.2 Side-Functionalized Fluorinated Oligomers

Ge et al. [69] prepared FPUs by fluorinated polyether glycol as a soft segment and 1,6-hexamethylene diisocyanate or toluene diisocyanate as a hard segment and proposed that the surface properties of side-functionalized fluorinated polymers were better than those with

fluorinated groups in the main chain. Fluorinated phosphatidylcholines attached to the hard block of PUs as a side chain [58, 70, 71] could promote the migration of functional groups to the surface of base polymers due to its low surface free energy of long fluorinated alkyl group, resulting in the reduction of protein adsorption and platelet adhesion.

Tan et al. [70] also designed and synthesized side-functionalized poly(carbonate urethane)s with fluorinated alkyl phosphatidylcholine side groups. The result by protein adsorption and platelet adhesion experiments suggested that only 5–12.5 mol% phosphatidylcholine (PC) could be enough for good hemo-compatibility, and they proposed that it can be used to bring the bioactive PC groups to the surface of the PC-containing PUs more effectively.

In addition, fluorine content plays a critical role in the improvement surface properties of the base polymers and their blood compatibility. A higher content of fluorine atoms exposed on the surface results in a lower surface free energy, a lower relative index of platelet adhesion, and a lower fibrinogen/albumin adsorption ratio (F/A ratio). The polyurethane containing a 50% molar ratio of fluorodiols 1H,1H,12H,12H-perfluoro-1,12-dodecanediol (PFDDOL) and 2,2,3,3-tetrafluoro-1,4-butanediol (TF) as a chain extender exhibited the lowest surface energy and superior blood compatibility [72]. Also, fluorinated phosphatidylcholine poly(carbonate urethane)s (FPCPCUs) blending with poly(ether urethane) (PEU) in different compositions improve blood compatibility of PUs. The results demonstrated when FPCPCU content reached to 40 wt% (40FPCPCU film), the number of adhered platelets decreased by 6 and 23 times, compared with that of FPCPCU and PEU, respectively [73].

Recent anti-biofouling strategies based on SMAs are to combine both fluorinated side chains and hydrophilic chains, which can be self-assembled to generate amphiphilic surfaces. These copolymers have low surface energy side chains as polydimethylsiloxane (PDMS) or fluorinated molecules [74] and enriched hydrophilic

side chains based on PEG. The amphiphilic surface would undergo an environment-dependent transformation in the surface when in contact with the extracellular polymeric substances for its anti-fouling nature, and it could be useful for applications to blood-contacting devices. Zhao et al. [75] designed amphiphilic membrane surfaces covered with enriched hydrophilic poly(ethylene oxide) (PEO) segments and low surface energy PDMS segments, which could prevent biofoulant adsorption and drive away the adsorbed biofoulants, respectively. The resulting surface exhibited better anti-fouling properties than that of polyethersulfone (PES) membrane, and it was also found that the biofouling could be significantly reduced by the coexistence of optimized hydrophilic and low surface energy microdomains.

13.3.3 Fluorinated Oligomers with Zwitterionic Structures

Zwitterionic surfactants are a relatively new class of surfactants, which combine the structural features of dimeric and **amphoteric surfactants** in one **molecule**. However, a few examples of these compounds have been reported with their difficult synthesis. Lin et al. [76] designed the facile synthesis of four fluorinated zwitterionic heterogemini surfactants with side-functionalized $\text{CF}_3\text{CF}_2\text{CF}_2\text{C}(\text{CF}_3)_2$ group with perfluoro-2-methyl-2-pentene as starting material, demonstrating that fluorinated zwitterionic heterogemini **surfactants** showed much better **surface activities** than the monomeric fluorinated surfactant.

Zhang and coworkers [77] also proposed that a novel amphiphilic copolymer with zwitterionic and fluorinated chains acted as additives with the hydrophilic zwitterionic carboxybetaine methyl acrylamide (CBMA) and low surface energy tridecafluorooctyl acrylate (TFOA) segments on the membrane surface, which could improve anti-fouling properties due to the binary cooperative effect of zwitterionic and low surface energy microdomains.

13.4 Conclusions

Despite significant efforts, thrombosis and biofouling induced by blood-contacting polymeric biomaterials limit their wider applications as long-term blood-containing implants. Therefore, studies related to the improvement of surface properties of blood-contacting polymeric biomaterials still have been receiving much attention. Among many surface treatment technologies, such as coating, grafting, and bulk blending, bulk blending is considered as effective and simple way to improve surface properties of biomaterials, which could overcome some drawbacks such as low adhesion stability for surface coatings and complex process. In this chapter, we have focused on polymeric additives with zwitterionic structures and/or fluoroalkyl groups that show functional surface active to improve blood compatibility of base polymers in different mechanisms. Zwitterionic groups can be hydrated with water molecules on the surface to reduce protein adsorption and cell adhesion, whereas polymers with fluoroalkyl groups can reduce the interfacial free energy, which induce less protein adsorption and platelet adhesion, due to the migration of fluorinated groups. In summary, bulk blending of these additives with based polymers to improve surface blood compatibility is an important technique for blood-contacting medical devices.

References

- Li S, Henry JJ (2011) Nonthrombogenic approaches to cardiovascular bioengineering. *Annu Rev Biomed Eng* 13:451–475
- Moellering RC Jr (2011) MRSA: the first half century. *J Antimicrob Chemother* 67(1):4–11
- Tu Q, Shen X, Liu Y et al (2019) A facile metal–phenolic–amine strategy for dual-functionalization of blood-contacting devices with antibacterial and anticoagulant properties. *Mater Chem Front* 3(2):265–275
- Vogler EA, Siedlecki CA (2009) Contact activation of blood–plasma coagulation. *Biomaterials* 30(10):1857–1869
- Frost MC, Reynolds MM, Meyerhoff ME (2005) Polymers incorporating nitric oxide releasing/generating substances for improved biocompatibility of blood-contacting medical devices. *Biomaterials* 26(14):1685–1693
- Surman F, Riedel T, Bruns M et al (2015) Polymer brushes interfacing blood as a route toward high performance blood contacting devices. *Macromol Biosci* 15(5):636–646
- Hucknall A, Rangarajan S, Chilkoti A (2009) In pursuit of zero: polymer brushes that resist the adsorption of proteins. *Adv Mater* 21(23):2441–2446
- Rodriguez-Emmenegger C, Brynda E, Riedel T, Houska M et al (2011) Polymer brushes showing non fouling in blood plasma challenge the currently accepted design of protein resistant surfaces. *ISO: Macromol Rapid Commun* 32(13):952–957
- Mosher DF (1993) Adhesive proteins and their cellular receptors. *Cardiovasc Pathol* 2(3):149–155
- Lopez-Donaire ML, Santerre JP (2014) Surface modifying oligomers used to functionalize polymeric surfaces: consideration of blood contact applications. *J Appl Polym Sci* 131(14)
- Alves NM, Pashkuleva I, Reis RL et al (2010) Controlling cell behavior through the design of polymer surfaces. *Small* 6(20):2208–2220
- Kingshott P, Andersson G, McArthur SL et al (2011) Surface modification and chemical surface analysis of biomaterials. *Curr Opin Chem Biol* 15(5):667–676
- Chen H, Yuan L, Song W et al (2008) Biocompatible polymer materials: role of protein–surface interactions. *Prog Polym Sci* 33(11):1059–1087
- Amiji M, Park K (1992) Prevention of protein adsorption and platelet adhesion on surfaces by PEO/PPO/PEO triblock copolymers. *Biomaterials* 13(10):682–692
- Chang Y, Chen WY, Yandi W et al (2009) Dual-thermoreponsive phase behavior of blood compatible zwitterionic copolymers containing nonionic poly (N-isopropyl acrylamide). *Biomacromolecules* 10(8):2092–2100
- Yang Z, Tu Q, Maitz MF et al (2012) Direct thrombin inhibitor–bivalirudin functionalized plasma polymerized allylamine coating for improved biocompatibility of vascular devices. *Biomaterials* 33(32):7959–7971
- Wang L-F, Wei Y-H, Chen K-Y et al (2004) Properties of phospholipid monolayer deposited on a fluorinated polyurethane. *J Biomater Sci Polym Ed* 15(8):957–969
- Hossfeld S, Nolte A, Hartmann H et al (2013) Bioactive coronary stent coating based on layer-by-layer technology for siRNA release. *Acta Biomater* 9(5):6741–6752
- Lim C-M, Hur J, Jang H et al (2019) Developing a thermal grafting process for zwitterionic polymers on cross-linked polyethylene with geometry-independent grafting thickness. *Acta Biomater* 85:180–191
- Lim C-M, Seo J, Jang H et al (2018) Optimizing grafting thickness of zwitterionic sulfobetaine polymer on cross-linked polyethylene surface to reduce friction coefficient. *Appl Surf Sci* 452:102–112
- Jiang H, Wang X, Li C et al (2011) Improvement of hemocompatibility of polycaprolactone film surfaces with zwitterionic polymer brushes. *Langmuir* 27(18):11575–11581

22. Flores JD, Xu X, Treat NJ et al (2009) Reversible “self-locked” micelles from a zwitterion-containing triblock copolymer. *Macromolecules* 42(14):4941–4945
23. Seo J-H, Matsuno R, Lee Y et al (2009) Conformational recovery and preservation of protein nature from heat-induced denaturation by water-soluble phospholipid polymer conjugation. *Biomaterials* 30(28):4859–4867
24. Hedayati M, Neufeld MJ, Reynolds MM et al (2019) The quest for blood-compatible materials: recent advances and future technologies. *Mater Sci Eng R Rep* 138:118–152
25. Ishihara K (2019) Revolutionary advances in 2-methacryloyloxyethyl phosphorylcholine polymers as biomaterials. *J Biomed Mater Res Part A* 107(5):933–943
26. Shimizu T, Goda T, Minoura N et al (2010) Superhydrophilic silicone hydrogels with interpenetrating poly (2-methacryloyloxyethyl phosphorylcholine) networks. *Biomaterials* 31(12):3274–3280
27. Liu P-S, Chen Q, Liu X et al (2009) Grafting of zwitterion from cellulose membranes via ATRP for improving blood compatibility. *Biomacromolecules* 10(10):2809–2816
28. Jiang S, Cao Z (2010) Ultralow-fouling, functionalizable, and hydrolyzable zwitterionic materials and their derivatives for biological applications. *Adv Mater* 22(9):920–932
29. Seo J-H, Matsuno R, Takai M et al (2009) Cell adhesion on phase-separated surface of block copolymer composed of poly (2-methacryloyloxyethyl phosphorylcholine) and poly (dimethylsiloxane). *Biomaterials* 30(29):5330–5340
30. Hasegawa T, Iwasaki Y, Ishihara K (2001) Preparation and performance of protein-adsorption-resistant asymmetric porous membrane composed of polysulfone/phospholipid polymer blend. *Biomaterials* 22(3):243–251
31. Anderson JM, Shive MS (1997) Biodegradation and biocompatibility of PLA and PLGA microspheres. *Adv Drug Deliv Rev* 28(1):5–24
32. Iwasaki Y, Sawada S-i, Ishihara K et al (2002) Reduction of surface-induced inflammatory reaction on PLGA/MPC polymer blend. *Biomaterials* 23(18):3897–3903
33. Ye SH, Watanabe J, Iwasaki Y et al (2002) Novel cellulose acetate membrane blended with phospholipid polymer for hemocompatible filtration system. *J Membr Sci* 210(2):411–421
34. Zhao Y-F, Zhu L-P, Yi Z et al (2013) Improving the hydrophilicity and fouling-resistance of polysulfone ultrafiltration membranes via surface zwitterionicalization mediated by polysulfone-based triblock copolymer additive. *J Membr Sci* 440:40–47
35. Meng S, Guo Z, Wang Q et al (2011) Studies on a novel multi-sensitive hydrogel: influence of the biomimetic phosphorylcholine end-groups on the PEO–PPO–PEO tri-block co-polymers. *J Biomater Sci Polym Ed* 22(4–6):651–664
36. Huang J, Gu S, Zhang R et al (2013) Synthesis, spectroscopic, and thermal properties of polyurethanes containing zwitterionic sulfobetaine groups. *J Therm Anal* 12(3):1289–1295
37. Cao J, Yang M, Lu A et al (2013) Polyurethanes containing zwitterionic sulfobetaines and their molecular chain rearrangement in water. *J Biomed Mater Res Part A* 101(3):909–918
38. Sechriest VF, Miao YJ, Niyibizi C et al (2000) GAG-augmented polysaccharide hydrogel: a novel biocompatible and biodegradable material to support chondrogenesis. *J Biomed Mater Res* 49(4):534–541
39. Jeon S, Lee J, Andrade J et al (1991) Protein—surface interactions in the presence of polyethylene oxide: I. Simplified theory. *J Colloid Interface Sci* 142(1):149–158
40. Jeon S, Andrade J (1991) Protein—surface interactions in the presence of polyethylene oxide: II. Effect of protein size. *J Colloid Interface Sci* 142(1):159–166
41. Ji J, Zhu H, Shen J (2004) Surface tailoring of poly (DL-lactic acid) by ligand-tethered amphiphilic polymer for promoting chondrocyte attachment and growth. *Biomaterials* 25(10):1859–1867
42. Tamada Y, Murata M, Makino K et al (1998) Anticoagulant effects of sulphonated polyisoprenes. *Biomaterials* 19(7–9):745–750
43. Silver JH, Hart AP, Williams EC et al (1992) Anticoagulant effects of sulphonated polyurethanes. *Biomaterials* 3(6):339–344
44. Tamada Y, Murata M, Hayashi T et al (2002) Anticoagulant mechanism of sulfonated polyisoprenes. *Biomaterials* 23(5):1375–1382
45. Nie S, Xue J, Lu Y (2012) Improved blood compatibility of polyethersulfone membrane with a hydrophilic and anionic surface. *Colloid Surf B Biointerfaces* 100:116–125
46. Chen HF, Ren YJ (2015) Design, synthesis, and anti-thrombotic evaluation of some novel fluorinated thrombin inhibitor derivatives. *Arch Pharm* 348(6):408–420
47. Nowatzki PJ, Koepsel RR, Stoodley P et al (2012) Salicylic acid-releasing polyurethane acrylate polymers as anti-biofilm urological catheter coatings. *Acta Biomater* 8(5):1869–1880
48. Nouman M, Jubeli E, Saunier J et al (2016) Exudation of additives to the surface of medical devices: impact on biocompatibility in the case of polyurethane used in implantable catheters. *J Biomed Mater Res Part A* 104(12):2954–2967
49. Suk DE, Chowdhury G, Matsuura T et al (2002) Study on the kinetics of surface migration of surface modifying macromolecules in membrane preparation. *Macromolecules* 35(8):3017–3021
50. Rana D, Matsuura T, Narbaitz RM (2006) Novel hydrophilic surface modifying macromolecules for polymeric membranes: polyurethane ends capped by hydroxy group. *J Membr Sci* 282(1–2):205–216
51. Theron JP, Knoetze JH, Sanderson RD et al (2010) Modification, crosslinking and reactive electrospinning of a thermoplastic medical polyurethane for vascular graft applications. *Acta Biomater* 6(7):2434–2447

52. Joung YK, Hwang IK, Park KD et al (2010) CD34 monoclonal antibody-immobilized electrospun polyurethane for the endothelialization of vascular grafts. *Macromol Res* 18(9):904–912
53. Sundaram HS, Cho YJ, Dimitriou MD et al (2011) Fluorinated amphiphilic polymers and their blends for fouling-release applications: the benefits of a triblock copolymer surface. *ACS Appl Mater Interfaces* 3(9):3366–3374
54. Pinchuk L (1994) A review of the biostability and carcinogenicity of polyurethanes in medicine and the new-generation of biostable polyurethanes. *J Biomater Sci Polym Ed* 6(3):225–267
55. Xie XY, Tan H, Li JH et al (2008) Synthesis and characterization of fluorocarbon chain end-capped poly(carbonate urethane)s as biomaterials: a novel bilayered surface structure. *J Biomed Mater Res Part A* 84A(1):30–43
56. Massa TM, Yang ML, Ho JYC et al (2005) Fibrinogen surface distribution correlates to platelet adhesion pattern on fluorinated surface-modified polyetherurethane. *Biomaterials* 26(35):7367–7376
57. Krafft MP, Riess JG (2007) Perfluorocarbons: life sciences and biomedical uses – dedicated to the memory of professor Guy Ourisson, a true RENAISSANCE man. *J Polym Sci A Polym Chem* 45(7):1185–1198
58. Tan H, Li JH, Guo M et al (2005) Phase behavior and hydrogen bonding in biomembrane mimicking polyurethanes with long side chain fluorinated alkyl phosphatidylcholine polar head groups attached to hard block. *Polymer* 46(18):7230–7239
59. Khulbe KC, Feng C, Matsuura T (2010) The art of surface modification of synthetic polymeric membranes. *J Appl Polym Sci* 115(2):855–895
60. Tang YW, Santerre JP, Labow RS et al (1996) Synthesis of surface-modifying macromolecules for use in segmented polyurethanes. *J Appl Polym Sci* 62(8):1133–1145
61. Hutchings LR, Narrienen AP, Thompson RL et al (2008) Modifying and managing the surface properties of polymers. *Polym Int* 57(2):163–170
62. Tang YW, Santerre JP, Labow RS et al (1997) Use of surface-modifying macromolecules to enhance the biostability of segmented polyurethanes. *J Biomed Mater Res* 35(3):371–381
63. Tonelli C, Ajroldi G, Turturro A et al (2001) Synthesis methods of fluorinated polyurethanes. 1. Effects on thermal and dynamic-mechanical behaviours. *Polymer* 42(13):5589–5598
64. Li JH, Zhang Y, Yang J et al (2013) Synthesis and surface properties of polyurethane end-capped with hybrid hydrocarbon/fluorocarbon double-chain phospholipid. *J Biomed Mater Res Part A* 101(5):1362–1372
65. El-Shehawey AA, Yokoyama H, Sugiyama K et al (2005) Precise synthesis of novel chain-end-functionalized polystyrenes with a definite number of perfluorooctyl groups and their surface characterization. *Macromolecules* 38(20):8285–8299
66. Hutchings LR, Narrienen AP, Eggleston SM et al (2006) Surface-active fluorocarbon end-functionalized polylactides. *Polymer* 47(24):8116–8122
67. Bergius WNA, Hutchings LR, Sarih NM et al (2013) Synthesis and characterisation of end-functionalised poly(N-vinylpyrrolidone) additives by reversible addition-fragmentation transfer polymerisation. *Polym Chem* 4(9):2815–2827
68. Hutchings LR, Sarih NM, Thompson RL (2011) Multi-end functionalised polymer additives synthesised by living anionic polymerisation-the impact of additive molecular structure upon surface properties. *Polym Chem* 2(4):851–861
69. Ge Z, Zhang XY, Dai JB et al (2009) Synthesis, characterization and properties of a novel fluorinated polyurethane. *Eur Polym J* 45(2):530–536
70. Tan H, Liu J, Li JH et al (2006) Synthesis and hemocompatibility of biomembrane mimicking poly(carbonate urethane)s containing fluorinated alkyl phosphatidylcholine side groups. *Biomacromolecules* 7(9):2591–2599
71. Tan H, Xie XY, Li JH et al (2004) Synthesis and surface mobility of segmented polyurethanes with fluorinated side chains attached to hard blocks. *Polymer* 45(5):1495–1502
72. Lin YH, Chou NK, Chang CH et al (2007) Blood compatibility of fluorodiol-containing polyurethanes. *J Polym Sci A Polym Chem* 45(15):3231–3242
73. Zhang XQ, Jiang X, Li JH et al (2008) Largely improved blood compatibility of polyurethane by blending with fluorinated phosphatidylcholine polyurethane. *Chin J Polym Sci* 26(2):203–211
74. Krishnan S, Ayothi R, Hexemer A et al (2006) Anti-biofouling properties of comblike block copolymers with amphiphilic side chains. *Langmuir* 22(11):5075–5086
75. Zhao XT, Su YL, Li YF et al (2014) Engineering amphiphilic membrane surfaces based on PEO and PDMS segments for improved antifouling performances. *J Membr Sci* 450:111–123
76. Lin C, Pan RM, Xing P et al (2018) Synthesis and surface activity study of novel branched zwitterionic heterogemini fluorosurfactants with CF₃CF₂CF₂C(CF₃)₂ group. *J Fluor Chem* 214:35–41
77. Zhang GF, Gao F, Zhang QH et al (2016) Enhanced oil-fouling resistance of poly(ether sulfone) membranes by incorporation of novel amphiphilic zwitterionic copolymers. *RSC Adv* 6(9):7532–7543